

THE ROLE OF GELATINOUS  
ZOOPLANKTON FOR MARINE  
ECOSYSTEMS AND THE  
CARBON CYCLE

BY

REBECCA MARY WRIGHT

FOR THE DEGREE OF

DOCTOR OF PHILOSOPHY

THESIS PRESENTED TO THE

UNIVERSITY OF EAST ANGLIA,  
SCHOOL OF ENVIRONMENTAL SCIENCES

JUNE 2019

This copy of the thesis has been supplied on condition that anyone who consults it is understood to recognise that its copyright rests with the author and that use of any information derived therefrom must be in accordance with current UK Copyright Law. In addition, any quotation or extract must include full attribution.



# ABSTRACT

There is increasing recognition of the importance of gelatinous zooplankton (GZ) within the ocean. However, observations of GZ and understanding of their ecosystem role, lags behind other zooplankton. Increasing pressures on the ocean, including climate change and overfishing, will likely impact GZ. This thesis aims to identify the role of GZ in the marine ecosystem and carbon cycle using observations and a model. This is achieved by (1) an analysis of GZ abundance and biomass from a global database, (2) the addition of GZ as a Plankton Functional Type in the global biogeochemical model PlankTOM11, (3) an analysis of the effect of GZ on carbon export in PlankTOM11 and (4) a case study on the effects of overfishing and climate change on GZ in PlankTOM11. Model developments made use of available vital rates and biomass data. Parameterisation of mortality was the largest source of uncertainty for GZ; therefore, mortality was tuned based on the resulting biomass generated by PlankTOM11. GZ had the largest influence on macrozooplankton biomass and influenced the whole plankton ecosystem through trophic cascades. PlankTOM11 showed trophic level as the most important characteristic of GZ for increasing export. There is evidence that GZ mortality plays an important role in export, but this is not replicated in PlankTOM11, likely due to particulate organic carbon (OC) representation as smaller and with slower sinking speeds than GZ carcasses. Further partitioning of OC should improve the representation of GZ mortality and its influence on export. The case study found overfishing reduced GZ biomass, in opposition to other studies. The lack of fish predation on GZ may be a key factor. Climate and overfishing acted synergistically on the ecosystem. GZ play a key role in marine ecosystems by influencing plankton community structures through trophic cascades, thus influencing carbon export.



# LIST OF CONTENTS

List of Tables	XI
List of Figures	XIV
List of Equations	XXIII
List of Appendices	XXIV
Acknowledgements	XXV
CHAPTER 1. INTRODUCTION	1
1.1 Opening Statement	3
1.2 What are Gelatinous Zooplankton	3
1.2.1 Life Cycle	6
1.2.2 The Benefits of Blooming	7
1.3 Climate Change & Gelatinous Zooplankton - the Jellyfish Paradigm	9
1.4 The Importance of Gelatinous Zooplankton	11
1.4.1 Economic Benefit	11
1.4.2 Economic Cost	11
1.4.3 Ecosystem Services	12
1.5 Biogeochemical Cycles & The Biological Carbon Pump	13
1.5.1 Excretion	15
1.5.2 Death	15
1.6 Drivers of Blooms	16
1.6.1 Temperature	16
1.6.2 Food	17
1.6.3 Fishing	18
1.6.4 Nutrients & Eutrophication	18
1.6.5 Hydrology	19
1.6.6 Others	19
1.7 Causes of Busts	20

1.7.1 Food	20
1.7.2 Parasites	21
1.7.3 Disease	21
1.7.4 Predation	21
1.7.5 Senescence Post-Spawning	22
1.7.6 Extreme Temperature	22
1.7.7 Intertidal Stranding	23
1.8 Trends in Gelatinous Zooplankton Populations	23
1.8.1 North East Atlantic	23
1.8.2 Mediterranean	25
1.8.3 Americas - Pacific	26
1.8.4 Americas - Atlantic	27
1.8.5 China	28
1.8.6 Southern Ocean	28
1.8.7 Global	29
1.9 Baselines	30
1.10 Seasonality	30
1.10.1 Seasonality Studies	31
1.10.2 Trends in Seasonality	31
1.11 The Difficulty with Sampling Gelatinous Zooplankton	32
1.11.1 Zooplankton Tows	33
1.11.2 Fishery Surveys	34
1.11.3 By-Proxy	34
1.11.4 Visual and Video Counts	35
1.11.5 Other Methods	35
1.12 Modelling Gelatinous Zooplankton	36
1.12.1 Fisheries Models – Ecopath	36
1.12.2 Stage-structured Models	37
1.12.3 Small-scale Ecosystem Models – NPZD	38

1.12.4 Physical Models	38
1.13 Plankton Functional Type Modelling	39
1.14 Thesis Outline	40
1.14.1 Thesis Objective	40
1.14.2 Thesis Structure	41
References	42
CHAPTER 2. GLOBAL & REGIONAL TRENDS IN GELATINOUS ZOOPLANKTON ABUNDANCE	59
Abstract	61
2.1 Introduction	63
2.1.1 Evidence of Trends and Variability in Gelatinous Zooplankton Abundance	64
2.1.2 Baselines in Gelatinous Zooplankton Populations	65
2.2 Methods	67
2.2.1 Data Handling	67
2.2.2 Seasonality in Longhurst Provinces	69
2.2.3 Global Baselines	70
2.3 Results	71
2.3.1 Bloom and Bust	71
2.3.2 Seasonality in Longhurst Provinces	71
2.3.3 Phylum Baselines	77
2.3.4 Global Gelatinous Zooplankton Baselines	81
2.4 Discussion	84
2.5 Conclusion	86
References	88
CHAPTER 3. INCORPORATING JELLYFISH IN A GLOBAL OCEAN BIOGEOCHEMISTRY MODEL	95
Abstract	97
3.1 Introduction	99

3.2 Methods	101
3.2.1 Model Description	101
3.2.2 Jellyfish PFT Development	103
3.2.2.1 Growth	104
3.2.2.2 Grazing	104
3.2.2.3 Respiration	107
3.2.2.4 Mortality	108
3.2.3 Additional Tuning	112
3.2.4 Model Simulations	113
3.3 Results	115
3.3.1 Ecosystem Properties of PlankTOM11	115
3.3.2 Jellyfish Biomass in PlankTOM11	119
3.3.3 Influence of Jellyfish on the PlankTOM Ecosystem	120
3.4 Discussion	125
3.5 Conclusion	127
References	129
CHAPTER 4. ROLE OF JELLYFISH FOR CARBON EXPORT	137
Abstract	139
4.1 Introduction	141
4.2 Methods	144
4.2.1 Export in PlankTOM11	144
4.2.2 Model Simulations	147
4.2.3 Export Efficiency	147
4.3 Results	149
4.3.1 Carbon Export in PlankTOM11	149
4.3.2 Role of Jellyfish Characteristics in Carbon Export	152
4.4 Discussion	164
4.5 Conclusion	168



References	170
CHAPTER 5. IMPACTS OF CLIMATE AND FISHERIES ON JELLYFISH IN THE BENGUELA CURRENT SYSTEM	175
Abstract	177
5.1 Introduction	179
5.1.1 Jellyfish in the Benguela Current System	181
5.1.2 A Brief History of Fishing in the Benguela Current System	183
5.1.3 Influence of Overfishing on Jellyfish Biomass	185
5.1.4 Influence of Climate Variability on Jellyfish Biomass	186
5.1.5 Models of Jellyfish in the Benguela Current System	187
5.2 Methods	189
5.2.1 Introducing Fishing Pressure to PlankTOM11	189
5.2.1.1 Fish Predation Preference	189
5.2.1.2 Mortality Through Predation	189
5.2.1.3 Fish Biomass and Proxy Predator Biomass	190
5.2.2 Model Validation	192
5.2.2.1 Plankton Observations	192
5.2.2.2 Physical Observations	194
5.2.3 Model Simulations	194
5.3 Results	196
5.3.1 The Northern Benguela	196
5.3.2 The Southern Benguela	201
5.3.3 Correlation to Physical Conditions	206
5.3.4 External Influence	209
5.4 Discussion	211
5.5 Conclusion	213
References	215
CHAPTER 6. CONCLUSION	221

6.1 Introduction	223
6.2 Key Questions and Findings	223
6.4 Future Work	226
6.5 Closing Statement	228
References	230

## LIST OF TABLES

Table 1.1	Taxonomic classification of groups of gelatinous zooplankton (see Appendices 1).	4
Table 2.1	Statistics of gelatinous zooplankton split into phylum from the gridded MAREDAT data. AM is the arithmetic mean, and GM is the geometric mean. No data for Ctenophora biomass was available in the dataset.	78
Table 2.2	PFT global biomass, adapted from Buitenhuis et al. (2013). Gelatinous data calculated according to methods described in Buitenhuis. All data from MAREDAT. In Buitenhuis et al. (2013) median depth profiles are the min, and AM (arithmetic mean) depth profiles are the max.	81
Table 2.3	Statistics of gelatinous zooplankton from the gridded MAREDAT data. AM is the arithmetic mean and GM is the geometric mean. The Northern Hemisphere is defined as 90°N-30°N, the Tropics is defined as 30°N-30°S and the Southern Hemisphere is defined as 30°S-90°S. For biomass, only the global value is given, all data points are in the Northern Hemisphere, except for one data point in the Tropics.	82
Table 3.1	Size range and descriptions of PFT groups used in PlankTOM11. Adapted from Le Quéré et al. (2016).	102
Table 3.2	Parameters used to calculate PFT specific growth rate with two-parameter fit (Eq. 3.2) and three-parameter fit (Eq. 3.3) in PlankTOM11.	105
Table 3.3	Relative preference, expressed as a ratio, of zooplankton for food (grazing) used in PlankTOM. For each zooplankton the preference ratio for diatoms is set to 1. Adapted from Le Quéré et al. (2016).	107
Table 3.4	Temperature dependent rates of respiration and mortality for macro- and jellyfish zooplankton. Where $\mu_0$ is the rate at 0°C and $Q_{10}$ is the temperature coefficient. See text for detail.	111
Table 3.5	Changes to non-jellyfish PFT parameters. PlankTOM10 (2016) is the latest published version of PlankTOM with 10 PFTs (Le Quéré et al., 2016).	112
Table 3.6	Global mean values for rates and biomass from observations and the PlankTOM11 and PlankTOM10 models averaged over 1985–2015. In parenthesis is the percentage share of the plankton type of the total Phytoplankton or Zooplankton biomass.	116

Table 3.7	Jellyfish (Cnidaria) biomass globally from observations (MAREDAT, see Chapter 2) and PlankTOM11. Three types of mean are given for the observations; Med is the median, AM is the arithmetic mean and GM is the geometric mean. The ratios are all scaled to mean = 1. All units are $\mu\text{g C L}^{-1}$ .	119
Table 3.8	Jellyfish (Cnidaria) biomass statistics for the coast of Alaska from observations (MAREDAT, see Chapter 2) and PlankTOM11. Mean is the arithmetic mean and SD is the standard deviation. PlankTOM11 is sampled at grid boxes where observations are available (see Fig. 3.9). All units are $\mu\text{mol C L}^{-1}$ .	121
Table 4.1	Temperature-dependent rates of macro- and jellyfish zooplankton. Respiration and mortality follow a simple exponential curve, where $\mu_0$ is the rate at $0^\circ\text{C}$ and $Q_{10}$ is the temperature coefficient. Growth has a bell-shaped curve with a temperature optimum, where $\mu_{\text{max}}$ is the maximum growth rate at $T_{\text{opt}}$ (the optimal temperature) and $dT$ is the temperature interval (see Chapter 3, section 3.2.2.1).	146
Table 4.2	Sensitivity simulations to test the addition of a jellyfish PFT to PlankTOM. The parameterisation of the 11 <sup>th</sup> PFT in PlankTOM as either jellyfish parameters (J) or macrozooplankton parameters (M) is indicated for each simulation. For grazing preferences, refer to Figure 4.2. For values used in growth, respiration and mortality parameters refer to Table 3.2 and Table 3.4.	147
Table 4.3	Global annual <i>ef</i> ratio, primary production and export production rates (Pg carbon/y) and total zooplankton biomass ( $\text{mol carbon/m}^3$ ) averaged over 0-100m in PlankTOM11 and PlankTOM10.5 simulations.	153
Table 5.1	The annual average (min – max) zooplankton biomass ( $\mu\text{mol C L}^{-1}$ ) in the Benguela for the top 200m. Observations are converted into $\mu\text{mol C L}^{-1}$ from Hutchings et al. (1991) for mesozooplankton and macrozooplankton, and from Fearon et al. (1992) for jellyfish, with the Lynam et al. (2006) snapshot observations in parenthesis. Jellyfish observations are converted into carbon weight using the conversions in Lucas et al. (2011). PlankTOM11 results are for 1950-2015, 0-200m, using the regional masks shown in Figure 5.3.	192
Table 5.2	PlankTOM11 simulations to assess the influence of climate variability and fisheries (as fish predation pressure) on the BCS ecosystem.	195

Table 5.3	The effect of climate and fishing on zooplankton and chlorophyll in the Northern Benguela. Each of the simulations TOM11-CF, TOM11-CN and TOM11-NF is subtracted from TOM11-NN (no climate or fishing). CN + NF is the addition of the results from TOM11-CN and TOM11-NF. Results are given as a total of 1950 - 2012 for all zooplankton ( $\mu\text{mol C L}^{-1}$ ) and chlorophyll ( $\mu\text{mol chl L}^{-1}$ ) and broken down into the total of each decade for macrozooplankton, jellyfish and chlorophyll.	199
Table 5.4	The effect of climate and fishing on zooplankton and chlorophyll in the Southern Benguela. Each of the simulations TOM11-CF, TOM11-CN and TOM11-NF is subtracted from TOM11-NN (no climate or fishing). CN + NF is the addition of the results from CN and NF. Results are given as a total of 1950 – 2012 for all zooplankton ( $\mu\text{mol C L}^{-1}$ ) and chlorophyll ( $\mu\text{mol chl L}^{-1}$ ) and broken down into the total of each decade for macrozooplankton, jellyfish and chlorophyll.	203

## LIST OF FIGURES

- |            |  |    |
|------------|--|----|
| Figure 1.1 | Photos of gelatinous zooplankton. (a) Lions mane jellyfish (Cnidaria; Smithsonian, 2017), (b) Moon jellyfish (Cnidaria; New England Aquarium, 2015), (c) Box jellyfish (Cnidaria; Generate Change, 2019), (d) Sea gooseberries (Ctenophora; Microscopy UK, 2019), (e) Sea walnut (Ctenophora; NIOZ, 2015), (f) Salp oozoid (Tunicata; Plankton Chronicles, 2016), (g) Salp chain (Tunicata; Plankton Chronicles, 2016).  | 4  |
| Figure 1.2 | Simplified anatomy of gelatinous zooplankton for typical (top) Cnidaria, (middle) Ctenophora and (bottom) Tunicata.  | 5  |
| Figure 1.3 | Life cycles of gelatinous zooplankton for (top) the moon jellyfish, <i>Aurelia aurita</i> , as a typical Cnidaria, (middle) the comb jelly, <i>Mnemiopsis leidyi</i> , as a typical Ctenophora and (bottom) the salp, <i>Thalia democratia</i> , as a typical Tunicata.  | 8  |
| Figure 1.4 | The biological carbon pump. CO <sub>2</sub> from the atmosphere dissolves into the ocean. Phytoplankton convert the dissolved CO <sub>2</sub> into particulate organic carbon (POC) via photosynthesis in the euphotic layer of the epipelagic zone. Zooplankton graze on phytoplankton, converting the POC and other organic matter in phytoplankton into faecal pellets, carcasses and other POC aggregates (marine snow), which are exported into the mesopelagic and bathypelagic zones by sinking and by the vertical migration of some zooplankton and fish. In the mesopelagic zone the marine snow (sinking particles) is converted into dissolved organic carbon (DOC) through microbial remineralisation which can be moved throughout the water column via physical vertical mixing of water. The marine snow is also grazed and repackaged by zooplankton, which are in turn predated by fish, squid and other deep ocean consumers, continuing the repackaging of POC and DOC in the mesopelagic zone. Below the sequestration depth carbon is deposited and stored for 100 years or more. Adapted from Turner et al. (2015). | 14 |
| Figure 1.5 | Authors personal photos from multiple trawls during a CEFAS scientific fishery survey of the North Sea, illustrating some of the difficulties in sampling and identifying GZ species from fishery surveys. Specimens are displayed on a board marked with centimetres. Unidentifiable gelatinous zooplankton (left) due to damage by net/other organisms in the net i.e. sea urchin, shells, fish spines. A damaged lions mane jellyfish, <i>Cyanea</i>  | 33 |

*capillata*, (top right) with no tentacles remaining and only a small section of oral arms remaining. A colourless specimen (usually red/burgundy in colour). A damaged moon jellyfish, *Aurelia aurita*, (bottom right) with sections missing from the mesoglea, no tentacles and some oral arms.

Figure 2.1	Number of data in MAREDAT for gelatinous zooplankton (top) abundance and (bottom) biomass, after binning the original raw data by month for 1938 – 2008 on a 1°x1° grid.	68
Figure 2.2	Number of raw abundance data for gelatinous zooplankton across (top) decades, and (bottom) months (summed across years), split into the Northern Hemisphere (green), Tropics (purple) and Southern Hemisphere (blue).	69
Figure 2.3	Percentage frequency of gelatinous zooplankton abundance (number of individuals/m <sup>3</sup> ) for the Northern Hemisphere (NH), Tropics (TR) and Southern Hemisphere (SH) from ungridded data. For top panels abundance is binned into 0, >0-1, 1-2, 2-3, etc. up to 9-10. For bottom panels abundance is binned into 0, >0-10, 10-20, 20-30, etc. up to 90-100, and then 100-1000, and >1000. Left panels show a difference percentage scale to right panels. The total number of samples for each of the three regions is given in the key.	72
Figure 2.4	Percentage frequency of gelatinous zooplankton biomass (µg carbon L <sup>-1</sup> ) for the Northern Hemisphere (NH) and Tropics (TR; there were no biomass samples for the Southern Hemisphere) from ungridded data. For top panels abundance is binned into 0, >0-0.01, 0.01-0.02, 0.02-0.03, etc. up to 0.09-0.10. For bottom panels abundance is binned into 0, >0-1, 1-2, 2-3, etc. up to 9-10, and then >10. Left panels show a difference percentage scale to right panels. The total number of samples for the two regions is given in the key.	73
Figure 2.5	Global map showing the Longhurst Provinces used in this analysis, each colour represents the area of a different Longhurst Province, labelled with the name. The Provinces are Alaska Coastal Downwelling Province (ALSK; dark blue), California Current Province (CALC; dark green), Northwest Atlantic Shelves Province (NWCS; red), Northeast Atlantic Shelves Province (NECS; light blue), Kuroshio Current Province (KURO; orange), North Pacific Subtropical West (NPSW; dark purple), North Pacific Equatorial Countercurrent Province (PNEC; light purple), Pacific Equatorial Divergence Province (PEQD; yellow) and the Indian Monsoon Gyres Province (MONS; light green).	74

Figure 2.6	Seasonal abundance of gelatinous zooplankton for nine ocean provinces shown in Fig. 5 (number of ind/m <sup>3</sup> ). For each month the light blue line shows the 5 <sup>th</sup> and 95 <sup>th</sup> percentile, the dark blue lines shows the 25 <sup>th</sup> and 75 <sup>th</sup> percentile, and the black line is the 50 <sup>th</sup> percentile/median. All the data points are shown in grey. For months with less than 4 data points, no percentiles are calculated. Across the top of each panel the number of data per month for that province is given. The graphs have been stretched at the lower values (0 – 25) as this is where the majority of the data occurs. All panels are on the same axis. See Figure 5 for locations and full name of each province.	76
Figure 2.7	Average gelatinous zooplankton abundance (individuals/m <sup>3</sup> ) on a 1x1 degree grid for Cnidaria, Tunicata, Ctenophora and Unclassified. Where abundance equals 0 the data is plotted in black.	79
Figure 2.8	Average gelatinous zooplankton (top) abundance (individuals/m <sup>3</sup> ) and (bottom) biomass (ug carbon/L) averaged for 1930 – 2008, on a 1x1 grid.	80
Figure 3.1	Schematic representation of the PlankTOM11 marine ecosystem model. The arrows represent the grazing fluxes by protozooplankton (orange), mesozooplankton (red), macrozooplankton (blue) and jellyfish zooplankton (purple). Only fluxes with relative preferences above 0.1 are shown (see Table 3.3).	103
Figure 3.2	Maximum growth rates for the 11 PFTs as a function of temperature from observations (grey circles). The fit to the data for two-parameters is the dark blue line, with the updated three-parameter fit in green. The Root Mean Square Error is given in each PFT panel coloured to the corresponding fit (blue for three-parameter and green for two-parameter). The two fits use the parameter values from Table 3.2. For full PFT names see Table 3.1.	106
Figure 3.3	Maximum (top) growth rates, (middle) respiration rates and (bottom) mortality rates for (left; purple) jellyfish and (right; blue) macrozooplankton PFTs as a function of temperature. The fit to the data is shown in black, using the parameter values from Table 3.2 and Table 3.4. Growth rates are the same as shown in Figure 2, on a different scale. For mortality the thin dashed line is the untuned fit, and the solid line is the tuned fit (Table 3.4).	109
Figure 3.4	Results from sensitivity tests on jellyfish mortality rates are shown by empty circles, the standard (tuned) PlankTOM11	110



simulation is shown by the black filled circle and the untuned simulation is shown by the grey filled circle; (top – middle) global mean PFT biomass for 0-200m depth, (bottom) regional mean surface chlorophyll concentration. For the regional mean chlorophyll and north/south ratio the grey lines show observations calculated from SeaWiFS. All data are averaged for 1985-2015, and between 30° and 55° latitude in both hemispheres: 140-240°E in the north and 140-290°E in the south. Observations for global PFT biomass are omitted as the results all fall within the min-max observational range. Phyto is the sum of all the phytoplankton PFTs.

- Figure 3.5 Annual mean surface chlorophyll ( $\mu\text{mol chl L}^{-1}$ ) and carbon biomasses ( $\mu\text{mol C L}^{-1}$ ) of JEL, MAC, MES and PRO for tuning of JEL mortality in PlankTOM11 (left) chosen simulation with 0.12 mortality/d<sup>-1</sup> and (right) untuned simulation with 0.02 mortality/d<sup>-1</sup>. Model results are shown for the surface box (0-10 meters) and averaged for 1985-2015. 111
- Figure 3.6 Global PFT biomass ( $\mu\text{mol C L}^{-1}$ ) averaged over 0-100m for PlankTOM11. Top is the total phytoplankton PFTs, middle is the total zooplankton PFTs and bottom is the jellyfish PFT. The grey line is the spin up period and the black line is the interannually varying forcing (see text for detail). The dashed line indicates the year 1985 after which the model data is used for analysis. 113
- Figure 3.7 Surface chlorophyll ( $\text{mg/m}^3$ ) averaged for (left) June to August and (right) November to January. Data are from (top) SeaWiFS satellite and results (bottom) from PlankTOM11. SeaWiFS is averaged for 1997-2006, and PlankTOM11 for 1985-2015. Model results are shown for the surface box (0-10 meters). The black boxes show the North, Tropic and South regions used in other figures. 115
- Figure 3.8 Annual mean surface carbon biomass ( $\mu\text{mol C L}^{-1}$ ) for each plankton functional type from PlankTOM11. Results are shown for the surface box (0-10 meters) and averaged for 1985-2015. All panels are scaled to the same key. 117
- Figure 3.9 Annual surface carbon biomasses ( $\mu\text{mol C L}^{-1}$ ) for the jellyfish PFT in PlankTOM11. Results are the mapped (top left) minimum over time, (middle left) average over time, and (bottom left) maximum over time, and (right) averaged over longitude for the minimum and maximum in thin black lines and average in the thick black line. All data is for 1985-2015. 118
- Figure 3.10 Carbon biomass of jellyfish from (left) observations and (right) 121

PlankTOM11 in  $\mu\text{mol C L}^{-1}$ , for the coast of Alaska (the region with the highest density of observations). The top panels show the annual mean jellyfish biomass and the bottom panels show the seasonal jellyfish biomass, with the mean in black and the minimum and maximum in blue. Observations and PlankTOM11 results are for 0-150m, as the depth range where >90% of the observations occur.

- |             |   |     |
|-------------|---|-----|
| Figure 3.11 | Surface chlorophyll concentration ( $\mu\text{g chl L}^{-1}$ ) for SeaWiFS satellite (green), PlankTOM11 (TOM11, black) and PlankTOM10 (TOM10, grey). North/south chlorophyll concentration ratio (left) and regional chlorophyll concentration (right) for the north (N), tropic (T) and south (S) regions shown in Figure 6.  | 122 |
| Figure 3.12 | Taylor diagram comparing the global distributions of in annual mean surface chlorophyll concentration ( $\mu\text{g chl L}^{-1}$ ) of PlankTOM11 (black circle) and PlankTOM10 (grey circle) to SeaWiFS satellite observations (green).   | 122 |
| Figure 3.13 | Mean surface carbon biomasses of all phytoplankton PFTs (green), protozooplankton (orange), mesozooplankton (red), macrozooplankton (blue) and jellyfish (purple). Global PFT biomass (top) in PgC for PlankTOM11 (TOM11) and PlankTOM10 (TOM10). Line plots shown regional PFT biomass in $\mu\text{mol C L}^{-1}$ for (left) PlankTOM11 and (right) PlankTOM10, for (middle) the north from January to December and (bottom) the south from July to June. All data are averaged for 1985-2015, and for the regions between 30° and 55° latitude in both hemispheres: 140-240°E in the north and 140-290°E in the south, as shown in Figure 3.6. | 124 |
| Figure 4.1  | The sources and sinks within PlankTOM11 for dissolved organic carbon (DOC) and small (POC) and large (GOC) particulate carbon. The sources (+) are additions to one or more of the organic carbon types and the sinks (-) are subtractions from one or more of the organic carbon types.  | 144 |
| Figure 4.2  | Relative preference of (left) macrozooplankton and (right) jellyfish grazing for food used in PlankTOM11. Small phytoplankton is $\text{N}_2$ -fixers, pico-phytoplankton and coccolithophores, large phytoplankton is mixed phytoplankton, diatoms and Phaeocystis, and particulate organic carbon is POC and GOC. For values see Chapter 3, Table 3.3.  | 146 |
| Figure 4.3  | PlankTOM11 results averaged for (left) June to August and (right) November to January. Data are for (top) primary production ( $\text{mol C/m}^2/\text{year}$ ) integrated over the top 100m,   | 150 |

- (middle) carbon export production at 100m ( $\text{mol C/m}^2/\text{year}$ ) and (bottom) *ef* ratio (export efficiency). All model results are averaged from 1985-2015.
- Figure 4.4 PlankTOM11 seasonal variation of primary production and export production ( $\text{mol/m}^2/\text{year}$ ) at regions; (left) North 30-90°N, (middle) Tropic 30°N-30°S and (right) South 30-90°S. Points are coloured by months of the year, averaged from 1985-2015. Straight black lines indicate *ef* ratios of 0.1, 0.2 and 0.4. 150
- Figure 4.5 PlankTOM11 correlations over time of the *ef* ratio with primary production (top left), sea surface temperature (top right), chlorophyll concentration (middle left), total zooplankton biomass (middle right), jellyfish biomass (bottom left) and macrozooplankton biomass (bottom right). Correlations are averaged over 0-100m except for sea surface temperature. Warm colours indicate a positive correlation, while cold colours indicate a negative correlation. Cross-hatched grid cells are where the correlation is not statistically significant (p values less than 0.05). 152
- Figure 4.6 Depth profiles of primary production, export production and total zooplankton biomass for PlankTOM11 (thick black line), PlankTOM10.5 (thin black line), PlankTOM10.5a (dark blue line; grazing preference), PlankTOM10.5b (green line; growth), PlankTOM10.5c (light blue line; respiration) and PlankTOM10.5d (red line; mortality). The top row of panels is results averaged for the Northern Hemisphere (30-90°N), the middle row is the Tropics (30°S-30°N) and the bottom row is the Southern Hemisphere (30-90°S). The left column of panels is for primary production ( $\text{mol/m}^2/\text{year}$ ), the middle column is export production ( $\text{mol/m}^2/\text{year}$ ) and the right column is total zooplankton biomass ( $\mu\text{m C L}^{-1}$ ). All results are averaged for 1985 – 2015. 155
- Figure 4.7 Annual mean (left) primary production from 0-100m and (right) carbon export at 100m ( $\text{mol/m}^2/\text{year}$ ). Results shown for (top) PlankTOM11, then below the difference between PlankTOM11 and the other simulations, in descending order PlankTOM10.5, PlankTOM10.5a (grazing), PlankTOM10.5b (growth), PlankTOM10.5c (respiration) and PlankTOM10.5d (mortality). All model results are averaged for 1985-2015. For the difference between PlankTOM11 and other simulations, warm colours indicate that the values of the other simulation are higher than PlankTOM11, while cold colours indicate that the values of the other simulation are lower than PlankTOM11. 157

Figure 4.8	Mean seasonal primary production, export production and the <i>ef</i> ratio for PlankTOM11 and the five PlankTOM10.5 simulations for the North (30-90°N). The <i>ef</i> ratio (dashed black line) is on the left vertical axis. Primary production (mol/m <sup>2</sup> ; green line) and export production (mol/m <sup>2</sup> ; black line) are on the right vertical axis. Export production is multiplied by a factor of 10 for visual clarity in comparison to primary production. Results are shown for (top left) PlankTOM11, (top right) PlankTOM10.5, (middle left) PlankTOM10.5a, (middle right) PlankTOM10.5b, (bottom left) PlankTOM10.5c, (bottom right) PlankTOM10.5d. All data are averaged for 1985-2015.	159
Figure 4.9	Mean seasonal PFT biomass for PlankTOM11 and the five PlankTOM10.5 simulations for the North (30-90°N). The PFTs are total phytoplankton (green), protozooplankton (orange), mesozooplankton (red), macrozooplankton (purple) and jellyfish (blue). PFT biomass is averaged from 0 – 100m. Results are shown for (top left) PlankTOM11, (top right) PlankTOM10.5, (middle left) PlankTOM10.5a, (middle right) PlankTOM10.5b, (bottom left) PlankTOM10.5c, (bottom right) PlankTOM10.5d. All data are averaged for 1985-2015.	160
Figure 5.1	The Benguela Current System with the key oceanographic features which form the Northern Benguela and Southern Benguela ecosystems. Upwelling cells (dark grey circles), the Angola-Benguela Front (light grey rectangle) and ocean currents (black arrows) are denoted in their approximate positions. See text for detail.	180
Figure 5.2	Stacked (top) fisheries catch and (bottom) fish biomass in million tons in the (left) Northern Benguela and (right) Southern Benguela for sardines and anchovies. Fisheries catch data from (FAO, 2017)) and fish biomass data collated from (FAO, 2017)) and Crawford (2007) . Note that the catch and biomass panels have difference scale bars.	184
Figure 5.3	The top panel shows the normalised fish biomass for the Northern Benguela (dark blue) and Southern Benguela (cyan) as used in PlankTOM11 to simulate fish PP. The normalised fish biomass is masked to the Northern and Southern Benguela, the area of these masks is shown in the bottom panel using the same colour key. The fish biomass data ends in 2012 so after this time the normalised fish biomass returns to 1.	191
Figure 5.4	Zooplankton biomass and upwelling for the BCS region. PlankTOM11 jellyfish (top left), macrozooplankton (top right) and mesozooplankton (middle left) biomass are in $\mu\text{molC L}^{-1}$	193

averaged over 0-200m. Upwelling is the vertical velocity in  $\text{m day}^{-1}$ , positive values indicate upwelling. PlankTOM11 upwelling (middle right) is averaged over 40-50m and upwelling modelled by Small et al. (2015) is at 45m (bottom; panels are adapted from Figure 5 in Small et al., 2015). All PlankTOM11 results are averaged over 1950 – 2015.

- Figure 5.5 The effect of climate and fishing on zooplankton and chlorophyll in the Northern Benguela. Each of the simulations TOM11-CF (red line), TOM11-CN (black line), TOM11-NF (green line) and TOM11-NN (dashed black line), is subtracted from TOM11-NN, so that the y-axis is the difference due to fish PP, climate or fish PP and climate. Results are shown for (top left) jellyfish, (top right) macrozooplankton, (middle left) mesozooplankton, (middle right) protozooplankton and (bottom left) surface chlorophyll. Fish PP (bottom right) for the Northern Benguela as in Figure 5.3 with the dashed line at 1 where fish predation does not have an influence on proxy predator biomass (Eq. 5.2). All simulation results are seasonally smoothed to show year to year variability, zooplankton are averaged over 0-200 meters in  $\mu\text{mol C L}^{-1}$  and chlorophyll is averaged over 0-10 meters in  $\mu\text{mol chl L}^{-1}$ . 197
- Figure 5.6 The effect of climate and fishing on zooplankton and chlorophyll in the Southern Benguela. Each of the simulations TOM11-CF (red line), TOM11-CN (black line), TOM11-NF (green line) and TOM11-NN (dashed black line), is subtracted from TOM11-NN, so that the y-axis is the difference due to fishing, climate or fishing and climate. Results are shown for (top left) jellyfish, (top right) macrozooplankton, (middle left) mesozooplankton, (middle right) protozooplankton and (bottom left) surface chlorophyll. Fish PP (bottom right) for the Northern Benguela as in Figure 5.3 with the dashed line at 1 where fish predation does not have an influence on proxy predator biomass (Eq. 5.3). All simulation results are seasonally smoothed to show year to year variability, zooplankton are averaged over 0-200 meters in  $\mu\text{mol C L}^{-1}$  and chlorophyll is averaged over 0-10 meters  $\mu\text{mol chl L}^{-1}$ . 202
- Figure 5.7 The correlation over time of jellyfish with (top) upwelling and (bottom) SST for the simulations (left) TOM11-CN (Climate & No fish predation) and (right) TOM11-CF (Climate & Fish predation). Correlations are calculated for 1950-2012 for the Northern and Southern Benguela masks where fish predation is applied, as shown in Figure 5.3. Warms colours indicate positive correlation and cold colours indicate negative 206

correlation. Cross-hatched grid cells are where the correlation is not statistically significant (p values less than 0.05).

- Figure 5.8 The spatial correlation of macrozooplankton with (top) upwelling and (bottom) SST for the simulations (left) TOM11-CN (climate and no fish PP) and (right) TOM11-CF (climate and fish PP). Correlations are calculated for 1950-2012 for the Northern and Southern Benguela masks where fish predation is applied, as shown in Figure 3. Warm colours indicate positive correlation and cold colours indicate negative correlation. Cross-hatched grid cells are where the correlation is not statistically significant (p values less than 0.05). 207
- Figure 5.9 Annual average maps of (left) jellyfish and (right) macrozooplankton biomass ( $\mu\text{mol C L}^{-1}$ ) for TOM11-CF from 1975 – 1984, covering a period of rapid increase in macrozooplankton biomass in the Northern Benguela. Note that the zooplankton are mapped to different scales. 210

## LIST OF EQUATIONS

Equation 3.1	$\frac{\partial Z_j}{\partial t} = \sum_k g_{F_k}^{Z_j} \times F_k \times MGE \times Z_j$ $- \sum_{k=j+1}^3 g_{Z_j}^{Z_k} \times Z_k \times Z_j - R_{0^\circ}^{Z_j} \times d_{Z_j}^T \times Z_j$ $- m_{0^\circ}^{Z_j} \times c_{Z_j}^T \times \frac{Z_j}{K^{Z_j} + Z_j} \times \sum_i P_i$	103
Equation 3.2	$\mu^T = \mu_0 \times Q_{10}^{T/10}$	104
Equation 3.3	$\mu^T = \mu_{max} \times \exp \left[ \frac{-(T - T_{opt})^2}{dT^2} \right]$	104
Equation 3.4	$g^T = \frac{u^T}{GGE}$	104
Equation 3.5	$GLM = \log_{10} RR = a + b \log_{10} BM + c T$	108
Equation 3.6	$cost\ function = \sum \left( \frac{\mu^T - \mu_{obs}^T}{\mu_{obs}^T} \right)^2$	108
Equation 4.1	$V_{GOC} = k_{GOC} \times \max(\rho_{GOC} - \rho_{seawater}, \rho_{min})^{S_{GOC}}$	145
Equation 4.2	$\frac{\partial DOC}{\partial t} = \sum \left[ (1 - \sigma)(1 - \zeta \right.$ $\left. - MGE) \sum_k g_{F_k}^{JEL} \times JEL \times F_k \right]$	145
Equation 4.3	$\frac{\partial POC}{\partial t} = - \sum [g_{POC}^{JEL} \times JEL \times POC]$	145
Equation 4.4	$\frac{\partial GOC}{\partial t} = \sum \zeta \sum_k [g_{F_k}^{JEL} \times JEL \times F_k]$ $+ \sum [m_{0^\circ}^{JEL} \times T \times JEL]$	146
Equation 4.5	$ef = \frac{E_P}{P_P}$	147

Equation 5.1	<i>zooplankton mortality</i>	189
	$= m_{0^{\circ}}^{Z_j} \times c_{Z_j}^T \times \frac{Z_j}{K^{Z_j} + Z_j} \times \sum_i P_i$	
Equation 5.2	$P_F^{NB} = \frac{B_F^{NB}}{B_F^{BCS}}$	190
Equation 5.3	$P_F^{SB} = \frac{B_F^{SB}}{B_F^{BCS}}$	191
Equation 5.4	$fish\ PP = P_F^{NB,SB} \times \sum_i P_i$	192

## LIST OF APPENDICES

Appendices		233
	Table A1. Taxonomic information for gelatinous zooplankton from MAREDAT. The last filled column for each row is the taxonomic level given in MAREDAT. Provided in parenthesis are alternative or historic names for the same organism.	235



## ACKNOWLEDGEMENTS

I would like to thank Professor Corinne Le Quéré for accepting me onto this PhD project and her unfailing support and encouragement at every stage. I would like to thank Dr Erik Buitenhuis for his support, particularly with the development and running of the PlankTOM model. I would also like to thank Dr Sophie Pitois and the fisheries scientists at CEFAS for providing me with the invaluable opportunity to experience the reality of sampling jellyfish onboard a scientific fisheries cruise, and to contribute to a database of jellyfish observations. I would like to thank Dr Mark Gibbons, Dr Lynne Shannon, Dr Marcello Vichi and everyone else at the University of Cape Town for their vital support in helping me to grasp the complexity of the Benguela Current and its history.

And finally, I would like to thank my parents for their everlasting support, Mikey for reminding me that a world exists outside of work and Willow for keeping me sane.



*The Sea, once it casts its spell, holds one in its net  
of wonder forever.*

Jaques Cousteau





# CHAPTER 1. INTRODUCTION



## 1.1 Opening Statement

There is a widespread perception that gelatinous zooplankton (GZ; defined below) populations are increasing globally due to climate change. There is, however, a severe paucity of data within the scientific literature backing up this claim, which has come to be known as the ‘jellyfish paradigm’ (Condon et al., 2012). There are several factors other than climate change thought to influence GZ abundance including overfishing, eutrophication and climate variability (Pitt et al., 2018). GZ blooms are responsible for economic losses to coastal industries and play a significant role within ecosystems. It is therefore important to improve our understanding of the relative impacts of these different factors on GZ occurrence and potential additive effects, to guide future management and mitigation. Studies of past climate variability have shown a link between warmer temperatures and increased GZ abundance, but we lack both the long-term observations and adequate models to infer the role of climate change (Condon et al., 2012, Condon et al., 2014, Lucas et al., 2014, Pitt et al., 2014).

## 1.2 What are Gelatinous Zooplankton?

The term GZ encompasses a wide range of organisms with the shared characteristics of gelatinous bodies, slow moving, a tendency to aggregate in large numbers (form blooms) and a (mostly) pelagic life feeding on plankton, which colloquially are often called jellyfish (Lucas and Dawson, 2014). The gelatinous bodies of GZ have an average wet weight water content of 96% and an average carbon content of 0.5% (Lucas et al., 2011), in comparison to other marine animals which have an average water content of 75% and carbon content of 8-10% (Vinogradov, 1953). GZ can be separated into three main groups; Cnidaria, often termed ‘true-jellyfish’, including the classes Scyphozoa, Cubozoa and Hydrozoa; Ctenophora, often termed ‘comb-jellies’, including the classes Tentaculata and Nuda; and the subphylum Tunicata, often termed ‘salps and doliolids’, including the classes Thaliacea, Ascidiacea and Appendicularia (Table 1, Fig. 1.1; Lucas and Dawson, 2014, Mills, 1995). For *Cnidaria*, the body form is characterised by a bell-shaped body (medusae) used for swimming by muscular pulsing contractions, below the medusae are tentacles and oral arms which contain stinging cells (nematocysts; Fig. 1.2). Cnidaria are largely non-visual generalist predators, feeding on zooplankton. For Ctenophores, the body-form is

**Table 1.1** Taxonomic classification of groups of gelatinous zooplankton (see Appendices 1).

Phylum	Subphylum	Class	Subclass	Order
Chordata	Tunicata	Thaliacea		
		Ascidiacea		
		Appendicularia		
Cnidaria	Medusozoa	Cubozoa		
		Hydrozoa		Limnomedusae
			Trachylina	Trachymedusae
			Hydroidolina	Anthoathecata
			Leptothecata	
			Siphonophorae	
Ctenophora		Scyphozoa		
		Nuda		
		Tentaculata		

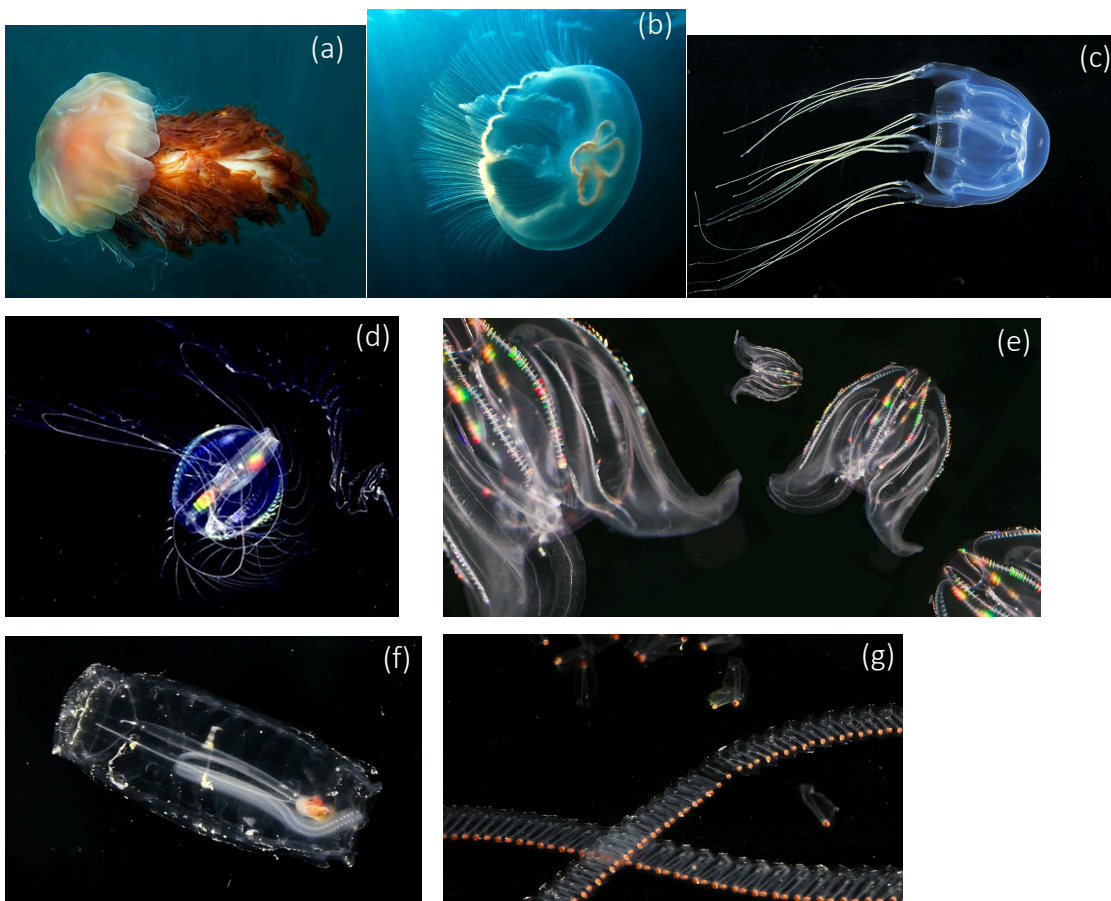


**Figure 1.1** Photos of gelatinous zooplankton. (a) Lions mane jellyfish (Cnidaria; Smithsonian, 2017), (b) Moon jellyfish (Cnidaria; New England Aquarium, 2015), (c) Box jellyfish (Cnidaria; Generate Change, 2019), (d) Sea gooseberries (Ctenophora; Microscopy UK, 2019), (e) Sea walnut (Ctenophora; NIOZ, 2015), (f) Salp oozoid (Tunicata; Plankton Chronicles, 2016), (g) Salp chain (Tunicata; Plankton Chronicles, 2016).



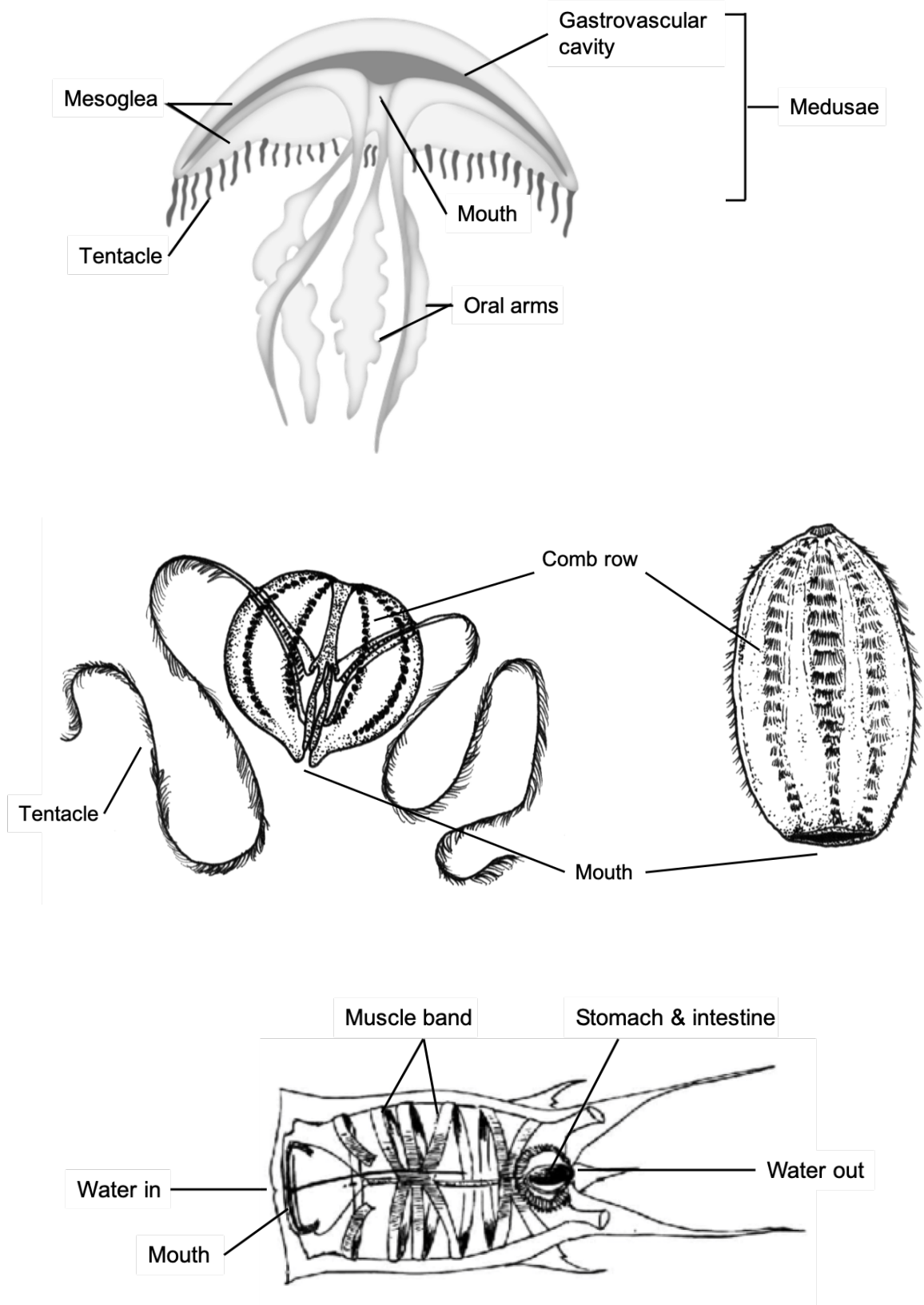


**Figure 1.2** Simplified anatomy of gelatinous zooplankton for typical Cnidaria (top; Exploring Our Fluid Earth, 2019), Ctenophora (middle; Canal Cederj, 2011) and Tunicata (bottom; Pascual, 2016).

characterised by eight rows of cilia evenly distributed around a normally egg-shaped body; Ctenophores beat the cilia to propel them through the water and occur with and without tentacles (Fig. 1.2). They are non-visual generalist predators feeding on zooplankton. (Richardson et al., 2009). For Tunicata, the body-form is cylindrical and species are either solitary or colonial, forming long chains (Fig. 1.2). They are filter feeders of particles between 1 – 10  $\mu\text{m}$ , ranging from small bacteria to large phytoplankton (Lucas and Dawson, 2014). In this thesis GZ will refer to all three groups outlined above (Cnidaria, Ctenophora and Tunicata), individual groups or species will be referred to where appropriate.

### 1.2.1 Life Cycle

GZ have many life cycle strategies, but they can be categorised into two groups; holoplanktonic, remaining in the plankton throughout their life cycle, and meroplanktonic, spending some of their life cycle in the plankton (Lucas and Dawson, 2014). Most Cnidaria are meroplanktonic species which spawn as adults (medusa) in the water column, the eggs are fertilized and develop into planula larvae, which settle onto hard substrate and develop into a polyp (scyphistomae). Polyps are often transparent and barely a couple of millimetres in length. The polyps of multiple species have been found to form hard protective casings known as cysts. The polyp can stay at this stage for several months over winter, until an environmental trigger causes the polyp to undergo asexual reproduction (strobilation) and bud multiple juveniles (ephyrae). Under favourable environmental conditions the ephyrae can rapidly grow into adult medusa, reach sexual maturity, and spawn. Strobilation and budding of ephyrae can occur multiple times during a season (Fig. 1.3). Ctenophora and some Cnidaria are holoplanktonic, skipping the benthic stage, with the planula larvae developing straight into ephyrae within the plankton (Fig. 1.3). In some species a small proportion of the adult population overwinters and spawns the following spring (Costello et al., 2006, Lucas et al., 2012, Lucas and Dawson, 2014). Tunicata are also holoplanktonic but reproduce in markedly different ways to Ctenophora and Cnidaria. Generally, the Tunicata life cycle begins with a solitary stage (oozoids) which asexually reproduce to form multiple chains (blastozooids), the blastozooids are hermaphrodites which internally fertilise, and then release an embryo which develops into an oozoid (Fig. 1.3; Loeb and Santora, 2012). These life cycle strategies,

particularly meroplanktonic species, allow GZ to survive when conditions are poor, and rapidly reproduce and grow when conditions improve (Brotz et al., 2012). The budding of multiple ephyrae from an individual polyp, essentially invisible to humans, and the rapid growth of ephyrae into adult medusa is the reason for apparent large and sudden aggregations of GZ, known as blooms. Blooms are generally short lived, lasting a few weeks, during which time spawning occurs. Intertidal stranding and death of GZ often follow coastal blooms (Lucas et al., 2012, Lucas and Dawson, 2014). Blooms can be categorised into two types; ‘true’ and ‘apparent’. A ‘true’ bloom is the increase in biomass in a region due to reproduction and growth, whilst an ‘apparent’ bloom is the increase in biomass in a region due to hydrodynamics and wind amassing individuals into one area (Graham et al., 2001, Lucas and Dawson, 2014).

### **1.2.2 The Benefits of Blooming**

GZ blooms are a natural ephemeral feature of marine ecosystems, with fossil evidence of large bloom formations dating back to the Cambrian Period (Graham et al., 2001, Young and Hagadorn, 2010). Bloom-forming gelatinous taxa have evolved independently multiple times, indicating its success as an adaptive strategy in the marine environment, which is characterized by patchy and ephemeral favourable conditions (Hamner and Dawson, 2009). The elements of a bloom-forming life cycle that take advantage of ephemeral conditions include rapid growth and development, early reproduction, high fecundity and a condensed period of sexual reproduction (Lucas et al., 2012, Lucas and Dawson, 2014). Another attribute of GZ that enables them to survive and thrive in harsh environments is high plasticity in feeding and physiology. This includes a generalized diet, continuous touch-feeding and the ability to shrink body size when prey abundance is low (Richardson et al., 2009). The same strategies that make GZ good survivors and adaptors also make them successful invaders. It is often the rapid proliferation of invasive GZ species that cause the most interference to, and attention from, humans (Richardson et al., 2009, Bayha and Graham, 2014). For example the Ctenophora, *Mnemiopsis leidyi*, invaded the Black Sea in the 1980s and has since spread into the Mediterranean (Boero, 2013) and into the North and Black Seas (Costello et al., 2012) and the Scyphozoa, *Phylolrhiza punctata*, successfully invaded the Gulf of Mexico (Graham and Bayha, 2008).

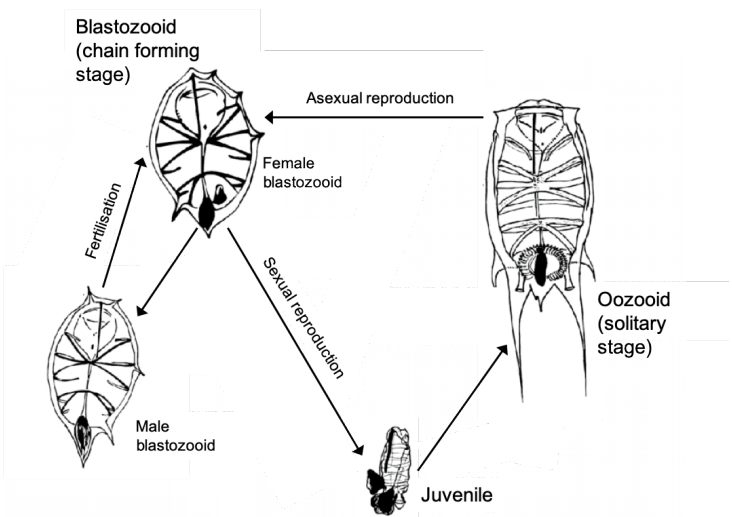
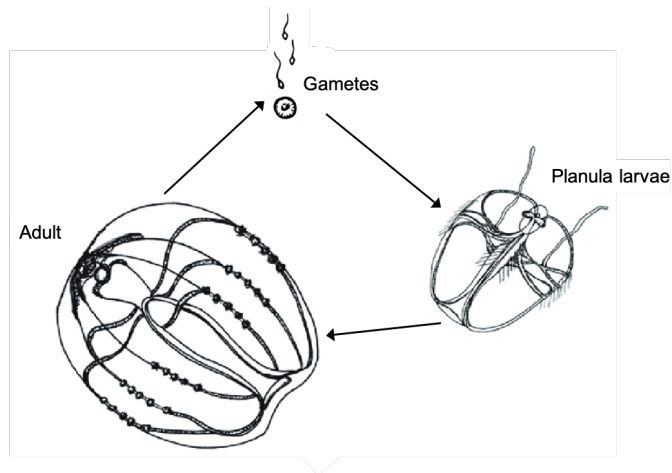
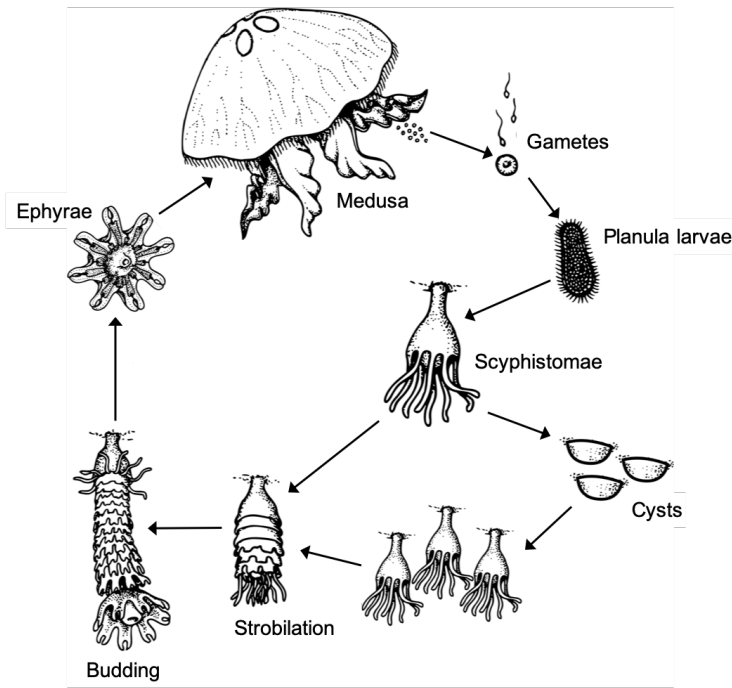


**Figure 1.3** Life cycles of gelatinous zooplankton for the moon jellyfish, *Aurelia aurita*, as a typical Cnidaria (top; adapted from BIODIDAC, 2019), the comb jelly, *Mnemiopsis leidyi*, as a typical Ctenophora (middle; adapted from Sea Gooseberries, 2019) and the salp, *Thalia democratia*, as a typical Tunicata (bottom; adapted from Pascual, 2016).

### 1.3 Climate Change & Gelatinous Zooplankton - the Jellyfish Paradigm

Rising atmospheric carbon dioxide concentration and climate change are driving changes in the marine environment, primarily increasing temperature and decreasing pH. This trend is set to continue into the coming decades (Rhein, 2013). Climate change will have significant impacts on marine ecosystems, many of which are already occurring such as increasing temperature triggering coral bleaching (Hoegh-Guldberg et al., 2018). Alterations to ocean temperature and acidity can directly impact species ranges, seasonal abundance and cause local extinctions, leading to indirect effects from climate change transferring throughout ecosystems via trophic cascades (Doney et al., 2012). GZ may be both directly and indirectly affected by climate change. Rising temperatures are likely to directly impact GZ through increasing growth and reproduction rates and through increasing species ranges (Brotz et al., 2012, Lucas and Dawson, 2014, Condon et al., 2014). In Australia some species of box jellyfish (Cubozoa) are predicted to increase their range north along the coast as sea surface temperatures increase (Richardson et al., 2009, Klein et al., 2014). Indirect impacts on GZ from climate change are likely to come from ocean warming increasing stratification, resulting in reduced mixing of nutrients, eutrophication and hypoxia. These changes to the physical marine environment will trigger bottom-up cascades changing the structure of the plankton food web, and thus GZ prey. What impact this will have on GZ populations is currently unclear (Gibbons and Richardson, 2013, Lucas and Dawson, 2014). Many species of GZ are tolerant to hypoxic and eutrophic conditions, which may allow them to outcompete other organisms as areas experiencing hypoxic and eutrophic conditions increase in size and frequency (Richardson and Gibbons, 2008, Richardson et al., 2009).

There is significant debate within the literature around the question of whether GZ have already, or will increase in the future due to climate change (Brotz et al., 2012, Condon et al., 2012, Condon et al., 2013, Gibbons and Richardson, 2013). The debate largely stems from a lack of long-term observational data, unknown baselines, and the difficulty in determining trends in GZ due to the large fluctuations in abundance over even small space and time scales, from apparent absence to large blooms containing millions of individuals over a few weeks. This perceived global increase in GZ lacks a backing of rigorous scientific data, and is known as the jellyfish paradigm (Brotz et al.,

2012, Condon et al., 2013, Gibbons and Richardson, 2013). Poor citation practices within the GZ scientific literature have also contributed to the jellyfish paradigm (Sanz-Martín et al., 2016). A few papers, each of which found an increase in a GZ species in a region correlated with rising ocean temperatures, suggested that this may be representative of trends in other regions and may suggest a global increase, were repeatedly mis-cited as direct evidence of a global increase across most GZ species directly linked to climate change (Sanz-Martín et al., 2016).

Human issues with GZ have increased in recent decades (Purcell et al., 2007, Purcell, 2012, Richardson et al., 2009, Doyle et al., 2014). Increased use of the marine environment for industry and tourism has brought GZ into direct conflict with humans more frequently (see section 4.1). Where a coastal bloom may have gone unnoticed in the past, infrastructure such as an aquaculture farm or a power plant, results in a ‘nuisance bloom’ likely to be picked up on by the media as a newsworthy story (Purcell, 2012). This is contributing to a public perception of the jellyfish paradigm. The public and media perception of more frequent blooms is based on a short frame of reference and may indicate a perceived, rather than actual, increase in GZ abundance in some areas (Condon et al., 2012, Duarte et al., 2013). Often the high-profile blooms are from invasive species (Dong et al., 2010, Boero, 2013, Bagheri et al., 2014), further contributing to the negative public perception of increasing GZ abundance (Bayha and Graham, 2014).

The influence of temperature on GZ abundance is probably the most studied factor, with positive correlation found for the majority of species, especially in temperate environments (Lucas and Dawson, 2014). The upper temperature threshold for GZ is higher than is found in many other marine species (Purcell, 2012). It is widely suggested that this high-threshold will allow GZ to become more prolific and expand their ranges as global temperatures increase. The positive correlation between GZ abundance and temperature has been picked up by the media, contributing to the current paradigm where GZ are perceived to be increasing globally due to climate change (Condon et al., 2012). The indirect effects from climate change on GZ are less clear and the overall effect of climate change on GZ abundance cannot be determined from current observational data (Purcell, 2005, Richardson et al., 2009, Gibbons and Richardson, 2013). Climate indices have been positively correlated to GZ abundance

in several regions, but negative correlation in other regions has also been shown (see Section 1.8; Condon et al., 2013). Overfishing and global ocean sprawl have also been correlated to increases in GZ abundance (see Section 1.6). Attributing an increase in GZ abundance directly to climate change is difficult and complicated due to the lack of knowledge on GZ baseline and variations with climate indices, and the many interactions between climate, ecosystems and all the other stressors imposed on the marine environment by mankind (Condon et al., 2012).

#### **1.4 The Importance of Gelatinous Zooplankton**

In general, GZ are viewed as negative components of the marine environment as they conspicuously disrupt many coastal industries. However they also have many beneficial and essential roles, which are often overlooked (Doyle et al., 2014, Purcell et al., 2007). Both the positive and negative impacts of GZ are introduced below.

##### **1.4.1 Economic Benefit**

GZ can provide an economic benefit through the GZ fishing industry (Richardson et al., 2009, Doyle et al., 2014). Certain species of Cnidaria have been historically fished in Asia (Dong et al., 2010) and the practice has recently been taken up in the Americas and Europe (Doyle et al., 2014). Another key benefit from GZ is their contribution to biotechnology and medicine, for example GZ collagen is currently being tested for use in treating rheumatoid arthritis and rebuilding muscle, cartilage and bone. In biotechnology the green fluorescent protein was first isolated from the GZ, *Aequorea victoria*, and is widely used to tag proteins and track changes of cellular process in living cells (Doyle et al., 2014).

##### **1.4.2 Economic Cost**

GZ are predominantly known for their negative impacts on coastal industries. The tourism industry can suffer economic loss from beach closures due to blooms and stings giving an area a bad reputation. For example, proliferations of box jellyfish species in touristic areas such as Australia's north coast have resulted in hospitalisation and human fatalities (Richardson et al., 2009, Gershwin et al., 2014). Recent years

have seen the number of fatalities from stings by numerous species of GZ increase in China (Dong et al., 2010). Several industries use large quantities of seawater taken up through pipelines, most notably nuclear power stations and desalination plants. GZ blooms in the area of such plants can be sucked up and clog the filtration system to such an extent that the plant has to stop operations in order for the filter to be cleared, resulting in economic losses (Purcell et al., 2007, Richardson et al., 2009, Dong et al., 2010). There are many reported cases of GZ killing fish within aquaculture pens, e.g. by stinging their gills to such an extent that they suffocate (Purcell et al., 2007, Richardson et al., 2009). GZ blooms can impact fisheries directly, by bursting nets and contaminating catches (Dong et al., 2010, Quinones et al., 2013), and indirectly through predation on and competition with commercial species (Roux et al., 2013). There are a high number of cases of direct impacts on Japanese and Chinese fisheries (Richardson et al., 2009, Dong et al., 2010, Purcell, 2012). GZ have also been cited as a potential factor in dangerous algal blooms via cascading ecosystem effects (Pitt et al., 2007, West et al., 2009).

### **1.4.3 Ecosystem Services**

Traditionally GZ have been largely ignored in marine ecosystem studies, with blooming events seen as unnatural and a signifier of a degraded ecosystem (Boero et al., 2008, Hays et al., 2018). The high-water content, and thus low carbon and nutrient content of GZ bodies, has strongly influenced the view of them as trophic dead ends, i.e. that nothing would bother to eat them. However, the rapid and low-energy digestion required for the consumption of GZ may counterbalance their low nutrient content. This rapid digestion of GZ and lack of hard body parts (i.e. bones, scales or carapace) has likely contributed to the idea that they were not consumed, as there is poor evidence of them in the traditional visual stomach analysis of fish or scat analysis of sea birds and marine mammals. The recent advances in DNA analysis and cheaper high-throughput testing are dismantling this idea (Lamb et al., 2017, McInnes et al., 2017, Hays et al., 2018). GZ have been viewed as trophic dead-ends, but research has now shown that they make up some of the diets of 124 fish species and 34 other marine species (Pauly et al., 2009). Some of these are specialist feeders relying on GZ for the majority of their diet, including the iconic and endangered leatherback turtle, *Dermochelys coriacea*, and the ocean sunfish, *Mola mola* (Houghton et al., 2006a,



Houghton et al., 2006b). Other species, such as penguins, are not traditionally viewed as predators of GZ, but four species have now been shown to actively predate GZ (Hosia et al., 2017). The importance of GZ in the diet of the majority of these species is unknown, as is the top-down influence of predators on GZ abundance (Hays et al., 2018). There has been an underestimation of GZ importance in pelagic food webs (Boero et al., 2008) as well as in benthic food webs where GZ carcasses are rapidly scavenged (Sweetman et al., 2014). GZ are efficient feeders of the plankton, able to rapidly clear large volumes of water, thus influencing the plankton structure and potentially the food web through trophic cascades (Pitt et al., 2007, Pitt et al., 2009, West et al., 2009). GZ were described by Pauly et al. 2009) as “arguably the most important predators of the sea”. There is also increasing evidence that GZ can play a substantial role in marine biogeochemical cycles, due to their bloom-forming capabilities (Lebrato et al., 2012, Chelsky et al., 2015).

### **1.5 Biogeochemical Cycles & The Biological Carbon Pump**

Biogeochemical cycles are the continuous reuse and cycling of nutrients and carbon through the marine environment, with a small proportion exiting the cycles through sedimentation. The plankton community plays a vital role in biogeochemical cycles, providing the link between carbon (C), nitrogen (N) and phosphorous (P) in the water column and larger marine animals higher up the food web (Steinberg and Landry, 2017). For the biogeochemical cycle of carbon, sequestration occurs through the sinking of plankton faeces and carcasses as marine snow (Pitt et al., 2009, Lebrato et al., 2012, Chelsky et al., 2015). The biological carbon pump (BCP) is the name given to the section of the biogeochemical cycle which focuses on the carbon pathways that are mediated by marine ecosystems, including the return flow through ocean circulation (see Fig. 1.4 for detail; Sanders et al., 2014). GZ blooms provide a large and sudden input of carbon and nutrients into the environment due to their bloom and bust dynamics, playing an important role in the carbon and biogeochemical cycles through two routes; waste produced during their lives through repackaging of carbon into mucus and faeces; and their death and subsequent decomposition and consumption. The mass deposition events from the rapid sinking of GZ carcasses during and after blooms are termed ‘jelly-falls’ (Lebrato et al., 2012). A relatively small amount of research has been done thus far into such roles, but this has increased

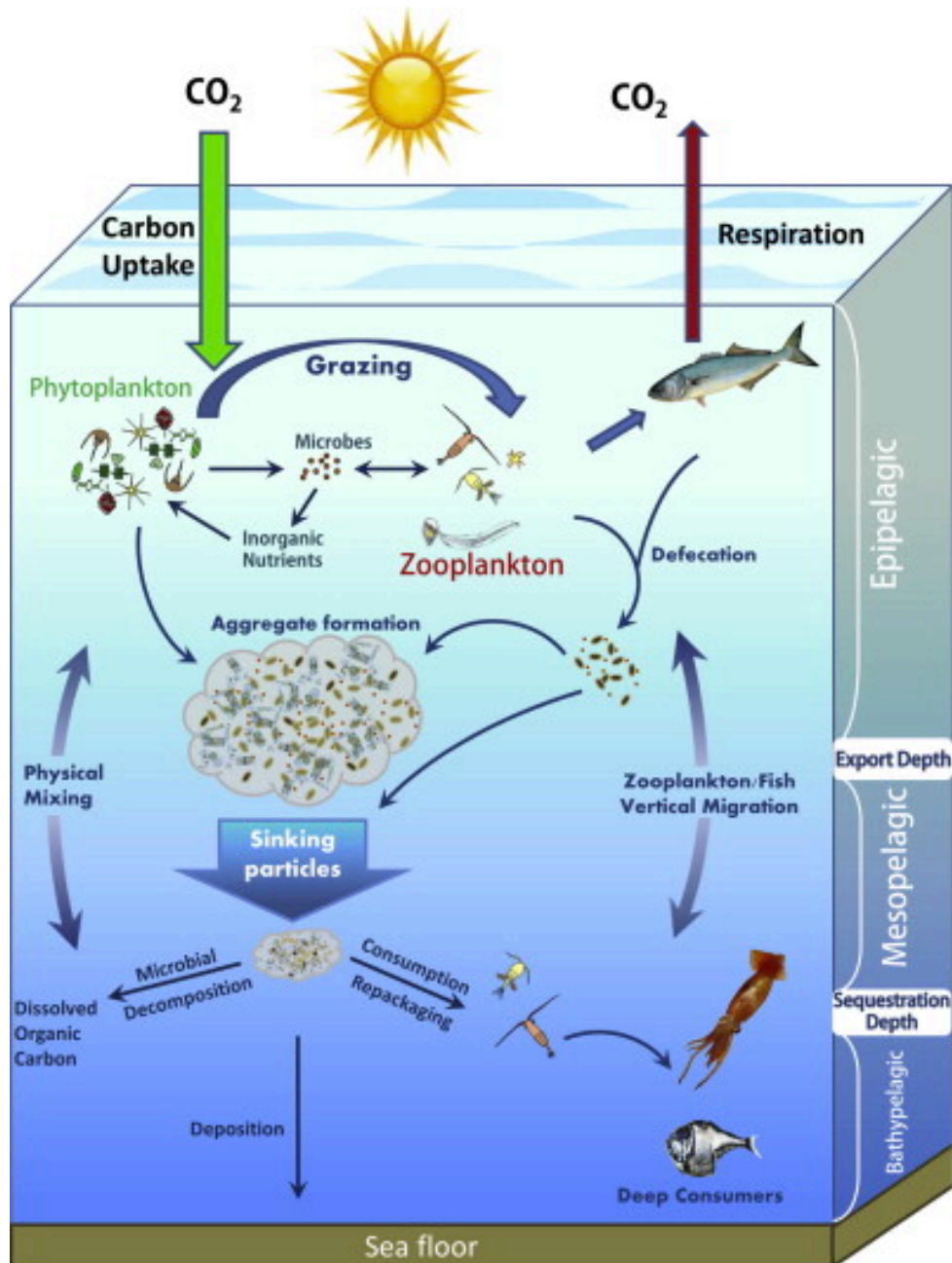


**Figure 1.4** The biological carbon pump. CO<sub>2</sub> from the atmosphere dissolves into the surface ocean. Phytoplankton convert the dissolved CO<sub>2</sub> into particulate organic carbon (POC) via photosynthesis in the euphotic layer of the epipelagic zone. Zooplankton graze on phytoplankton, converting the POC and other organic matter in phytoplankton into faecal pellets, carcasses and other POC aggregates (marine snow), which are exported into the mesopelagic and bathypelagic zones by sinking and by the vertical migration of some zooplankton and fish. In the mesopelagic zone the marine snow (sinking particles) is converted into dissolved organic carbon (DOC) through microbial remineralisation which can be moved throughout the water column via physical vertical mixing of water. The marine snow is also grazed and repackaged by zooplankton, which are in turn preyed upon by fish, squid and other deep ocean consumers, continuing the repackaging of POC and DOC in the mesopelagic zone. Below the sequestration depth carbon is deposited and stored for 100 years or more. Adapted from Turner (2015).

in recent years and this trend is likely to continue (Billett et al., 2006, Pitt et al., 2009, Lebrato et al., 2012, Chelsky et al., 2015, Stone and Steinberg, 2018). Climate change will alter the biogeochemical and carbon cycles and the role that zooplankton play in the cycles, including the role of GZ (Steinberg and Landry, 2017, McKinley et al., 2017, Chelsky et al., 2015).

### **1.5.1 Excretion**

Pitt et al. 2009) reviewed C, N and P in relation to Cnidaria and Ctenophora and found a handful of laboratory studies on faeces production. Temperature appears to have a significant influence on the rate of excretion (Pitt et al., 2009), suggesting potential implications with climate change. The sinking rate of salp (Tunicata) faecal pellets is considerably faster than euphausiids and significantly faster than copepods; faster pellet sinking rates result in less time for remineralisation, thus a greater proportion of C, N and P exiting the cycle through sedimentation (Doyle et al., 2014). A study in the Antarctic found a high proportion of the marine snow under a salp bloom to contain salp faeces. The focus of the study was on krill bloom effects on marine snow and sediment composition, which were found to be significant (Atkinson et al., 2012). It is a fair assumption that large salp blooms are likely to also have an impact on the local sediment (Doyle et al., 2014). Scyphozoa excretion during a bloom can double phytoplankton biomass, largely due to an increase in diatoms through the biological pump (West et al., 2009). A study on carbon flux found no difference in the total particulate organic carbon in treatments with and without *Mnemiopsis leidyi* (Ctenophora) and *Chrysaora chesapeakei* (Scyphozoa), but the presence of the GZ decreased the copepod faecal pellet carbon flux by 50% due to a reduction in copepod abundance through predation by the GZ (Stone and Steinberg, 2018). GZ may play an important role in the BCP through their structuring of the plankton community by trophic cascades.

### **1.5.2 Death**

The review by Pitt et al. 2009) also looked at Cnidaria and Ctenophora bloom decomposition after a jelly-fall. They find that the decomposition of a bloom will release C, which may support microbial production, and N and P, which may support

algal production. The oxygen demand from microbes and algae to decompose the GZ tissues could result in localized hypoxia (Pitt et al., 2009). Lebrato et al. 2012) summarises data on jelly-falls up to 2012 and finds evidence of the importance of the falls in transferring carbon and nutrients to shelf- and deep-sea habitats. The authors hypothesize that increasing GZ blooms at the surface will increase particulate organic matter transport to the bottom and may provide a “natural-compensation” for predicted reduction in particulate organic matter. GZ are also a potential vector of carbon export (Lebrato et al., 2013b), particularly because of the fast sinking rate of gelatinous-biomass compared to other plankton exports due to their relatively large structures (Lebrato et al., 2013a). There is evidence that the carbon from a single jelly-fall provides four times the annual carbon input to the seafloor (Lebrato and Jones, 2009), whilst another study found that a jelly-fall exceeded the annual downward flux of carbon by more than an order of magnitude, with a standing stock of up to 78g Cm<sup>2</sup> (Billett et al., 2006). GZ are likely to be an important carbon sink in the global carbon cycle, but are currently ignored in global studies (Doyle et al., 2014, Qu et al., 2014, Lebrato et al., 2012, Lebrato et al., 2013a).

## **1.6 Drivers of GZ Blooms**

There are many drivers of GZ blooms suggested within the literature, including climate change, temperature, nutrients, fishing, currents, hard substrate, zooplankton, wind mixing, precipitation and climate indices (Purcell et al., 2007, Hamner and Dawson, 2009). Many of the drivers are interconnected, with the increasing strength of one contributing to another i.e. eutrophication from nutrient run off may be enhanced by stratification from higher temperatures. Multiple drivers are often occurring simultaneously in the marine environment, particularly in coastal areas where human impacts are more direct (Lucas and Dawson, 2014).

### **1.6.1 Temperature**

GZ populations follow seasonal cycles, particularly in temperate environments, with the greatest abundance occurring during the summer months. Many studies have found positive correlation between GZ abundance and temperature, with the most significant correlations in temperate environments. Temperature had been argued as the main

cause of blooms by several reviews (Purcell, 2012, Qu et al., 2014, Xu et al., 2013). This positive correlation is supported by laboratory studies investigating temperature effects on many stages of GZ life cycles. For Cnidaria, the number of ephyrae produced per polyp, the rate of polyp development, the frequency of strobilation cycles and the growth of ephyrae into medusa have all been positively correlated with temperature (Lucas et al., 2012, Purcell et al., 2012, Robinson and Graham, 2014). A review by Purcell et al. (2007) found that 18 of 24 temperate GZ species abundances increased as waters warmed. Unusually high temperatures have been shown to decrease production (see Section 1.7), but the temperature tolerance range of many GZ species is greater than that of other marine species (Purcell, 2012, Pitt et al., 2014). This may allow GZ to expand their range and bloom-forming season as climate change progresses (Gershwin, 2007, Gershwin and Zeidler, 2008, Xu et al., 2013).

### 1.6.2 Food

Cnidaria and Ctenophora feed on a wide range of zooplankton species and ichthyoplankton (fish eggs and larvae). Smaller species and juveniles generally feed on micro- and some phytoplankton. Tunicata feed on phytoplankton by drawing water through their siphon and filtering out particles. The large body size to carbon content ratio of GZ creates a low maintenance, large feeding structure, which combined with continuous (day and night) touch-feeding allows for efficient clearance rates of the plankton (Lucas and Dawson, 2014, Acuña et al., 2011). This feeding strategy also allows GZ to outcompete other predators of zooplankton such as planktivorous fish, which actively hunt prey by sight, restricting feeding time to daylight hours (Acuña et al., 2011). Prey concentration has been positively correlated with rates of budding from polyps and the growth of ephyrae into medusa (Han and Uye, 2010, Lucas and Dawson, 2014). The relationship between zooplankton and GZ abundance can also be seen in the seasonal cycle where GZ blooms closely follow plankton blooms, i.e. spring, summer and autumn blooms (West et al., 2009, Garcia-Comas et al., 2011, Pitt et al., 2014). Chiaverano et al. (2013) demonstrated a strong positive relationship of the box jellyfish *Alatina moseri* (Cubozoa) to zooplankton biomass. A stage-structured matrix model of the moon jellyfish *Aurelia aurita* (Scyphozoa) found prey availability to be an important ecological driver of blooms, by moving the population structure from the polyp stage to the medusae stage (Goldstein and Steiner, 2017). The

same study also found that introducing projected climate change scenarios to the matrix model only caused small changes in population.

### **1.6.3 Fishing**

The collapse of fisheries in many locations around the world has been correlated to an increase in GZ abundance (Purcell, 2012, Robinson et al., 2014). It is argued that human interference, namely overfishing and pollution, worked together to cause the fisheries collapse, creating a space in the ecosystem which GZ rapidly took advantage of, rather than the collapse of a fishery being caused by a rise in GZ abundance (Purcell et al., 2007, Robinson et al., 2014). Overfishing is thought to increase GZ populations in two main ways; firstly by reducing competition for prey, as many species of planktivorous fish are commercially exploited (Robinson et al., 2014) and secondly by reducing predation pressure, as GZ are eaten by many commercial species of fish (Lamb et al., 2017). Overfishing may change the food web to such an extent that an ecosystem shift occurs, where the structure and function of the ecosystem shifts from one stable state i.e. planktivorous fish dominated, to another contrasting state i.e. GZ dominated (Roux et al., 2013). The ecosystem shift, from fish dominated to GZ dominated, that can be brought about by overfishing is thought to be entrenched due to a high consumption of ichthyoplankton by GZ, and strong competition for food with juvenile and/or adult fish, depending on the species. High consumption of ichthyoplankton reduces the recruitment success of the remaining fish population. The feeding strategy of GZ as continuous passive touch-feeders is likely to outcompete fish which are selective, active hunters restricted to daylight (Acuña et al., 2011). These factors may make the recovery of fisheries to pre-collapse levels very difficult (Roux et al., 2013, Robinson et al., 2014).

### **1.6.4 Nutrients & Eutrophication**

The number and size of areas of coastal waters experiencing eutrophication is increasing globally (Doney et al., 2012, Purcell, 2012, Rhein, 2013). This is mostly due to increased nutrient run-off from land and riverine inputs, largely from the increased use of fertilisers. Global warming can enhance eutrophication and may lead to hypoxia, as warmer waters hold less oxygen and are more stratified, reducing

mixing with deeper cooler oxygen rich waters (Doney et al., 2012). Eutrophication and hypoxia do not appear to directly cause GZ blooms, rather GZ are more tolerant of low oxygen conditions than many other marine species, as they do not have complex breathing structures or a high oxygen demand (Purcell et al., 2001). Also, Cnidaria and Ctenophora are able to switch their feeding from zooplankton, which are generally not tolerant to hypoxia, to flagellates, which proliferate in hypoxic conditions. These two features can allow GZ to survive and dominate in hypoxic regions where many other species cannot (Purcell et al., 2001, 2007). Some studies have correlated higher eutrophication and increased GZ abundance (Xu et al., 2013).

### **1.6.5 Hydrology**

Localized hydrology can have a strong influence on the formation and location of GZ blooms (Graham et al., 2001). A strong current in the Mediterranean had a clustering effect on smaller blooms, creating large formations of ‘apparent’ blooms (Benedetti-Cecchi et al., 2015). GZ are likely to take advantage of both stratification and mixing. In stratified environments GZ may outcompete fish and other predators due to their unselective feeding, higher tolerance of extreme physical conditions (see above). In mixed environments there is usually a high abundance of plankton due to increased nutrients, which may lead to higher GZ abundance from increased food availability (Graham et al., 2001).

### **1.6.6 Others**

Other physical forcings have been suggested to influence the formation of GZ blooms including acidification, precipitation and salinity, but with tenuous and limited evidence (Graham et al., 2001, Pitt et al., 2018). GZ generally lack calcified parts that could be negatively affected by acidification, but it has been suggested that they may benefit from reduced competition with marine organisms that are negatively affected by acidification (Attrill et al., 2007). The low selectivity of prey by GZ may allow them to avoid a reduction in food due to the changing structure of the plankton community, although evidence of this is currently minimal (Richardson and Gibbons, 2008). Climate change is likely to shift the ‘interaction web’ of the plankton

community (Francis et al., 2012) which may favour GZ over other planktivores due to their unselective feeding (Roux et al., 2013, Acuña et al., 2011).

These factors are all, either directly or indirectly, influenced by human activities. Anthropogenic climate change affects temperature, salinity, pH, currents, wind-mixing and precipitation. Global ocean sprawl including fishing, hard substrate additions and species translocation, as well as nutrient enrichment from fertiliser runoff, are likely to act synergistically to benefit GZ (Duarte et al., 2013). As discussed above, much of the evidence for the influence of anthropogenic stressors on GZ is correlative or based on conceptual models of how stressors may influence blooms rather than direct evidence of causation (Pitt et al., 2018).

## **1.7 Causes of Busts**

Most research on GZ has focused on the causes of blooms, with very little done on why the blooms collapse. Predicting how long a bloom may persist is important for management of industry and understanding impacts on the local ecosystem, as reduced GZ abundance will release predation and competition pressure on zooplankton. But, GZ also act as shelter to many species of juvenile fish and invertebrates (Condon et al., 2014, Pitt et al., 2014). The length of a bloom will also impact the biogeochemical cycling of nutrients and carbon (Lucas et al., 2011, Pitt et al., 2009). Pitt et al. 2014) identify the major drivers of bloom collapse from the literature, although note “rarely was the cause of the decline in the population reliably identified; however, authors frequently speculated about the cause of mortality”. The major drivers of GZ population collapse (bust) are outlined below.

### **1.7.1 Food**

Food limitation is regularly cited as a major cause of bust (Pitt et al., 2014). GZ are highly efficient consumers of plankton, as previously mentioned. Once the rate of predation by medusa exceeds secondary production of zooplankton, medusa growth can be inhibited and may shrink their body size to compensate for food limitation (Purcell and Decker, 2005). Goldstein & Steiner (2017) note that in their experiments on *A. aurita* medusa all individuals in the ‘low food treatment’ had died after 4



months, whilst all individuals in the ‘high food treatment’ were alive after the same time period.

### **1.7.2 Parasites**

Many parasites are known to infest GZ (including hyperiid amphipods, digenean trematodes and parasitic anemones), which are also parasites to many other marine species (Pitt et al., 2014). Rates of infestation within blooms are likely to be high, as abundance of parasites is positively correlated to the density of hosts (Arneberg et al., 1998). GZ parasites can damage body parts, including feeding and swimming apparatus. Population crashes due to parasite infestation in marine species such as fish and krill are well documented; it is likely a similar pattern widely occurs in GZ blooms (Pitt et al., 2014).

### **1.7.3 Disease**

Disease is regularly suggested as a potential cause of bust, but very few studies have investigated this. Mills (1993) found bacterial infection on 80% of a bloom population near the end of the season. GZ appear able to recover from bacterial infection if there is sufficient food available, likely making them vulnerable to infections when food becomes limited after a sustained bloom (Mills, 1993). Pathogens other than bacteria (e.g. fungi and viruses) are likely to infect and affect blooms but no studies exist (Pitt et al., 2014).

### **1.7.4 Predation**

Traditionally GZ have been seen as trophic dead ends, with the exception of specialised predation by a few iconic species (i.e. leatherback turtles and ocean sunfish). Recent studies indicate that a wide range of fish and other marine species predate GZ, including other GZ, however the levels of consumption and the impact on bloom populations are still unknown (Arai, 2005, Pauly et al., 2009), but are beginning to be quantified (Lamb et al., 2017, Hays et al., 2018). In the Irish Sea genetic analysis of fish gut samples found Scyphozoa DNA in 20.3% of herring sampled, 9.5% of dragonet, 7.7% of whiting and 7.4% of lesser-spotted dogfish, as well as in grey

gurnards, poor cod, squid, dover sole and spat (Lamb et al., 2017). The authors of this study suggest that these common fish species preying on GZ, even at low levels, could exert a greater predation pressure on GZ populations in the Irish Sea than the rare obligate GZ predators such as the ocean sunfish. A study in the Southern Ocean documented almost 200 cases of targeted predation on GZ by four species of penguin. Predation occurred at all of the locations in the study (Thiebot et al., 2017). The authors note that GZ may be a ubiquitous but underrepresented trophic link in the Southern Ocean. The impact on bloom populations of targeted predation on GZ by a wide range of marine species is currently unknown and can only be speculated on, specifically whether the level of predation on high density blooms will have an impact on overall GZ abundance.

### **1.7.5 Senescence Post-Spawning**

Senescence post-spawning has been observed in GZ populations several times (Pitt et al., 2014). Although it seems more likely that death after spawning events can be attributed to starvation, through loss of feeding tentacles, or the funnelling of nutrients to the growth of gonads, and through increased parasitism, than to the spawning event itself (Pitt et al., 2014).

### **1.7.6 Extreme Temperature**

Blooms are generally observed to decline into the autumn and winter as sea surface temperature (SST) decreases, but this is likely due to temperature interacting with other parts of the ecosystem such as reducing zooplankton abundance, making the water temperature not the driving factor behind such seasonal declines (Pitt et al., 2014). Extreme water temperatures have been shown to cause bloom mortality, although in limited cases. Only in Chesapeake Bay has cold temperature been robustly attributed to GZ death, of the Scyphozoan, *Chrysaora quinquecirrha* (Sexton et al., 2010). In an enclosed marine lake sustained high water temperature and abnormal stratification was attributed to the disappearance of 1.5 million *Mastigias* medusa (Martin et al., 2006, Dawson et al., 2001). However, this high temperature did not affect the *Aurelia* medusa population in the same lake. A key difference between these Scyphozoa species is that *Mastigias* has a photo-symbiotic relationship with

zooxanthellae, whilst *Aurelia* does not. The authors note that the high temperature may have disrupted this symbiosis, contributing to the *Mastigias* decline (Dawson et al., 2001).

### **1.7.7 Intertidal Stranding**

Large stranding events are common and highly conspicuous along shorelines. It is likely that such events are a result of other factors mentioned above reducing the swimming ability of GZ so that they are less able to orientate in relation to tides, winds and currents to avoid stranding (Pitt et al., 2014). Doyle et al. 2007) found that stranded GZ along the Irish coast were already lacking tentacles and oral arms. Stranding events in Hawaii are closely synchronised to the full moon creating strong tides (Chiaverano et al., 2013).

It is likely that busts are due to a combination of several factors acting synergistically, particularly limited food availability increasing susceptibility to other factors. Secondary impacts from parasitic damage to the body include reduced feeding capability and reduced swimming ability to orientate away from shore.

## **1.8 Trends in Gelatinous Zooplankton Populations**

As mentioned previously, it can be difficult to separate the large fluctuations in GZ abundance intra- and inter-annually from any longer-term trends that may indicate a growing population caused by climate change. This problem is compounded by the paucity in long-term regional data sets. Henson et al. 2010) suggests that time series of at least 40 years are necessary to separate inter-annual variability and climate indices from trends in plankton due to climate change. Unfortunately, such long, continuous and quantitative records of GZ are rare (Purcell, 2012), making it difficult to attribute GZ trends to climate change. The large variability in GZ populations between years also increases the difficulty of interpreting the data, and separate studies of the same area can give conflicting results. Key studies investigating trends in GZ populations are given below. For a clear summary of the evidence, papers are grouped by region.

### **1.8.1 Northeast Atlantic**

The following series of papers demonstrate both the complexity of the North Sea and the Northeast Atlantic, their relation to the North Atlantic Oscillation (NAO) and the difficulties and disagreements in analysing GZ data.

The North Sea is a complex region, influenced by the NAO, with distinct sub-regions. Lynam et al. (2004, 2005) use by-catch data from pelagic fishing surveys covering a 15 year period during 1970s – ‘80s. They report catches of medusa (various Cnidaria species) ranging in diameter from 1-47cm, and use abundance, as the number of medusa per trawl, for the analysis. The studies find a negative correlation between the NAO and medusa abundance, except in a region north of Scotland where the trend is reversed (Lynam et al., 2004, Lynam et al., 2005). Attrill et al. 2007) use data from the Continuous Plankton Recorder (CPR), covering a 43-year period from 1958. The CPR is too small to capture medusa; instead the presence or absence of tissue or nematocysts (stinging cells) is used to infer the presence/absence of medusa, which is used as percentage frequency of occurrence in the CPR. Attrill et al. 2007) find a positive correlation between the NAO and medusa occurrence, and point out the direct contradiction with Lynam et al. (2004, 2005). Attrill et al. 2007) argue that the contradiction is due to the shorter time series, and removal of a high outlying data point for 1983 by Lynam et al., to strengthen the negative correlation. However, Attrill et al. 2007) also use the removal of one outlier for 1979 to strengthen their positive correlation. Attrill et al. 2007) concludes that as the NAO moves into a stronger positive phase with global warming, the frequency of medusa outbreaks will increase. Haddock 2008) queries the strength of Attrill et al.’s analysis, on the apparent selective removal of one outlier and not another, and from this that the conclusions are ‘overstated’. Haddock 2008) recommends greater conservancy in drawing conclusions about climate change trends, in particular for press releases, noting Attrill et al.’s press statement “... all climate projections expect the North Sea to become warmer, so jellyfish will become more and more common in our waters” (Sample, 2007).

Gibbons and Richardson 2009) also used CPR data to investigate Cnidaria medusa occurrence, but they argue that the CPR data includes records of Ctenophora tissue, where the previous CPR studies assume only Cnidaria are recorded. The Gibbons and Richardson study covers a larger area of the North Atlantic, comparing shelf sea and

oceanic populations. The data covers 60 years, from 1946 – 2005. They found clear multi-decadal cycles for both shelf sea and oceanic populations, with the last decade on an upward trend. It is noted however that the current level is lower than previous peaks since 1946. The oceanic populations were found to be related to zooplankton abundance and temperature, but not to the NAO or chlorophyll, whilst there was no correlation found between the shelf sea populations and any environmental variables tested (Gibbons and Richardson, 2009). These conclusions again differ from those drawn by Atrill et al. 2007) and Lynam et al. (2004, 2005). Another analysis of the CPR data (assuming only Cnidaria records) from 1958 – 2007 finds an increase in the North Sea in medusa since the early 1980s ‘coincident’ with a change from a cold to warm hydroclimatic regime (Licandro et al., 2010). Over the Northeast Atlantic they also find increases in frequency since 2002, especially in winter, where medusa appear earlier in the year and persist for longer.

A long-term study (50 years) on four Scyphomedusae species in the western Dutch Wadden Sea found no relation between patterns of mean abundance and climate change (measured as increasing SST) in the area. But all the species occurred earlier in the year in recent decades with warming SST (Van Walraven et al., 2015).

### **1.8.2 Mediterranean**

A study looking at a rare long-term record in the Western Mediterranean (180 years, from 1785 – 1965, visual presence/absence of *Pelagia noctiluca*), found ‘outbursts’ occurring periodically every 12 years or so. Climatic variables, primarily temperature, precipitation and atmospheric pressure were found to predict the presence of *P. noctiluca* (Goy et al., 1989). Kogovšek et al. 2010) collated presence/absence data from a variety of published sources for five Scyphozoa species in the Northern Adriatic (Northeast Mediterranean) covering a period of 219 years, from 1790-2009. They found three periods of greatly increased presence for all species, with two occurring since the 1980’s. A wavelet analysis showed periodicity of around 3 and 8 - 12 years for all species, and also that this periodicity has shortened in recent decades whilst recurrence of blooms has increased (Kogovsek et al., 2010). Within the same study the wavelet analysis technique was also applied to the data from Goy et al. 1989) and reconfirmed the 12-year periodicity.

A quantitative record from a zooplankton survey of several Cnidaria species and one Ctenophora species in the Northwest Mediterranean (1966 to 1993) found that abundance was related to climate indices, with strength of relationship intensifying with increasing high positive anomalies in temperature (Molinero et al., 2005). The study also found that high abundance of Cnidaria and Ctenophora were linked to decline in the abundance of copepods. Garcia-Comas et al. (2011) used data from the same zooplankton survey for a different, but overlapping, time period (1974 to 2003). They found that Cnidaria and Ctenophora abundance followed large-scale climate driven temperature during the 1970s and 80s but decreased slightly from 1990 despite increasing temperature. The authors suggest that low winter temperatures and stronger mixing in the water column during the 1980s increased nutrient enrichment into surface waters. This is supported by lower than average abundance in 1990s, and higher than average in the 1980s in the five other (non-gelatinous) zooplankton groups studied (Garcia-Comas et al., 2011).

Lebrato et al. 2013b) utilised a large-scale benthic trawling survey, covering the continental margin of the Northwest Mediterranean, from 1994 – 2005. Quantitative data of jelly-carbon ( $\text{mgC m}^2$ ) was used, from the species *Pyrosoma atlanticum* (Thaliacea). Decadal scale changes in jelly-carbon were correlated to hydroclimatic modifications (including NAO), with high jelly-carbon deposits strongly temperature driven and chlorophyll only playing a minor role in variation. A significant increase in deposits was found post 2001 (Lebrato et al., 2013b).

### **1.8.3 Americas – Pacific**

Video data, collected from 1990 to 1998, in Monterey Bay, California showed significant differences in Hydrozoa abundance and depths, varying with species, in relation to two El Niño Southern Oscillation (ENSO) events. Seldom-seen species were observed in high numbers, whilst common species became rare during the ENSO events (Raskoff, 2001). Fourteen years of monthly beach counts in Hawaii (1988 – 2011) of *Alatina moseri* (Cubozoa) showed strong positive relationship to the North Pacific Gyre Oscillation (NPGO) index, as well as primary production and >2mm (non-gelatinous) zooplankton biomass (Chiaverano et al., 2013). A 43-year timeseries

off the coast of Peru (1972-2014), using GZ bycatch data from fishery surveys, found that *Chrysaora plocamia* (Scyphozoa) biomass fluctuated with ENSO and El Viejo regime warm events (Quiñones et al., 2015).

An 8-year study (2000 – 2007) of *Chrysaora fuscescens* (Scyphozoa) and *Aequorea* sp. (Hydrozoa) abundance in the Northern California Current found a strong negative correlation to the Pacific Decadal Oscillation (PDO), with higher abundance in cooler years (negative PDO; Suchman et al., 2012). In this region negative PDO is associated with stronger upwelling, bringing cold, nutrient rich waters to surface and resulting in high marine productivity, which the populations of *C. fuscescens* and *Aequorea* appear to follow. The authors note the importance of this negative correlation in an upwelling region, as it “run[s] counter to the prevailing trend for temperate species that warm temperatures lead to increased numbers” (Suchman et al., 2012).

Anderson and Piatt 1999) found increasing Scyphozoa populations in the Gulf of Alaska, over the period 1953 to 1997, collected as part of a wider trawl survey, which found a wider marine community reorganisation triggered by a shift in the ocean climate regime. A series of studies investigated Bering Sea fisheries trawl samples of GZ from 1975, and 1979 – 2005 (Brodeur et al., 1999, 2002, 2008). Density-dependent interactions between GZ biomass (>90% composed of the Scyphozoa, *Chrysaora melanaster*) and ice cover, SST (in spring and summer), wind mixing, juvenile fish stock and zooplankton biomass were found. The authors suggest that with further warming in the area the *C. melanaster* populations may remain at similar levels but with a shift northward into the Arctic Ocean (Brodeur et al., 1999, 2002, 2008). Decker et al. 2013) reviews and summarises GZ (>85% composed of *C. melanaster*) trends in the Bering Sea and finds that they do not support the hypothesis of long-term sustained population growth, rather that the populations show variable oscillation over decadal timescales, similar to other populations worldwide Decker et al. (2013), (Condon et al., 2013).

#### **1.8.4 Americas - Atlantic**

Graham 2001) used data on *Chrysaora quinquecirrha* and *Aurelia aurita* (Scyphozoans) from a Northern Gulf of Mexico fisheries trawl survey from 1985 –

1997, collected twice yearly in the summer and autumn. In 2/10 regions *C. quinquecirrha* showed statistically significant long-term increase, while in 6/10 regions *A. aurita* experience significant long-term increase. Long-term is defined as the total length of the study. The author suggests a number of causes for the increase, including natural (climate indices and climate change) and human-induced (coastal fertilisation, overfishing and ocean sprawl), but none of the suggested causes are tested against the data (Graham, 2001). A later study using the same fisheries trawl survey, over an extended period (1985 – 2007) found *C. quinquecirrha* and *A. aurita* populations were positively related to ENSO, Atlantic Multi-Decadal Oscillation (AMDO), and PDO, but negatively correlated to the Great Plains Lower Jet. The two species also showed higher production during wet and warm years (Robinson and Graham, 2013).

Greene et al. 2015) integrated fisheries trawl data for the Puget Sound, Washington, from 1971 – 2011 (40 years). They found no significant climate effects in GZ catch, despite an increase in GZ over time, but a positive relationship to human population density and commercial fishing (Greene et al., 2015). Stomach content analysis of the spiny dogfish, from 1981 – 2000, across the continental shelf of Northeast USA, found a significant increase in the percentage occurrence of Ctenophora over the time period (Link and Ford, 2006). The authors hypothesise that the increase is due to warming SST and overfishing.

### **1.8.5 China**

A 13-year study in the Yellow Sea and East China Sea (1998 – 2010) found that increasing SST and eutrophication levels favoured the long-term increase in *Nemopilema nomurai* (Scyphozoa) abundance. The authors suggest that continued rising SST would favour a rise in *N. nomurai* in this region (Xu et al., 2013).

### **1.8.6 Southern Ocean**

Atkinson et al. 2004) investigated krill (*Euphasia superba*) and salp (*Salpa thompsoni*, Thaliacea) density across the Southern Ocean, from 1926 – 2003. Salp density



increased south of the Southern Boundary Current (SBC), with a mixture of increase, decrease and no-change north of the SBC. There was no relationship between salp and sea ice indices found. The authors suggest that warming temperatures in the Southern Ocean benefit salp over krill, as does the lower food requirement of salp (Atkinson et al., 2004). Lee et al. (2010) investigated the same krill and salp species from 1975-2002. They found no significant relationship between abiotic factors (temperature, salinity, sea-ice and nutrients) and salp or krill abundance, but did note that salp abundance was generally higher in years with higher sea water temperature, lower sea-ice extent and lower nutrient levels, with krill abundance having the opposite pattern for all three factors (Lee et al., 2010).

### **1.8.7 Global**

A small number of reviews on global long-term trends in GZ populations have been carried out. Purcell (2005) reviews studies of Cnidaria and Ctenophora abundance that are related to climate variations (SST, salinity, NAO, NPO and ENSO) up to 2005. Eleven species reviewed had positive relationships between warm temperature and increased abundance, whilst four species did not. The author concludes that warming SST, as a result of climate change, is likely to change the ranges, expand the seasonality and increase the abundance of temperate GZ species (Purcell, 2005). A later review by Purcell (2012) finds numerous correlations between elevated Cnidaria and Ctenophora abundance and increased SST and low forage fish. Purcell states, “Global warming will provide a rising baseline against which climate cycles will cause fluctuations in jelly populations” (Purcell, 2012). In this second review it is restated that the ranges and seasonality of Cnidaria and Ctenophora will change, and greater emphasis is given to the combined impact from other anthropogenic perturbations to the marine environment (Purcell, 2012, Brodeur et al., 2008). Another global review in the same year by Brotz et al. (2012) found 28/45 (or 62%) of Large Marine Ecosystems showed increasing trends in GZ abundance, 3 showed decreasing and 14 were stable, from 1950 to present. 33% of the conclusions were of high certainty, and that two thirds of these (10/15) were in the Large Marine Ecosystems showing increasing trends in GZ abundance (Brotz et al., 2012).

GZ abundance appears to be increasing in many coastal regions around the globe, in recent decades, with the exception of some species and some areas, on the evidence currently available. This increase in GZ abundance has not been robustly linked to climate change. In many regions, abundance has been positively correlated to climate oscillations, but this again has exceptions and inconsistencies. Significant areas of the global ocean, especially away from shelf seas, do not have long-term studies on GZ abundance leaving large uncertainty in the hypothesis that GZ are increasing globally (Condon et al., 2013), such that GZ abundance cannot be said to be increasing globally. Boero et al. 2008) suggests that with the combined anthropogenic (i.e. pollution and the removal of fish and marine mammals) and climate change effects, global oceans may ‘de-evolve’ to conditions similar to those 500 million years ago, resulting in a ‘Medusozoan dominant’ ecosystem.

## **1.9 Baselines**

Part of the difficulty in determining trends in GZ populations is the lack of information on baseline populations, from which changes may be determined. In recent years two global studies have begun to address this problem, through the Jellyfish Database Initiative (JeDI) (Lilley et al., 2011, Lucas et al., 2014). JeDI is a publicly available online database of GZ. Lilley et al. 2011) carried out a meta-analysis using JeDI, from which 58 locations across the globe, from 1967 – 2009, were included. GZ biomass decreased significantly with increasing total water column depth, with coastal sites (<50m) typically experiencing 742 times the biomass of deep ocean sites (>2000m) (Lilley et al., 2011). Lucas et al. 2014) extracted data on GZ carbon biomass from JeDI, covering the period 1934 – 2011, and mapped it to a 5° grid. The global geometric mean (and standard deviation) of total biomass was 0.53 ( $\pm 16.16$ ) mg C m<sup>-3</sup>, with the greatest biomass in the subtropical and boreal Northern Hemisphere (Lucas et al., 2014).

## **1.10 Seasonality**

Most of the studies discussed here only measure GZ (quantitatively or qualitatively) for a small section of the year, often during the summer. Whilst many studies investigating seasonality in GZ only sample for 1 or 2 years (Nogueira Junior et al.,

2010, Bravo et al., 2011), and the large inter-annual variability displayed by GZ make these inadequate to realistically demonstrate seasonality. There is a general knowledge that GZ populations peak in abundance (bloom) at some point during the summer, but the variation in timing and amplitude in blooms over different regions is poorly known (Sullivan and Kremer, 2011, Aubert et al., 2018). Shifts in the timing of GZ blooms are likely to have a significant impact on the local ecosystem through trophic cascade effects (Robinson and Graham, 2014).

### **1.10.1 Seasonality Studies**

Gibbons and Richardson 2009) compared shelf sea and oceanic populations of Cnidaria and Ctenophora in the North Atlantic Ocean, from 1946 - 2005. Oceanic populations peaked slightly earlier (June – July) and declined faster than shelf sea populations (July – October). A significant relationship was also found between the duration of GZ blooms, for both population groups, and latitude, so that peaks flattened towards southern latitudes with shorter productive seasons (Gibbons and Richardson, 2009). A study in Hawaii found no seasonal trend in 14-years of monthly collected samples of Cubozoa, but still large inter- and intra-annual variability (Chiaverano et al., 2013). Zavolokin and Glebov 2009) found that the abundance of *A. forskalea* and *C. capillata* in the Bering Sea increased from summer to autumn, whilst the abundance of *C. melanaster* declined from summer to autumn (study period 2002 – 2007, with data collected from summer to autumn). Panasiuk-Chodnicka and Zmijewska 2010) found abrupt peaks in Cnidaria abundance in the middle (January) and end (April) of summer around the Antarctic Peninsula, with two Siphonophorae species peaking throughout the summer, and one Siphonophorae peaking in the winter. Data were collected from December 1985 – February 1986, February – April 1988 and June - August and 1989 (Panasiuk-Chodnicka and Zmijewska, 2010). Suchman et al. (2012) found *C. fuscescens* to peak in abundance in July - August and *Aequorea* sp. peaked in June in the Northern Californian Current. Data were collected from 2000 – 2007 from April to September (Suchman et a., 2012).

### **1.10.2 Trends in Seasonality**

Sullivan et al. 2001) found a seasonal expansion in blooms of *Mnemiopsis leidyi* between the periods 1950 – 1979 and 1980 – 1999, along the Northeast coast of the USA. This shifted the seasonal peak to earlier in the year and was linked with increasing water temperature over the period. Higher water temperatures in the region are associated with positive NAO phases (Sullivan et al., 2001). A 50-year data set, in the Dutch Wadden Sea, found earlier occurrence of all four Scyphozoa species sampled over time. For two species the duration significantly increased over time, and remained constant for the one other species (Van Walraven et al., 2015).

Several reviews hypothesise that the length of the blooming season of GZ will increase with climate change as spring warming triggers earlier blooms (Purcell, 2005, Purcell, 2012, Purcell et al., 2007, Robinson and Graham, 2013), but so far there is limited observational data to robustly back up this hypothesis as a global trend.

### **1.11 The Difficulty with Sampling Gelatinous Zooplankton**

As mentioned previously, there is a shortage of robust long-term GZ abundance data. There are several reasons for this including difficulties in sampling and exclusion from ecosystem surveys (Boero et al., 2008). GZ are inherently difficult to sample, due to their patchy, short-lived and fragile gelatinous nature. Traditional net sampling, as used in fishery surveys, can often destroy the fragile bodies of large Cnidaria and Ctenophora and not retain smaller species or juveniles (Condon et al., 2012), whilst zooplankton sampling methods exclude medusa and can often exclude juveniles, whether intentionally or unintentionally (Brotz et al., 2012). The limited availability of resources, particularly ship time, to GZ researchers is another factor in the data shortage (Bastian et al., 2010). The availability of resources is improving, but historically GZ were not a focus for ecosystem surveys, and easily overlooked in a sample (Boero et al., 2008, Lynam et al., 2011). The nature of the GZ life cycle, with high temporal and spatial variability in adult abundance (the most conspicuous stage), even over small distances, adds to the difficulties in studying long-term trends in abundance (Boero et al., 2008).

The various ways GZ are sampled for population studies are outlined below, along with the pros and cons of each. GZ are recorded in one of two ways, either qualitative

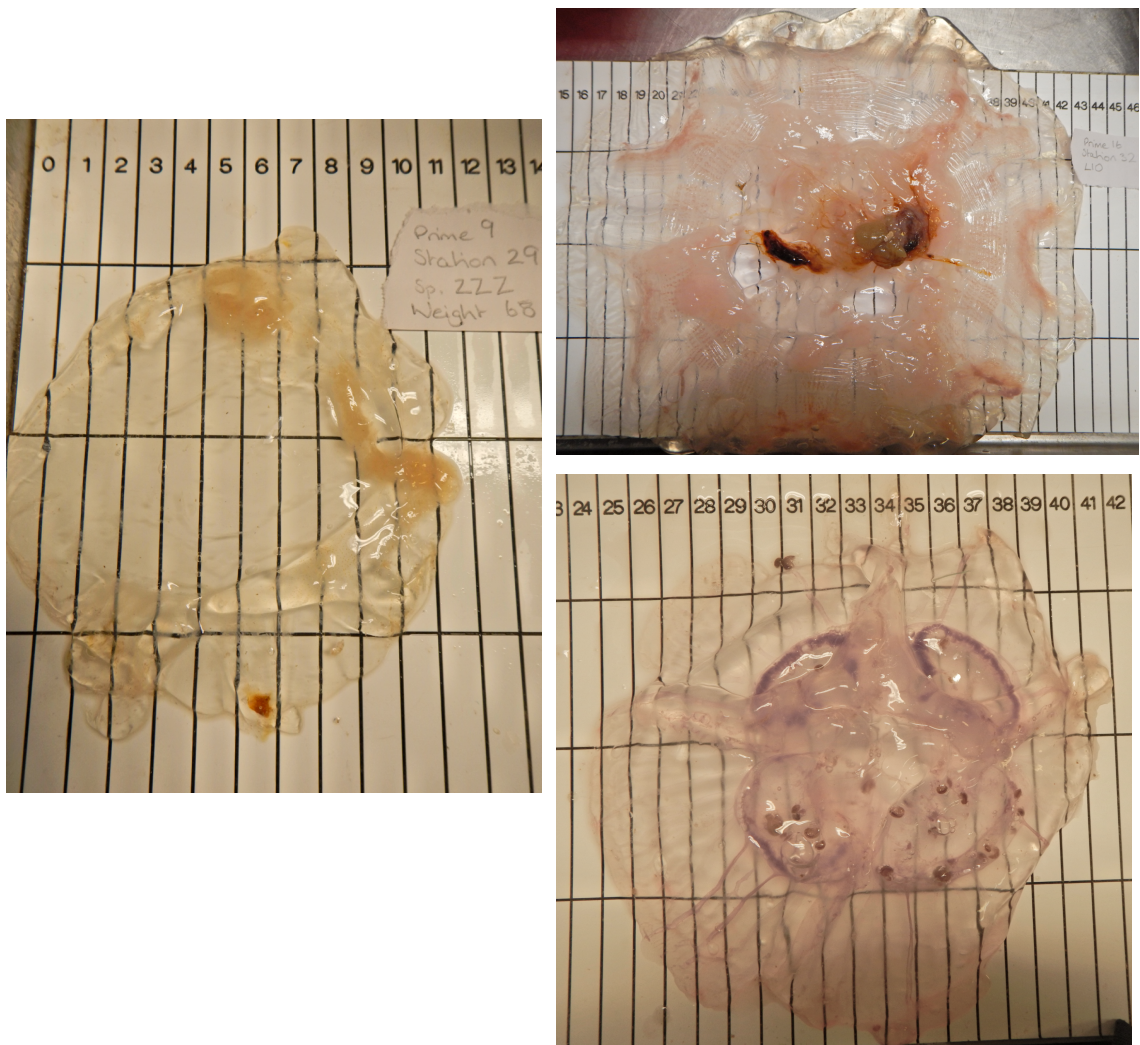


**Figure 1.5** Authors personal photos from multiple trawls during a CEFAS scientific fishery survey of the North Sea, illustrating some of the difficulties in sampling and identifying GZ species from fishery surveys. Specimens are displayed on a board marked with centimetres. Unidentifiable gelatinous zooplankton (left) due to damage by net/other organisms in the net i.e. sea urchins, shells, fish spines. A damaged lions mane jellyfish, *Cyanea capillata*, (top right) with no tentacles remaining and only a small section of oral arms remaining. A colourless specimen (usually red/burgundy in colour). A damaged moon jellyfish, *Aurelia aurita*, (bottom right) with sections missing from the mesoglea, no tentacles and some oral arms.

(as presence or absence), or quantitative (as wet weight, dry weight, number of individuals, carbon biomass etc.).

### 1.11.1 Zooplankton Tows

Nets traditionally used for sampling zooplankton have small rigid openings, which will exclude large GZ and often destroy smaller delicate organisms (Suchman et al., 2012). The largest long-term plankton survey is the CPR; GZ data from this is from counts of

nematocysts (stinging cells) and tissue, because the net mesh does not retain intact individuals. The species of GZ sampled is impossible to determine without costly and time-consuming genetic analysis (Baxter et al., 2010). There is disagreement within the literature over which species or groups of GZ are being sampled or excluded in the CPR (Gibbons and Richardson, 2009). It is useful that CPR data has been collected using the same method since 1946, providing a rare long-term continuous dataset, however the method is not ideal for sampling GZ and only provides presence/absence data and no species data (Gibbons and Richardson, 2009, Baxter et al., 2010, Lynam et al., 2010).

### **1.11.2 Fishery Surveys**

Many countries carry out fishery surveys annually as a means of assessing commercial fish stocks and more general marine ecosystem health. Historically GZ caught in these trawls were ignored. Recently however, more surveys are regularly identifying and counting medusa caught, providing a relatively cheap and logistically easy way to study inter-annual trends in GZ abundance (Bastian et al., 2010, Aubert et al., 2018, Brodeur et al., 2016). However, there are negatives associated with using fishery by-catch data; large mesh size may allow smaller organisms (i.e. Tunicata) to slip through, a high density bloom can rapidly clog the net preventing the filtering of the required volume of water, trawls are often only carried out at one depth, and individuals may be too damaged for reliable identification and weighing (Fig 1.5; Bastian et al., 2010, Suchman et al., 2012).

### **1.11.3 By-Proxy**

GZ have occasionally been measured as a proxy to study more enigmatic species, often with larger resources available to researchers. Aerial surveys were used to map GZ blooms around Ireland, in order to locate and survey the ocean sunfish and the leatherback turtle (Houghton et al., 2006a, Houghton et al., 2006b) and in the north-east Atlantic and Mediterranean Sea also to survey the ocean sunfish (Grémillet et al., 2017). These studies provide qualitative data on bloom size and location, and good spatial coverage over a large area, but they are rare.

#### **1.11.4 Visual and Video Counts**

A survey of GZ in the Irish and Celtic Seas used surface counts from ships of opportunity and shoreline surveys of strandings (Doyle et al., 2008, Doyle et al., 2007). These provide good spatial coverage for a low cost, reasonable identification to species level and semi-qualitative data. Visual confirmations of GZ blooms are also being used in citizen-science projects in the UK, Mediterranean and several other countries (JellyWatch, 2016). Video cameras towed behind boats or moored can provide fine-scale qualitative GZ data, but only cover small areas (Raskoff, 2001, Bamstedt et al., 2003). Video photography can be useful to quantify large GZ, such as adult Cnidaria and Ctenophora, under sea ice where other methods cannot sample (Purcell et al., 2018). Video photography on drones has recently been used to survey larger species of GZ in Australia (Raoult and Gaston, 2018), But these methods can only offer semi-quantitative data i.e. abundance but not carbon biomass.

#### **1.11.5 Other Methods**

Acoustic methods have been under development for a number of years for GZ sampling, but currently still require other sampling methods (such as nets) to verify counts and identify species, and are yet to be widely used (Bamstedt et al., 2003, Brierley et al., 2001, Graham et al., 2010). Environmental DNA (eDNA) surveys can detect trace amounts of organismal DNA from seawater samples, indicating the presence of a species in that environment. The eDNA methods for detecting GZ are in development, and may in the future allow for large areas of the ocean to be sampled at low cost (Minamoto et al., 2017). Dietary DNA is a rapidly growing field, due to reducing costs, where the gut contents of fish and scat samples of sea birds are analysed for DNA traces of GZ (Lamb et al., 2017, McInnes et al., 2017). Dietary DNA can provide qualitative information and can identify to varying taxonomic levels depending on the methods used.

GZ are becoming increasingly recognised as an important component of marine ecosystems and global biogeochemical cycles, subsequently data collection is increasing. Unfortunately, historic data collection has been patchy and sporadic with few long-term (>10 years) studies, different sampling techniques, and most areas only

sampled once, or not at all. Peaks in data collection often follow high-profile bloom events (i.e. the *M. leidyi* invasion in the Mediterranean during the 1980's), after which collection dries up. Different sampling techniques show selectivity towards different GZ groups and result in widely varying estimates of abundance. For example, a study examining the difference between sampling techniques found that at the same location and time a macrozooplankton trawl gave a GZ abundance of 1.4 ind/1000m<sup>3</sup>, whilst a multinet trawl gave a GZ abundance of 468 ind/1000m<sup>3</sup> (Hosia et al., 2017). The inclusion of GZ in increasing numbers of ecosystem and annual fisheries surveys will provide essential data for future long-term studies on population trends (Brodeur et al., 2016, Aubert et al., 2018). Currently, however, the data available are not sufficient to attribute an increasing trend in GZ abundance to climate change (Purcell et al., 2007, Condon et al., 2012).

## **1.12 Modelling Gelatinous Zooplankton**

GZ have been included in a range of models to test various hypotheses. The majority of GZ modelling has been in fisheries-based ecosystem models (Pauly et al., 2009), but has also been used to investigate potential GZ locations from ecological niches (Bentlage et al., 2009, 2013). Some key GZ modelling studies and findings are outlined below.

### **1.12.1 Fisheries Models - Ecopath**

Ecopath, including Ecopath with Ecosim, is one of the most commonly used ecosystem modelling approaches, and this follows through into GZ, where it seems to be the most common model type containing a representation of GZ (Pauly et al., 2009). An Ecopath model of the East China Sea was developed containing *Cyanea* sp. and *Stomolophus* sp. (Cnidaria) to investigate fisheries interactions Hong et al. (2008). The study found a possible positive pelagic feedback system, where due to mutual competition and predation between the Cnidaria sp. and *Stromatidae* fish, exploitation of *Stromatidae* fish allowed for Cnidaria blooms to form (Hong et al., 2008). An Ecopath model of the Northern Humboldt Current system was developed to investigate the interaction of *Chrysaora plocamia* (Scyphozoa) with planktivorous fisheries (Chiaverano et al., 2018). Results suggest that *C. plocamia* blooms and fishing have



important effects on the ecosystem structure, with forced increases of planktivorous fish decreasing *C. plocamia* productivity and vice versa (Chiaverano et al., 2018). A series of papers used an Ecopath model of the northern and southern Benguela Upwelling System (Roux and Shannon, 2004, Roux et al., 2013, Shannon et al., 2009) to investigate the interaction between Cnidaria populations and planktivorous fisheries. Results suggest that Cnidaria biomass generally increases when fish biomass decreases, and declines when fish biomass is increased (Roux et al., 2013).

Ecopath models are useful for positioning GZ with higher trophic levels, i.e. fish and marine mammal interactions. However, Pauly et al. (2009) notes that the representation of GZ in Ecopath models is generally poor, with simple inclusion and parameterisation, that is highly variable between different Ecopath models. Ecopath models often use wet weight as model currency; the high water content of GZ make wet weight a poor and biased estimate of GZ biomass (Pauly et al., 2009), especially when comparing GZ biomass to other marine organisms, such as fish. Ecopath models also do not include hydrodynamics or spatial variability (Shannon et al., 2009), which have been shown to influence the formation of GZ blooms.

### **1.12.2 Stage-structured Models**

Stage-structured matrix models partition the GZ life cycle stages with different parameters. A stage-structured model of *A. aurita* (Scyphozoa) was developed including larvae, polyps, ephyrae and medusa under two food regimes, of high and low food availability, and projected winter warming from climate change (Goldstein and Steiner, 2017). The study found enhanced bloom and bust dynamics under higher food conditions, compared to low food, whilst winter warming had a low impact on bloom development at both high and low food conditions (Goldstein and Steiner, 2017). A stage-structured model of *M. leidy* (Ctenophora) was developed including egg, juvenile, transitional and adult, under three food regimes and five temperature regimes, ranging from 10 – 30°C (Salihoglu et al., 2011). The study found that changes to temperature have a similar influence on all life-stages, as does a decrease in food, whilst an increase in food favoured the transitional and adult stages over the egg and juvenile stages (Salihoglu et al., 2011).

Stage-structured models are useful for investigating the life stage-dynamics of GZ, and how each stage responds to different environmental perturbations (Goldstein and Steiner, 2017). However, stage-structured models have no representation of predators or wider ecosystem dynamics, they could be included in end-to-end models to assess the influence of GZ on the wider ecosystem (Salihoglu et al., 2011) and the influence of the wider ecosystem on GZ life-stages.

### 1.12.3 Small-scale Ecosystem Models - NPZD

Nutrient Phytoplankton Zooplankton Detritus (NPZD) models are small-scale ecosystem, simple community models and are usually developed for a specific region to address a specific question. They usually include one or two elements, normally carbon and/or nitrogen, which operate as model currency. An NPZD model of an enclosed or semi-enclosed temperate coastal ecosystem was developed with nitrogen, detritus, one phytoplankton, one zooplankton and two GZ, representing holoplanktonic and meroplanktonic life cycles respectively (Schnedler-Meyer et al., 2018). The study found high GZ biomass would reduce zooplankton biomass, releasing grazing pressure on phytoplankton, resulting in a summer phytoplankton bloom, which were not present when GZ biomass was low (Schnedler-Meyer et al., 2018). A classical NPZD model of a coastal temperate environment was developed with a stage-resolved copepod (*Pseudocalanus* sp.) and Scyphozoa (*A. aurita*) model (Ramirez-Romero et al., 2018). The study found high abundance of *A. aurita* occurred related to high winter temperatures and generated an ecosystem shift from copepod dominance, to *A. aurita* dominance (Ramirez-Romero et al., 2018).

NPZD models allow for the inclusion of life-cycle dynamics with food web interactions. However, they are regionally specific and contain a highly simplified plankton food web, with one phytoplankton and one zooplankton in addition to the GZ component, and therefore include no competition with, or predation of GZ.

### 1.12.4 Physical Models

A model was developed of Chesapeake Bay using *C. quinquecirrha* (Scyphozoa) abundance and temperature and salinity observations to predict the probability of *C.*

*quinquecirrha* occurrence and concentration Decker et al. (2007). The model outputs were found to explain seasonal and spatial variation reasonably well compared to observations (Decker et al., 2007). The physical model works reasonably well in a semi-enclosed, well sampled region, but has not been shown to work on a larger scale. The model also does not include any biological interactions such as prey availability.

### **1.13 Plankton Functional Type Modelling**

The interactions between climate and marine ecosystems, as well as possible feedback mechanisms, are highly complex. The types of models discussed above cannot address these interactions. Dynamic Green Ocean Models (DGOMs) combine physical forcings and representations of biology as plankton functional types (PFTs) to aid understanding of the global biochemical cycle through the interactions between ecosystems and the environment (Le Quéré et al., 2005, Le Quéré et al., 2016). These complex models have provided insight into net primary production (Buitenhuis et al., 2013), the role of oceans in the carbon pump (Hauck et al., 2015, Heinze et al., 2015) and the role of PFTs in ecosystem processes (Hashioka et al., 2013, Le Quéré et al., 2016) and biogeochemical fluxes (Buitenhuis et al., 2006, Buitenhuis et al., 2010), although there are still many challenges and improvements ahead (Heinze et al., 2015).

DGOM development was inspired by terrestrial Dynamic Global Vegetation Models, which successfully applied the concept of functional types (Smith et al., 2001, Steffen, 1996) to reduce global biological complexity to a level manageable within the modelling context (Le Quéré et al., 2005). The criteria for defining functional types as PFTs in DGOMs are given in Le Quéré et al. (2005) and are paraphrased here; each PFT should (a) have an explicit biogeochemical role, (b) be defined by a distinct group of physiological, environmental, or nutrient requirements controlling its biomass and productivity, (c) have distinct effects on other PFTs e.g. through grazing, and (d) be of quantitative importance in at least some region of the ocean. DGOM models do not yet include a representation of GZ, which are likely to have a significant impact on the structure of the plankton web and biogeochemical and carbon cycles. The need for GZ inclusion in global biogeochemical models has been noted in the literature (Lebrato et al., 2013a, Fuentes et al., 2018, Burd et al., 2016). There has been some criticism within the literature of the lumping together of the GZ group in modelling studies and

poor parametrisation, which is likely a result of limited biological data on GZ as a whole and even more so on each GZ group (Gibbons and Richardson, 2013, Pauly et al., 2009). The availability of data on each GZ group will be used in Chapters 2 and 3 to assess the appropriate grouping to use for adding a gelatinous type to a DGOM. The physiological requirements of zooplankton PFTs which control their biomass and productivity are growth rates (which then informs grazing rates) respiration rates and mortality rates (Le Quéré et al., 2005).

This thesis uses the PlankTOM PFT ocean biogeochemical model which first began development in 2003 (Aumont et al., 2003), with two phytoplankton and two zooplankton groups, and now includes ten PFTs, called PlankTOM10 (Le Quéré et al., 2005, Buitenhuis et al., 2006, Buitenhuis et al., 2010, Buitenhuis et al., 2013, Le Quéré et al., 2016). PlankTOM includes 39 tracers, including the full biogeochemical cycles of carbon, phosphate, silicate and oxygen and a simplified iron cycle. Of the ten PFTs in PlankTOM three represent zooplankton types; protozooplankton (5-200  $\mu\text{m}$ , such as heterotrophic flagellates and ciliates), mesozooplankton (200-2000  $\mu\text{m}$ , primarily copepods) and macrozooplankton (>2000  $\mu\text{m}$ , crustaceans; Le Quéré et al., 2016). This thesis adds an eleventh PFT representing GZ to the PlankTOM10 model, making PlankTOM11. The PlankTOM PFT ocean biogeochemical model is described in greater detail in Chapter 3. Increasing the number of PFTs will improve understanding of the BCP, as increasingly explicit pathways and feedback mechanisms for carbon are included (Burd et al., 2016). The use of the PlankTOM PFT model allows for the integration of many of the aspects covered in the separate, simpler model types outlined in the previous section.

## **1.14 Thesis Outline**

### **1.14.1 Thesis Objective**

There is still a deficit of information on the role of GZ in the marine ecosystem and global carbon cycle. Part of this deficit comes from a historical lack of data on GZ, outside of a few small locations. Before we can confidently predict the role of future climate change in jellyfish populations, we must understand their role in and influence on the global marine ecosystem. The central goal of this PhD thesis is to investigate

the role of GZ in the marine ecosystem, in particular the influence on other zooplankton, and how this may influence the carbon cycle. An important step of this work was to parameterise GZ for their inclusion in the biogeochemical model PlankTOM11 as a PFT, and subsequent model tuning. Numerous factors are attributed to GZ blooms; two key ones are climate change and overfishing. The secondary goal of this thesis was to assess the relative and cumulative effect of climate change and overfishing to GZ populations. A key step of this work was including the influence of historical fishing pressure on planktivorous fish stocks, and thus on PFTs in the model. From these general goals five questions are addressed:

- 1) Can GZ be represented in a global biogeochemical model?
- 2) What is the global biomass of GZ and how does it compare to other zooplankton types?
- 3) How do jellyfish affect the marine ecosystem structure?
- 4) What is the role of jellyfish in global carbon export?
- 5) What is the relative effect on jellyfish biomass of overfishing and climate variability?

#### **1.14.2 Thesis Structure**

This thesis begins by investigating GZ data extracted from a global plankton dataset for global patterns of abundance and biomass (Chapter 2). Seasonal baselines for GZ are generated for nine regions where there is enough data to inform the full seasonal cycle. Ranges are generated of the global carbon biomass for GZ, and each GZ group where data are sufficient. These seasonal baselines and global biomass are used to quantify GZ and to validate GZ biomass and spatial distribution in PlankTOM11. Chapter 3 describes the development of PlankTOM11, where a PFT representing Cnidaria (jellyfish) was added to PlankTOM10. PlankTOM11 is assessed for the replication of Cnidaria with regards to observations and the ecosystem effects of this additional zooplankton, in particular the effect on other PFTs is investigated. Chapter 4 uses PlankTOM11 to assess the effect of the Cnidaria PFT on the global BCP, specifically the carbon sink. Each characteristic of Cnidaria, which informs its physiological representation with the model, is individually tested for its influence on the carbon sink. Chapter 5 adds a representation of overfishing to PlankTOM11 for a region that has experienced historical overfishing and now reports large blooms of

Cnidaria as a result. The question of whether climate or overfishing has a larger impact on Cnidaria biomass is addressed, as well as if the additive effect of both occurring simultaneously has an even greater impact. Chapters 2 – 5 are written to be self-contained and the basis of publications. Chapter 6 brings the earlier chapters together to address the five questions given above and suggests future avenues of research arising from this thesis.

## References

- ACUÑA, J. L., LÓPEZ-URRUTIA, Á. & COLIN, S. 2011. Faking giants: the evolution of high prey clearance rates in jellyfishes. *Science*, 333, 1627-1629.
- ANDERSON, P. J. & PIATT, J. F. 1999. Community reorganization in the Gulf of Alaska following ocean climate regime shift. *Marine Ecology Progress Series*, 189, 117-123.
- ARAI, M. N. 2005. Predation on pelagic coelenterates: a review. *Journal of the Marine Biological Association of the United Kingdom*, 85, 523-536.
- ARNEBERG, P., SKORPING, A., GRENFELL, B. & READ, A. F. 1998. Host densities as determinants of abundance in parasite communities. *Proceedings of the Royal Society B-Biological Sciences*, 265, 1283-1289.
- ATKINSON, A., SCHMIDT, K., FIELDING, S., KAWAGUCHI, S. & GEISSLER, P. A. 2012. Variable food absorption by Antarctic krill: Relationships between diet, egestion rate and the composition and sinking rates of their fecal pellets. *Deep-Sea Research Part II-Topical Studies in Oceanography*, 59, 147-158.
- ATKINSON, A., SIEGEL, V., PAKHOMOV, E. & ROTHERY, P. 2004. Long-term decline in krill stock and increase in salps within the Southern Ocean. *Nature*, 432, 100-103.
- ATTRILL, M., WRIGHT, J. & EDWARDS, M. 2007. Climate-related increases in jellyfish frequency suggest a more gelatinous future for the North Sea. *Limnology and Oceanography*, 52, 480-485.
- AUBERT, A., ANTAJAN, E., LYNAM, C., PITOIS, S., PLIRU, A., VAZ, S. & THIBAUT, D. 2018. No more reason for ignoring gelatinous zooplankton in ecosystem assessment and marine management: Concrete cost-effective methodology during routine fishery trawl surveys. *Marine Policy*, 89, 100-108.
- BAGHERI, S., NIERMANN, U., MANSOR, M. & YEOK, F. S. 2014. Biodiversity, distribution and abundance of zooplankton in the Iranian waters of the Caspian Sea off Anzali during 1996-2010. *Journal of the Marine Biological Association of the United Kingdom*, 94, 129-140.
- BAMSTEDT, U., KAARTVEDT, S. & YOUNGBLUTH, M. 2003. An evaluation of acoustic and video methods to estimate the abundance and vertical distribution of jellyfish. *Journal of Plankton Research*, 25, 1307-1318.

- BASTIAN, T., LILLEY, M. K. S., STOKES, D., BEGGS, S. E., LYNAM, C. P., HAYS, G. C., DAVENPORT, J. & DOYLE, T. K. 2010. How fish surveys provide a 'backbone' for jellyfish research. . Nantes, France: ICES Annual Science Conference. 20-24 September 2010.
- BAXTER, E. J., WALNE, A. W., PURCELL, J. E., MCALLEN, R. & DOYLE, T. K. 2010. Identification of jellyfish from Continuous Plankton Recorder samples. *Hydrobiologia*, 645, 193-201.
- BAYHA, K. M. & GRAHAM, W. M. 2014. Nonindigenous marine jellyfish: invasiveness, invasibility, and impacts. *Jellyfish Blooms*. Springer.
- BENEDETTI-CECCHI, L., CANEPA, A., FUENTES, V., TAMBURELLO, L., PURCELL, J. E., PIRAINO, S., ROBERTS, J., BOERO, F. & HALPIN, P. 2015. Deterministic Factors Overwhelm Stochastic Environmental Fluctuations as Drivers of Jellyfish Outbreaks. *PloS one*, 10, e0141060.
- BENTLAGE, B., PETERSON, A. T., BARVE, N. & CARTWRIGHT, P. 2013. Plumbing the depths: extending ecological niche modelling and species distribution modelling in three dimensions. *Global Ecology and Biogeography*, 22, 952-961.
- BENTLAGE, B., PETERSON, A. T. & CARTWRIGHT, P. 2009. Inferring distributions of chirodropid box-jellyfishes (Cnidaria: Cubozoa) in geographic and ecological space using ecological niche modeling. *Marine Ecology Progress Series*, 384, 121-133.
- BILLETT, D. S. M., BETT, B. J., JACOBS, C. L., ROUSE, I. P. & WIGHAM, B. D. 2006. Mass deposition of jellyfish in the deep Arabian Sea. *Limnology and Oceanography*, 51, 2077-2083.
- BOERO, F. 2013. *Review of jellyfish blooms in the Mediterranean and Black Sea*.
- BOERO, F., BOUILLON, J., GRAVILI, C., MIGLIETTA, M. P., PARSONS, T. & PIRAINO, S. 2008. Gelatinous plankton: irregularities rule the world (sometimes). *Marine Ecology Progress Series*, 356, 299-310.
- BRAVO, V., PALMA, S. & SILVA, N. 2011. Seasonal and vertical distribution of medusae in Aysen region, southern Chile. *Latin American Journal of Aquatic Research*, 39, 359-377.
- BRIERLEY, A. S., AXELSEN, B. E., BUECHER, E., SPARKS, C. A., BOYER, H. & GIBBONS, M. J. 2001. Acoustic observations of jellyfish in the Namibian Benguela. *Marine Ecology Progress Series*, 210, 55-66.



- BRODEUR, R. D., DECKER, M. B., CIANNELLI, L., PURCELL, J. E., BOND, N. A., STABENO, P. J., ACUNA, E. & HUNT JR, G. L. 2008. Rise and fall of jellyfish in the eastern Bering Sea in relation to climate regime shifts. *Progress in Oceanography*, 77, 103-111.
- BRODEUR, R. D., LINK, J. S., SMITH, B. E., FORD, M., KOBAYASHI, D. & JONES, T. T. 2016. Ecological and economic consequences of ignoring jellyfish: a plea for increased monitoring of ecosystems. *Fisheries*, 41, 630-637.
- BRODEUR, R. D., MILLS, C. E., OVERLAND, J. E., WALTERS, G. E. & SCHUMACHER, J. D. 1999. Evidence for a substantial increase in gelatinous zooplankton in the Bering Sea, with possible links to climate change. *Fisheries Oceanography*, 8, 296-306.
- BRODEUR, R. D., SUGISAKI, H. & HUNT, G. L. 2002. Increases in jellyfish biomass in the Bering Sea: implications for the ecosystem. *Marine Ecology Progress Series*, 233, 89-103.
- BROTZ, L., CHEUNG, W. W. L., KLEISNER, K., PAKHOMOV, E. & PAULY, D. 2012. Increasing jellyfish populations: trends in Large Marine Ecosystems. *Hydrobiologia*, 690, 3-20.
- BUITENHUIS, E., LE QUÉRÉ, C., AUMONT, O., BEAUGRAND, G., BUNKER, A., HIRST, A., IKEDA, T., O'BRIEN, T., PIONTKOVSKI, S. & STRAILE, D. 2006. Biogeochemical fluxes through mesozooplankton. *Global Biogeochemical Cycles*, 20.
- BUITENHUIS, E. T., HASHIOKA, T. & LE QUERE, C. 2013. Combined constraints on global ocean primary production using observations and models. *Global Biogeochemical Cycles*, 27, 847-858.
- BUITENHUIS, E. T., RIVKIN, R. B., SAILLEY, S. & QUÉRÉ, C. L. 2010. Biogeochemical fluxes through microzooplankton. *Global Biogeochemical Cycles*, 24.
- BURD, A., BUCHAN, A., CHURCH, M. J., LANDRY, M. R., MCDONNELL, A. M., PASSOW, U., STEINBERG, D. K. & BENWAY, H. M. 2016. Towards a transformative understanding of the ocean's biological pump: Priorities for future research-Report on the NSF Biology of the Biological Pump Workshop. Ocean Carbon & Biogeochemistry (OCB) Program.

- CHELSKY, A., PITT, K. A. & WELSH, D. T. 2015. Biogeochemical implications of decomposing jellyfish blooms in a changing climate. *Estuarine Coastal and Shelf Science*, 154, 77-83.
- CHIAVERANO, L. M., HOLLAND, B. S., CROW, G. L., BLAIR, L. & YANAGIHARA, A. A. 2013. Long-Term Fluctuations in Circalunar Beach Aggregations of the Box Jellyfish *Alatina moseri* in Hawaii, with Links to Environmental Variability. *Plos One*, 8.
- CHIAVERANO, L. M., ROBINSON, K. L., TAM, J., RUZICKA, J. J., QUIÑONES, J., ALEKSA, K. T., HERNANDEZ, F. J., BRODEUR, R. D., LEAF, R. & UYE, S.-I. 2018. Evaluating the role of large jellyfish and forage fishes as energy pathways, and their interplay with fisheries, in the Northern Humboldt Current System. *Progress in oceanography*, 164, 28-36.
- CONDON, R. H., DUARTE, C. M., PITT, K. A., ROBINSON, K. L., LUCAS, C. H., SUTHERLAND, K. R., MIANZAN, H. W., BOGEBERG, M., PURCELL, J. E., DECKER, M. B., UYE, S.-I., MADIN, L. P., BRODEUR, R. D., HADDOCK, S. H. D., MALEJ, A., PARRY, G. D., ERIKSEN, E., QUINONES, J., ACHA, M., HARVEY, M., ARTHUR, J. M. & GRAHAM, W. M. 2013. Recurrent jellyfish blooms are a consequence of global oscillations. *Proceedings of the National Academy of Sciences of the United States of America*, 110, 1000-1005.
- CONDON, R. H., GRAHAM, W. M., DUARTE, C. M., PITT, K. A., LUCAS, C. H., HADDOCK, S. H. D., SUTHERLAND, K. R., ROBINSON, K. L., DAWSON, M. N., DECKER, M. B., MILLS, C. E., PURCELL, J. E., MALEJ, A., MIANZAN, H., UYE, S.-I., GELCICH, S. & MADIN, L. P. 2012. Questioning the Rise of Gelatinous Zooplankton in the World's Oceans. *Bioscience*, 62, 160-169.
- CONDON, R. H., LUCAS, C. H., PITT, K. A. & UYE, S.-I. 2014. Jellyfish blooms and ecological interactions. *Marine Ecology Progress Series*, 510, 109-110.
- COSTELLO, J., BAYHA, K., MIANZAN, H., SHIGANOVA, T. & PURCELL, J. 2012. The ctenophore *Mnemiopsis leidyi*: transitions from a native to an exotic species. *Hydrobiologia*, 690, 21-46.
- COSTELLO, J., SULLIVAN, B. K., GIFFORD, D., VAN KEUREN, D. & SULLIVAN, L. 2006. Seasonal refugia, shoreward thermal amplification, and

- metapopulation dynamics of the ctenophore *Mnemiopsis leidyi* in Narragansett Bay, Rhode Island. *Limnology and Oceanography*, 51, 1819-1831.
- DAWSON, M. N., MARTIN, L. E. & PENLAND, L. K. 2001. Jellyfish swarms, tourists, and the Christ-child. *Jellyfish Blooms: Ecological and Societal Importance*. Springer.
- DECKER, M. B., BROWN, C. W., HOOD, R. R., PURCELL, J. E., GROSS, T. F., MATANOSKI, J. C., BANNON, R. O. & SETZLER-HAMILTON, E. M. 2007. Predicting the distribution of the scyphomedusa *Chrysaora quinquecirrha* in Chesapeake Bay. *Marine Ecology Progress Series*, 329, 99-113.
- DECKER, M. B., LIU, H., CIANNELLI, L., LADD, C., CHENG, W. & CHAN, K.-S. 2013. Linking changes in eastern Bering Sea jellyfish populations to environmental factors via nonlinear time series models. *Marine Ecology Progress Series*, 494, 179-189.
- DONEY, S. C., RUCKELSHAUS, M., DUFFY, J. E., BARRY, J. P., CHAN, F., ENGLISH, C. A., GALINDO, H. M., GREBMEIER, J. M., HOLLOWED, A. B., KNOWLTON, N., POLOVINA, J., RABALAIS, N. N., SYDEMAN, W. J. & TALLEY, L. D. 2012. Climate Change Impacts on Marine Ecosystems. *Annual Review of Marine Science*, Vol 4, 4, 11-37.
- DONG, Z., LIU, D. & KEESING, J. K. 2010. Jellyfish blooms in China: Dominant species, causes and consequences. *Marine Pollution Bulletin*, 60, 954-963.
- DOYLE, T. K., DE HAAS, H., COTTON, D., DORSCHER, B., CUMMINS, V., HOUGHTON, J. D. R., DAVENPORT, J. & HAYS, G. C. 2008. Widespread occurrence of the jellyfish *Pelagia noctiluca* in Irish coastal and shelf waters. *Journal of Plankton Research*, 30, 963-968.
- DOYLE, T. K., HAYS, G. C., HARROD, C. & HOUGHTON, J. D. 2014. Ecological and societal benefits of jellyfish. *Jellyfish blooms*. Springer.
- DOYLE, T. K., HOUGHTON, J. D. R., BUCKLEY, S. M., HAYS, G. C. & DAVENPORT, J. 2007. The broad-scale distribution of five jellyfish species across a temperate coastal environment. *Hydrobiologia*, 579, 29-39.
- DUARTE, C. M., PITT, K. A., LUCAS, C. H., PURCELL, J. E., UYE, S.-I., ROBINSON, K., BROTZ, L., DECKER, M. B., SUTHERLAND, K. R., MALEJ, A., MADIN, L., MIANZAN, H., GILI, J.-M., FUENTES, V., ATIENZA, D., PAGES, F., BREITBURG, D., MALEK, J., GRAHAM, W. M.

- & CONDON, R. H. 2013. Is global ocean sprawl a cause of jellyfish blooms? *Frontiers in Ecology and the Environment*, 11, 91-97.
- FRANCIS, T. B., SCHEUERELL, M. D., BRODEUR, R. D., LEVIN, P. S., RUZICKA, J. J., TOLIMIERI, N. & PETERSON, W. T. 2012. Climate shifts the interaction web of a marine plankton community. *Global Change Biology*, 18, 2498-2508.
- FUENTES, V. L., PURCELL, J. E., CONDON, R. H., LOMBARD, F. & LUCAS, C. H. 2018. Jellyfish blooms: advances and challenges. *Marine Ecology Progress Series*, 591, 3-5.
- GARCIA-COMAS, C., STEMMANN, L., IBANEZ, F., BERLINE, L., MAZZOCCHI, M. G., GASPARINI, S., PICHERAL, M. & GORSKY, G. 2011. Zooplankton long-term changes in the NW Mediterranean Sea: Decadal periodicity forced by winter hydrographic conditions related to large-scale atmospheric changes? *Journal of Marine Systems*, 87, 216-226.
- GERSHWIN, L.-A. 2007. Malo kingi: A new species of Irukandji jellyfish (Cnidaria : Cubozoa : Carybdeida), possibly lethal to humans, from Queensland, Australia. *Zootaxa*, 55-68.
- GERSHWIN, L.-A., CONDIE, S. A., MANSBRIDGE, J. V. & RICHARDSON, A. J. 2014. Dangerous jellyfish blooms are predictable. *Journal of the Royal Society Interface*, 11.
- GERSHWIN, L.-A. & ZEIDLER, W. 2008. Two new jellyfishes (Cnidaria : Scyphozoa) from tropical Australian waters. *Zootaxa*, 41-52.
- GIBBONS, M. J. & RICHARDSON, A. J. 2009. Patterns of jellyfish abundance in the North Atlantic. *Hydrobiologia*, 616, 51-65.
- GIBBONS, M. J. & RICHARDSON, A. J. 2013. Beyond the jellyfish joyride and global oscillations: advancing jellyfish research. *Journal of Plankton Research*, 35, 929-938.
- GOLDSTEIN, J. & STEINER, U. K. 2017. Ecological and demographic drivers of jellyfish blooms. *bioRxiv*.
- GOY, J., MORAND, P. & ETIENNE, M. 1989. Long-term fluctuations of *Pelagia noctiluca* (Cnidaria, Scyphomedusa) in the western Mediterranean Sea. Prediction by climatic variables. *Deep Sea Research Part A. Oceanographic Research Papers*, 36, 269-279.

- GRAHAM, T. R., HARVEY, J. T., BENSON, S. R., RENFREE, J. S. & DEMER, D. A. 2010. The acoustic identification and enumeration of scyphozoan jellyfish, prey for leatherback sea turtles (*Dermochelys coriacea*), off central California. *Ices Journal of Marine Science*, 67, 1739-1748.
- GRAHAM, W., PAGÈS, F. & HAMNER, W. 2001. A physical context for gelatinous zooplankton aggregations: a review. *Hydrobiologia*, 451, 199-212.
- GRAHAM, W. M. 2001. Numerical increases and distributional shifts of *Chrysaora quinquecirrha* (Desor) and *Aurelia aurita* (Linne) (Cnidaria : Scyphozoa) in the northern Gulf of Mexico. *Hydrobiologia*, 451, 97-111.
- GRAHAM, W. M. & BAYHA, K. M. 2008. Biological invasions by marine jellyfish. *Biological invasions*. Springer.
- GREENE, C., KUEHNE, L., RICE, C., FRESH, K. & PENTTILA, D. 2015. Forty years of change in forage fish and jellyfish abundance across greater Puget Sound, Washington (USA): anthropogenic and climate associations. *Marine Ecology Progress Series*, 525, 153-170.
- GRÉMILLET, D., WHITE, C. R., AUTHIER, M., DORÉMUS, G., RIDOUX, V. & PETTEX, E. 2017. Ocean sunfish as indicators for the 'rise of slime'. *Current Biology*, 27, R1263-R1264.
- HADDOCK, S. H. D. 2008. Reconsidering evidence for potential climate-related increases in jellyfish. *Limnology and Oceanography*, 53, 2759-2762.
- HAMNER, W. M. & DAWSON, M. N. 2009. A review and synthesis on the systematics and evolution of jellyfish blooms: advantageous aggregations and adaptive assemblages. *Hydrobiologia*, 616, 161-191.
- HAN, C.-H. & UYE, S.-I. 2010. Combined effects of food supply and temperature on asexual reproduction and somatic growth of polyps of the common jellyfish *Aurelia aurita* sl. *Plankton and Benthos Research*, 5, 98-105.
- HASHIOKA, T., VOGT, M., YAMANAKA, Y., LE QUERE, C., BUITENHUIS, E. T., AITA, M., ALVAIN, S., BOPP, L., HIRATA, T. & LIMA, I. D. 2013. Phytoplankton competition during the spring bloom in four plankton functional type models.
- HAUCK, J., VÖLKER, C., WOLF-GLADROW, D., LAUFKÖTTER, C., VOGT, M., AUMONT, O., BOPP, L., BUITENHUIS, E. T., DONEY, S. C. & DUNNE, J. 2015. On the Southern Ocean CO<sub>2</sub> uptake and the role of the biological carbon pump in the 21st century. *Global Biogeochemical Cycles*, 29, 1451-1470.

- HAYS, G. C., DOYLE, T. K. & HOUGHTON, J. D. 2018. A paradigm shift in the trophic importance of jellyfish? *Trends in ecology & evolution*.
- HEINZE, C., MEYER, S., GORIS, N., ANDERSON, L., STEINFELDT, R., CHANG, N., LE QUERE, C. & BAKKER, D. C. 2015. The ocean carbon sink-impacts, vulnerabilities and challenges. *Earth System Dynamics*, 6, 327.
- HENSON, S. A., SARMIENTO, J. L., DUNNE, J. P., BOPP, L., LIMA, I. D., DONEY, S. C., JOHN, J. & BEAULIEU, C. 2010. Detection of anthropogenic climate change in satellite records of ocean chlorophyll and productivity.
- HOEGH-GULDBERG, O., JACOB, D., TAYLOR, M., BINDI, M., BROWN, S., CAMILLONI, I., DIEDHIU, A., DJALANTE, R., EBI, K. & ENGELBRECHT, F. 2018. Impacts of 1.5 °C global warming on natural and human systems.
- HONG, J., HE-QIN, C., HAI-GEN, X., ARREQUIN-SANCHEZ, F., ZETINA-REJON, M. J., LUNA, P. D. M. & LE QUESNE, W. J. F. 2008. Trophic controls of jellyfish blooms and links with fisheries in the East China Sea. *Ecological Modelling*, 212, 492-503.
- HOSIA, A., FALKENHAUG, T., BAXTER, E. J. & PAGÈS, F. 2017. Abundance, distribution and diversity of gelatinous predators along the northern Mid-Atlantic Ridge: A comparison of different sampling methodologies. *PloS one*, 12, e0187491.
- HOUGHTON, J. D. R., DOYLE, T. K., DAVENPORT, J. & HAYS, G. C. 2006a. The ocean sunfish *Mola mola*: insights into distribution, abundance and behaviour in the Irish and Celtic Seas. *Journal of the Marine Biological Association of the United Kingdom*, 86, 1237-1243.
- HOUGHTON, J. D. R., DOYLE, T. K., WILSON, M. W., DAVENPORT, J. & HAYS, G. C. 2006b. Jellyfish Aggregations and Leatherback Turtle Foraging Patterns in a Temperate Coastal Environment. *Ecology*, 87, 1967-1972.
- JELLYWATCH. 2016. Available: <http://www.jellywatch.org/regional> [Accessed 10/05/2016 2016].
- KLEIN, S. G., PITT, K. A., RATHJEN, K. A. & SEYMOUR, J. E. 2014. Irukandji jellyfish polyps exhibit tolerance to interacting climate change stressors. *Global Change Biology*, 20, 28-37.

- KOGOVSEK, T., BOGUNOVIC, B. & MALEJ, A. 2010. Recurrence of bloom-forming scyphomedusae: wavelet analysis of a 200-year time series. *Hydrobiologia*, 645, 81-96.
- LAMB, P. D., HUNTER, E., PINNEGAR, J. K., CREER, S., DAVIES, R. G. & TAYLOR, M. I. 2017. Jellyfish on the menu: mtDNA assay reveals scyphozoan predation in the Irish Sea. *Royal Society Open Science*, 4.
- LE QUÉRÉ, C., BUITENHUIS, E. T., MORIARTY, R., ALVAIN, S., AUMONT, O., BOPP, L., CHOLLET, S., ENRIGHT, C., FRANKLIN, D. J., GEIDER, R. J., HARRISON, S. P., HIRST, A., LARSEN, S., LEGENDRE, L., PLATT, T., PRENTICE, I. C., RIVKIN, R. B., SATHYENDRANATH, S., STEPHENS, N., VOGT, M., SAILLEY, S. & VALLINA, S. M. 2016. Role of zooplankton dynamics for Southern Ocean phytoplankton biomass and global biogeochemical cycles. *Biogeosciences Discuss.*, 12, 11935-11985.
- LE QUÉRÉ, C., HARRISON, S. P., COLIN PRENTICE, I., BUITENHUIS, E. T., AUMONT, O., BOPP, L., CLAUSTRE, H., COTRIM DA CUNHA, L., GEIDER, R., GIRAUD, X., KLAAS, C., KOHFELD, K. E., LEGENDRE, L., MANIZZA, M., PLATT, T., RIVKIN, R. B., SATHYENDRANATH, S., UITZ, J., WATSON, A. J. & WOLF-GLADROW, D. 2005. Ecosystem dynamics based on plankton functional types for global ocean biogeochemistry models. *Global Change Biology*, 11, 2016-2040.
- LEBRATO, M. & JONES, D. O. B. 2009. Mass deposition event of *Pyrosoma atlanticum* carcasses off Ivory Coast (West Africa). *Limnology and Oceanography*, 54, 1197-1209.
- LEBRATO, M., MENDES, P. D. J., STEINBERG, D. K., CARTES, J. E., JONES, B. M., BIRSA, L. M., BENAVIDES, R. & OSCHLIES, A. 2013a. Jelly biomass sinking speed reveals a fast carbon export mechanism. *Limnology and Oceanography*, 58, 1113-1122.
- LEBRATO, M., MOLINERO, J.-C., CARTES, J. E., LLORIS, D., MÉLIN, F. & BENI-CASADELLA, L. 2013b. Sinking jelly-carbon unveils potential environmental variability along a continental margin. *PloS one*, 8, e82070.
- LEBRATO, M., PITT, K. A., SWEETMAN, A. K., JONES, D. O., CARTES, J. E., OSCHLIES, A., CONDON, R. H., MOLINERO, J. C., ADLER, L. & GAILLARD, C. 2012. Jelly-falls historic and recent observations: a review to drive future research directions. *Hydrobiologia*, 690, 227-245.

- LEE, C. I., PAKHOMOV, E., ATKINSON, A. & SIEGEL, V. 2010. Long-term relationships between the marine environment, krill and salps in the Southern Ocean. *Journal of Marine Biology*, 2010.
- LICANDRO, P., CONWAY, D. V. P., YAHIA, M. N. D., FERNANDEZ DE PUELLES, M. L., GASPARINI, S., HECQ, J. H., TRANTER, P. & KIRBY, R. R. 2010. A blooming jellyfish in the northeast Atlantic and Mediterranean. *Biology Letters*, 6, 688-691.
- LILLEY, M. K. S., BEGGS, S. E., DOYLE, T. K., HOBSON, V. J., STROMBERG, K. H. P. & HAYS, G. C. 2011. Global patterns of epipelagic gelatinous zooplankton biomass. *Marine Biology*, 158, 2429-2436.
- LINK, J. S. & FORD, M. D. 2006. Widespread and persistent increase of Ctenophora in the continental shelf ecosystem off NE USA. *Marine Ecology Progress Series*, 320, 153-159.
- LOEB, V. & SANTORA, J. 2012. Population dynamics of *Salpa thompsoni* near the Antarctic Peninsula: growth rates and interannual variations in reproductive activity (1993–2009). *Progress in Oceanography*, 96, 93-107.
- LUCAS, C. H. & DAWSON, M. N. 2014. What Are Jellyfishes and Thaliaceans and Why Do They Bloom? *Jellyfish blooms*. Springer.
- LUCAS, C. H., GRAHAM, W. M. & WIDMER, C. 2012. JELLYFISH LIFE HISTORIES: ROLE OF POLYPS IN FORMING AND MAINTAINING SCYPHOMEDUSA POPULATIONS. *Advances in Marine Biology, Vol 63*, 63, 133-196.
- LUCAS, C. H., JONES, D. O. B., HOLLYHEAD, C. J., CONDON, R. H., DUARTE, C. M., GRAHAM, W. M., ROBINSON, K. L., PITT, K. A., SCHILDHAUER, M. & REGETZ, J. 2014. Gelatinous zooplankton biomass in the global oceans: geographic variation and environmental drivers. *Global Ecology and Biogeography*, 23, 701-714.
- LUCAS, C. H., PITT, K. A., PURCELL, J. E., LEBRATO, M. & CONDON, R. H. 2011. What's in a jellyfish? Proximate and elemental composition and biometric relationships for use in biogeochemical studies. *ESA Ecology*, 92, 1704.
- LYNAM, C. P., ATTRILL, M. J. & SKOGEN, M. D. 2010. Climatic and oceanic influences on the abundance of gelatinous zooplankton in the North Sea.



- Journal of the Marine Biological Association of the United Kingdom*, 90, 1153-1159.
- LYNAM, C. P., HAY, S. J. & BRIERLEY, A. S. 2004. Interannual variability in abundance of North Sea jellyfish and links to the North Atlantic Oscillation. *Limnology and Oceanography*, 49, 637-643.
- LYNAM, C. P., HAY, S. J. & BRIERLEY, A. S. 2005. Jellyfish abundance and climatic variation: contrasting responses in oceanographically distinct regions of the North Sea, and possible implications for fisheries. *Journal of the Marine Biological Association of the United Kingdom*, 85, 435-450.
- LYNAM, C. P., LILLEY, M. K. S., BASTIAN, T., DOYLE, T. K., BEGGS, S. E. & HAYS, G. C. 2011. Have jellyfish in the Irish Sea benefited from climate change and overfishing? *Global Change Biology*, 17, 767-782.
- MARTIN, L. E., DAWSON, M. N., BELL, L. J. & COLIN, P. L. 2006. Marine lake ecosystem dynamics illustrate ENSO variation in the tropical western Pacific. *Biology Letters*, 2, 144-147.
- MCINNES, J. C., ALDERMAN, R., LEA, M. A., RAYMOND, B., DEAGLE, B. E., PHILLIPS, R. A., STANWORTH, A., THOMPSON, D. R., CATRY, P. & WEIMERSKIRCH, H. 2017. High occurrence of jellyfish predation by black-browed and Campbell albatross identified by DNA metabarcoding. *Molecular ecology*, 26, 4831-4845.
- MCKINLEY, G. A., FAY, A. R., LOVENDUSKI, N. S. & PILCHER, D. J. 2017. Natural variability and anthropogenic trends in the ocean carbon sink. *Annual review of marine science*, 9, 125-150.
- MILLS, C. E. 1993. NATURAL MORTALITY IN NE PACIFIC COASTAL HYDROMEDUSAE - GRAZING PREDATION, WOUND-HEALING AND SENESCENCE. *Bulletin of Marine Science*, 53, 194-203.
- MILLS, C. E. 1995. Medusae, siphonophores, and ctenophores as planktivorous predators in changing global ecosystems. *ICES Journal of Marine Science*, 52, 575-581.
- MINAMOTO, T., FUKUDA, M., KATSUHARA, K. R., FUJIWARA, A., HIDAKA, S., YAMAMOTO, S., TAKAHASHI, K. & MASUDA, R. 2017. Environmental DNA reflects spatial and temporal jellyfish distribution. *PloS one*, 12, e0173073.

- MOLINERO, J. C., IBANEZ, F., NIVAL, P., BUECHER, E. & SOUSSI, S. 2005. North Atlantic climate and northwestern Mediterranean plankton variability. *Limnology and Oceanography*, 50, 1213-1220.
- NOGUEIRA JUNIOR, M., NAGATA, R. M. & HADDAD, M. A. 2010. Seasonal variation of macromedusae (Cnidaria) at North Bay, Florianopolis, southern Brazil. *Zoologia*, 27, 377-386.
- PANASIUK-CHODNICKA, A. A. & ZMIJEWSKA, M. I. 2010. Cnidaria from the Croker passage (Antarctic Peninsula) with a special focus on Siphonophorae. *Polar Biology*, 33, 1131-1143.
- PAULY, D., GRAHAM, W., LIBRALATO, S., MORISSETTE, L. & PALOMARES, M. L. D. 2009. Jellyfish in ecosystems, online databases, and ecosystem models. *Hydrobiologia*, 616, 67-85.
- PITT, K. A., BUDARF, A. C., BROWNE, J. G. & CONDON, R. H. 2014. Bloom and Bust: Why Do Blooms of Jellyfish Collapse? *In*: PITT, K. A. & LUCAS, C. H. (eds.) *Jellyfish Blooms*. Springer.
- PITT, K. A., KINGSFORD, M. J., RISSIK, D. & KOOP, K. 2007. Jellyfish modify the response of planktonic assemblages to nutrient pulses. *Marine Ecology Progress Series*, 351, 1-13.
- PITT, K. A., LUCAS, C. H., CONDON, R. H., DUARTE, C. M. & STEWART-KOSTER, B. 2018. Claims that anthropogenic stressors facilitate jellyfish blooms have been amplified beyond the available evidence: a systematic review. *Frontiers in Marine Science*, 5, 451.
- PITT, K. A., WELSH, D. T. & CONDON, R. H. 2009. Influence of jellyfish blooms on carbon, nitrogen and phosphorus cycling and plankton production. *Hydrobiologia*, 616, 133-149.
- PURCELL, J. & DECKER, M. 2005. Effects of climate on relative predation by scyphomedusae and ctenophores on copepods in Chesapeake Bay during 1987-2000. *Limnology and Oceanography*, 50, 376-387.
- PURCELL, J. E. 2005. Climate effects on formation of jellyfish and ctenophore blooms: a review. *Journal of the Marine Biological Association of the United Kingdom*, 85, 461-476.
- PURCELL, J. E. 2012. Jellyfish and ctenophore blooms coincide with human proliferations and environmental perturbations. *Annual Review of Marine Science*, 4, 209-235.

- PURCELL, J. E., ATIENZA, D., FUENTES, V., OLARIAGA, A., TILVES, U., COLAHAN, C. & GILI, J.-M. 2012. Temperature effects on asexual reproduction rates of scyphozoan species from the northwest Mediterranean Sea. *Hydrobiologia*, 690, 169-180.
- PURCELL, J. E., BREITBURG, D. L., DECKER, M. B., GRAHAM, W. M., YOUNGBLUTH, M. J. & RASKOFF, K. A. 2001. Pelagic cnidarians and ctenophores in low dissolved oxygen environments: A review. *In*: RABALAIS, N. N. (ed.) *Coastal and Estuarine Sciences, Vol 58: Coastal Hypoxia: Consequences for Living Resources and Ecosystems*.
- PURCELL, J. E., JUHL, A. R., MAŃKO, M. K. & AUMACK, C. F. 2018. Overwintering of gelatinous zooplankton in the coastal Arctic Ocean. *Marine Ecology Progress Series*, 591, 281-286.
- PURCELL, J. E., UYE, S.-I. & LO, W.-T. 2007. Anthropogenic causes of jellyfish blooms and their direct consequences for humans: a review. *Marine Ecology Progress Series*, 350, 153-174.
- QU, C.-F., SONG, J.-M. & LI, N. 2014. Causes of jellyfish blooms and their influence on marine environment. *Ying yong sheng tai xue bao = The journal of applied ecology / Zhongguo sheng tai xue xue hui, Zhongguo ke xue yuan Shenyang ying yong sheng tai yan jiu suo zhu ban*, 25, 3701-12.
- QUIÑONES, J., MIANZAN, H., PURCA, S., ROBINSON, K. L., ADAMS, G. D. & ACHA, E. M. 2015. Climate-driven population size fluctuations of jellyfish (*Chrysaora plocamia*) off Peru. *Marine biology*, 162, 2339-2350.
- QUINONES, J., MONROY, A., MARCELO ACHA, E. & MIANZAN, H. 2013. Jellyfish bycatch diminishes profit in an anchovy fishery off Peru. *Fisheries Research*, 139, 47-50.
- RAMIREZ-ROMERO, E., MOLINERO, J. C., PAULSEN, M., JAVIDPOUR, J., CLEMMESSEN, C. & SOMMER, U. 2018. Quantifying top-down control and ecological traits of the scyphozoan *Aurelia aurita* through a dynamic plankton model. *Journal of Plankton Research*, 40, 678-692.
- RAOULT, V. & GASTON, T. 2018. Rapid biomass and size-frequency estimates of edible jellyfish populations using drones. *Fisheries Research*, 207, 160-164.
- RASKOFF, K. A. 2001. The impact of El Niño events on populations of mesopelagic hydromedusae. *Hydrobiologia*, 451, 121-129.

- RHEIN, M. S. R. R., S. AOKI, E. CAMPOS, D. CHAMBERS, R.A. FEELY, S. GULEV, G.C. JOHNSON, S.A. JOSEY, A. KOSTIANOY, C. MAURITZEN, D. ROEMMICH, L.D. TALLEY AND F. WANG, 2013. Observations: Ocean. *In: STOCKER, T. F., D. QIN, G.-K. PLATTNER, M. TIGNOR, S.K. ALLEN, J. BOSCHUNG, A. NAUELS, Y. XIA, V. BEX AND P.M. MIDGLEY (ed.) Climate Change 2013: The Physical Science Basis. Contribution of Working Group I to the Fifth Assessment Report of the Intergovernmental Panel on Climate Change.* Cambridge University Press, Cambridge, United Kingdom and New York, NY, USA.
- RICHARDSON, A. J., BAKUN, A., HAYS, G. C. & GIBBONS, M. J. 2009. The jellyfish joyride: causes, consequences and management responses to a more gelatinous future. *Trends in Ecology & Evolution*, 24, 312-322.
- RICHARDSON, A. J. & GIBBONS, M. J. 2008. Are jellyfish increasing in response to ocean acidification? *Limnology and Oceanography*, 53, 2040-2045.
- ROBINSON, K. L. & GRAHAM, W. M. 2013. Long-term change in the abundances of northern Gulf of Mexico scyphomedusae *Chrysaora* sp and *Aurelia* spp. with links to climate variability. *Limnology and Oceanography*, 58, 235-253.
- ROBINSON, K. L. & GRAHAM, W. M. 2014. Warming of subtropical coastal waters accelerates *Mnemiopsis leidyi* growth and alters timing of spring ctenophore blooms. *Marine Ecology Progress Series*, 502, 105-115.
- ROBINSON, K. L., RUZICKA, J. J., DECKER, M. B., BRODEUR, R. D., HERNANDEZ, F. J., QUIÑONES, J., ACHA, E. M., UYE, S.-I., MIANZAN, H. & GRAHAM, W. M. 2014. Jellyfish, forage fish, and the world's major fisheries. *Oceanography*, 27, 104-115.
- ROUX, J. & SHANNON, L. 2004. Ecosystem approach to fisheries management in the northern Benguela: the Namibian experience. *African Journal of Marine Science*, 26, 79-93.
- ROUX, J.-P., VAN DER LINGEN, C. D., GIBBONS, M. J., MOROFF, N. E., SHANNON, L. J., SMITH, A. D. & CURY, P. M. 2013. Jellyfication of marine ecosystems as a likely consequence of overfishing small pelagic fishes: lessons from the Benguela. *Bulletin of Marine Science*, 89, 249-284.
- SALIHOGU, B., FACH, B. A. & OGUZ, T. 2011. Control mechanisms on the ctenophore *Mnemiopsis* population dynamics: A modeling study. *Journal of Marine Systems*, 87, 55-65.

- SAMPLE, I. 2007. Jellyfish surge endangers fish stocks. *The Guardian*.
- SANDERS, R., HENSON, S. A., KOSKI, M., CHRISTINA, L., PAINTER, S. C., POULTON, A. J., RILEY, J., SALIHOGLU, B., VISSER, A. & YOOL, A. 2014. The biological carbon pump in the North Atlantic. *Progress in Oceanography*, 129, 200-218.
- SANZ-MARTÍN, M., PITT, K. A., CONDON, R. H., LUCAS, C. H., NOVAES DE SANTANA, C. & DUARTE, C. M. 2016. Flawed citation practices facilitates the unsubstantiated perception of a global trend toward increased jellyfish blooms.
- SCHNEDLER-MEYER, N. A., KIØRBOE, T. & MARIANI, P. 2018. Boom and Bust: Life History, Environmental Noise, and the (un)Predictability of Jellyfish Blooms. *Frontiers in Marine Science*, 5.
- SEXTON, M. A., HOOD, R. R., SARKODEE-ADOO, J. & LISS, A. M. 2010. Response of *Chrysaora quinquecirrha* medusae to low temperature. *Hydrobiologia*, 645, 125-133.
- SHANNON, L. J., COLL, M., NEIRA, S., CURY, P. & ROUX, J.-P. 2009. Impacts of fishing and climate change explored using trophic models.
- SMITH, B., PRENTICE, I. C. & SYKES, M. T. 2001. Representation of vegetation dynamics in the modelling of terrestrial ecosystems: comparing two contrasting approaches within European climate space. *Global Ecology and Biogeography*, 10, 621-637.
- STEFFEN, W. L. 1996. A periodic table for ecology? A chemist's view of plant functional types. *Journal of Vegetation Science*, 7, 425-430.
- STEINBERG, D. K. & LANDRY, M. R. 2017. Zooplankton and the ocean carbon cycle. *Annual review of marine science*, 9, 413-444.
- STONE, J. P. & STEINBERG, D. K. 2018. Influence of top-down control in the plankton food web on vertical carbon flux: A case study in the Chesapeake Bay. *Journal of Experimental Marine Biology and Ecology*, 498, 16-24.
- SUCHMAN, C. L., BRODEUR, R. D., DALY, E. A. & EMMETT, R. L. 2012. Large medusae in surface waters of the Northern California Current: variability in relation to environmental conditions. *Hydrobiologia*, 690, 113-125.
- SULLIVAN, B., VAN KEUREN, D. & CLANCY, M. 2001. Timing and size of blooms of the ctenophore *Mnemiopsis leidyi* in relation to temperature in Narragansett Bay, RI. *Hydrobiologia*, 451, 113-120.

- SULLIVAN, L. J. & KREMER, P. 2011. Gelatinous Zooplankton and Their Trophic Roles. *Treatise on Estuarine and Coastal Science*. Waltham: Academic Press.
- SWEETMAN, A. K., SMITH, C. R., DALE, T. & JONES, D. O. 2014. Rapid scavenging of jellyfish carcasses reveals the importance of gelatinous material to deep-sea food webs. *Proceedings of the Royal Society B: Biological Sciences*, 281, 20142210.
- THIEBOT, J. B., ARNOULD, J. P., GÓMEZ-LAICH, A., ITO, K., KATO, A., MATTERN, T., MITAMURA, H., NODA, T., POUPART, T. & QUINTANA, F. 2017. Jellyfish and other gelata as food for four penguin species—insights from predator-borne videos. *Frontiers in Ecology and the Environment*, 15, 437-441.
- VAN WALRAVEN, L., LANGENBERG, V. T., DAPPER, R., WITTE, J. I., ZUUR, A. F. & VAN DER VEER, H. W. 2015. Long-term patterns in 50 years of scyphomedusae catches in the western Dutch Wadden Sea in relation to climate change and eutrophication. *Journal of Plankton Research*, 37, 151-167.
- VINOGRADOV, A. 1953. The elementary chemical composition of marine organisms. *New Haven*.
- WEST, E. J., PITT, K. A., WELSH, D. T., KOOP, K. & RISSIK, D. 2009. Top-down and bottom-up influences of jellyfish on primary productivity and planktonic assemblages. *Limnology and Oceanography*, 54, 2058-2071.
- XU, Y., ISHIZAKA, J., YAMAGUCHI, H., SISWANTO, E. & WANG, S. 2013. Relationships of interannual variability in SST and phytoplankton blooms with giant jellyfish (*Nemopilema nomurai*) outbreaks in the Yellow Sea and East China Sea. *Journal of Oceanography*, 69, 511-526.
- YOUNG, G. A. & HAGADORN, J. W. 2010. The fossil record of cnidarian medusae. *Palaeoworld*, 19, 212-221.
- ZAVOLOKIN, A. V. & GLEBOV, I. I. 2009. SUMMER-FALL DISTRIBUTION, STRUCTURE AND ABUNDANCE TREND OF JELLYFISH IN THE WESTERN BERING SEA. *Zoologicheskyy Zhurnal*, 88, 1411-1424.

# CHAPTER 2. GLOBAL & REGIONAL TRENDS IN GELATINOUS ZOOPLANKTON ABUNDANCE

An analysis of the MARine Ecosystem biomass DATA  
(MAREDAT) database





## Abstract

Understanding and predicting changes to GZ populations in a changing climate is impeded by poor knowledge of the starting point, or ‘baselines’, both for global and regional biomass and for seasonal dynamics. The aim of this chapter is to provide a best estimate of the global biomass and characterise the seasonal dynamics of GZ over large ocean regions. This analysis is based on the MAREDAT global plankton database, which includes 107,156 abundance data of GZ, and 3,406 carbon biomass data, from 1930 – 2008. The GZ data was binned on to a global  $1^{\circ}\times 1^{\circ}$  degree grid at monthly resolution. The data were also divided by phyla (Cnidaria, Ctenophora and Tunicata) and into Longhurst Provinces. Regional analysis is carried out on six Longhurst Provinces in the Northern Hemisphere and three in the Tropics, where sufficient data are available. This is the first study to establish seasonal baselines from long-term, multi-source data. Each Province exhibits its own seasonality, background abundance, and bloom characteristics. The tropical Indian Ocean had the lowest GZ baseline, the two equatorial Pacific regions had the highest baseline, and the north-west Atlantic had the highest bloom abundance. Of the phyla, Tunicata were the most abundant with a median of 0.43 individuals/m<sup>3</sup>, whilst Cnidaria had the highest biomass with a median of 0.28  $\mu\text{g C L}^{-1}$ . The best estimate for the global biomass of GZ is for a range of 0.14 to 1.33 PgC, based on the spread between the median and the arithmetic mean, following previous studies. The GZ biomass is similar to that of other zooplankton groups, confirming their importance. The exact biomass cannot be assessed with more precision from the data available because of the poor data coverage and the bloom and bust nature of GZ populations. These findings provide a historical baseline to help assess future GZ abundance and biomass in a changing climate. The quantitative and qualitative information presented here supports the development and validation of global ocean models that represent GZ explicitly.



## 2.1 Introduction

There is significant debate within the scientific literature around the question of whether gelatinous zooplankton (GZ) have already, or will increase in the future due to climate change (Purcell, 2005, Attrill and Edwards, 2008, Haddock, 2008, Condon et al., 2012, Condon et al., 2013, Gibbons and Richardson, 2013, Purcell, 2012, Sanz-Martín et al., 2016). The debate largely stems from a lack of long-term observational data, unknown mean conditions (called ‘baselines’ here), and important heterogeneity in time and space. Indeed, GZ abundance fluctuates over small spatial scales, and can evolve from apparent absence to large blooms of millions of individuals over a few weeks only. The perceived global increase in GZ due to climate change lacks demonstration with rigorous scientific data (Brotz et al., 2012, Sanz-Martín et al., 2016). GZ include gelatinous taxa within the Cnidaria, Ctenophora and Tunicata groups and are widely reported to have an increasingly negative impact on coastal ecology and economic activities, including fish stocks, aquaculture and tourism (Pauly et al., 2009). GZ are also increasingly recognised as an important food source for many species (Doyle et al., 2014, Lamb et al., 2017) and as a route for carbon export through the biological carbon pump (Lebrato et al., 2012).

Temperature increases due to climate change are probably the most studied driver of change for GZ abundance, with positive correlation between water temperatures and abundance found for the majority of GZ species studied. Experiments have shown that higher temperatures also increase GZ growth and reproduction (Lucas et al., 2012, Purcell et al., 2012, Robinson and Graham, 2014). The upper temperature threshold for GZ, above which the rate of growth or development begins to decrease, is higher than for many other marine species. Their high temperature threshold could allow GZ to become more prolific and expand their ranges as global temperatures increase (Purcell, 2012, Klein et al., 2014, Lynam et al., 2011, Gibbons and Richardson, 2009). Ocean acidification due to climate change has not been well linked to GZ abundance, although there are a limited number of studies on the topic. GZ are generally considered as a non-calcifying group and direct impacts from acidification have not been shown (Richardson and Gibbons, 2008). Ocean acidification will cause widespread changes to the plankton community (Mostofa et al., 2016), which is likely to indirectly impact GZ through changes to their prey and competition for resources.

The direct impacts of rising temperature and increased acidity from rising carbon dioxide concentrations and climate change on marine organisms can lead to indirect effects throughout marine ecosystems via trophic cascades (Doney et al., 2012, Mostofa et al., 2016). Phytoplankton and zooplankton community assemblages and biomass have been shown to vary substantially with climate variability (Francis et al., 2012, Boyce et al., 2010). These variations in the plankton community can cascade up trophic pathways through zooplankton, fish and into marine mammals, propagating the climate signal throughout the ecosystem (Brotz et al., 2012, Lucas and Dawson, 2014, Doney et al., 2012). The indirect effects of climate change on GZ through trophic cascades are difficult to study *in situ* (Purcell, 2009) and therefore the overall effect of climate change on GZ abundance cannot be determined from current observational data (Purcell, 2005, Richardson et al., 2009, Gibbons and Richardson, 2013).

Attributing changes in GZ abundance to climate change is difficult and complicated due to the lack of knowledge on GZ baselines and variability, and the many interactions between climate, ecosystems and all the other stressors imposed on the marine environment by mankind (Condon et al., 2012).

### **2.1.1 Evidence of Trends and Variability in Gelatinous Zooplankton Populations**

It can be difficult to separate the large fluctuations in GZ abundance intra- and inter-annually from any longer-term trend that may indicate a growing population caused by climate change. This problem is compounded by the paucity in long-term regional data sets (Condon et al., 2012, Condon et al., 2013). Long, continuous and quantitative records of GZ are rare, making it difficult to attribute GZ trends to climate change rather than other factors such as climate indices (Purcell, 2012, Condon et al., 2013). The large variability in GZ abundance between years also increases the difficulty of interpreting the data, and separate studies of the same area can give conflicting results, even when similar methodologies are used (Suchman et al., 2012, Molinero et al., 2008, Condon et al., 2013, Purcell, 2012). Such conflicting results are exemplified in studies of the North Atlantic Oscillation (NAO), where negative, positive and minimal correlation between the NAO and GZ abundance have been found (Attrill et al., 2007, Gibbons and Richardson, 2009, Lynam et al., 2004, Lynam et al., 2005, Lynam et al.,

2010). There is a general consensus among these studies that local conditions likely interact with the NAO causing differences in trophic cascades through the plankton ecosystem, which in turn influence local GZ abundance and may explain the different findings among studies.

The evidence for global long-term trends in GZ populations has been reviewed a few times (see Chapter 1). Purcell (2012) points out that direct evidence for human perturbations causing a rise in GZ abundance is lacking for the majority of cases, but that numerous correlations between elevated GZ abundance and increased SST exist and are often also correlated with low forage fish abundance due to over fishing. Another global review found 28/45 of Large Marine Ecosystems showed increasing trends in GZ abundance, 14 were stable and 3 showed decreasing trends. Of these, 15 Large Marine Ecosystems trends were of high certainty and 10 of the high certainty were for increasing trends in GZ abundance (Brotz et al., 2012). Information on trends in GZ abundance is missing for most of the ocean, especially in the open ocean, leaving large uncertainty in the hypothesis that GZ are increasing globally (Condon et al., 2013).

### **2.1.2 Baselines in Gelatinous Zooplankton Populations**

Part of the difficulty in determining trends in GZ populations comes from the lack of information on baseline populations, from which changes may be determined. In recent years two global studies have focused on characterising global GZ baselines, through the Jellyfish Database Initiative (JeDI; Lilley et al., 2011, Lucas et al., 2014). JeDI is an online database of GZ including quantitative, categorical, presence-absence and presence only records from 1790 – 2011 (Condon et al., 2014). Lilley et al. (2011) used JeDI to analyse GZ biomass from 1967 – 2009 at 58 locations. GZ biomass was found to decrease significantly with increasing total water column depth, with coastal sites (<50m) on average experiencing 742 times the biomass of deep ocean sites (>2000m) (Lilley et al., 2011). Lucas et al. (2014) also used JeDI to analyse GZ biomass over the period 1934 – 2011. The global mean carbon biomass of GZ was found to be 0.53 ( $\pm 16.16$ )  $\mu\text{g C L}^{-1}$ , with the greatest biomass in the subtropical and boreal Northern Hemisphere oceans (Lucas et al., 2014).

The MAREDAT database includes carbon biomass and abundance data for zooplankton, including GZ (Buitenhuis et al., 2013). The GZ (including Cnidaria, Ctenophora and Tunicata) sub-set within MAREDAT has yet to be analysed independently from the global zooplankton data (Moriarty et al., 2013), which also included Gastropoda, Heteropoda, Pteropoda, Chaetognatha, Polychaeta, Amphipoda, Stomatopoda, Mysida, Decapoda and Euphausiacea. JeDI and MAREDAT have overlapping data but they differ through their focus. MAREDAT is designed for use in the validation of PFTs in global biogeochemical models, with much of the data coming from zooplankton surveys, while JeDI is designed to collate both quantitative and qualitative data on GZ. Ideally JeDI and MAREDAT would be harmonised and extended to include data from recent years, to provide the most comprehensive database of GZ abundance and biomass. However, following an exploration of both databases, such harmonisation and extension was found to be outside the realm and timescale of this thesis, where the primary aim is to include GZ in a global biogeochemical model.

Many studies addressing multi-year trends only measure GZ (quantitatively or qualitatively) for a month or two of the year, often during the summer, spring/summer or summer/autumn, which is insufficient to determine the seasonality. Likewise, many studies directly investigating seasonality in GZ only sampled for 1 or 2 years (Nogueira Junior et al., 2010, Bravo et al., 2011), which is not sufficient to determine robust seasonal baselines. Shifts in the timing of GZ blooms are likely to have a significant impact on the local ecosystem through trophic cascade effects (Graham et al., 2014).

The aim of this chapter is to determine a global baseline of GZ abundance and biomass and seasonal baselines for ocean regions. To achieve this aim, I will examine abundance and carbon biomass of GZ in the MAREDAT database, investigating the spatial and temporal spread of the data. The GZ biomass calculated from the MAREDAT database will be compared to the biomass of other zooplankton in the same database, and to the biomass of GZ calculated from the JeDI database. The GZ abundance data will also be used to find seasonal baselines for ocean regions with sufficient data coverage. The seasonal baselines will provide information on the mean and variations in timing, strength and bloom duration.

## 2.2 Methods

### 2.2.1 Data handling

MAREDAT is a database compiled of global ocean plankton abundance and biomass, harmonised to common units. It contains carbon biomass, calculated where possible, and is open source available online (Moriarty et al., 2013, Buitenhuis et al., 2013). MAREDAT contains global quantitative observations of GZ abundance and biomass as part of the generic macrozooplankton group (Moriarty et al., 2013). The GZ sub-set of data has not been analysed independently yet.

For this study, all MAREDAT records under the group GZ were extracted and examined. This included Cnidaria, Ctenophora and Tunicata, as well as ‘unspecified jellyfish’. The taxonomic level within the database varies from phylum down to species and is provided in Appendix 1. The data covers the period from August 1930 to August 2008. The data contains abundance in the form of number of individuals (107,156 data points) and carbon biomass (3,406 data points). The data were collected at depths ranging from 0 to 2442m. The majority of the data (97.9%) was collected in the top 200m with an average depth of 65.2m ( $\pm$  42.3m), compared to total average depth of 71.5m ( $\pm$  68.6m). The majority of the data are from two net types that integrate over a specific depth, dividing the data by this depth gives abundance in individuals/m<sup>3</sup>. Carbon biomass is calculated from wet weight/dry weight conversion factors for species where data records are sufficient (Moriarty et al., 2013).

The raw (ungridded) abundance data were binned into 1°x1° degree boxes at monthly resolution, as in Moriarty et al. (2013), reducing the number of (gridded) abundance data points to 7,832. The same method was applied to the carbon biomass data, reducing the number of (gridded) biomass data points to 849 (Fig. 2.1). The ungridded abundance and biomass data were split into phylum where possible, with all other samples marked as ‘jellyfish unspecified’ and then gridded as above. The phyla groups are Cnidaria, Ctenophora and Tunicata.

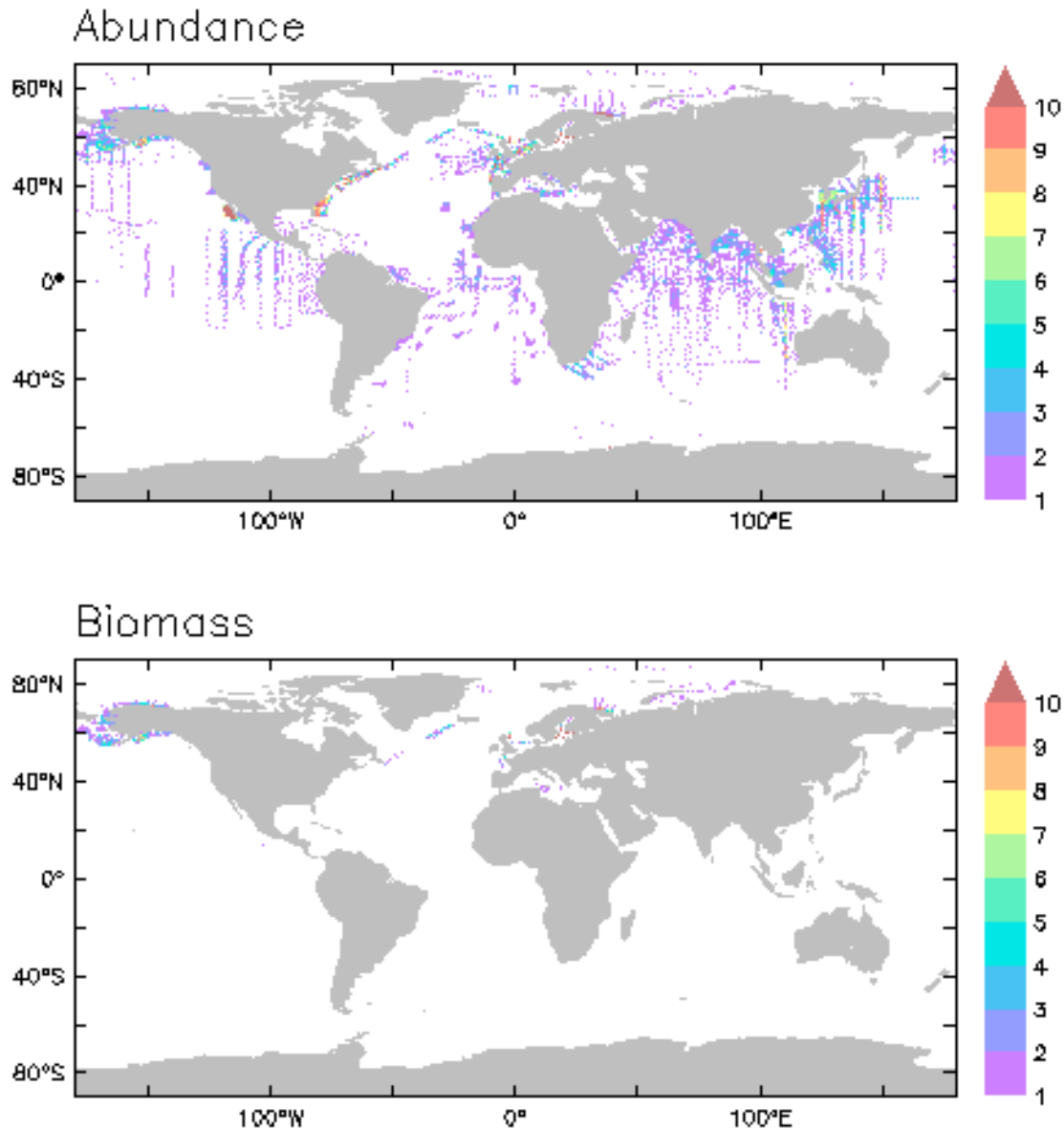


**Figure 2.1** Number of data in MAREDAT for gelatinous zooplankton (top) abundance and (bottom) biomass, after binning the original raw data by month for 1938 – 2008 on a 1°x1° grid.

The ungridded data set was split into the Northern Hemisphere (90°N – 30°N), Tropics (30°N – 30°S) and the Southern Hemisphere (30°S – 90°S) to investigate sampling distribution spatially, temporally and across seasons. It was then grouped into decades and months (Fig. 2.2). For the Southern Hemisphere, sampling occurs in every month and from the 1960's to the 1980's. For the Tropics, sampling occurs in every month and from the 1950's to the 2000's, with a strong peak in sampling in the 1960's. For the Northern Hemisphere, sampling occurs in every month and from the 1930's to the 2000's, with low sampling in the first two decades (Fig. 2.2). Sampling is much more



consistent in all regions across the seasons, with every month sampled, than across the decades. The data set is appropriate for calculating a GZ global mean and assessing GZ seasonality. A long-term time series analysis was deemed inappropriate for this data due to the inconsistencies in sampling across decades.

### 2.2.2 Seasonality in Longhurst Provinces

Despite the higher spatial coverage for abundance in the Northern Hemisphere and in the Tropics, many sites have only been sampled once (Fig. 2.1). Biomass data is generally sparse (Fig. 2.1). The gridded abundance was grouped into areas of coherent water mass following the definition of Longhurst Provinces (Longhurst, 2007). Provinces were excluded from the analysis if they had more than three months with less than four data points in each month, as they were assessed to be unsuitable for the analysis of full seasonality. Six provinces in the Northern hemisphere and three

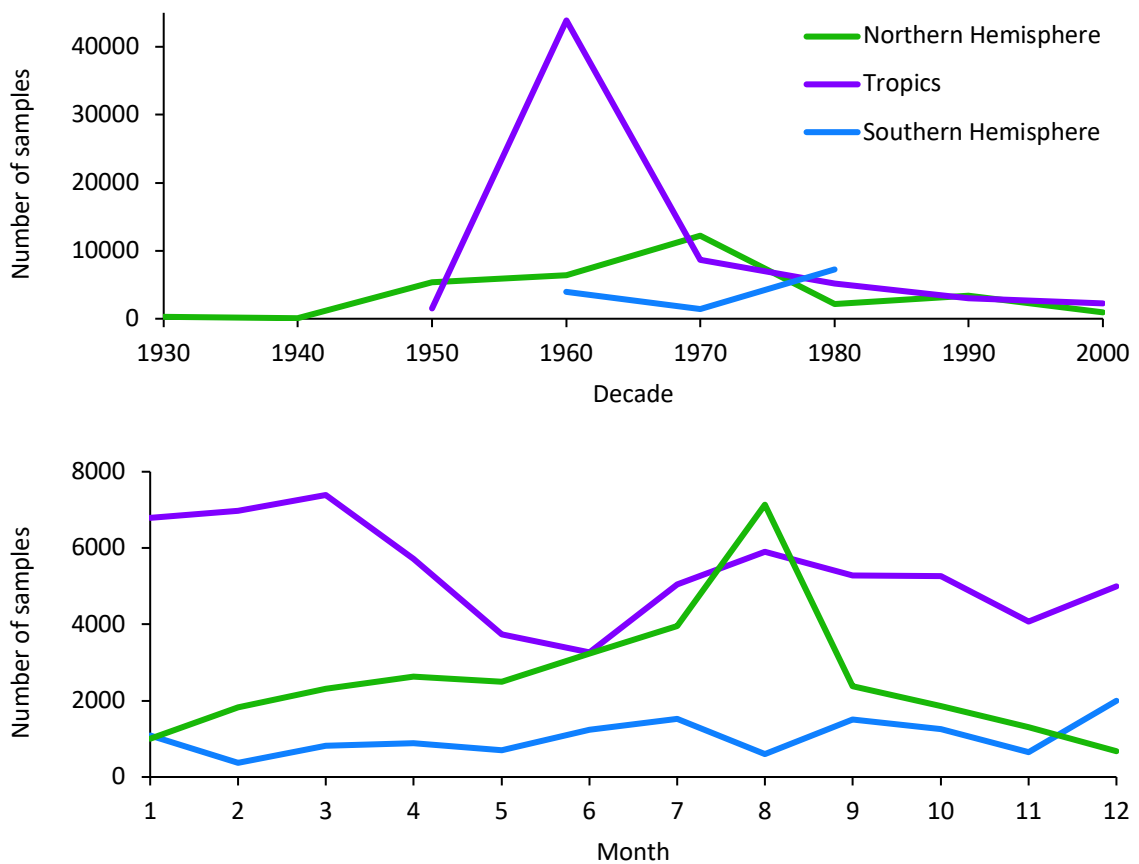


**Figure 2.2** Number of raw abundance data for gelatinous zooplankton across (top) decades, and (bottom) months (summed across years), split into the Northern Hemisphere (green), Tropics (purple) and Southern Hemisphere (blue).

provinces in the Tropics met the criteria. The provinces are (following Longhurst naming) Alaska Coastal Downwelling Province (ALSK), California Current Province (CALC), Northwest Atlantic Shelves Province (NWCS), Northeast Atlantic Shelves Province (NECS), Kuroshio Current Province (KURO), North Pacific Subtropical West Province (NPSW), North Pacific Equatorial Countercurrent Province (PNEC), Pacific Equatorial Divergence Province (PEQD) and the Indian Monsoon Gyres Province (MONS; Longhurst, 2007). Five percentiles were calculated for each month in each Province that had more than four data points. The percentiles used are the 5<sup>th</sup>, 25<sup>th</sup>, 50<sup>th</sup> (or median), 75<sup>th</sup> and 95<sup>th</sup> (see section 2.3.2).

### **2.2.3 Global Baselines**

Multiple methods were used here to calculate average values because of the patchiness of the data, to improve the robustness of results. Firstly, the arithmetic mean (AM) which is equal to the sum of the values of each observation divided by the total number of observations; secondly, the geometric mean (GM) which is the  $n$ th root of the product of  $n$  observations and thirdly, the median which is the central value of observations. The gridded data were split into the Northern Hemisphere, Tropics, and Southern Hemisphere (as in the explorative tests above) to examine the differences between regions.

To compare to the other PFTs within the MAREDAT database, global GZ biomass was calculated according to the methods in Buitenhuis et al. (2013). Buitenhuis et al. (2013) calculate a biomass range, using the median as the minimum and the AM as the maximum. The MAREDAT database is designed to be used for the validation of global biogeochemical models. The GZ biomass range calculated here will be used to validate the new GZ component in the PlankTOM model (Chapter 3). To compare to the GZ estimate of Lucas et al. (2014) based on the JeDI database, global GZ biomass from MAREDAT was calculated according to the methods in Lucas et al. (2014), using GM.

## 2.3 Results

### 2.3.1 Bloom and Bust

The abundance distribution varies by several orders of magnitude. For the Northern Hemisphere, 18% of the GZ abundance data is reported as zero. A large portion of the GZ abundance data ranges between  $>0$  and  $1 \text{ ind/m}^3$  (38%; Fig. 2.3 top panels) and about 60% of the abundance data ranges between  $>0$  and  $10 \text{ ind/m}^3$  (Fig. 2.3 bottom panels). The frequency rapidly declines as abundance increases (Fig. 2.3). For the Tropics there is a similar pattern to the Northern Hemisphere, but a greater portion of the abundance data is zero (34%), with 38% ranging between  $>0$  and  $1 \text{ ind/m}^3$  (Fig. 2.3). For the Southern Hemisphere, the majority of abundance data is reported as zero (73%), with 18% ranging from  $>0$  to  $1 \text{ ind/m}^3$ , and only 22% ranging from  $>0$  to  $10 \text{ ind/m}^3$  (Fig. 2.3). GZ is most abundant and most likely to reach high abundance in the Northern Hemisphere, and second most abundant and likely to reach high abundance in the Tropics. In the Southern Hemisphere GZ are most likely to not be present, and occasionally reach high abundance.

Substantially less data are available for GZ biomass than for abundance, with no biomass data in the Southern Hemisphere and only 62 data points in the Tropics (Fig. 2.4). The Northern Hemisphere has 3,344 biomass data points, with 0.03% of the GZ biomass data reported as zero. Most of the GZ biomass data ranges between  $>0$  and  $0.01 \mu\text{g C L}^{-1}$  (49%), and around 86% of the data ranges between  $>0$  and  $1 \mu\text{g C L}^{-1}$  (Fig. 2.4). The Tropics has a greater portion of zero biomass data (32%) than the Northern Hemisphere, and the highest portion of data in the Tropics ranges from  $>0$  to  $1 \mu\text{g C L}^{-1}$  (52%), with only 8% from  $>0$  to  $0.01 \mu\text{g C L}^{-1}$ . Only the Northern Hemisphere has biomass data above  $8 \mu\text{g C L}^{-1}$ , the lack of higher biomass in the Tropics is likely due to the very limited number of data points (Fig. 2.4). The biomass data from the Tropics must be regarded with caution as it all is from one area, in one month.

### 2.3.2 Seasonality in Longhurst Provinces

Seasonal patterns in GZ abundance were analysed for Longhurst Provinces that had sufficient data. The nine Provinces selected are shown in Figure 2.5. To best explain

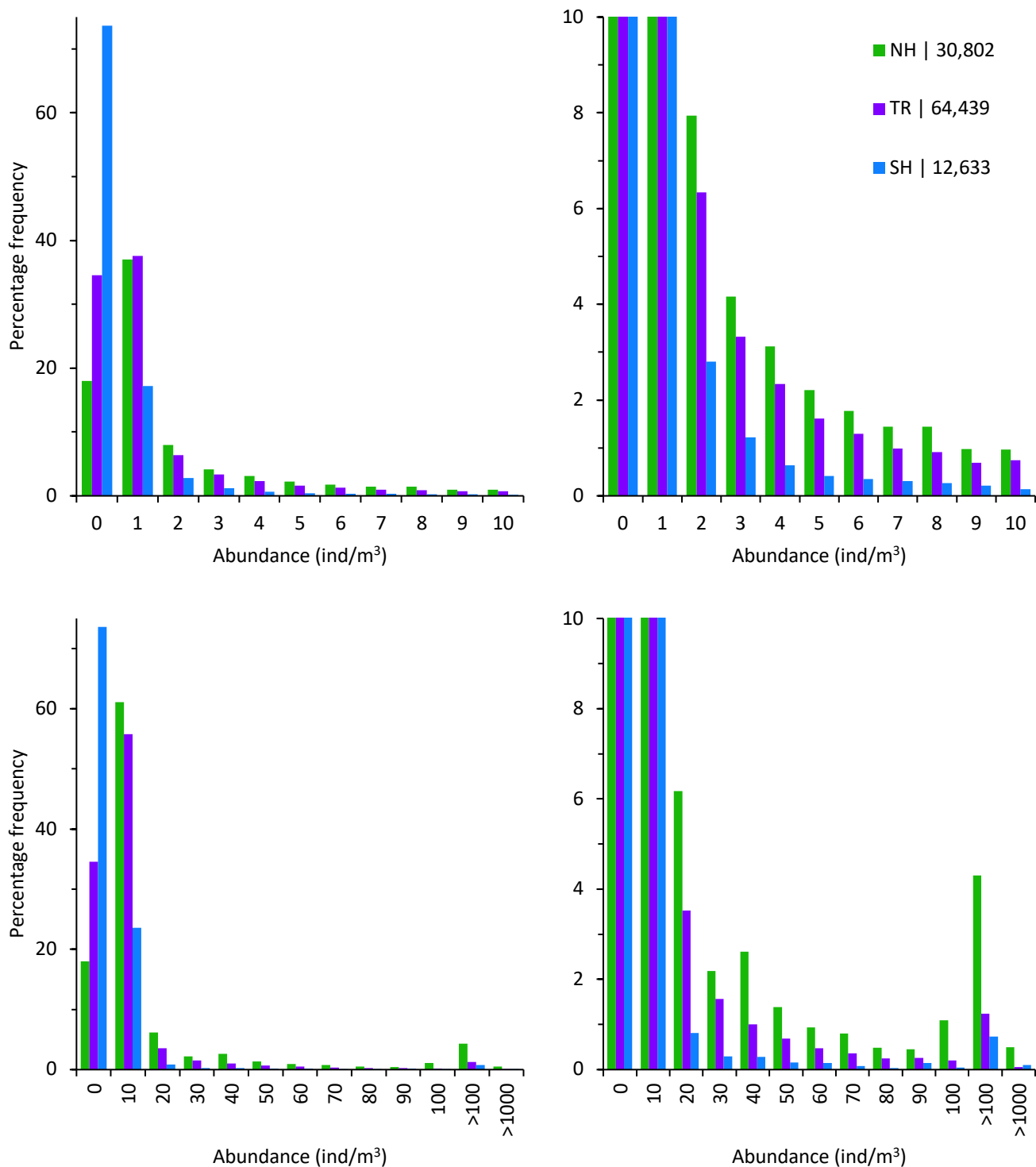


**Figure 2.3** Percentage frequency of gelatinous zooplankton abundance (number of individuals/m<sup>3</sup>) for the Northern Hemisphere (NH), Tropics (TR) and Southern Hemisphere (SH) from ungridded data. For top panels abundance is binned into 0, >0-1, 1-2, 2-3, etc. up to 9-10 ind/m<sup>3</sup>. For bottom panels abundance is binned into 0, >0-10, 10-20, 20-30, etc. up to 90-100, and then 100-1000, and >1000 ind/m<sup>3</sup>. Left panels show a difference percentage scale to right panels. The total number of samples for each of the three regions is given in the key.

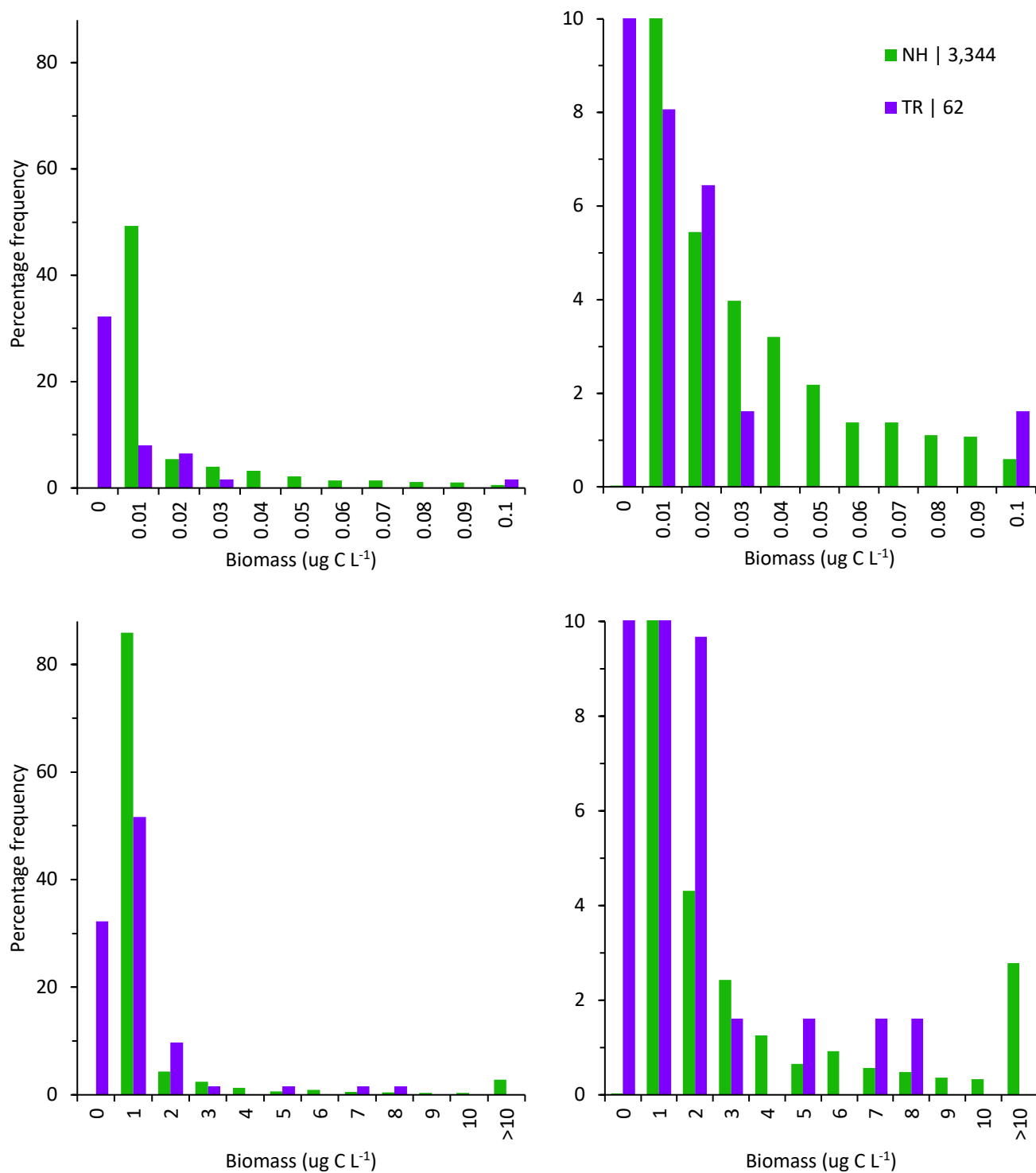


**Figure 2.4** Percentage frequency of gelatinous zooplankton biomass ( $\mu\text{g carbon L}^{-1}$ ) for the Northern Hemisphere (NH) and Tropics (TR; there were no biomass samples for the Southern Hemisphere) from ungridded data. For top panels abundance is binned into 0, >0-0.01, 0.01-0.02, 0.02-0.03, etc. up to 0.09-0.10  $\text{ind/m}^3$ . For bottom panels abundance is binned into 0, >0-1, 1-2, 2-3, etc. up to 9-10, and then >10  $\text{ind/m}^3$ . Left panels show a difference percentage scale to right panels. The total number of samples for the two regions is given in the key.

the widely fluctuating GZ abundance due to their bloom and bust dynamics, a range of percentiles are used (Fig. 2.6). The percentiles calculated are the 5<sup>th</sup>, 25<sup>th</sup>, 50<sup>th</sup> (median), 75<sup>th</sup> and 95<sup>th</sup>, to demonstrate the spread of abundance data, and the chance of a certain abundance occurring in each month. The median (50<sup>th</sup> percentile) shows the background abundance observed 50% of the time, whilst the 75<sup>th</sup> and 95<sup>th</sup> percentiles represent occasional and rare blooms (Fig. 2.6).

The Northern Hemisphere Provinces (ALSK, CALC, NWCS, NECS, KURO and NPSW; Fig. 2.5) show a mostly low background abundance of GZ (median of <2 ind/m<sup>3</sup>) punctuated with strong peaks in abundance (i.e. 75<sup>th</sup> percentile >20 ind/m<sup>3</sup>). The Northern Hemisphere Provinces differ mostly in the timing and amplitude of the peaks (Fig. 2.6).

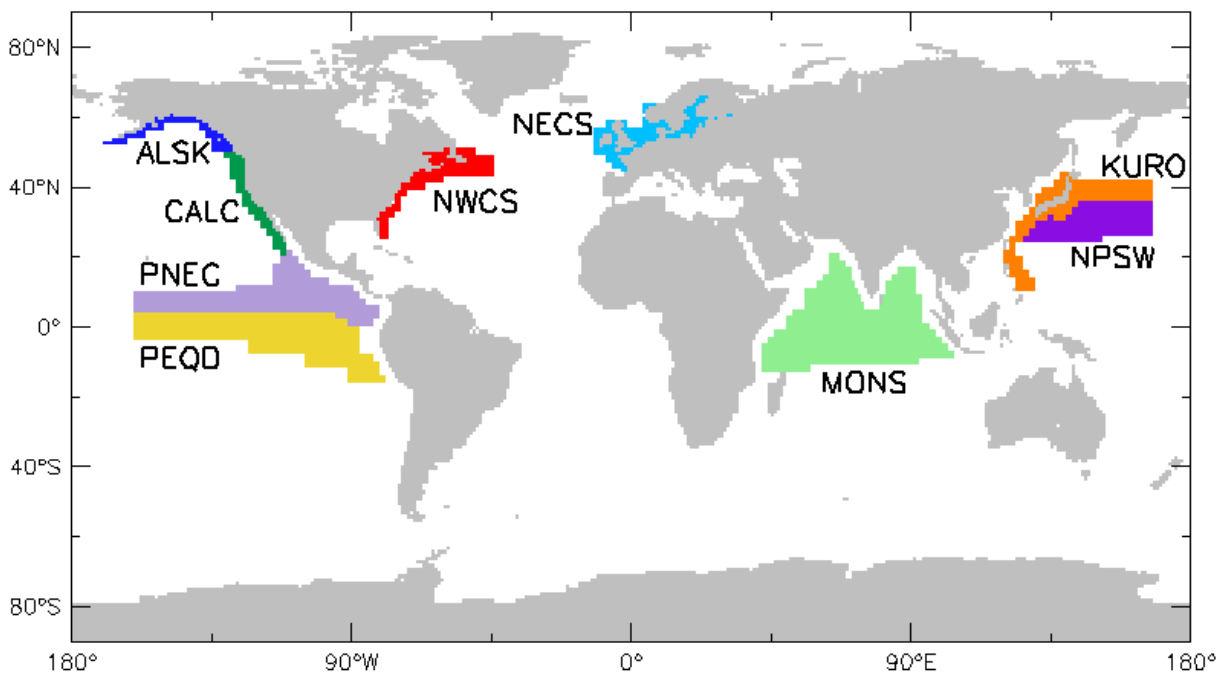


**Figure 2.5** Global map showing the Longhurst Provinces used in this analysis, each colour represents the area of a different Longhurst Province, labelled with the name. The Provinces are Alaska Coastal Downwelling Province (ALSK; dark blue), California Current Province (CALC; dark green), Northwest Atlantic Shelves Province (NWCS; red), Northeast Atlantic Shelves Province (NECS; light blue), Kuroshio Current Province (KURO; orange), North Pacific Subtropical West (NPSW; dark purple), North Pacific Equatorial Countercurrent Province (PNEC; light purple), Pacific Equatorial Divergence Province (PEQD; yellow) and the Indian Monsoon Gyres Province (MONS; light green).

The seasonal cycle for ALSK shows peaks in abundance in June, August and November, with the strongest bloom in August exceeding 25 ind/m<sup>3</sup> (75<sup>th</sup> percentile), with a median of 11 ind/m<sup>3</sup> (Fig. 2.6). For the rest of the year (where data are available) the median abundance is around 1 ind/m<sup>3</sup>. A strong bloom (>25 ind/m<sup>3</sup>) occasionally occurs (in the 95<sup>th</sup> percentile) in July and November (Fig. 2.6).

The seasonal cycle for CALC shows peaks in abundance in May (median of 5 ind/m<sup>3</sup>, 75<sup>th</sup> percentile 20 ind/m<sup>3</sup>) and November (median of 8 ind/m<sup>3</sup>, 75<sup>th</sup> percentile 9 ind/m<sup>3</sup>). There are some occurrences of blooms in February with the 95<sup>th</sup> percentile of 16 ind/m<sup>3</sup> and a median of 3 ind/m<sup>3</sup> (Fig. 2.5). For the rest of the year (except December, where no data are available) the 75<sup>th</sup> percentile is around 3 ind/m<sup>3</sup> or less (Fig. 2.6). A strong bloom (>25 ind/m<sup>3</sup>) occasionally occurs (in the 95<sup>th</sup> percentile) in May and November (Fig. 2.6).

The seasonal cycle for NWCS shows peaks in abundance for a large portion of the year, with the high abundance (75<sup>th</sup> percentile over 10 ind/m<sup>3</sup>) found in January, February, July to September, November and December (Fig. 2.6). The median is zero ind/m<sup>3</sup> for most of the year, except for February, July and November. A strong bloom (>25 ind/m<sup>3</sup>) occasionally occurs (in the 95<sup>th</sup> percentile) in every month except for May, October and November (Fig. 2.6).

The seasonal cycle for NECS shows peaks in abundance in March (median of 50 ind/m<sup>3</sup>, 75<sup>th</sup> percentile of 200 ind/m<sup>3</sup>) and August (median of 4 ind/m<sup>3</sup>, 75<sup>th</sup> percentile of 48 ind/m<sup>3</sup>). For the rest of the year the median abundance is zero ind/m<sup>3</sup> (Fig. 2.6). A strong bloom (>25 ind/m<sup>3</sup>) occasionally occurs (in the 95<sup>th</sup> percentile) from March to September (Fig. 2.6).

The seasonal cycle for KURO shows peaks in abundance from March to April, July to August and November with the 75<sup>th</sup> percentile mostly over 10 ind/m<sup>3</sup> (Fig. 2.6). Throughout the year KURO has a persistent background abundance with the median between 1 – 5 ind/m<sup>3</sup>, and few data showing zero abundance. A strong bloom (>25 ind/m<sup>3</sup>) occasionally occurs (in the 95<sup>th</sup> percentile) from March to April, and July to August (Fig. 2.6).

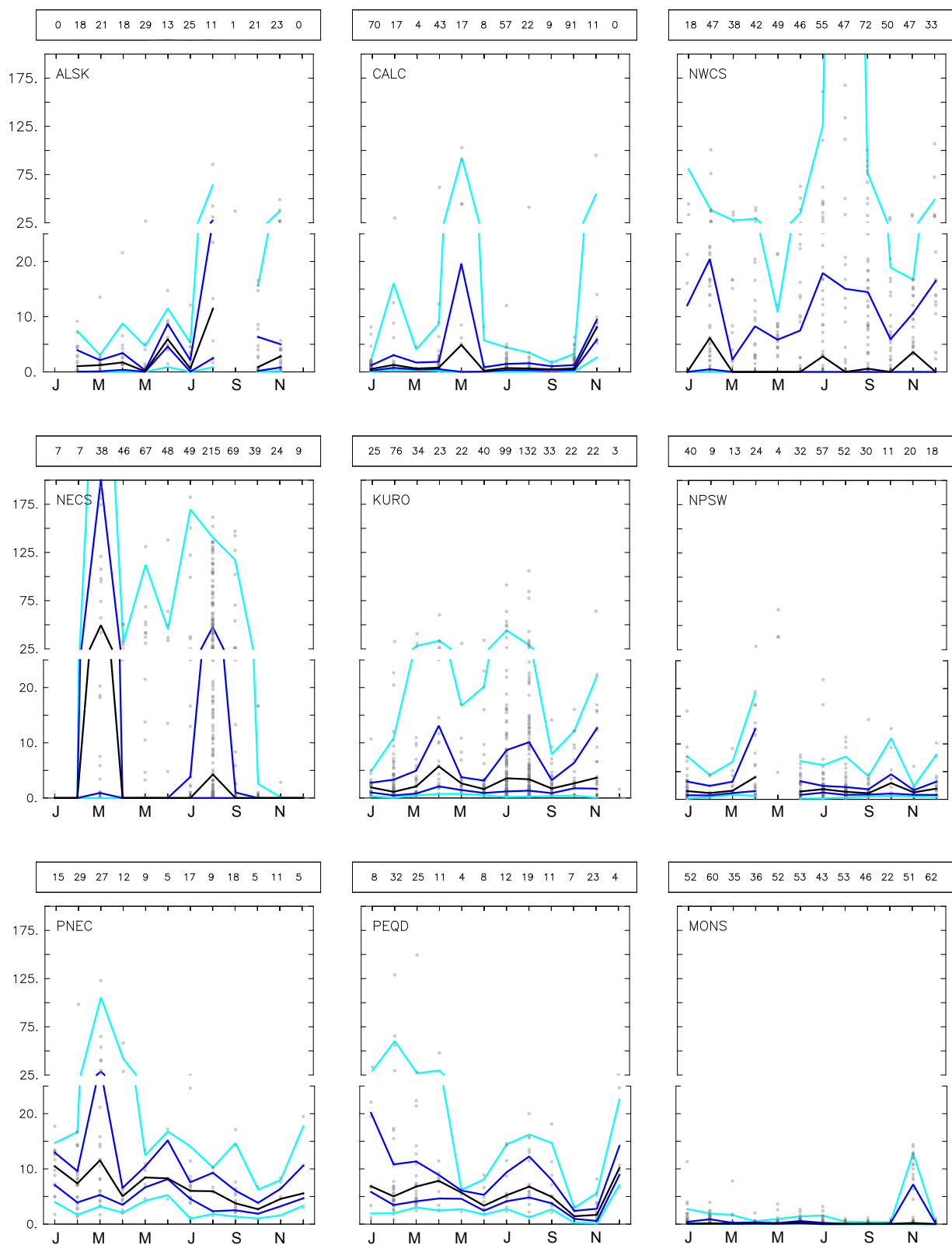


**Figure 2.6** Seasonal abundance of gelatinous zooplankton for nine ocean provinces shown in Fig. 2.5 (number of ind/m<sup>3</sup>). For each month the light blue line shows the 5<sup>th</sup> and 95<sup>th</sup> percentile, the dark blue lines shows the 25<sup>th</sup> and 75<sup>th</sup> percentile, and the black line is the 50<sup>th</sup> percentile/median. All the data points are shown in grey. For months with less than 4 data points, no percentiles are calculated. Across the top of each panel the number of data per month for that province is given. The graphs have been stretched at the lower values (0 – 25) as this is where the majority of the data occurs. All panels are on the same axis. See Figure 2.5 for locations and full name of each province.



The seasonal cycle for NPSW has a peak in abundance in April, with a 75<sup>th</sup> percentile of 12 ind/m<sup>3</sup>. Throughout the year the median is around 2 – 4 ind/m<sup>3</sup>, and in every month except for April, the 75<sup>th</sup> percentile is from 3 – 5 ind/m<sup>3</sup> (Fig. 2.6). The highest 95<sup>th</sup> percentile is in April when the abundance is 20 ind/m<sup>3</sup> (Fig. 2.6).

The two Provinces covering the Pacific equatorial upwelling (PNEC and PEQD) have similar seasonal cycle patterns. PNEC has peaks in abundance in January, March, June and December, and PEQD has peaks in abundance from January to March, August and December (75<sup>th</sup> percentiles over 10 ind/m<sup>3</sup>; Fig. 2.6). PNEC and PEQD have the highest background year-round abundance of all the Provinces, with the median only dropping below 5 ind/m<sup>3</sup> in the autumn. A strong bloom (>25 ind/m<sup>3</sup>) occasionally occurs (in the 95<sup>th</sup> percentile) in PNEC from March to April, and in PEQD from January to April (Fig. 2.6).

The seasonal cycle for MONS has a peak in abundance in April, with a 75<sup>th</sup> percentile of 7 ind/m<sup>3</sup>. MONS has the lowest year-round abundance of all the Provinces, with the median always <1 ind/m<sup>3</sup>, and the 95<sup>th</sup> percentile only getting above 3 ind/m<sup>3</sup> in November (Fig. 2.6).

### 2.3.3 Phylum Baselines

Most of the data in the MAREDAT database is for Tunicata, followed by Cnidaria, Ctenophora and Unclassified samples (Table 2.1, Fig. 2.7). This difference in the amount of data is most likely due to sampling techniques, where Ctenophora are often overlooked in samples due to specimens disintegrating, are simply not targeted during surveys, or are actively excluded, as is often the case for all GZ groups (Purcell, 2009). Ctenophora also have the highest number of 0 abundance recorded (Fig. 2.7).

For abundance (ind/m<sup>3</sup>), Tunicata are the dominant phyla with the highest arithmetic mean (AM; 12.69), geometric mean (GM; 1.62) and median (0.43), followed by Cnidaria (AM 3.57, GM 0.77 and median 0.02), and then Ctenophora (AM 0.13, GM 0.03 and median 0.00). Cnidaria have a significantly higher carbon biomass (AM 3.61, GM 0.95 and median 0.29 µg C L<sup>-1</sup>) than Tunicata (AM 0.09, GM 0.05 and median 0.002 µg C L<sup>-1</sup>; Table 2.1). These patterns are consistent across the three averaging

**Table 2.1** Statistics of gelatinous zooplankton split into phylum from the gridded MAREDAT data. AM is the arithmetic mean, and GM is the geometric mean. No data for Ctenophora biomass was available in the dataset.

Phylum	<i>n</i>	AM	Median	GM	Min	Max	SD
<b>Abundance (individuals/m<sup>3</sup>)</b>							
<b>Tunicata</b>	7487	12.69	0.43	1.62	0.00	5040.49	96.13
<b>Cnidaria</b>	6192	3.57	0.02	0.77	0.00	1645.93	31.22
<b>Ctenophora</b>	4081	0.13	0.00	0.03	0.00	284.56	4.51
<b>Unclassified</b>	2476	1.02	0.00	0.35	0.00	161.09	5.35
<b>Biomass (µg carbon L<sup>-1</sup>)</b>							
<b>Tunicata</b>	669	0.09	0.002	0.05	0.00	13.50	0.79
<b>Cnidaria</b>	653	3.61	0.29	0.95	0.00	156.00	12.62

methods giving a high confidence in the qualitative results. Overall Tunicata were found to be the most abundant phyla group, but Cnidaria exhibit the largest biomass. This is consistent with group characteristics; Tunicata are generally the smallest sized phyla group and some types live in colonies comprising hundreds of individuals, while the Cnidaria phyla contains the largest sized individuals and make up the most conspicuous bloom formations (Chapter 1, Lucas and Dawson 2014). For example, in two blooms with equal biomass, one comprising of Tunicata and one of Cnidaria, the Tunicata bloom would be likely to have a higher number of individuals than the Cnidaria bloom to make up the same biomass.

Lucas et al. (2015) found the GM for Tunicata biomass to be 0.09 µg C L<sup>-1</sup>, similar to the GM biomass of 0.05 µg C L<sup>-1</sup> from MAREDAT (Table 2.1). There is a greater difference between the datasets for Cnidaria GM biomass, 4.43 µg C L<sup>-1</sup> (Lucas et al., 2015) compared to 0.95 µg C L<sup>-1</sup> (Table 2.1). This difference may be due to a number of reasons including the distribution of the data, the number of data and the methods with which data were collected (i.e. plankton tow vs fishing nets; see Chapter 1).

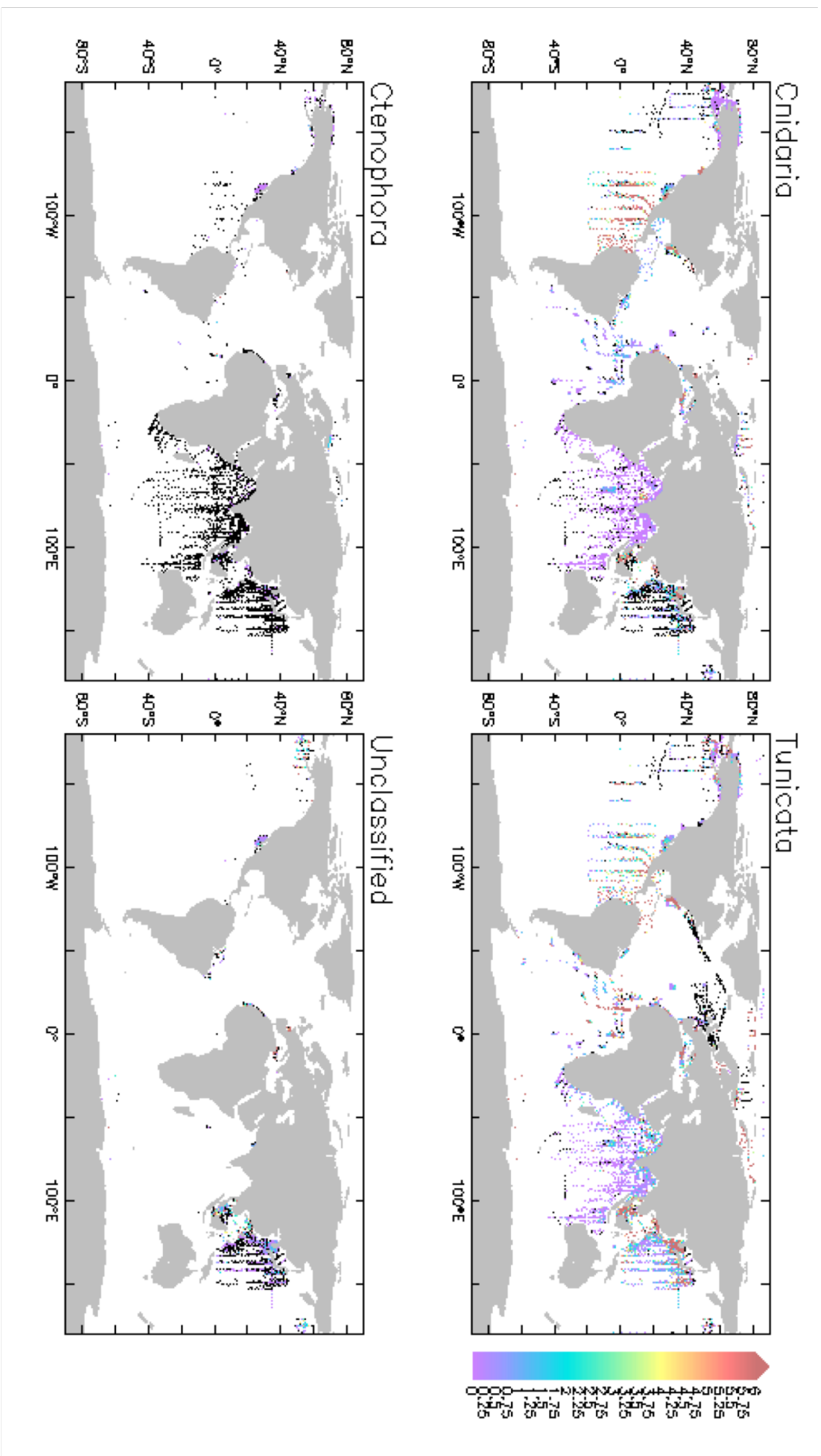


**Figure 2.7** Average Gelatinous Zooplankton abundance (individuals/m<sup>3</sup>) on a 1x1 degree grid for Cnidaria, Tunicata, Ctenophora and Unclassified. Where abundance equals 0 the data is plotted in black.

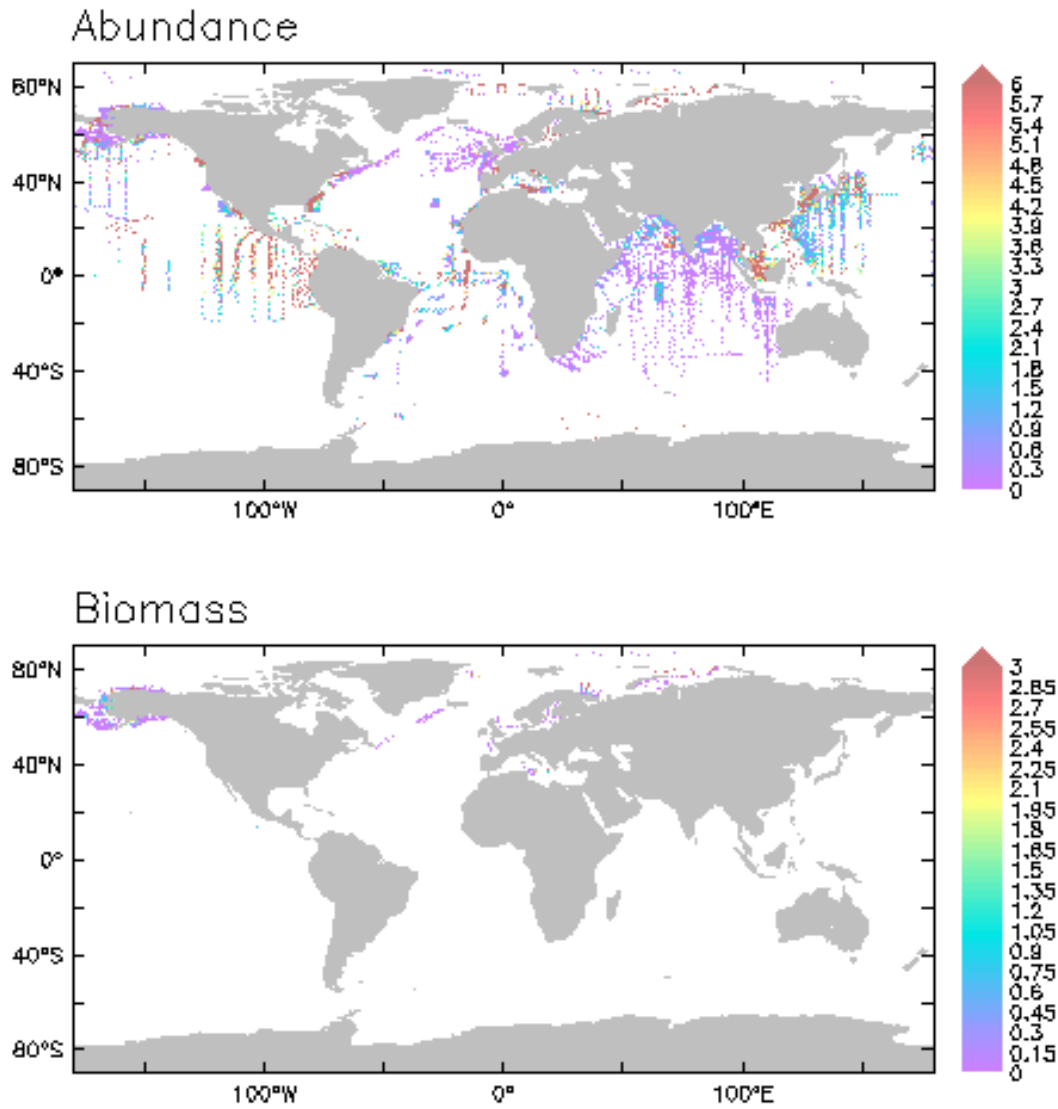


**Figure 2.8** Average gelatinous zooplankton (top) abundance (individuals/m<sup>3</sup>) and (bottom) biomass (ug carbon/L) averaged for 1930 – 2008, on a 1x1 grid.

Table 2.2 compares GZ to the other plankton types in the MAREDAT database using median (min) and AM (max). Cnidaria biomass is almost as high as the microzooplankton and higher than meso- and macrozooplankton (Table 2.2).

Cnidarian biomass data is only present in the Northern Hemisphere where GZ are more abundant which may skew the data (Fig. 2.4). Another caveat to the data is that a substantially smaller frequency of zeros is reported for biomass than for abundance (Fig. 2.3 and Fig. 2.4). Under reporting of zero values will increase the average, regardless of the averaging method used.

**Table 2.2** PFT global biomass, adapted from Buitenhuis et al. (2013). Gelatinous data calculated according to methods described in Buitenhuis. All data from MAREDAT. In Buitenhuis et al. (2013) median depth profiles are the min, and AM (arithmetic mean) depth profiles are the max.

	PFT global biomass (PgC)		
	SD	Median	AM
<b>Autotrophs</b>			
Picophytoplankton	22.1	0.28	0.64
Diazotrophs	27.4	0.008	0.12
Coccolithophores	2.4	0.001	0.03
Phaeocystis	96.0	0.11	0.71
Diatoms	104.7	0.10	0.94
<b>Heterotrophs</b>			
Picoheterotrophs	6.0	1.00	1.10
Microzooplankton	17.1	0.48	0.73
Formaninifers	0.05	0.0009	0.003
Mesozooplankton	10.6	0.33	0.59
Pteropods	25.4	0.026	0.67
Macrozooplankton	67.7	0.22	1.52
Gelatinous zooplankton		0.14	1.33
Cnidaria		0.459	3.11

### 2.3.4 Global Gelatinous Zooplankton Baselines

The GZ abundance data shows relatively good spatial coverage across the Northern Hemisphere coastal regions, as well as the Tropical Atlantic, Indian and east Pacific Oceans (Fig. 2.8). However, there are large areas with no data, particularly throughout the Southern Hemisphere as well as in the northern open ocean in the Atlantic and central Pacific (Fig. 2.8). The GZ biomass data is generally poor, with data mostly in coastal regions in the Northern Hemisphere (Fig. 2.8). The maximum abundance recorded was

**Table 2.3** Statistics of gelatinous zooplankton from the gridded MAREDAT data. AM is the arithmetic mean and GM is the geometric mean. The Northern Hemisphere is defined as 90°N-30°N, the Tropics is defined as 30°N-30°S and the Southern Hemisphere is defined as 30°S-90°S. For biomass, only the global value is given, all data points are in the Northern Hemisphere, except for one data point in the Tropics.

Area	<i>n</i>	AM	Median	GM	Min	Max	SD
<b>Abundance (individuals/m<sup>3</sup>)</b>							
<b>Global</b>	7832	10.87	0.70	1.78	0.00	3208.00	72.73
<b>Northern Hemisphere</b>	3612	16.60	0.45	2.00	0.00	2678.19	89.17
<b>Tropics</b>	3924	6.03	0.99	1.74	0.00	3208.00	55.07
<b>Southern Hemisphere</b>	296	5.18	0.01	0.40	0.00	697.32	44.78
<b>Biomass (µg carbon/L)</b>							
<b>Global</b>	849	0.60	0.001	0.18	0.00	45.73	3.11

3208 individuals/m<sup>3</sup> in the Tropics, whilst the highest biomass is 45.73 µg C L<sup>-1</sup> (Table 2.3).

There are large differences in mean values from the averaging methods because of the large spread in the data (Table 2.3). From the AM, the Northern Hemisphere has the highest abundance of GZ, around three times the Tropics or Southern Hemisphere (16.60 compared to 6.03 and 5.18 ind/m<sup>3</sup> respectively). From the median, the Tropics has the highest abundance (0.99 ind/m<sup>3</sup>), over double that of the Northern Hemisphere (0.45 ind/m<sup>3</sup>) and almost a hundred times that of the Southern Hemisphere (0.01 ind/m<sup>3</sup>). From the GM, the Northern Hemisphere also has the highest abundance, followed by the Tropics, but the difference between the means is markedly smaller (2.00 compared to 1.74 ind/m<sup>3</sup>) than for the arithmetic mean (Table 2.3).

The global abundance (ind/m<sup>3</sup>) of GZ ranges from a median of 0.70, to a GM of 1.78, up to an AM of 10.87. The global carbon biomass (µg C L<sup>-1</sup>) of GZ ranges from a median of 0.001, to a GM of 0.18, up to an AM of 0.60 (Table 2.3).

Buitenhuis et al. (2013) calculated a range of global plankton biomasses from MAREDAT, using the median as minimum and the AM as the maximum, and multiplying by the ocean volume of the top 200m to provide an estimate in PgC. Using this same approach, the range of GZ biomass is therefore 0.14 (median) to 1.33 PgC (AM; Table 2.2). The GZ biomass is similar to and possibly lower than macrozooplankton biomass of 0.22 – 1.52 PgC (Table 2.2), where macrozooplankton is defined as crustaceans such as krill (Buitenhuis et al., 2013). In Moriarty et al. (2013) macrozooplankton is defined as all zooplankton in MAREDAT with an adult size greater than 2mm, this includes the GZ data analysed here, the macrozooplankton in Table 2.2 as well as Gastropoda, Heteropoda, Pteropoda, Chaetognatha, Polychaeta, Amphipoda, Stomatopoda, Mysida, Decapoda and Euphausiids. The >2mm zooplankton biomass of 0.02 – 1.06 PgC (Moriarty et al., 2013) is similar to and lower than the GZ biomass and the macrozooplankton biomass (Table 2.2). Many of the data points for the groups within the MAREDAT >2mm zooplankton subset are not co-located (Moriarty et al., 2013).

These varying biomass values highlight the importance of categorising zooplankton by more than just size, including characteristics such as body type and trophic level. Even within the GZ taxa, Cnidaria biomass was 140 times larger than Tunicata for the median, and 19 times larger for the GM (Table 2.1).

Lucas et al. (2014) report a GM of global GZ biomass of 0.038 PgC, from the JeDI database. Using the same method with the MAREDAT database produces a GM global GZ biomass of 0.014 PgC (Table 2.2), less than half of the biomass found by Lucas et al. (2014). The difference likely arises from several disparities between the two databases. Firstly, a greater proportion of biomass of zero are recorded in the MAREDAT database than the JeDI database. Secondly, MAREDAT has a greater depth range than Lucas (0-200m), although the majority of data in MAREDAT (97.9%) was from the top 200m. Thirdly, in the MAREDAT database all but 1 data point for carbon biomass occur in the Northern Hemisphere (north of 30°N), whereas JeDI has coverage in the Tropics and Southern Hemisphere (Lucas et al., 2014). The difference in global GZ biomass is larger between the averaging methods than it is between the two databases, despite these disparities between the databases.

## 2.4 Discussion

Global marine biogeochemical models are gradually increasing the complexity of the modelled plankton food web to better understand biogeochemical cycles and assess the implications of climate change (Le Quéré et al., 2016). The lack of global assessments of PFT biomasses has been a key hindrance to model development. This study adds to the growing base of data products that can be used to validate global ocean models (Buitenhuis et al., 2006, Buitenhuis et al., 2010, Buitenhuis et al., 2013, Moriarty et al., 2013).

The description of GZ seasonal baselines for nine Longhurst Provinces is a key result from this study (Fig. 2.6). This is the first study to establish seasonal baselines from long-term, multi-source data. Previously only studies based on single locations had determined seasonal baselines from longer-term data, generally for inshore coastal areas (Molinero et al., 2008, Sullivan et al., 2001, Van Walraven et al., 2015). The seasonal baselines provide statistical information on the likely timing of bloom conditions, and their strength and frequency. It is this information on bloom timing and frequency that is of most use to coastal industries. Coastal industries, including aquaculture farms, nuclear power plants and beach tourism are negatively impacted by GZ blooms (Purcell et al., 2007, Quinones et al., 2013, Gibbons and Richardson, 2013). Better understanding the likely timing, frequency and intensity of blooms can help planning and mitigation efforts (Richardson et al., 2009, Gershwin et al., 2010, Gershwin et al., 2014, Graham et al., 2014). The seasonal baselines also provide global and regional validation data to inform model development, and can serve to evaluate future changes such as shifts in seasonality due to climate change (Molinero et al., 2008, Sullivan et al., 2001, Van Walraven et al., 2015, Graham et al., 2014). The MAREDAT data was insufficient to establish seasonal baselines for provinces in the Southern Hemisphere.

The bloom and bust nature of GZ is dominant in the data (Fig. 2.3 and Fig. 2.4) and creates challenges for averaging abundance and biomass values, as for many other patchy plankton data, that also exhibit strong seasonal cycles of bloom and bust (Buitenhuis et al., 2013). There is a greater variance between the results from the different averaging methods than between the MAREDAT and JeDI databases. Use of



all three averaging methods, AM, GM and median together provides a more representative view of global and regional baselines, and the spread of the data.

Data reporting of GZ is generally skewed towards coastal regions with large human populations, and/or coastal regions with large commercial fisheries. Studies and funding of GZ are often targeted to areas where they are known to bloom and cause issues for industries (Sullivan and Kremer, 2011). This bias in data reporting occurs for many marine organisms outside of the GZ group (McRae et al., 2017, Purcell, 2012, Sullivan and Kremer, 2011). Growing evidence points towards an increase in GZ populations from human influences on the coastal marine environment (Purcell et al., 2007, Purcell, 2012, Greene et al., 2015), which may skew the calculation of a global baseline towards higher values. Human influences on the coastal marine environment include increasing artificial hard substrates from the development of ports, coastal defence, renewable energy structures and more. These artificial hard substrates have been linked to increasing GZ populations, particularly Cnidaria, where a benthic stage to the life cycle of many species benefits from the additional hard substrate available for settling (Lucas et al., 2012, Purcell, 2012, Duarte et al., 2013). Over-fishing, particularly of planktivorous species such as sardines, is thought to increase GZ populations, through the removal of competitors for prey (Pauly et al., 2009, Flynn et al., 2012, Jensen et al., 2012, Purcell, 2012, Roux et al., 2013). Open ocean regions and the Southern Hemisphere are the most under reported (Fig. 2.2), and they are likely to have lower concentrations compared with coastal areas.

The sampling of GZ has increased in intensity over recent decades (Condon et al., 2012, Pitt et al., 2018). If GZ populations have increased over this same time period then the baselines calculated from the data will be skewed towards a higher value, giving a 'sliding frame of reference' (Condon et al., 2012) more representative of recent decades than a longer time period. However, the GZ subset of the MAREDAT database does not follow this general trend of increasing sampling over time and is more likely biased towards intensive sampling in the 1960's in the Tropics and the 1970's in the Northern Hemisphere (Fig. 2.2). The peaks and troughs in sampling are due to inconsistencies in funding and attention for GZ research, as they have not traditionally been included in regular marine ecosystem or fisheries surveys, although this is beginning to change (Aubert et al., 2018). Unfortunately, both the MAREDAT

and JeDI databases have not been updated for several years (ending in 2008 and 2011 respectively), during which time the trend of increasing sampling has continued. For both databases this is due to the cessation of funding. The notion of extending GZ samples in MAREDAT past 2008 was discussed during the execution of this work, but it was decided that it was outside the scope and timescale of this PhD, where the primary aim is to include GZ in a global biogeochemical model.

Under reporting of zero biomass also has the potential to lead to over-estimated GZ baselines. This issue occurs for both abundance and biomass data but is emphasised in this analysis through the large difference in zero frequency between the abundance and biomass data (Fig. 2.3 and Fig. 2. 4). Analysis of abundance and biomass of GZ is therefore likely to overestimate values, this overestimation applies to the analysis carried out in this Chapter as well as other analysis of GZ abundance and biomass (Lucas et al., 2014). Including reports of zero biomass for taxa within ecosystem surveys is as important as records greater than zero, recording zero biomass in an area or time is very different to having no records.

The large difference in the number of data available between abundance and biomass is due to low-quality reporting of GZ (Fig. 2.2; Gibbons and Richardson, 2013). Biomass can only be calculated where either dry weight or wet weight is reported along with species level. For the majority of GZ data in MAREDAT only the number of individuals is recorded, with taxonomic identification only to phylum (Buitenhuis et al., 2013). The caveats of the GZ subset of MAREDAT are similar as those for the broader zooplankton subset of MAREDAT (Moriarty et al., 2013) and for the whole database (Buitenhuis et al., 2013). The key caveat in the GZ subset is that the data is not uniformly distributed spatially or temporally and not proportionally distributed between various biomes of the ocean, with abundance skewed to coastal regions and biomass only in the coastal Northern Hemisphere.

## **2.5 Conclusion**

It is hard to untangle which factors, and to what extent each factor is playing in influencing the GZ biomass, even with an idea of baselines and trends of biomass (Pauly et al., 2009). Such factors could include direct metabolic changes driven by

rising temperatures, earlier springs and longer summers, or indirect climatic-driven changes to the prey and competitors of GZ. Biogeochemical modelling can help to untangle these factors. The availability of global baseline GZ biomass and seasonality will help improve and validate global ocean models (Gibbons and Richardson, 2013).

The bloom and bust dynamics of GZ populations is confirmed by this analysis to be widespread in the Northern Hemisphere and to some extent in the equatorial Pacific. This study has established GZ seasonal baselines, on the likely timing of bloom conditions and their strength and frequency, for nine Longhurst Provinces in the Northern Hemisphere and Tropics. Future work could apply the methods used here to other GZ databases such as JeDI to increase global coverage. Within the uncertainties discussed above, carbon biomass for GZ appears equivalent with carbon biomass for macrozooplankton (crustacean), mesozooplankton and microzooplankton calculated from MAREDAT, confirming the importance of GZ in global marine ecosystems. Carbon biomass for GZ varies more between statistical methods than between databases. It is recommended that all studies into GZ biomass use a range of averaging methods to best represent the baseline and range of data. An assessment of a trend over time is not possible at this stage because of the combination of an incomplete database (especially carbon biomass) and the bloom and bust dynamics of GZ. It is also recommended that there is an integration of the GZ subset of the MAREDAT database with the JeDI database, and that the databases are updated to include the numerous sampling efforts of recent years, to give a fuller picture of GZ abundance and biomass.

## References

- ATTRILL, M., WRIGHT, J. & EDWARDS, M. 2007. Climate-related increases in jellyfish frequency suggest a more gelatinous future for the North Sea. *Limnology and Oceanography*, 52, 480-485.
- ATTRILL, M. J. & EDWARDS, M. 2008. Reply to Haddock, S. H. D. Reconsidering evidence for potential climate-related increases in jellyfish. *Limnology and Oceanography*, 53, 2763-2766.
- AUBERT, A., ANTAJAN, E., LYNAM, C., PITOIS, S., PLIRU, A., VAZ, S. & THIBAUT, D. 2018. No more reason for ignoring gelatinous zooplankton in ecosystem assessment and marine management: Concrete cost-effective methodology during routine fishery trawl surveys. *Marine Policy*, 89, 100-108.
- BOERO, F., BOUILLON, J., GRAVILI, C., MIGLIETTA, M. P., PARSONS, T. & PIRAINO, S. 2008. Gelatinous plankton: irregularities rule the world (sometimes). *Marine Ecology Progress Series*, 356, 299-310.
- BOYCE, D. G., LEWIS, M. R. & WORM, B. 2010. Global phytoplankton decline over the past century. *Nature*, 466, 591.
- BRAVO, V., PALMA, S. & SILVA, N. 2011. Seasonal and vertical distribution of medusae in Aysen region, southern Chile. *Latin American Journal of Aquatic Research*, 39, 359-377.
- BRODEUR, R. D., DECKER, M. B., CIANNELLI, L., PURCELL, J. E., BOND, N. A., STABENO, P. J., ACUNA, E. & HUNT JR, G. L. 2008. Rise and fall of jellyfish in the eastern Bering Sea in relation to climate regime shifts. *Progress in Oceanography*, 77, 103-111.
- BROTZ, L., CHEUNG, W. W. L., KLEISNER, K., PAKHOMOV, E. & PAULY, D. 2012. Increasing jellyfish populations: trends in Large Marine Ecosystems. *Hydrobiologia*, 690, 3-20.
- BUITENHUIS, E., LE QUÉRE, C., AUMONT, O., BEAUGRAND, G., BUNKER, A., HIRST, A., IKEDA, T., O'BRIEN, T., PIONTKOVSKI, S. & STRAILE, D. 2006. Biogeochemical fluxes through mesozooplankton. *Global Biogeochemical Cycles*, 20.
- BUITENHUIS, E. T., RIVKIN, R. B., SAILLEY, S. & QUÉRE, C. L. 2010. Biogeochemical fluxes through microzooplankton. *Global Biogeochemical Cycles*, 24.

- BUITENHUIS, E. T., VOGT, M., MORIARTY, R., BEDNARSEK, N., DONEY, S. C., LEBLANC, K., LE QUERE, C., LUO, Y. W., O'BRIEN, C., O'BRIEN, T., PELOQUIN, J., SCHIEBEL, R. & SWAN, C. 2013. MAREDAT: towards a world atlas of MARine Ecosystem DATa. *Earth System Science Data*, 5, 227-239.
- CONDON, R., LUCAS, C., DUARTE, C. & PITT, K. 2014. Jellyfish Database Initiative: Global records on gelatinous zooplankton for the past 200 years, collected from global sources and literature. *In: PROJECT, T. B. (ed.). Biological and Chemical Oceanography Data Management Office (BCO-DMO).*
- CONDON, R. H., DUARTE, C. M., PITT, K. A., ROBINSON, K. L., LUCAS, C. H., SUTHERLAND, K. R., MIANZAN, H. W., BOGEBERG, M., PURCELL, J. E., DECKER, M. B., UYE, S.-I., MADIN, L. P., BRODEUR, R. D., HADDOCK, S. H. D., MALEJ, A., PARRY, G. D., ERIKSEN, E., QUINONES, J., ACHA, M., HARVEY, M., ARTHUR, J. M. & GRAHAM, W. M. 2013. Recurrent jellyfish blooms are a consequence of global oscillations. *Proceedings of the National Academy of Sciences of the United States of America*, 110, 1000-1005.
- CONDON, R. H., GRAHAM, W. M., DUARTE, C. M., PITT, K. A., LUCAS, C. H., HADDOCK, S. H. D., SUTHERLAND, K. R., ROBINSON, K. L., DAWSON, M. N., DECKER, M. B., MILLS, C. E., PURCELL, J. E., MALEJ, A., MIANZAN, H., UYE, S.-I., GELCICH, S. & MADIN, L. P. 2012. Questioning the Rise of Gelatinous Zooplankton in the World's Oceans. *Bioscience*, 62, 160-169.
- DONEY, S. C., RUCKELSHAUS, M., DUFFY, J. E., BARRY, J. P., CHAN, F., ENGLISH, C. A., GALINDO, H. M., GREBMEIER, J. M., HOLLOWED, A. B., KNOWLTON, N., POLOVINA, J., RABALAIS, N. N., SYDEMAN, W. J. & TALLEY, L. D. 2012. Climate Change Impacts on Marine Ecosystems. *Annual Review of Marine Science, Vol 4*, 4, 11-37.
- DOYLE, T. K., HAYS, G. C., HARROD, C. & HOUGHTON, J. D. 2014. Ecological and societal benefits of jellyfish. *Jellyfish blooms*. Springer.
- DUARTE, C. M., PITT, K. A., LUCAS, C. H., PURCELL, J. E., UYE, S.-I., ROBINSON, K., BROTZ, L., DECKER, M. B., SUTHERLAND, K. R., MALEJ, A., MADIN, L., MIANZAN, H., GILI, J.-M., FUENTES, V., ATIENZA, D., PAGES, F., BREITBURG, D., MALEK, J., GRAHAM, W. M.

- & CONDON, R. H. 2013. Is global ocean sprawl a cause of jellyfish blooms? *Frontiers in Ecology and the Environment*, 11, 91-97.
- FLYNN, B. A., RICHARDSON, A. J., BRIERLEY, A. S., BOYER, D. C., AXELSEN, B. E., SCOTT, L., MOROFF, N. E., KAINGE, P. I., TJIZOO, B. M. & GIBBONS, M. J. 2012. Temporal and spatial patterns in the abundance of jellyfish in the northern Benguela upwelling ecosystem and their link to thwarted pelagic fishery recovery. *African Journal of Marine Science*, 34, 131-146.
- FRANCIS, T. B., SCHEUERELL, M. D., BRODEUR, R. D., LEVIN, P. S., RUZICKA, J. J., TOLIMIERI, N. & PETERSON, W. T. 2012. Climate shifts the interaction web of a marine plankton community. *Global Change Biology*, 18, 2498-2508.
- GERSHWIN, L.-A., CONDIE, S. A., MANSBRIDGE, J. V. & RICHARDSON, A. J. 2014. Dangerous jellyfish blooms are predictable. *Journal of the Royal Society Interface*, 11.
- GERSHWIN, L.-A., DE NARDI, M., WINKEL, K. D. & FENNER, P. J. 2010. Marine Stingers: Review of an Under-Recognized Global Coastal Management Issue. *Coastal Management*, 38, 22-41.
- GIBBONS, M. J. & RICHARDSON, A. J. 2009. Patterns of jellyfish abundance in the North Atlantic. *Hydrobiologia*, 616, 51-65.
- GIBBONS, M. J. & RICHARDSON, A. J. 2013. Beyond the jellyfish joyride and global oscillations: advancing jellyfish research. *Journal of Plankton Research*, 35, 929-938.
- GRAHAM, W. M., GELCICH, S., ROBINSON, K. L., DUARTE, C. M., BROTZ, L., PURCELL, J. E., MADIN, L. P., MIANZAN, H., SUTHERLAND, K. R., UYE, S.-I., PITT, K. A., LUCAS, C. H., BOGEBERG, M., BRODEUR, R. D. & CONDON, R. H. 2014. Linking human well-being and jellyfish: ecosystem services, impacts, and societal responses. *Frontiers in Ecology and the Environment*, 12, 515-523.
- GREENE, C., KUEHNE, L., RICE, C., FRESH, K. & PENTTILA, D. 2015. Forty years of change in forage fish and jellyfish abundance across greater Puget Sound, Washington (USA): anthropogenic and climate associations. *Marine Ecology Progress Series*, 525, 153-170.
- HADDOCK, S. H. D. 2008. Reconsidering evidence for potential climate-related increases in jellyfish. *Limnology and Oceanography*, 53, 2759-2762.

- HENSON, S. A., SARMIENTO, J. L., DUNNE, J. P., BOPP, L., LIMA, I. D., DONEY, S. C., JOHN, J. & BEAULIEU, C. 2010. Detection of anthropogenic climate change in satellite records of ocean chlorophyll and productivity. *Biogeosciences*, 7, 621-640.
- JENSEN, O. P., BRANCH, T. A. & HILBORN, R. 2012. Marine fisheries as ecological experiments. *Theoretical Ecology*, 5, 3-22.
- KLEIN, S. G., PITT, K. A., RATHJEN, K. A. & SEYMOUR, J. E. 2014. Irukandji jellyfish polyps exhibit tolerance to interacting climate change stressors. *Global Change Biology*, 20, 28-37.
- LAMB, P. D., HUNTER, E., PINNEGAR, J. K., CREER, S., DAVIES, R. G. & TAYLOR, M. I. 2017. Jellyfish on the menu: mtDNA assay reveals scyphozoan predation in the Irish Sea. *Royal Society Open Science*, 4.
- LE QUÉRÉ, C., BUITENHUIS, E. T., MORIARTY, R., ALVAIN, S., AUMONT, O., BOPP, L., CHOLLET, S., ENRIGHT, C., FRANKLIN, D. J., GEIDER, R. J., HARRISON, S. P., HIRST, A., LARSEN, S., LEGENDRE, L., PLATT, T., PRENTICE, I. C., RIVKIN, R. B., SATHYENDRANATH, S., STEPHENS, N., VOGT, M., SAILLEY, S. & VALLINA, S. M. 2016. Role of zooplankton dynamics for Southern Ocean phytoplankton biomass and global biogeochemical cycles. *Biogeosciences*, 13, 4111-4133.
- LEBRATO, M., PITT, K. A., SWEETMAN, A. K., JONES, D. O., CARTES, J. E., OSCHLIES, A., CONDON, R. H., MOLINERO, J. C., ADLER, L. & GAILLARD, C. 2012. Jelly-falls historic and recent observations: a review to drive future research directions. *Hydrobiologia*, 690, 227-245.
- LILLEY, M. K. S., BEGGS, S. E., DOYLE, T. K., HOBSON, V. J., STROMBERG, K. H. P. & HAYS, G. C. 2011. Global patterns of epipelagic gelatinous zooplankton biomass. *Marine Biology*, 158, 2429-2436.
- LONGHURST, A. R. 2007. *Ecological geography of the sea*, Burlington, MA, Academic Press.
- LUCAS, C. H. & DAWSON, M. N. 2014. What Are Jellyfishes and Thaliaceans and Why Do They Bloom? *Jellyfish blooms*. Springer.
- LUCAS, C. H., GRAHAM, W. M. & WIDMER, C. 2012. Jellyfish Life Histories: role of polyps in forming and maintaining scyphomedusa populations. *Advances in Marine Biology*, Vol 63, 63, 133-196.

- LUCAS, C. H., JONES, D. O. B., HOLLYHEAD, C. J., CONDON, R. H., DUARTE, C. M., GRAHAM, W. M., ROBINSON, K. L., PITT, K. A., SCHILDHAUER, M. & REGETZ, J. 2014. Gelatinous zooplankton biomass in the global oceans: geographic variation and environmental drivers. *Global Ecology and Biogeography*, 23, 701-714.
- LYNAM, C. P., ATTRILL, M. J. & SKOGEN, M. D. 2010. Climatic and oceanic influences on the abundance of gelatinous zooplankton in the North Sea. *Journal of the Marine Biological Association of the United Kingdom*, 90, 1153-1159.
- LYNAM, C. P., HAY, S. J. & BRIERLEY, A. S. 2004. Interannual variability in abundance of North Sea jellyfish and links to the North Atlantic Oscillation. *Limnology and Oceanography*, 49, 637-643.
- LYNAM, C. P., HAY, S. J. & BRIERLEY, A. S. 2005. Jellyfish abundance and climatic variation: contrasting responses in oceanographically distinct regions of the North Sea, and possible implications for fisheries. *Journal of the Marine Biological Association of the United Kingdom*, 85, 435-450.
- LYNAM, C. P., LILLEY, M. K. S., BASTIAN, T., DOYLE, T. K., BEGGS, S. E. & HAYS, G. C. 2011. Have jellyfish in the Irish Sea benefited from climate change and overfishing? *Global Change Biology*, 17, 767-782.
- MCRAE, L., DEINET, S. & FREEMAN, R. 2017. The diversity-weighted living planet index: controlling for taxonomic bias in a global biodiversity indicator. *PLoS One*, 12, e0169156.
- MOLINERO, J. C., CASINI, M. & BUECHER, E. 2008. The influence of the Atlantic and regional climate variability on the long-term changes in gelatinous carnivore populations in the northwestern Mediterranean. *Limnology and Oceanography*, 53, 1456-1467.
- MORIARTY, R., BUITENHUIS, E. T., LE QUERE, C. & GOSSELIN, M. P. 2013. Distribution of known macrozooplankton abundance and biomass in the global ocean. *Earth System Science Data*, 5, 241-257.
- MOSTOFA, K. M., LIU, C. Q., ZHAI, W., MINELLA, M., VIONE, D. V., GAO, K., MINAKATA, D., ARAKAKI, T., YOSHIOKA, T. & HAYAKAWA, K. 2016. Reviews and Syntheses: Ocean acidification and its potential impacts on marine ecosystems. *Biogeosciences*, 13, 1767-1786.



- NOGUEIRA JUNIOR, M., NAGATA, R. M. & HADDAD, M. A. 2010. Seasonal variation of macromedusae (Cnidaria) at North Bay, Florianopolis, southern Brazil. *Zoologia*, 27, 377-386.
- PAULY, D., GRAHAM, W., LIBRALATO, S., MORISSETTE, L. & PALOMARES, M. L. D. 2009. Jellyfish in ecosystems, online databases, and ecosystem models. *Hydrobiologia*, 616, 67-85.
- PITT, K. A., LUCAS, C. H., CONDON, R. H., DUARTE, C. M. & STEWART-KOSTER, B. 2018. Claims that anthropogenic stressors facilitate jellyfish blooms have been amplified beyond the available evidence: a systematic review. *Frontiers in Marine Science*, 5, 451.
- PURCELL, J. E. 2005. Climate effects on formation of jellyfish and ctenophore blooms: a review. *Journal of the Marine Biological Association of the United Kingdom*, 85, 461-476.
- PURCELL, J. E. 2009. Extension of methods for jellyfish and ctenophore trophic ecology to large-scale research. *Hydrobiologia*, 616, 23-50.
- PURCELL, J. E. 2012. Jellyfish and ctenophore blooms coincide with human proliferations and environmental perturbations. *Annual Review of Marine Science*, 4, 209-235.
- PURCELL, J. E., UYE, S.-I. & LO, W.-T. 2007. Anthropogenic causes of jellyfish blooms and their direct consequences for humans: a review. *Marine Ecology Progress Series*, 350, 153-174.
- QUINONES, J., MONROY, A., MARCELO ACHA, E. & MIANZAN, H. 2013. Jellyfish bycatch diminishes profit in an anchovy fishery off Peru. *Fisheries Research*, 139, 47-50.
- RICHARDSON, A. J., BAKUN, A., HAYS, G. C. & GIBBONS, M. J. 2009. The jellyfish joyride: causes, consequences and management responses to a more gelatinous future. *Trends in Ecology & Evolution*, 24, 312-322.
- RICHARDSON, A. J. & GIBBONS, M. J. 2008. Are jellyfish increasing in response to ocean acidification? *Limnology and Oceanography*, 53, 2040-2045.
- ROUX, J.-P., VAN DER LINGEN, C. D., GIBBONS, M. J., MOROFF, N. E., SHANNON, L. J., SMITH, A. D. & CURY, P. M. 2013. Jellyfication of marine ecosystems as a likely consequence of overfishing small pelagic fishes: lessons from the Benguela. *Bulletin of Marine Science*, 89, 249-284.

- SANZ-MARTÍN, M., PITT, K. A., CONDON, R. H., LUCAS, C. H., NOVAES DE SANTANA, C. & DUARTE, C. M. 2016. Flawed citation practices facilitates the unsubstantiated perception of a global trend toward increased jellyfish blooms. *Global Ecology and Biogeography*, 25, 1039-1049.
- SUCHMAN, C. L., BRODEUR, R. D., DALY, E. A. & EMMETT, R. L. 2012. Large medusae in surface waters of the Northern California Current: variability in relation to environmental conditions. *Hydrobiologia*, 690, 113-125.
- SULLIVAN, B., VAN KEUREN, D. & CLANCY, M. 2001. Timing and size of blooms of the ctenophore *Mnemiopsis leidyi* in relation to temperature in Narragansett Bay, RI. *Hydrobiologia*, 451, 113-120.
- SULLIVAN, L. J. & KREMER, P. 2011. Gelatinous Zooplankton and Their Trophic Roles. *Treatise on Estuarine and Coastal Science*. Waltham: Academic Press.
- VAN WALRAVEN, L., LANGENBERG, V. T., DAPPER, R., WITTE, J. I., ZUUR, A. F. & VAN DER VEER, H. W. 2015. Long-term patterns in 50 years of scyphomedusae catches in the western Dutch Wadden Sea in relation to climate change and eutrophication. *Journal of Plankton Research*, 37, 151-167.

CHAPTER 3. INCORPORATING  
JELLYFISH IN A GLOBAL  
OCEAN BIOGEOCHEMISTRY  
MODEL

The development of PlankTOM11



## Abstract

Jellyfish (here referring to Cnidaria) are increasingly recognised as important components of the marine ecosystem. However, the specific role of jellyfish in the ecosystem is less well understood than that of other zooplankton groups. Global biogeochemical models that include plankton food webs can be used to help understand processes. Here I developed the PlankTOM11 model by introducing jellyfish as the 11<sup>th</sup> plankton functional type (PFT) in the PlankTOM model series. Jellyfish is the fourth zooplankton in the model. PlankTOM11 is used to estimate the global biomass of jellyfish and assess the influence of jellyfish on the structure of the plankton community. PlankTOM11 is the first global biogeochemical model that represents jellyfish explicitly. Jellyfish are parameterised using observations of growth, grazing, respiration and mortality rates as a function of temperature. The trophic level of jellyfish is determined from observations on feeding preferences for other PFTs. Compared to the last published version of the PlankTOM model, the growth rate as a function of temperature was updated for all PFTs from a  $Q_{10}$  function (two parameters) to an optimum function (three parameters). PlankTOM11 was then tuned to reproduce available carbon biomass observations from the MAREDAT global database as well as satellite chlorophyll data. Jellyfish mortality rate was used as the key tuning parameter because it has the highest uncertainty. A control simulation was carried out, identical to PlankTOM11, but excluding the jellyfish PFT, called PlankTOM10. This control simulation is used to determine the influence of jellyfish on the biomass of the other PFTs. The global mean biomass of jellyfish in PlankTOM11 is 0.13 PgC, which is towards the lower end of the observation range (Chapter 2). Global mean phytoplankton and zooplankton biomasses are also within the observation range, at 1.01 PgC and 0.82 PgC respectively. The presence of jellyfish mainly influences macrozooplankton, with secondary effects on mesozooplankton. These changes to macro- and mesozooplankton influence the rest of the plankton community structure through trophic cascades. PlankTOM11 successfully replicates chlorophyll patterns spatially and seasonally, although with concentrations somewhat below observations. The model also achieves a high north/south chlorophyll ratio, closer to observations than the ratio achieved in PlankTOM10. The zooplankton community in PlankTOM11 was highly sensitive to the jellyfish mortality rate, with low jellyfish mortality allowing jellyfish to dominate the zooplankton. This sensitivity of the

zooplankton community to the mortality of jellyfish could help explain why jellyfish may be increasing globally, as pressures on their mortality in early-life stages decrease, allowing them to outcompete other zooplankton. However, the mortality rate is the most poorly constrained parameter for jellyfish, which may influence this sensitivity of the zooplankton community.

### 3.1 Introduction

Gelatinous zooplankton (GZ) are increasingly recognised as influential organisms in the marine environment, not just for the disruptions they can cause to coastal economies (fisheries, aquaculture and cooling intakes for power plants etc.), but also as components in marine biogeochemical cycles and key consumers of plankton. The term GZ can encompass a wide range of organisms across three phyla: Tunicata (salps), Ctenophora (comb-jellies), and Cnidaria (true jellyfish). This study focuses on Cnidaria (including Hydrozoa, Cubozoa and Scyphozoa), as they contribute 92% of the total global biomass of gelatinous zooplankton (Lucas et al., 2014). Cnidaria exhibit a radially symmetrical body plan with one opening for both feeding and excretion (gastrovascular cavity; see Fig. 1.2). They feed mostly on zooplankton using tentacles filled with stinging cells called nematocysts. Cnidaria generally have two stages in the life cycle (polyp and medusa) within which there is large reproductive and life cycle variety (Chapter 1). The other GZ groups, Tunicata and Ctenophora, are excluded from this study. There are far less data available on biomass and vital rates for Tunicata and Ctenophora than for Cnidaria. Tunicata have a different trophic level to Cnidaria, as filter feeders of phytoplankton. Ctenophora have a similar diet and trophic level to Cnidaria which results in them being considered together in some studies (Gibbons and Richardson 2013, Lucas and Dawson 2014). They are separated here as the dominance of Cnidaria in the data may misrepresent Ctenophora vital rates. Cnidaria are both independent enough from other gelatinous zooplankton, and cohesive enough to be represented as a single plankton functional type (PFT) for global modelling (Chapter 1 and 2). In this study the term jellyfish refers to Cnidaria medusa.

Jellyfish are significant consumers of plankton, especially zooplankton. The large body size to carbon content ratio of jellyfish creates a low maintenance, large feeding structure, which combined with continuous (day and night) touch-feeding allows for efficient clearance rates of the plankton (Lucas and Dawson, 2014, Acuña et al., 2011). Jellyfish are connected to lower trophic levels, with the ability to influence the plankton ecosystem structure and thus the larger marine ecosystem through trophic cascades (Pitt et al., 2007, Pitt et al., 2009, West et al., 2009). Jellyfish have the ability to rapidly form large high-density aggregations known as blooms (see Chapter 1)

which can temporarily dominate local ecosystems. Jellyfish contribute to the biogeochemical cycle through two main routes; from life through feeding processes, (including the excretion of faecal pellets, mucus and messy-eating) and from death, through the sinking of carcasses (Lebrato et al., 2012, Lebrato et al., 2013a, Chelsky et al., 2015, Pitt et al., 2009). The high biomass achieved during jellyfish blooms, and the rapid sinking of excretions from feeding and carcasses from such blooms, make them a potentially significant vector for carbon export (Lebrato et al., 2013a, Lebrato et al., 2013b).

Anthropogenic impacts from climate change (such as increasing temperature and acidity) and fishing (the removal of predators) impact the plankton, including jellyfish (Rhein, 2013, Doney et al., 2012). Multiple co-occurring impacts make it difficult to understand the role of jellyfish in the marine ecosystem, and how this role may be changed by these impacts. The paucity of historical jellyfish biomass data, especially outside of the Northern Hemisphere, has made it difficult to establish jellyfish global spatial distribution and biomass from observations (Chapter 2). PlankTOM11 will help to quantify global jellyfish biomass and the exact role of jellyfish for the global ecosystem in this chapter and in Chapter 4. The PlankTOM11 model will then be used to assess the relative influence of climate change and fisheries in a selected ocean area (Chapter 5).

This chapter describes the addition of jellyfish to the PlankTOM10 global biogeochemical model, which we call PlankTOM11. PlankTOM10 included three zooplankton: protozooplankton (mainly heterotrophic flagellates and ciliates), mesozooplankton (mainly copepods) and macrozooplankton (as crustaceans; Le Quéré et al., 2016). Jellyfish is the fourth zooplankton group, therefore introducing an additional trophic level. The jellyfish PFT was parameterised as described in this chapter using observed physiological process rates and then tuned to observed biomass data. PlankTOM11 is used to test the influence of jellyfish on ecosystem properties, by comparing PlankTOM11 simulation to an identical simulation with no jellyfish.



## 3.2 Methods

### 3.2.1 Model Description

PlankTOM11 was developed from the last published version of the PlankTOM model series (Le Quéré et al., 2016), by introducing jellyfish as an additional trophic level at the top of the plankton food web (Fig. 3.1). A full description of PlankTOM10 is published in Le Quéré et al. (2016), including all equations and parameters. Here we provide an overview of the model, focussing on the parameterisation of the growth and loss rates of jellyfish and how these compare to macrozooplankton. We also describe the update of the growth rate as a function of temperature and subsequent tuning. Growth rate is the only parameterisation that changed since the previous version of the model (Le Quéré et al., 2016).

PlankTOM11 is a global ocean biogeochemistry model that simulates plankton ecosystem processes and their interactions with the environment through the representation of 11 PFTs. The 11 PFTs consist of six autotrophs (picophytoplankton, nitrogen-fixing cyanobacteria, coccolithophores, mixed phytoplankton, diatoms and *Phaeocystis*) and five heterotrophs (bacteria, protozooplankton, mesozooplankton, macrozooplankton and jellyfish zooplankton). See Table 3.1 for further details on the PFTs and Figure 3.1 for the food web interactions. Physiological parameters are fixed within each PFT, and therefore, within-PFT diversity is not included. Spatial variability within PFTs is represented through parameter-dependence on environmental conditions including temperature, nutrients, light and food availability.

The model contains 39 biogeochemical tracers, with full marine cycles of key elements carbon, oxygen, phosphorous and silicon, and simplified cycles of nitrogen and iron (Le Quéré et al., 2016). There are three detrital pools; dissolved organic carbon (OC), small particulate OC, and large particulate OC. The elements enter through riverine fluxes and are cycled and generated through the PFTs via feeding, fecal matter, messy-eating and carcasses (Buitenhuis et al., 2006, Buitenhuis et al., 2013a, Buitenhuis et al., 2010, Le Quéré et al., 2016). Model parameters are based on observations where available. The model is tuned using a global database (MAREDAT, Chapter 2) of PFT carbon biomass that was designed for model studies (Buitenhuis et al., 2013b).

**Table 3.1** Size range and descriptions of PFT groups used in PlankTOM11. Adapted from Le Quéré et al. (2016).

Name	Abbreviation	Size Range $\mu\text{m}$	Description/Includes
<b>Autotrophs</b>			
Pico-phytoplankton	PIC	0.5 – 2	Pico-eukaryotes and non N <sub>2</sub> -fixing cyanobacteria such as <i>Synechococcus</i> and <i>Prochlorococcus</i>
N <sub>2</sub> -fixers	FIX	0.7 – 2	<i>Trichodesmium</i> and N <sub>2</sub> -fixing unicellular cyanobacteria
Coccolithophores	COC	5 – 10	
Mixed-phytoplankton	MIX	2 – 200	e.g. autotrophic dinoflagellates and chrysophytes
Diatoms	DIA	20 – 200	
Phaeocystis	PHA	120 – 360	Colonial <i>Phaeocystis</i>
<b>Heterotrophs</b>			
Bacteria	BAC	0.3 – 1	Here used to subsume both heterotrophic <i>Bacteria</i> and <i>Archaea</i>
Proto-zooplankton	PRO	5 – 200	e.g. heterotrophic flagellates and ciliates
Meso-zooplankton	MES	200 – 2000	Predominantly copepods
Macro-zooplankton	MAC	>2000	Euphausiids, amphipods, and others, called ‘macrozooplankton’
Jellyfish zooplankton	JEL	200 – >20,000	Cnidaria medusa, ‘true jellyfish’

The PlankTOM11 marine biogeochemistry component is coupled online to the global ocean general circulation model Nucleus for European Modeling of the Ocean version 3.5 (NEMO 3.5). We used the global configuration with a horizontal resolution of 2° longitude by a mean resolution of 1.1° latitude using a tripolar orthogonal grid. The vertical resolution is 10m for the top 100m, decreasing to a resolution of 500m at 5km depth, and a total of 30 vertical z-levels (Madec, 2008). The ocean is described as a fluid using the Navier-Stokes equations and a nonlinear equation of state (Madec, 2008). NEMO 3.5 explicitly calculates vertical mixing at all depths using a turbulent kinetic energy model and sub-grid eddy induced mixing. The model is interactively coupled to a thermodynamic sea-ice model (LIM version 2; Timmermann et al., 2005).

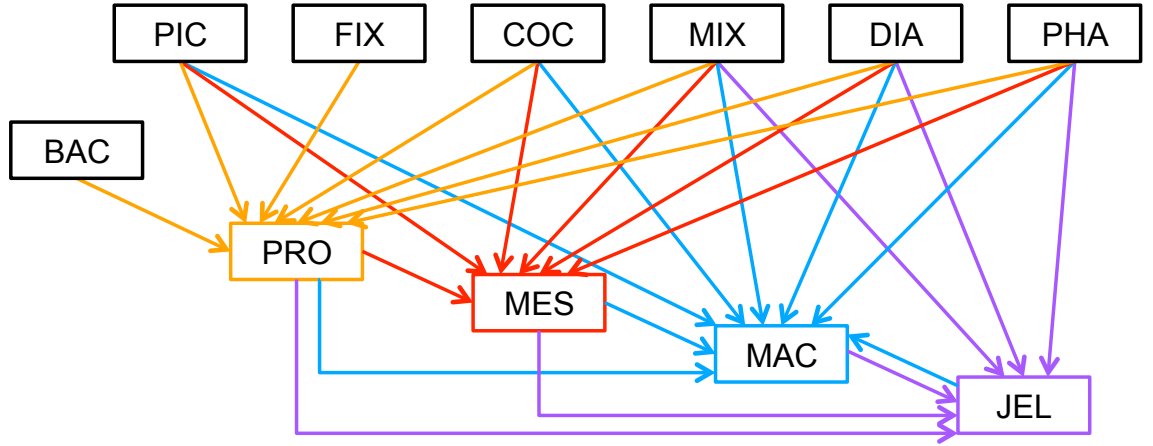


**Figure 3.1** Schematic representation of the PlankTOM11 marine ecosystem model. The arrows represent the grazing fluxes by protozooplankton (orange), mesozooplankton (red), macrozooplankton (blue) and jellyfish zooplankton (purple). Only fluxes with relative preferences above 0.1 are shown (see Table 3.3).

### 3.2.2 Jellyfish PFT Development

Jellyfish was parameterised through the formulation of growth and loss rates, following the methods used for the other zooplankton (Buitenhuis et al., 2010, Le Quéré et al., 2016). The temporal ( $t$ ) evolution of zooplankton concentration ( $Z_j$ ), is described as follows:

$$\frac{\partial Z_j}{\partial t} = \sum_k g_{F_k}^{Z_j} \times F_k \times MGE \times Z_j - \sum_{k=j+1}^3 g_{Z_j}^{Z_k} \times Z_k \times Z_j - R_{0^\circ}^{Z_j} \times d_{Z_j}^T \times Z_j \quad (3.1)$$

*growth through grazing – loss through grazing – basal respiration*

$$- m_{0^\circ}^{Z_j} \times c_{Z_j}^T \times \frac{Z_j}{K^{Z_j} + Z_j} \times \sum_i P_i$$

*– mortality through predation*

For growth through grazing,  $g_{F_k}^{Z_j}$  is the grazing of zooplankton  $Z_j$  on food source  $F_k$  and  $MGE$  is the model growth efficiency. For loss through grazing,  $g_{Z_j}^{Z_k}$  is the unassimilated fraction (messy-eating and faecal pellets)  $Z_k$  of zooplankton. For basal respiration,  $R_{0^\circ}^{Z_j}$  is the respiration rate at  $0^\circ\text{C}$ ,  $T$  is temperature,  $d_{Z_j}$  is the temperature dependence of respiration ( $d^{10} = Q_{10}$ ). For mortality through predation,  $m_{0^\circ}^{Z_j}$  is the mortality rate at  $0^\circ\text{C}$  and  $c_{Z_j}$  is the temperature dependence of the mortality ( $c^{10} = Q_{10}$ ) and  $K^{Z_j}$  is the half saturation constant for mortality.  $\sum P_i$  is the sum of all PFTs,

excluding bacteria, and is used as a proxy for the biomass of predators not explicitly included in the model. More details on each term are provided below.

### 3.2.2.1 Growth

Growth rate is the trait that most distinguishes PFTs in models (Buitenhuis et al., 2006, Buitenhuis et al., 2013a). Jellyfish growth rates were compiled as a function of temperature from the literature. In previous iterations of PlankTOM, growth as a function of temperature ( $\mu^T$ ) was fitted with two parameters:

$$\mu^T = \mu_0 \times Q_{10}^{T/10} \quad (3.2)$$

where  $\mu_0$  is the growth at 0°C,  $Q_{10}$  is the derived temperature dependence of growth and  $T$  is the observed temperature (Le Quéré et al., 2016). The jellyfish growth data had a poor fit to the exponential calculation, which resulted in a misrepresentation of the rates. The growth calculation has now been updated to a three-parameter growth rate, which produces a bell-shaped curve (Fig. 3.2 and Table 3.2). The three parameter fit is suitable for the global modelling of plankton because it can represent an exponential increase if the data support this (Schoemann et al., 2005). The growth rate as a function of temperature ( $\mu^T$ ) is now defined by; the optimal temperature ( $T_{opt}$ ), maximum growth rate ( $\mu_{max}$ ) at  $T_{opt}$ , and the temperature interval ( $dT$ ):

$$\mu^T = \mu_{max} \times \exp\left[\frac{-(T-T_{opt})^2}{dT^2}\right] \quad (3.3)$$

The three-parameter fit to the observations gives a lower Root Mean Square Error (RSME), than the two-parameter fit, for ten of the eleven PFTs. For the other PFT, the RSME is equal for both parameter fits (Fig. 3.2). The available observations measure growth rate, but the model requires specification of the grazing rate (Eq. 2). Growth of zooplankton and grazing ( $g^T$ ) are related through the gross growth efficiency (GGE):

$$g^T = \frac{u^T}{GGE} \quad (3.4)$$

GGE is the portion of grazing that is converted to biomass, which was obtained from the literature (Moriarty, 2009).

### 3.2.2.2 Grazing

The food web, and thus the trophic level of PFTs is determined through grazing preferences. The relative preference of jellyfish zooplankton for the other PFTs was

determined through a literature search and personal communications (Flynn and Gibbons, 2007, Purcell, 1992, Purcell, 1997, Stoecker, 1987, Purcell, 2003, Colin et al., 2005, Malej et al., 2007, Uye and Shimauchi, 2005, Gibbons, 2018). The dominant food source was mesozooplankton (specifically copepods), followed by proto-zooplankton and then macrozooplankton (Table 3.3). There is little evidence in the literature for jellyfish actively consuming autotrophs. One of the few pieces of evidence is a gut content analysis where ‘unidentified protists... some chlorophyll bearing’ were found (Colin et al., 2005). The ephyrae stage of jellyfish are likely to have a higher preference for autotrophs, due to their smaller size, but this will have a minimal effect on the overall preferences and the biomass consumed (Gibbons, 2018). Table 3.3 shows the relative preference of jellyfish zooplankton for its prey assigned in the model, along with the preferences of the other zooplankton PFTs. The preference ratios are weighted using the global carbon biomass for each type, calculated from the MAREDAT database, following the methodology used for the other PFTs (Buitenhuis et al., 2013b, Le Quéré et al., 2016).

**Table 3.2** Parameters used to calculate PFT specific growth rate with two-parameter fit (Eq. 3.2) and three-parameter fit (Eq. 3.3) in PlankTOM11.

PFT	Two-parameter fit		Three-parameter fit		
	$\mu_0$ (d <sup>-1</sup> )	$Q_{10}$	$\mu_{max}$ (d <sup>-1</sup> )	$T_{opt}$ (°C)	$dT$ (°C)
FIX	0.03	1.57	0.20	27.60	8.20
PIC	0.16	1.78	0.80	24.80	11.20
COC	0.31	1.35	1.00	20.40	7.40
MIX	0.20	1.57	1.10	34.00	20.00
PHA	0.70	1.11	1.40	15.60	13.00
DIA	0.36	1.66	1.30	23.20	17.20
BAC	0.12	1.20	0.40	18.80	20.00
PRO	0.40	1.00	0.40	22.00	20.00
MES	0.02	2.22	0.40	31.60	20.00
MAC	0.01	2.75	0.20	33.20	20.00
JEL	0.05	2.03	0.20	23.60	18.80

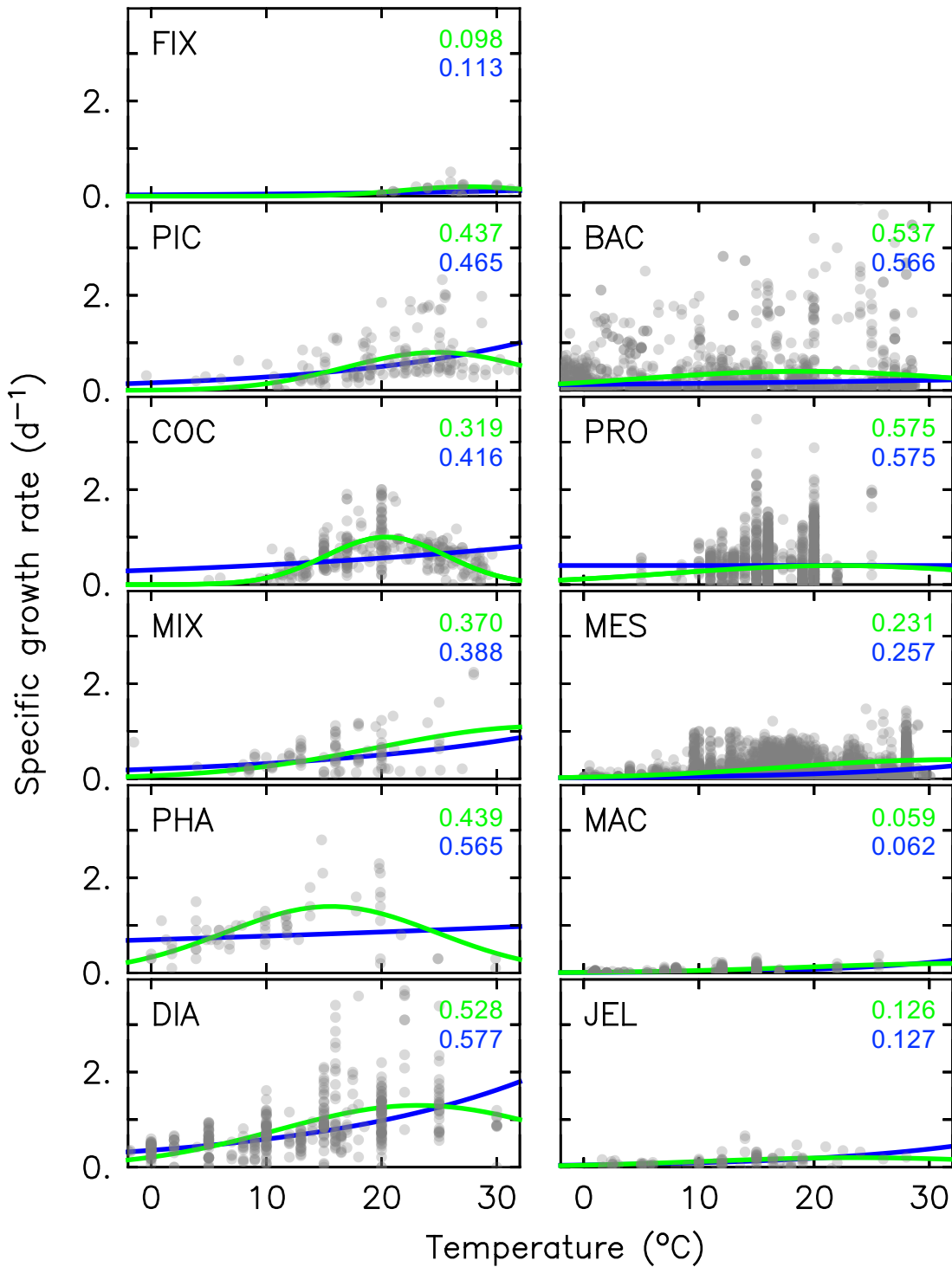


**Figure 3.2** Maximum growth rates for the 11 PFTs as a function of temperature from observations (grey circles). The fit to the data for two-parameters is the blue line, with the updated three-parameter fit in green. The Root Mean Square Error is given in each PFT panel coloured to the corresponding fit (blue for three-parameter and green for two-parameter). The two fits use the parameter values from Table 3.2. For full PFT names see Table 3.1.

**Table 3.3** Relative preference, expressed as a ratio, of zooplankton for food (grazing) used in PlankTOM. For each zooplankton the preference ratio for diatoms is set to 1. Adapted from Le Quéré et al. (2016).

PFT	PRO	MES	MAC	JEL
<b>Autotrophs</b>				
FIX	2	0.1	0.1	0.1
PIC	3	0.75	0.5	0.1
COC	2	0.75	1	0.1
MIX	2	0.75	1	1
DIA	1	1	1	1
PHA	2	1	1	1
<b>Heterotrophs</b>				
BAC	4	0.1	0.1	0.1
PRO	0	2	1	7.5
MES	0	0	2	10
MAC	0	0	0	5
JEL	0	0	0.5	0
<b>Particulate matter</b>				
Small organic particles	0.1	0.1	0.1	0.1
Large organic particles	0.1	0.1	0.1	0.1

### 3.2.2.3 Respiration

Previous analysis of respiration rates of jellyfish found that temperature manipulation experiments with  $Q_{10}$  values of  $>3$  were flawed because temperature was changed too rapidly (Purcell, 2009, Purcell et al., 2010). In a natural environment, jellyfish gradually acclimatise to temperature changes which has a smaller effect on their respiration rates. Purcell et al. instead collated values from experiments that measured respiration at ambient temperatures, providing a range of temperature data across different studies. They found that  $Q_{10}$  for respiration was 1.67 for *Aurelia* species (Purcell, 2009, Purcell et al., 2010). Moriarty (2009) collated a respiration dataset for zooplankton, including GZ, using a similar selectivity as Purcell (2009) for

experimental temperature, feeding, time in captivity and activity levels. Cnidaria medusae were extracted from the Moriarty (2009) dataset, which also included experiments on non-adult and non-Aurelia species medusa, unlike the Purcell et al. (2010) dataset. The relationship between temperature and respiration is heavily skewed by body mass (Purcell et al., 2010). The data was thus normalised by fitting it to a general linear model (GLM) using a least squares cost function, to reduce the effect of body mass on respiration rates (Ikeda, 1985, Le Quéré et al., 2016).

$$GLM = \log_{10}RR = a + b \log_{10}BM + c T \quad (3.5)$$

$$cost\ function = \sum \left( \frac{\mu^T - \mu_{obs}^T}{\mu_{obs}^T} \right)^2 \quad (3.6)$$

Where  $RR$  is the respiration rate,  $BM$  is the body mass, and  $T$  and  $\mu^T$  are the observed temperature and associated respiration rate. The parameter values were then calculated using  $\mu_0 = e^a$ , and  $Q_{10} = (e^c)^{10}$ , where  $e$  is the exponential function. The resulting fit to data is shown in Figure 3.3. The parameter values for respiration used in the model are given in Table 3.4. Macrozooplankton respiration values are also given in Figure 3.3 and Table 3.4, to provide a comparison to another zooplankton PFT. The respiration rates of jellyfish and macrozooplankton are comparable to each other, with rates mostly between 0 – 0.2 d<sup>-1</sup>. Macrozooplankton respiration is lower than jellyfish respiration at low temperatures and higher than jellyfish respiration at high temperatures (Fig. 3.3).

### 3.2.2.4 Mortality

There is limited data on mortality rates for jellyfish and to use mortality data from the literature on any zooplankton group some assumptions must be made (Acevedo et al., 2013, Almeda et al., 2013, Malej and Malej, 1992, Moriarty, 2009, Rosa et al., 2013). These assumptions are: that the population is in a steady state where mortality equals recruitment, reproduction is constant and that mortality is independent of age (Moriarty, 2009). All models with zooplankton mortality rates follow these assumptions. In reality the mortality of a zooplankton population is highly variable. Steady states are balanced over a long period (if a population remains viable), reproduction is restricted to certain times of year and the early stages of life cycles are many times more vulnerable to mortality. Despite these assumptions, with the limited data on mortality rates, the larger uncertainty lies with the data rather than the



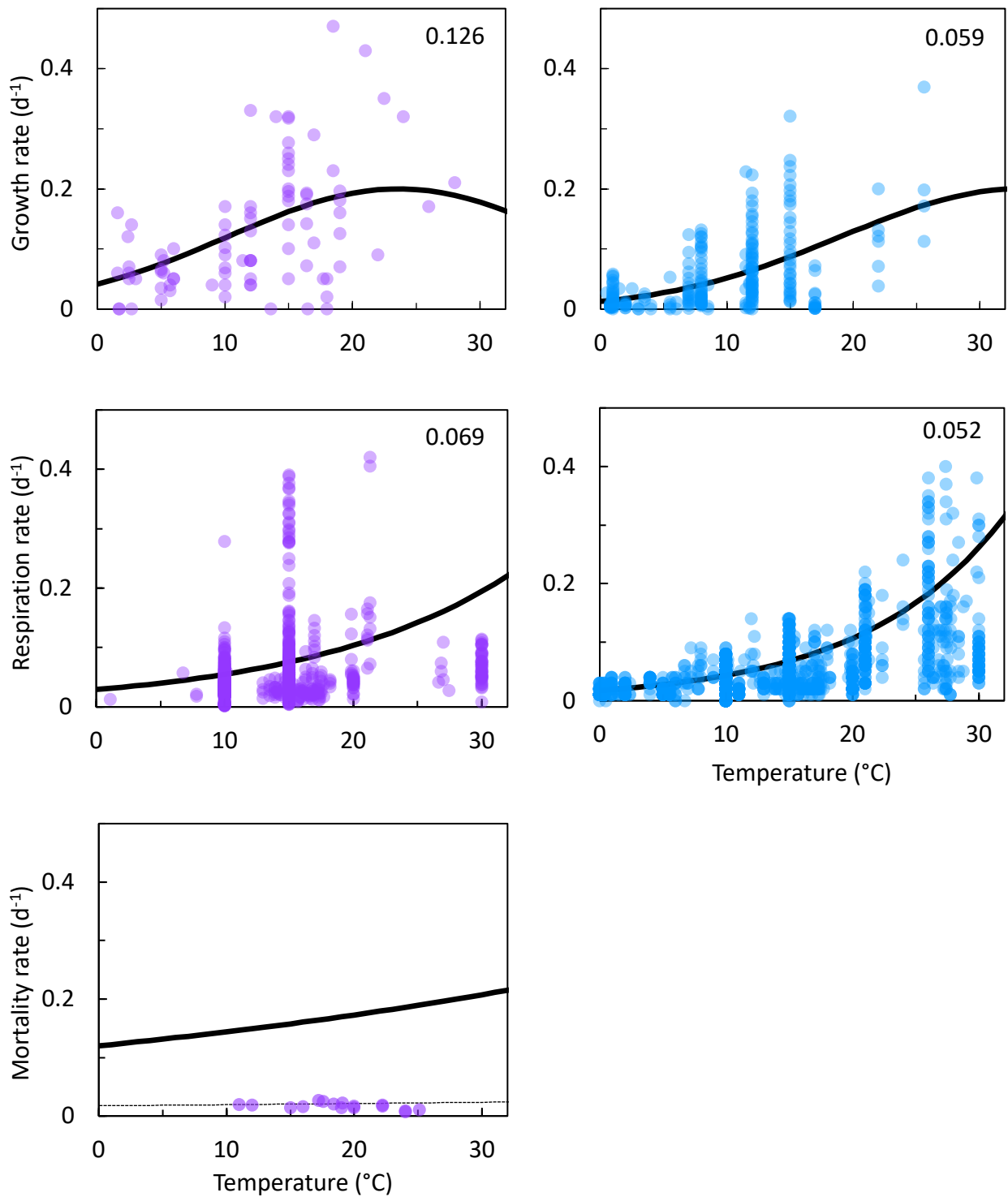


**Figure 3.3** Maximum (top) growth rates, (middle) respiration rates and (bottom) mortality rates for (left; purple) jellyfish and (right; blue) macrozooplankton PFTs as a function of temperature. The fit to the data is shown in black, using the parameter values from Table 3.2 and Table 3.4. The Root Mean Square Error for the fit to growth and respiration are shown in the corresponding panels. Growth rates are the same as shown in Figure 2, on a different scale. For mortality the thin dashed line is the untuned fit, and the solid line is the tuned fit (Table 3.4).

assumptions (Moriarty, 2009). In the small amount of data available and suitable for use in the model (16 data points from two studies) mortality ranged from 0.006 – 0.026

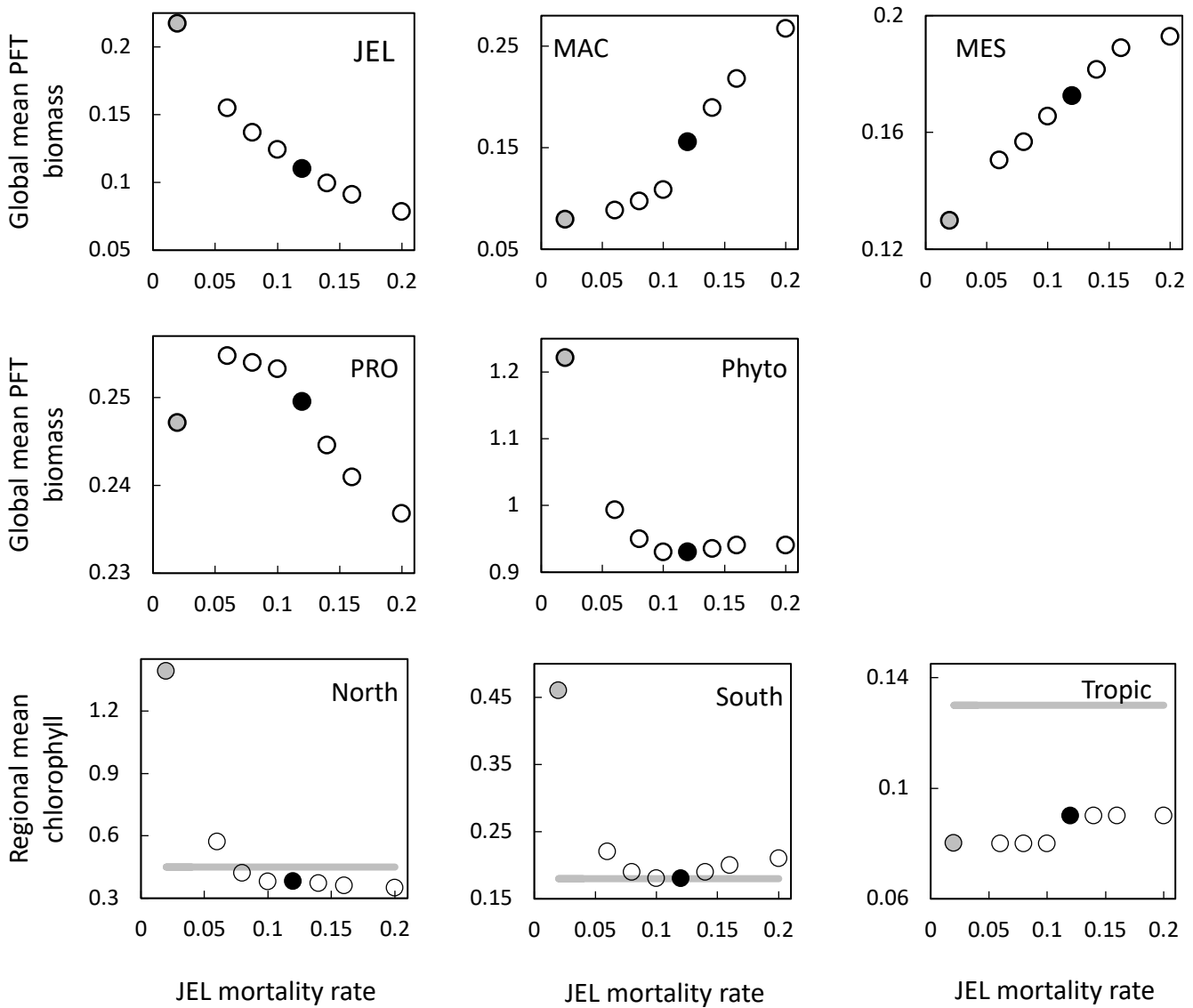


**Figure 3.4** Results from sensitivity tests on jellyfish mortality rates are shown by empty circles, the standard (tuned) PlankTOM11 simulation is shown by the black filled circle and the untuned simulation is shown by the grey filled circle; (top - middle) global mean PFT biomass ( $\mu\text{mol C L}^{-1}$ ) for 0-200m depth, (bottom) regional mean surface chlorophyll concentration ( $\mu\text{g chl L}^{-1}$ ). For the regional mean chlorophyll and north/south ratio the grey lines show observations calculated from SeaWiFS. All data are averaged for 1985-2015, and between  $30^\circ$  and  $55^\circ$  latitude in both hemispheres:  $140\text{-}240^\circ\text{E}$  in the north and  $140\text{-}290^\circ\text{E}$  in the south. Observations for global PFT biomass are omitted as the results all fall within the min-max observational range. Phyto is the sum of all the phytoplankton PFTs.

per day (Acevedo et al., 2013, Malej and Malej, 1992). Applying the exponential fit to this data gave a mortality rate at  $0^\circ\text{C}$  ( $m_{0^\circ}^{Z_j}$  in Eq. 3.1) of 0.018 per day (Fig. 3.3).

Sensitivity tests were carried out from this mortality rate due to low confidence in the value. Results from a subset of the sensitivity tests are shown in Figure 3.4. The model was found to best represent a range of observations (of plankton from MAREDAT and chlorophyll from SeaWiFS; Fig. 3.4) when jellyfish mortality was increased to 0.12 per day. Although the tuned fit is far higher than the observations (Fig. 3.3), it was

**Table 3.4** Temperature dependent rates of respiration and mortality for macro- and jellyfish zooplankton. Where  $\mu_0$  is the rate at 0°C and  $Q_{10}$  is the temperature coefficient. See text for detail.

Parameters	JEL		MAC	
	$\mu_0$ (d <sup>-1</sup> )	$Q_{10}$	$\mu_0$ (d <sup>-1</sup> )	$Q_{10}$
Respiration	0.03	1.88	0.01	2.46
Mortality	0.12	1.20	0.02	3.00

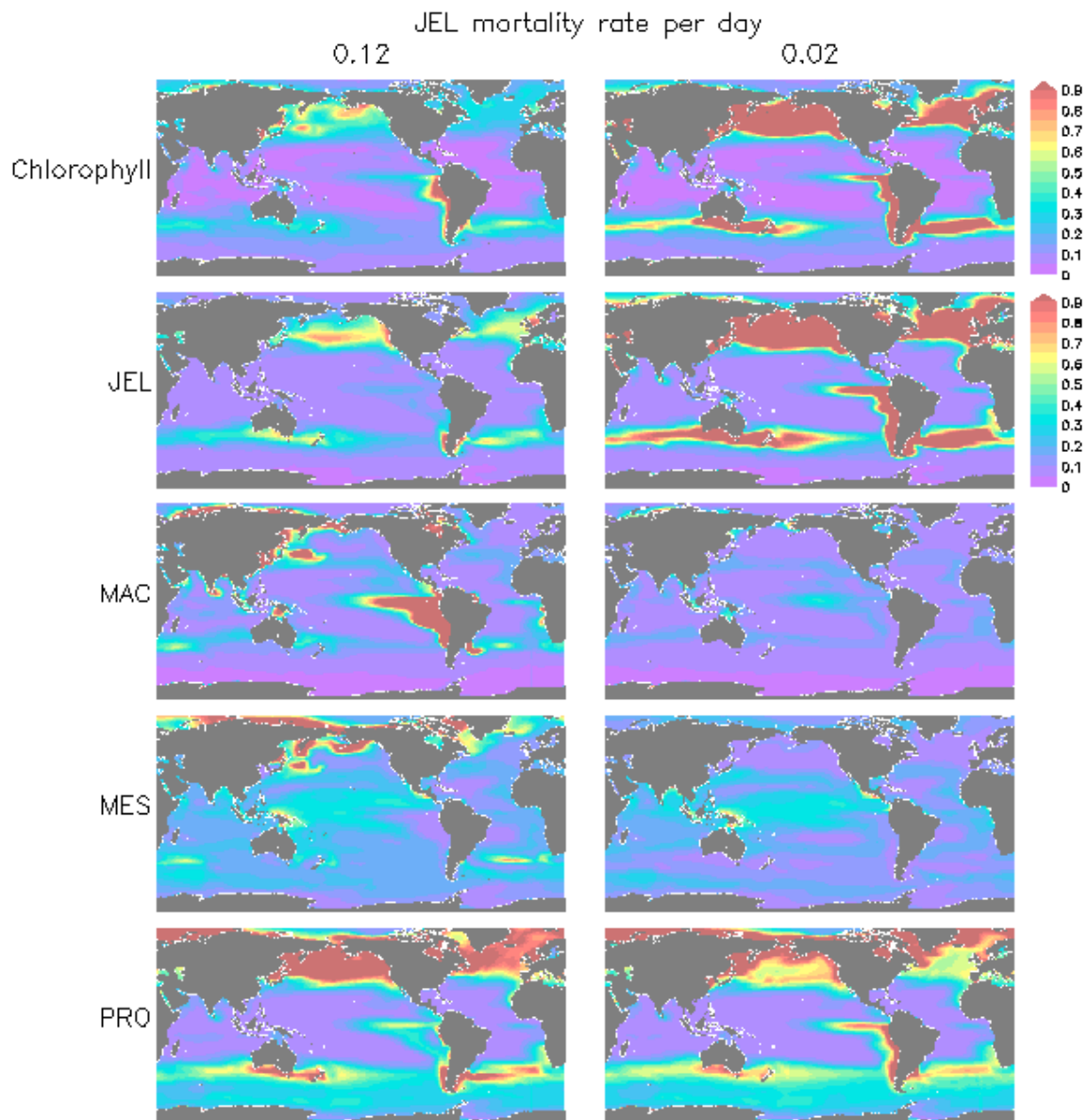


**Figure 3.5** Annual mean surface chlorophyll ( $\mu\text{g chl L}^{-1}$ ) and carbon biomasses ( $\mu\text{mol C L}^{-1}$ ) of JEL, MAC, MES and PRO for tuning of JEL mortality in PlankTOM11 (left) chosen simulation with 0.12 mortality/d<sup>-1</sup> and (right) untuned simulation with 0.02 mortality/d<sup>-1</sup>. Model results are shown for the surface box (0-10 meters) and averaged for 1985-2015.

selected for use in the model for two central reasons, firstly, that the observational mortality data is limited (as discussed above) and secondly, that the tuning provides a model much closer to a range of observations. Mortality rate values closer to 0.018 per day allowed jellyfish to dominate macro- and mesozooplankton, greatly reducing their biomass (Fig. 3.4 and Fig. 3.5). Low jellyfish mortality also resulted in higher chlorophyll concentrations than observed, especially in the high latitudes (Fig. 3.4 and Fig. 3.5, Bar-On et al., 2018, Buitenhuis et al., 2013b). The higher mortality rate may be accounting for the greater vulnerability to mortality experienced during the early stages of the life cycle. The half saturation constant for mortality ( $K^{Zj}$  in Eq. 3.1) is set to  $20 \mu\text{mol C L}^{-1}$ .

### 3.2.3 Additional Tuning

As shown in Equation 1, there is a component in the mortality of zooplankton to represent predation by organism types not included in the model. The jellyfish PFT is a significant grazer of macrozooplankton and mesozooplankton (Table 3.3). To account for this additional grazing the mortality term for macrozooplankton and the respiration term for mesozooplankton were reduced (Table 3.5, PlankTOM11). Respiration is used in place of mortality for mesozooplankton as the mortality term has already been reduced to zero to account for predation (Le Quéré et al., 2016).

From the change to the growth rate calculation all PFT rates are lower, but the change is most drastic for *Phaeocystis*, diatoms, bacteria and protozooplankton (Fig. 3.2). Further tuning is carried out to address this, as the model has been tuned previously to the higher growth rates. The model was tuned by increasing the grazing ratio preference of mesozooplankton for *Phaeocystis*, within observations, and decreasing

**Table 3.5** Changes to non-jellyfish PFT parameters. PlankTOM10 (2016) is the latest published version of PlankTOM with 10 PFTs (Le Quéré et al., 2016).

Parameters	PlankTOM10 (2016)	PlankTOM11	PlankTOM10 (this study)
MAC mortality	0.020	0.005	0.012
MES respiration	0.014	0.001	0.014

the half saturation constant of *Phaeocystis* for iron. The tuning resulted in a reduction of *Phaeocystis* biomass and an increase in diatom biomass, without disrupting the rest of the ecosystem. Diatom respiration was increased to reduce their biomass towards observations. Bacterial biomass was increased closer to observations by reducing the half saturation constant of bacteria for dissolved organic carbon.

### 3.2.4 Model Simulations

The PlankTOM11 simulations are run from 1920 to 2015, forced by meteorological data including daily wind stress, cloud cover, precipitation and freshwater riverine input (NCEP/ NCAR reanalysed fields from Kalnay et al., 1996). The simulations start with a 28-year spin up forced with year 1980 as an ‘average year’, with no strong El Nino/La Nina, followed by interannually varying forcing from 1948-2015. All analysis

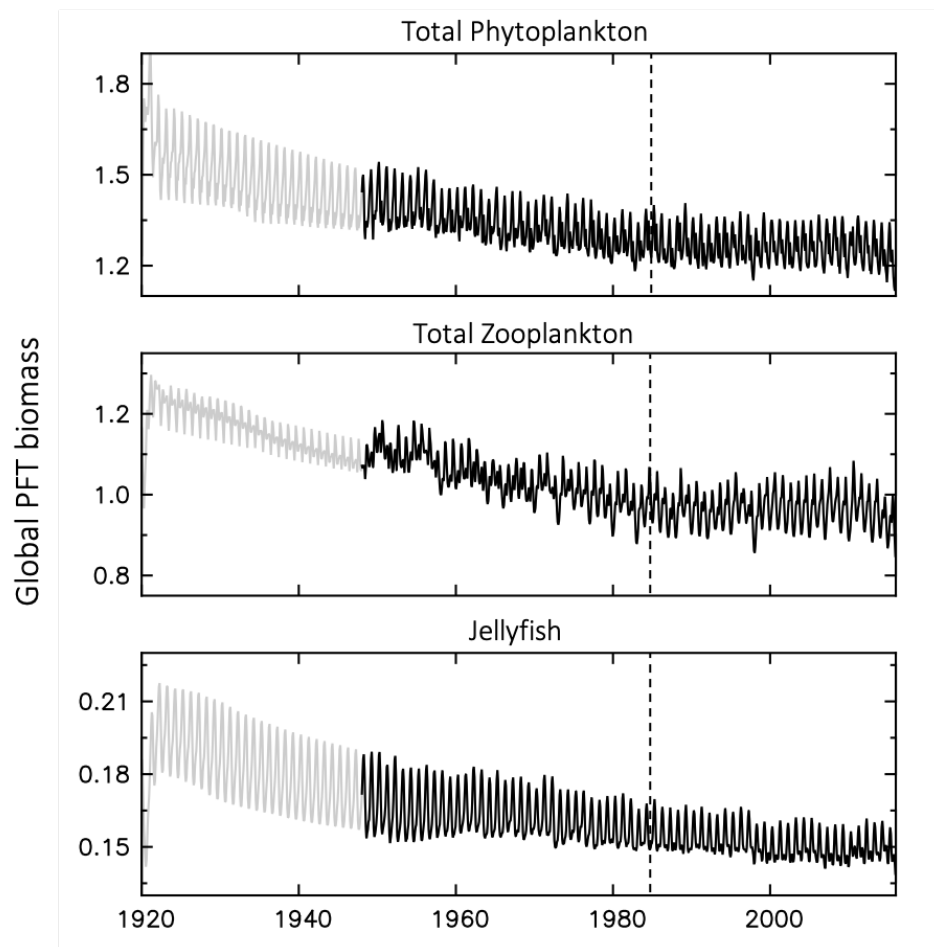


**Figure 3.6** Global PFT biomass ( $\mu\text{mol C L}^{-1}$ ) averaged over 0-100m for PlankTOM11. Top is the total phytoplankton PFTs, middle is the total zooplankton PFTs and bottom is the jellyfish PFT. The grey line is the spin up period and the black line is the interannually varying forcing (see text for detail). The dashed line indicates the year 1985 after which the model data is used for analysis.

is carried out on the last 31-year period of 1985-2015 when drift in the model is reduced (Fig. 3.6). PlankTOM11 is initialised with observations of dissolved inorganic carbon and alkalinity (Key et al., 2004),  $\text{NO}_3$ ,  $\text{PO}_4$ ,  $\text{SiO}_3$ ,  $\text{O}_2$ , temperature and salinity from the World Ocean Atlas (Antonov et al., 2010).

A comparison simulation was carried out in order to test the addition of a zooplankton representing jellyfish to PlankTOM. The comparison simulation is PlankTOM10, where jellyfish growth is set to 0, so that there are 10 PFTs active, as a replication of PlankTOM10 in Le Quéré et al. (2016) with the updated growth and tuning presented above. All other setup is identical to PlankTOM11 except for the top predator mortality term for meso- and macrozooplankton, which were returned to pre-jellyfish values, to account for the lack of predation by jellyfish. Macrozooplankton mortality was then tuned from this value to account for the change to the growth calculation (Table 3.5).

### 3.3 Results

#### 3.3.1 Ecosystem Properties of PlankTOM11

PlankTOM11 reproduces the main characteristics of surface chlorophyll observations, with high chlorophyll concentration in the high latitudes, low concentration in the subtropics and elevated concentrations around the equator (Fig. 3.7). PlankTOM11 also reproduces higher chlorophyll concentrations in the Northern Hemisphere than the Southern, and higher concentrations in the southern Atlantic than the southern Pacific Ocean (Fig. 3.7). Overall the model underestimates chlorophyll concentrations, as is standard with models of this type (Le Quéré et al., 2016) particularly in the central and north Atlantic (Fig. 3.7). PlankTOM11 also captures the seasonality of chlorophyll, with concentrations increasing in summer compared to the winter for each hemisphere (Fig. 3.7).

PlankTOM11 underestimates global primary production by 10 PgC  $y^{-1}$ , export production and N<sub>2</sub> fixation are within the observational range, and CaCO<sub>3</sub> export is slightly overestimated by 0.2 PgC  $y^{-1}$  (Table 3.6).

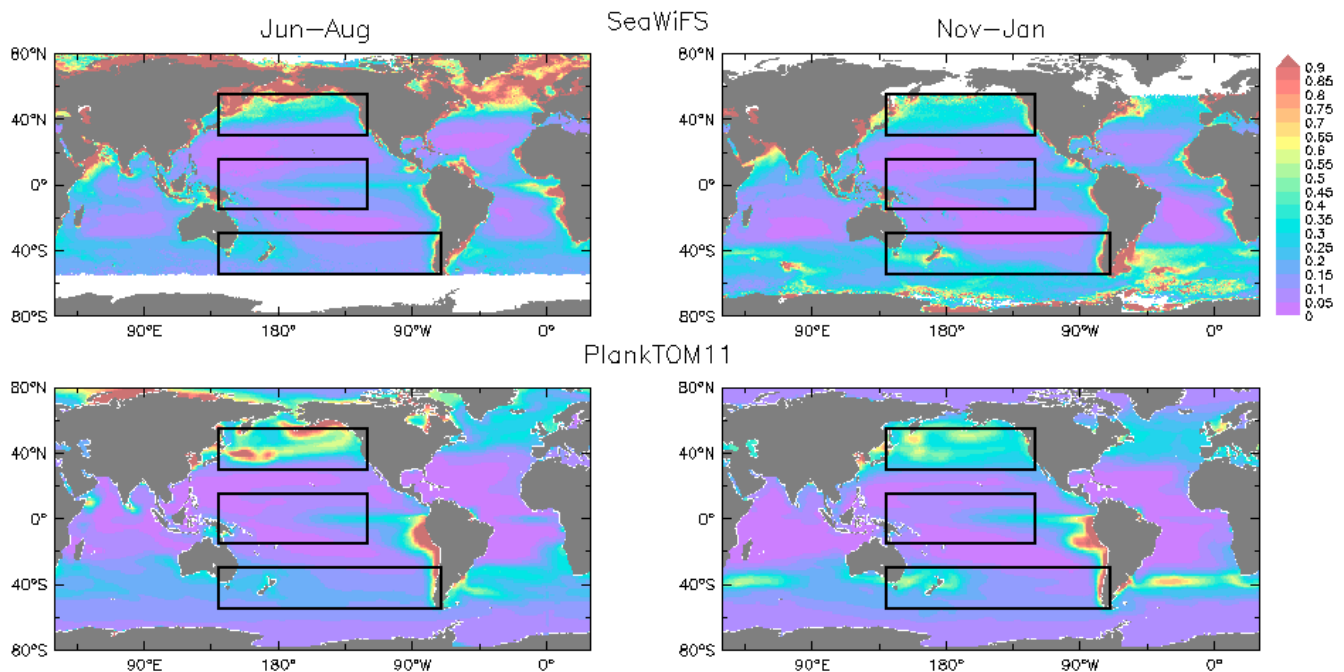


**Figure 3.7** Surface chlorophyll ( $\mu\text{g chl L}^{-1}$ ) averaged for (left) June to August and (right) November to January. Data are from (top) SeaWiFS satellite and results (bottom) from PlankTOM11. SeaWiFS is averaged for 1997-2006, and PlankTOM11 for 1985-2015. Model results are shown for the surface box (0-10 meters). The black boxes show the North, Tropic and South regions used in other figures.

**Table 3.6** Global mean values for rates and biomass from observations and the PlankTOM11 and PlankTOM10 models averaged over 1985–2015. In parenthesis is the percentage share of the plankton type of the total Phytoplankton or Zooplankton biomass. Adapted from Le Quéré et al. (2016).

	PlankTOM11	PlankTOM10	Data	Reference for the data
<i>Rates</i>				
Primary production (PgC y <sup>-1</sup> )	41.6	43.4	51-65	Buitenhuis et al. (2013b)
Export production at 100m (PgC y <sup>-1</sup> )	7.1	7.0	5-13	Henson et al. (2011), Palevsky et al. (2018)
CaCO <sub>3</sub> export at 100m (PgC y <sup>-1</sup> )	1.3	1.2	0.6-1.1	Lee (2001); Sarmiento et al. (2002)
N <sub>2</sub> fixation (TgN y <sup>-1</sup> )	97.2	95.9	60-200	Gruber (2008)
<i>Phytoplankton biomass 0-200 m (PgC)</i>				
N <sub>2</sub> -fixers	0.065 (6.1%)	0.075 (7.2%)	0.008-0.12 (2-8%)	Luo et al. (2012)
Picophytoplankton	0.141 (13%)	0.153 (15%)	0.28-0.52 (35-68%)	Buitenhuis et al. (2012b)
Coccolithophores	0.248 (23%)	0.212 (20%)	0.001-0.032 (0.2-2%)	O'Brien et al. (2013)
Mixed-phytoplankton	0.263 (24%)	0.268 (26%)	-	-
<i>Phaeocystis</i>	0.177 (16%)	0.170 (16%)	0.11-0.69 (27-46%)	Vogt et al. (2012)
Diatoms	0.183 (17%)	0.167 (16%)	0.013-0.75 (3-50%)	Le Blanc et al. (2012)
Total Phytoplankton biomass	1.077	1.046	0.412 – 2.112	
<i>Heterotrophs biomass 0-200 m (PgC)</i>				
Bacteria	0.041	0.046	0.25-0.26	Buitenhuis et al. (2012a)
Protozooplankton	0.295 (36%)	0.330 (32.7%)	0.10-0.37 (27-31%)	Buitenhuis et al. (2010)
Mesozooplankton	0.193 (23%)	0.218 (21.6%)	0.21-0.34 (25-66%)	Moriarty and O'Brien (2013)
Macrozooplankton	0.205 (25%)	0.460 (45.6%)	0.01-0.64 (3-47%)	Moriarty et al. (2013)
Jellyfish zooplankton (Cnidaria)	0.129 (16%)	-	0.1-3.11	Bar-On et al. (2018), Lucas et al. (2014), Chapter 2
Total Zooplankton biomass	0.823	1.008	0.42 – 4.46	



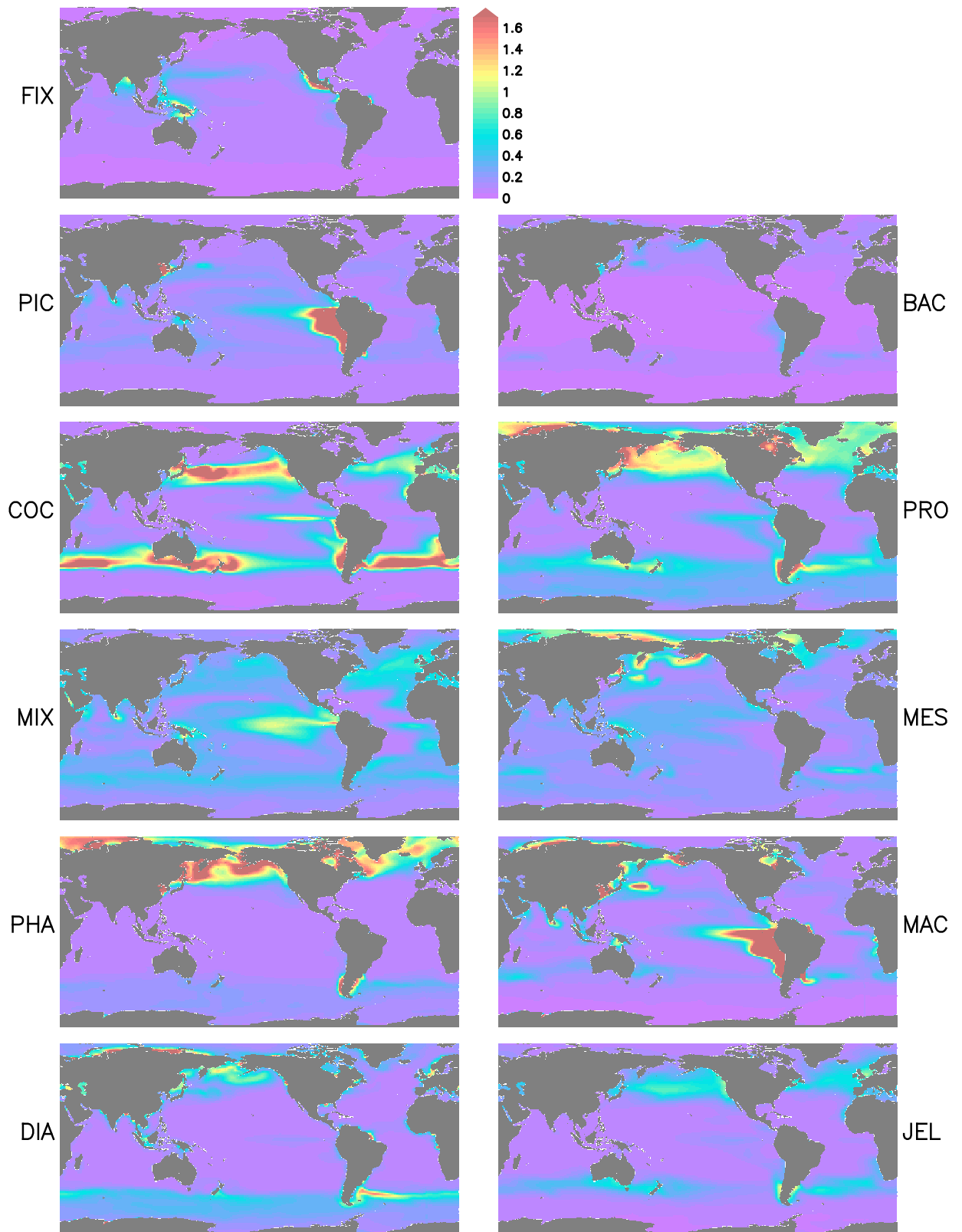


**Figure 3.8** Annual mean surface carbon biomass ( $\mu\text{mol C L}^{-1}$ ) for each plankton functional type from PlankTOM11. Results are shown for the surface box (0-10 meters) and averaged for 1985-2015. All panels are scaled to the same key.

In PlankTOM11 each PFT shows unique spatial distribution in carbon biomass (Fig. 3.8). The total biomass of phytoplankton is within the range of observations, but the partitioning of this biomass between phytoplankton types differs from observations (Table 3.6). PlankTOM11 is dominated by mixed-phytoplankton and coccolithophores, together making up 47% of the total phytoplankton biomass. Diatoms and *Phaeocystis* are the next most abundant and fall within the observed range, followed by Picophytoplankton with around half the observed biomass (Table 3.6). The observations are dominated by picophytoplankton, followed by *Phaeocystis* and Diatoms (Table 3.6). The modelled mixed-phytoplankton is likely taking up the ecosystem niche of picophytoplankton. Coccolithophores are overestimated by a factor of 10 and may also be filling the ecosystem niche of picophytoplankton in the model.

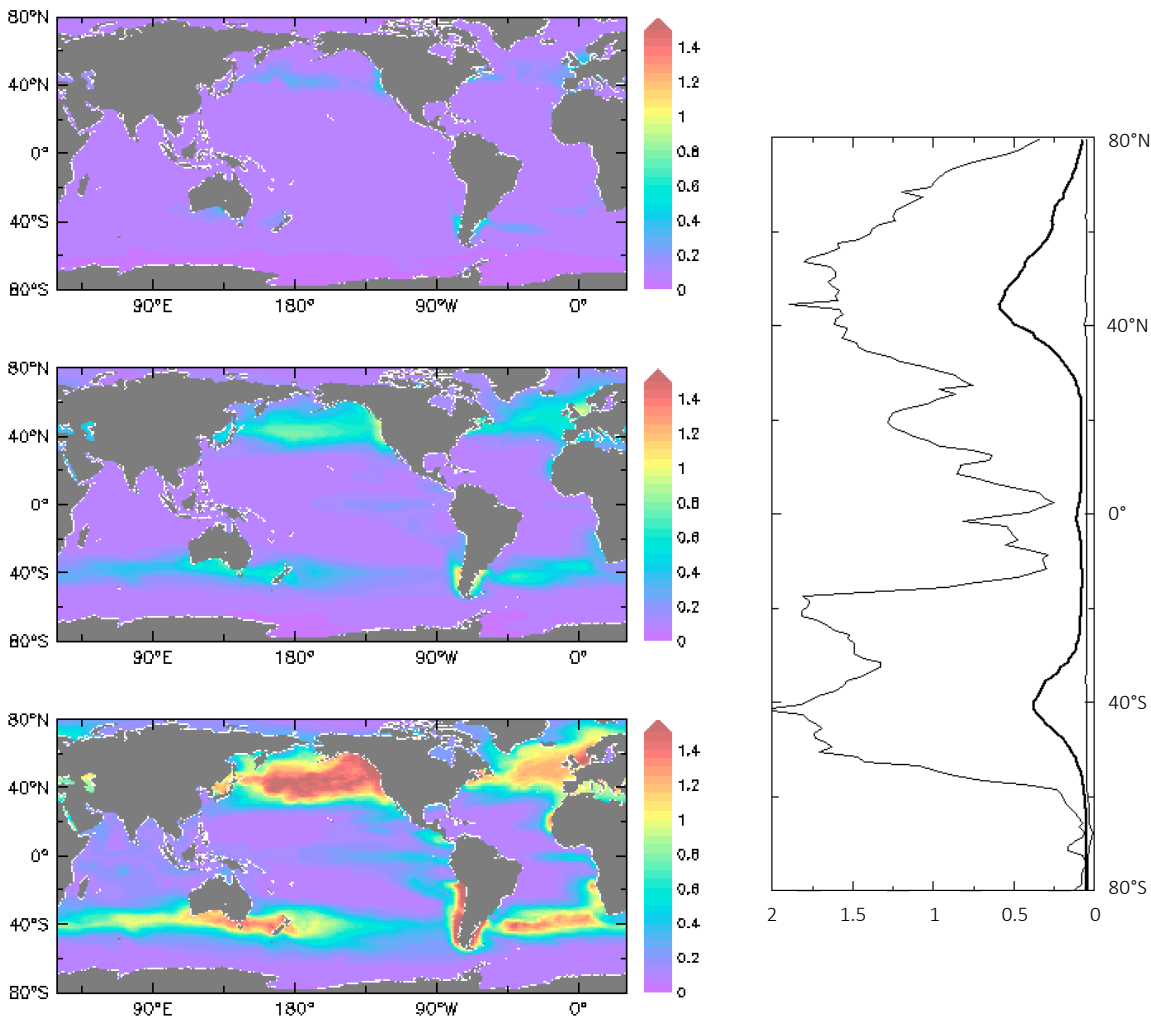


**Figure 3.9** Annual surface carbon biomass ( $\mu\text{mol C L}^{-1}$ ) for the jellyfish PFT in PlankTOM11. Results are the mapped (top left) minimum over time, (middle left) average over time, and (bottom left) maximum over time, and (right) averaged over longitude for the minimum and maximum in thin black lines and average in the thick black line. All data is for 1985-2015.

PlankTOM11 underestimates bacterial biomass by a factor of ten (Table 3.6). This is in the same range, but slightly higher than, previous published versions of PlankTOM; 0.031 in PlankTOM10 and 0.030 in PlankTOM6 (Le Quéré et al., 2016). Le Quéré et al. (2016) suggests that the underestimation of bacterial biomass is due to the PlankTOM model only representing highly active bacteria, while a significant portion of observed bacterial biomass is from low activity bacteria and ghost cells.

### 3.3.2 Jellyfish Biomass in PlankTOM11

The global jellyfish biomass estimated by various studies gives a range of results: 0.1 PgC (Bar-On et al., 2018),  $0.32 \pm 0.49$  PgC (Lucas et al., 2014), 0.26 PgC from MAREDAT following Lucas et al., (2014) methods, and 0.46 PgC from MAREDAT following Buitenhuis et al., (2013b) methods (see Chapter 2 for details). Jellyfish biomass in PlankTOM11 is within the range but towards the lower end of observations at 0.13 PgC (Table 3.6). When biomass was tuned to match the higher biomass observations by adjusting the mortality rate (Fig 3.4, Fig. 3.5) jellyfish dominate the entire ecosystem, significantly reducing levels of other PFTs to far below observations.

PlankTOM11 generally replicates the patterns of jellyfish biomass with observations. High biomass occurs at around 50-60°N across the oceans, with the highest average biomass in the North Pacific (Fig. 3.9, Chapter 2; Lucas et al., 2014). PlankTOM11 also replicates low biomass in the Indian Ocean, and the eastern half of the tropical Pacific shows higher biomass than other open ocean areas in agreement with patterns

**Table 3.7** Jellyfish (Cnidaria) biomass globally from observations (MAREDAT, see Chapter 2) and PlankTOM11. Three types of mean are given for the observations; Med is the median, AM is the arithmetic mean and GM is the geometric mean. The ratios are all scaled to mean = 1. All units are  $\mu\text{g C L}^{-1}$ .

		Mean	Max	Ratio
<b>Observations</b>	<b>AM</b>	3.61	156.00	1 : 43
	<b>GM</b>	0.95	156.00	1 : 165
	<b>Med</b>	0.29	156.00	1 : 538
<b>PlankTOM11</b>	<b>AM</b>	1.18	98.90	1 : 84

in observations (Fig. 3.9, Chapter 2; Lucas et al., 2014). The lack of biomass observations around 40°S makes it hard to say if the peak in jellyfish biomass in PlankTOM11 at this latitude is representative of reality. The modelled maximum biomass in the southern hemisphere is mostly around coastal areas i.e. South America and southern Australia. This is expected from the reports and papers on jellyfish in these areas (Condon et al., 2013, Purcell et al., 2007 and references therein). However, the high modelled biomass in the southern Atlantic open ocean around 40°S may be unrealistic as there is no data from this region (Fig. 3.9). A prevalence of jellyfish in coastal areas is apparent, in line with observations, even without any specific coastal advantages for jellyfish in the model (see macrozooplankton in Le Quéré et al., 2016; Fig. 3.9).

Jellyfish are characterised by their bloom and bust dynamics, resulting in patchy and ephemeral biomass (Chapter 1 & 2). The mean:max biomass ratio of observations (MAREDAT; Chapter 2) was compared to the same ratio for PlankTOM11 to assess the replication of this characteristic. The observations give a range of ratios depending on the type of mean used (Table 3.7). The PlankTOM11 ratio falls within this range, but towards the lower end. PlankTOM11 replicates some of the patchy and ephemeral biomass of jellyfish.

Observations of jellyfish biomass in MAREDAT have poor global spatial coverage (Chapter 2). The region around the coast of Alaska has the highest density of observations (Fig. 3.10) and is used here to evaluate the mean and seasonality of the carbon biomass of jellyfish as represented in PlankTOM11. PlankTOM11 reproduces the observed mean jellyfish biomass (0.16 compared to 0.13), but it underestimates the maximum and spread of the observations (Table 3.8). The spatial patchiness is somewhat replicated in PlankTOM11, although with a smaller variation (Fig. 3.10). PlankTOM11 replicates the mean seasonal shape and biomass of jellyfish with a small peak over the summer followed by a large peak in September in the observations and in October in PlankTOM11. PlankTOM11 underestimates the maximum biomass and temporal patchiness of the observations (Fig. 3.10).

### **3.3.3 Influence of Jellyfish on the PlankTOM Ecosystem**

**Table 3.8** Jellyfish (Cnidaria) biomass statistics for the coast of Alaska from observations (MAREDAT, see Chapter 2) and PlankTOM11. Mean is the arithmetic mean and SD is the standard deviation. PlankTOM11 is sampled at grid boxes where observations are available (see Fig. 3.9). All units are  $\mu\text{mol C L}^{-1}$ .

	Mean	Min	Max	SD
Observations	0.134	0.000	7.410	0.483
PlankTOM11	0.161	0.048	1.078	0.164

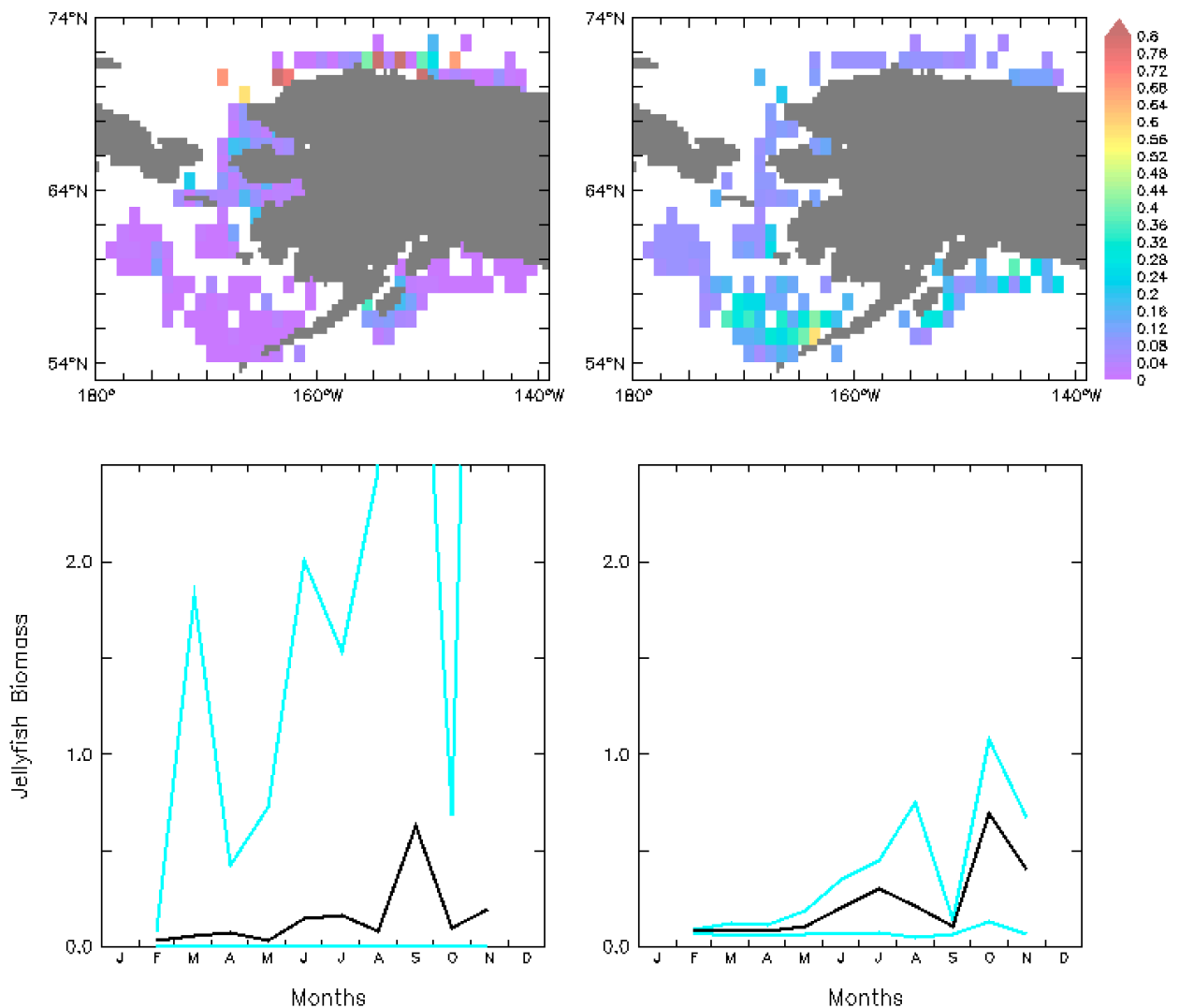


**Figure 3.10** Carbon biomass of jellyfish from (left) observations and (right) PlankTOM11 in  $\mu\text{mol C L}^{-1}$ , for the coast of Alaska (the region with the highest density of observations). The top panels show the annual mean jellyfish biomass and the bottom panels show the seasonal jellyfish biomass, with the mean in black and the minimum and maximum in blue. Observations and PlankTOM11 results are for 0-150m, as the depth range where >90% of the observations occur.

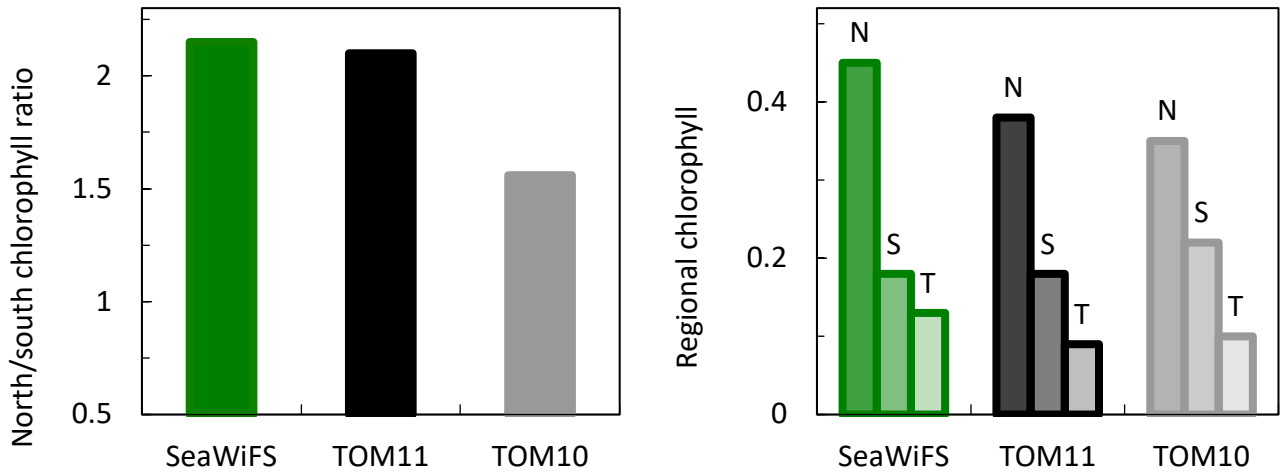


**Figure 3.11** Surface chlorophyll concentration ( $\mu\text{g chl L}^{-1}$ ) for SeaWiFS satellite (green), PlankTOM11 (TOM11, black) and PlankTOM10 (TOM10, grey). North/south chlorophyll concentration ratio (left) and regional chlorophyll concentration (right) for the north (N), tropic (T) and south (S) regions shown in Figure 3.6.

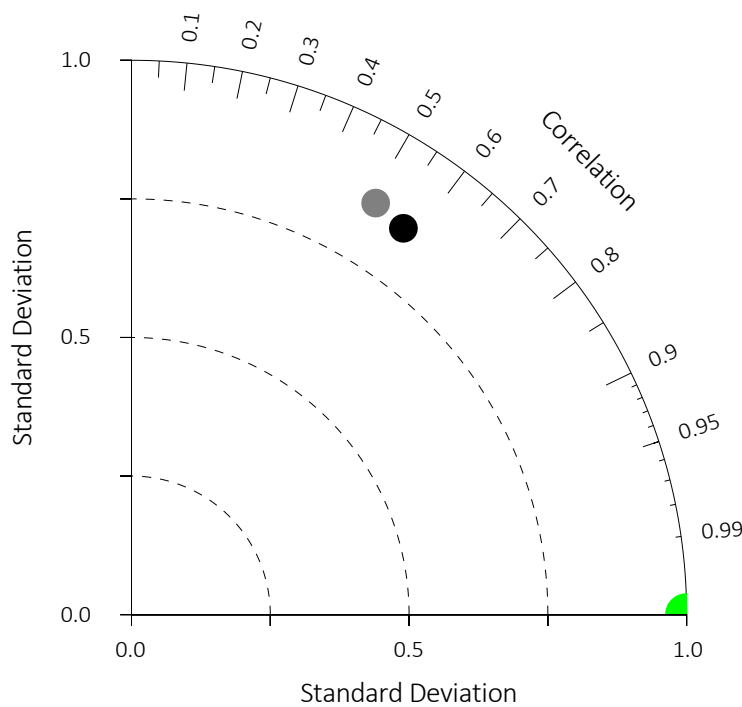


**Figure 3.12** Taylor diagram comparing the global distributions of in annual mean surface chlorophyll concentration ( $\mu\text{g chl L}^{-1}$ ) of PlankTOM11 (black circle) and PlankTOM10 (grey circle) to SeaWiFS satellite observations (green).

To assess the effect of adding jellyfish to PlankTOM, an additional simulation was conducted where jellyfish growth is set to zero (PlankTOM10). The simulation is otherwise identical to PlankTOM11, except for predation on meso- and macrozooplankton (see Table 3.5).

PlankTOM11 closely replicates the observed chlorophyll concentration as well as the ratio between the north and south of 2.1, compared to the observed ratio of 2.2 (Fig. 3.11). PlankTOM10 underestimates the observed chlorophyll concentration as well as the North/South ratio (1.56, Fig. 3.11). In the tropics (T) PlankTOM10 and PlankTOM11 chlorophyll concentration is similar and is below observations (Fig. 3.11). In the north (N) PlankTOM10 chlorophyll concentration is slightly below PlankTOM11 (0.35 and 0.38  $\mu\text{g chl L}^{-1}$ ) although both are below observations of 0.45  $\mu\text{g chl L}^{-1}$  (Fig. 3.11). In the south (S) PlankTOM11 chlorophyll concentration is the same as observations at 0.18  $\mu\text{g chl L}^{-1}$ , where in PlankTOM10 chlorophyll is higher (Fig. 3.11). Overall, the two simulations show similar spatial patterns of surface chlorophyll, but different concentration levels. Globally comparing to observations, PlankTOM11 and PlankTOM10 perform the same for standard deviation and PlankTOM11 performs better for correlation (Fig. 3.12).

Introducing jellyfish to PlankTOM, PlankTOM10 (this study) to PlankTOM11, decreases primary production and increases export (Table 3.6). The mechanisms behind this are explored in depth in Chapter 4. The total surface PFT biomass increases slightly from PlankTOM10 to PlankTOM11, due to the increase in total phytoplankton biomass (Fig. 3.13). The biomass of macrozooplankton decreases from 0.46 to 0.26 PgC, which likely accounts for the increase in phytoplankton biomass because of reduced grazing from macrozooplankton (Fig. 3.13). The biomass of macrozooplankton is reduced due to predation by jellyfish and competition with jellyfish for resources (both graze on meso- and protozooplankton). The biomass of meso- and protozooplankton is very similar in PlankTOM10 and PlankTOM11, even though the biomass of their predators (macrozooplankton in PlankTOM10 and macrozooplankton plus jellyfish in PlankTOM11) is lower in PlankTOM11 (Fig. 3.13). The lower biomass of the predators in PlankTOM11 is offset by the high grazing preference of jellyfish for zooplankton.

In PlankTOM11 there is a clear distinction between the biomass in the north and south, with higher biomass for each PFT in the north compared to the south (Fig. 3.13). Plankton types have higher concentrations in the respective hemisphere's summer, and a double peak in phytoplankton in the north (Fig. 3.13). In both regions protozooplankton have the highest zooplankton biomass, the other zooplankton have

similar biomass to each other, which vary in dominance over the seasons (Fig. 3.13). PlankTOM10 also has higher biomass of each PFT in the north compared to the south, but the difference is smaller than that in PlankTOM11 (Fig. 3.13). The key difference between the two models is the biomass of macrozooplankton. In PlankTOM10 macrozooplankton are the dominant zooplankton, especially in late summer and autumn where their biomass matches and even exceeds the biomass of phytoplankton in the region (Fig. 3.13). In PlankTOM11 neither macrozooplankton, nor any other zooplankton, come close to matching the biomass of phytoplankton. The largest influence of jellyfish in these regions is its control on macrozooplankton biomass.

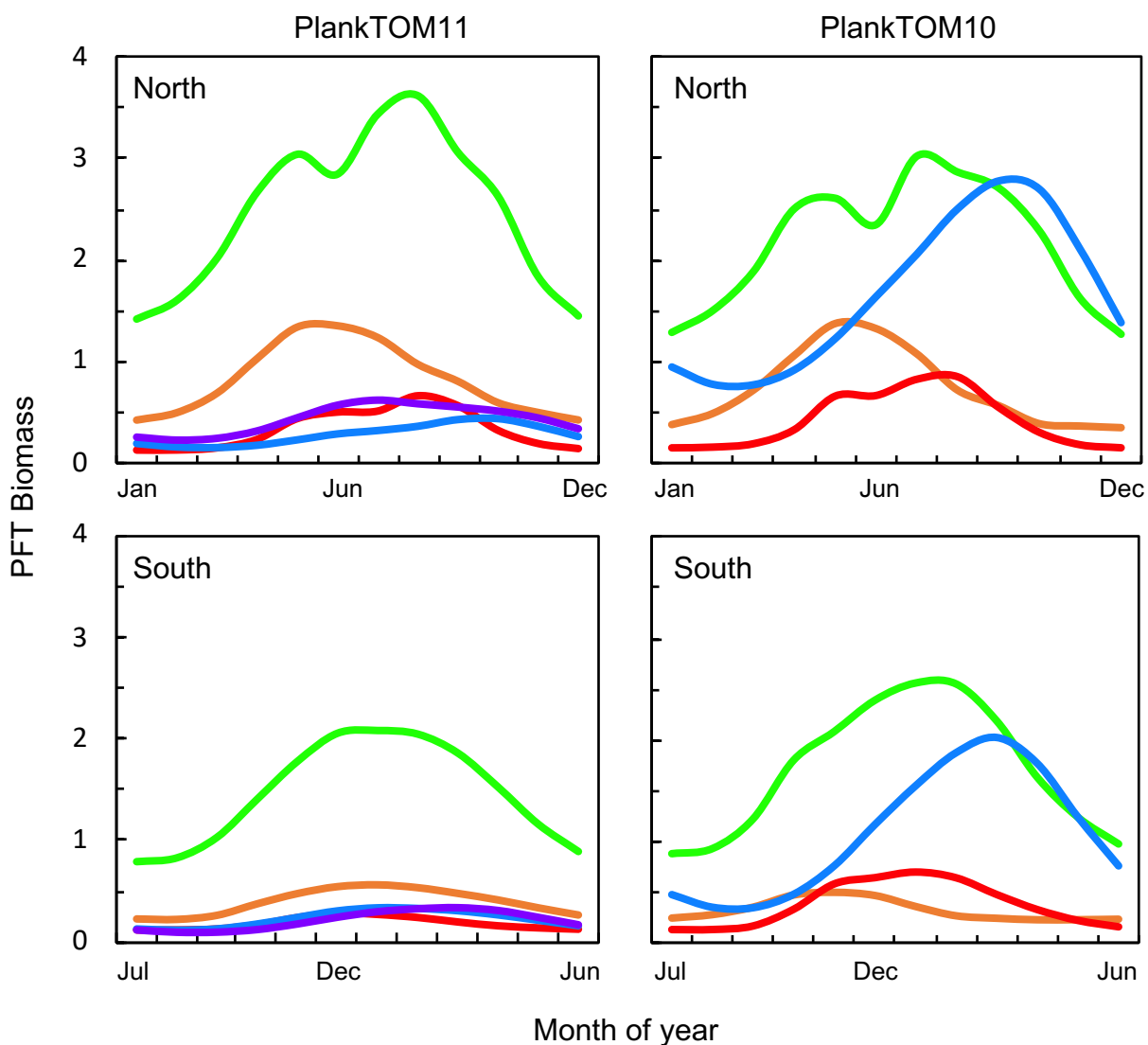


**Figure 3.13** Mean surface carbon biomass of all phytoplankton PFTs (green), protozooplankton (orange), mesozooplankton (red), macrozooplankton (blue) and jellyfish (purple). Line plots shown regional PFT biomass in  $\mu\text{mol C L}^{-1}$  for (left) PlankTOM11 and (right) PlankTOM10, for (middle) the north from January to December and (bottom) the south from July to June. All data are averaged for 1985-2015, and for the regions between  $30^{\circ}$  and  $55^{\circ}$  latitude in both hemispheres:  $140\text{-}240^{\circ}\text{E}$  in the north and  $140\text{-}290^{\circ}\text{E}$  in the south, as shown in Figure 3.6.



### 3.4 Discussion

PlankTOM11 uses a mortality rate for jellyfish that is much higher than the observations (Fig. 3.4 and Fig. 3.5). Lower jellyfish mortality is likely to be more representative of adult life stages, as jellyfish experience high mortality during juvenile life stages, especially as planulae larvae and during settling (Lucas et al., 2012). The limited observations of jellyfish mortality were from mostly adult organisms, which may explain the dominance of jellyfish in the model when parameterised with observed mortality. The higher mortality used for this study may be more representative of an average across all life stages.

PlankTOM11 results suggest high competition between macrozooplankton (crustaceans) and jellyfish, the top two zooplankton in the model. The growth rate of jellyfish is higher than that of macrozooplankton for the majority of the ocean (where the temperature is less than 25°C) but the mortality of jellyfish is also significantly higher than macrozooplankton, again for the majority of the ocean. In situations where jellyfish mortality is reduced (but still higher than macrozooplankton mortality), jellyfish outcompete macrozooplankton for grazing. Because jellyfish also prey directly on macrozooplankton, the biomass of macrozooplankton rapidly decreases (a positive feedback). This sensitivity of the composition of the zooplankton community to the mortality of jellyfish could help explain why jellyfish may be increasing globally. A reduction in jellyfish mortality during early life-stages i.e. through reduced predation on planulae larvae and juveniles by fish, or increased survivability of larvae due to the increased availability of hard substrates for settling (Duarte et al., 2013, Lucas et al., 2012), could quickly allow jellyfish to outcompete other zooplankton, especially macro- and mesozooplankton. However, jellyfish mortality is the least constrained parameter for the jellyfish PFT which may affect this sensitivity of the zooplankton community to jellyfish mortality.

The high patchiness of jellyfish in the observations is partly but not fully captured in PlankTOM11 (Fig. 3.10 and Table 3.7). The mean:max ratio of PlankTOM11 is within the range of observations, but towards the lower end (Table 3.7). This demonstrates that even without replication of high patchiness, PlankTOM11 still achieved some ephemeral blooms where jellyfish achieved a high biomass. The reasons for limited

patchiness include the coarse model resolution of  $1 \times 1^\circ$  which doesn't allow for the representation of small-scale physical mixing such as eddies and frontal regions, which have been shown to influence bloom formation (Graham et al., 2001, Benedetti-Cecchi et al., 2015). Physical processes are likely to be more responsible for jellyfish patchiness than behaviours, due to their simplistic locomotion (Chapter 1). For example, many jellyfish blooms occur around fronts, upwelling regions, tidal and estuarine regions, and shelf-breaks where currents can aggregate and retain organisms (Graham et al., 2001). A few large individuals of certain species have been found to have the capacity to actively swim counter current and orientate themselves with currents to aid bloom formation and retention (Fossette et al., 2015). However, this active swimming behaviour does not appear to be representative across the group and would only move the jellyfish within an area less than the resolution of the model. There is insufficient data and incomplete understanding of such swimming behaviours to include it in a global model.

A key limitation of jellyfish representation in the model is the lack of a life cycle. Many jellyfish alternate between asexual (budding during the polyp stage) and sexual (broadcast spawning) reproduction (Chapter 1). Temperature cues have been found to trigger budding of ephyrae, increasing the medusa population (Lucas and Dawson, 2014, Han and Uye, 2010). However, data on the polyp stage of jellyfish is significantly less than on medusa and modelling of jellyfish life cycles is still relatively new, with the focus of previous modelling studies on a small area and individual species only (Henschke et al., 2018, Schnedler-Meyer et al., 2018). The inclusion of jellyfish life cycles into PlankTOM would be a large undertaking, outside the scope of this study. The aim of this study was not to reproduce small-scale blooms, but rather to assess at the large and global scale the influence of jellyfish on the plankton ecosystem and biogeochemistry. There is currently no coastal advantage for jellyfish included in the model, as there is for macrozooplankton, which have a coastal and under-ice advantage for increased recruitment in these areas (Le Quéré et al., 2016). Introducing a similar advantage for jellyfish could introduce an element of life cycle benefits i.e. the increased recruitment and settlement of planulae larvae onto hard substrate in coastal regions (Lucas et al., 2012), without the large computational costs and uncertainty of including a full life cycle.

Another limitation of jellyfish representation in the model is the lack of body size representation. Most biological activity is from small individuals, while most of the biomass is from large individuals. The size distribution of body mass in jellyfish is particularly wide compared to other PFTs (Table 3.1), so representing jellyfish activity by an average sized individual could well skew the results.

Trophic interactions explain the improvement of spatial chlorophyll pattern with the introduction of jellyfish to the model (PlankTOM10 to PlankTOM11), especially the North/South ratio. The two simulations have identical physical environments, with the influence of jellyfish as the only alteration, so any differences between the two can be attributed to the ecosystem structure. Jellyfish are the highest trophic level represented in PlankTOM11, with grazing preference for meso-, followed by proto-, and then macrozooplankton. However, the largest influence of jellyfish is on the macrozooplankton, rather than on mesozooplankton, for which it has the highest preference. This is because as jellyfish graze, the grazing pressure on mesozooplankton from macrozooplankton is reduced, and the grazing on protozooplankton by macro- and mesozooplankton is reduced. The top down trophic cascade from jellyfish on the other zooplankton also releases some of the grazing pressure on the phytoplankton.

Jellyfish biomass does not show a clear trend over time in PlankTOM11, after 1985 when model drift is reduced (Fig. 3.6). This should be taken as a preliminary finding, as longer climatological runs would be required to fully investigate the trend in jellyfish biomass over time, preferably along with the improvements to the jellyfish PFT suggested in this discussion. The global trends in observations show a possible increase in jellyfish biomass since around 2000 (see Chapter 2). However, observations are largely restricted to coastal regions, so a future analysis of PlankTOM11 looking at global, regional, and coastal vs open ocean trends would provide the most constructive and informative analysis.

### **3.5 Conclusion**

Jellyfish have been included as a PFT in a global biogeochemical ocean model for the first time as far as we can tell. The model provides reasonable overall replication of

global ecosystem properties and reasonable surface chlorophyll, particularly the north/south ratio. The replication of global mean jellyfish biomass, 0.13 PgC, is within the observational range (Chapter 2, Lucas et al., 2014, Bar-On et al., 2018), and in the region with the highest density of observations PlankTOM11 closely replicates the mean jellyfish biomass, but underestimates the maximum biomass. Jellyfish exert control over the other zooplankton, with the greatest influence on macrozooplankton. Through trophic cascades jellyfish also influence the phytoplankton and chlorophyll. PlankTOM11 is a successful first step in the inclusion of jellyfish in global biogeochemical modelling. The model raises interesting questions about the sensitivity of the zooplankton community to changes in jellyfish mortality. Future work could include an exploration of the full life cycle, coastal advantages, higher resolution ocean physical processes to enhance patchiness, and the long-term effect of climate change on jellyfish biomass. However, this model version is deemed suitable to explore pathways to carbon export mediated by jellyfish (Chapter 4) and the relative importance of fisheries and changing climate for jellyfish biomass (Chapter 5).

## References

- ACEVEDO, M. J., FUENTES, V. L., OLARIAGA, A., CANEPA, A., BELMAR, M. B., BORDEHORE, C. & CALBET, A. 2013. Maintenance, feeding and growth of *Carybdea marsupialis* (Cnidaria: Cubozoa) in the laboratory. *Journal of Experimental Marine Biology and Ecology*, 439, 84-91.
- ACUÑA, J. L., LÓPEZ-URRUTIA, Á. & COLIN, S. 2011. Faking giants: the evolution of high prey clearance rates in jellyfishes. *Science*, 333, 1627-1629.
- ALMEDA, R., WAMBAUGH, Z., CHAI, C., WANG, Z., LIU, Z. & BUSKEY, E. J. 2013. Effects of crude oil exposure on bioaccumulation of polycyclic aromatic hydrocarbons and survival of adult and larval stages of gelatinous zooplankton. *PLoS One*, 8, e74476.
- ANTONOV, J. I., SEIDOV, D., BOYER, T., LOCARNINI, R., MISHONOV, A., GARCIA, H., BARANOVA, O., ZWENG, M. & JOHNSON, D. 2010. World Ocean Atlas 2009. U.S. Government Printing Office, Washington, D.C.: S. Levitus, Ed. NOAA Atlas NESDIS 69.
- BAR-ON, Y., PHILLIPS, R. & MILO, R. 2018. The biomass distribution on Earth. *Proceedings of the National Academy of Sciences of the United States of America*, 115, 6506-6511.
- BENEDETTI-CECCHI, L., CANEPA, A., FUENTES, V., TAMBURELLO, L., PURCELL, J. E., PIRAINO, S., ROBERTS, J., BOERO, F. & HALPIN, P. 2015. Deterministic Factors Overwhelm Stochastic Environmental Fluctuations as Drivers of Jellyfish Outbreaks. *PloS one*, 10, e0141060.
- BUITENHUIS, E., LE QUÉRÉ, C., AUMONT, O., BEAUGRAND, G., BUNKER, A., HIRST, A., IKEDA, T., O'BRIEN, T., PIONTKOVSKI, S. & STRAILE, D. 2006. Biogeochemical fluxes through mesozooplankton. *Global Biogeochemical Cycles*, 20.
- BUITENHUIS, E. T., HASHIOKA, T. & LE QUERE, C. 2013a. Combined constraints on global ocean primary production using observations and models. *Global Biogeochemical Cycles*, 27, 847-858.
- BUITENHUIS, E. T., LI, W. K. W., LOMAS, M. W., KARL, D. M., LANDRY, M. R. & JACQUET, S. 2012a. Picoheterotroph (Bacteria and Archaea) biomass distribution in the global ocean. *Earth Syst. Sci. Data*, 4, 101-106.

- BUITENHUIS, E. T., LI, W. K. W., VAULOT, D., LOMAS, M. W., LANDRY, M. R., PARTENSKY, F., KARL, D. M., ULLOA, O., CAMPBELL, L., JACQUET, S., LANTOINE, F., CHAVEZ, F., MACIAS, D., GOSSELIN, M. & MCMANUS, G. B. 2012b. Picophytoplankton biomass distribution in the global ocean. *Earth Syst. Sci. Data*, 4, 37-46.
- BUITENHUIS, E. T., RIVKIN, R. B., SAILLEY, S. & LE QUÉRÉ, C. 2010. Biogeochemical fluxes through microzooplankton. *Global Biogeochemical Cycles*, 24, GB4015.
- BUITENHUIS, E. T., VOGT, M., MORIARTY, R., BEDNARSEK, N., DONEY, S. C., LEBLANC, K., LE QUERE, C., LUO, Y. W., O'BRIEN, C., O'BRIEN, T., PELOQUIN, J., SCHIEBEL, R. & SWAN, C. 2013b. MAREDAT: towards a world atlas of MARine Ecosystem DATa. *Earth System Science Data*, 5, 227-239.
- CHELSKY, A., PITT, K. A. & WELSH, D. T. 2015. Biogeochemical implications of decomposing jellyfish blooms in a changing climate. *Estuarine Coastal and Shelf Science*, 154, 77-83.
- COLIN, S. P., COSTELLO, J. H., GRAHAM, W. M. & HIGGINS III, J. 2005. Omnivory by the small cosmopolitan hydromedusa *Aglaura hemistoma*. *Limnology and Oceanography*, 50, 1264-1268.
- DONEY, S. C., RUCKELSHAUS, M., DUFFY, J. E., BARRY, J. P., CHAN, F., ENGLISH, C. A., GALINDO, H. M., GREBMEIER, J. M., HOLLOWED, A. B., KNOWLTON, N., POLOVINA, J., RABALAIS, N. N., SYDEMAN, W. J. & TALLEY, L. D. 2012. Climate Change Impacts on Marine Ecosystems. *Annual Review of Marine Science*, Vol 4, 4, 11-37.
- DUARTE, C. M., PITT, K. A., LUCAS, C. H., PURCELL, J. E., UYE, S.-I., ROBINSON, K., BROTZ, L., DECKER, M. B., SUTHERLAND, K. R., MALEJ, A., MADIN, L., MIANZAN, H., GILI, J.-M., FUENTES, V., ATIENZA, D., PAGES, F., BREITBURG, D., MALEK, J., GRAHAM, W. M. & CONDON, R. H. 2013. Is global ocean sprawl a cause of jellyfish blooms? *Frontiers in Ecology and the Environment*, 11, 91-97.
- FLYNN, B. & GIBBONS, M. 2007. A note on the diet and feeding of *Chrysaora hysoscella* in Walvis Bay Lagoon, Namibia, during September 2003. *African Journal of Marine Science*, 29, 303-307.

- FOSSETTE, S., GLEISS, A., CHALUMEAU, J., BASTIAN, T., ARMSTRONG, C., VANDENABEELE, S., KARPYTECHEV, M. & HAYS, G. 2015. Current-Oriented Swimming by Jellyfish and Its Role in Bloom Maintenance. *Current Biology*, 25, 342-347.
- GIBBONS, M. 2018. *RE: Personal communication*.
- GRAHAM, W., PAGÈS, F. & HAMNER, W. 2001. A physical context for gelatinous zooplankton aggregations: a review. *Hydrobiologia*, 451, 199-212.
- GRUBER, N. 2008. The marine nitrogen cycle: Overview of distributions and processes. *In: CAPONE, D. G. (ed.) Nitrogen in the Marine Environment*, Amsterdam: Elsevier.
- HAN, C.-H. & UYE, S.-I. 2010. Combined effects of food supply and temperature on asexual reproduction and somatic growth of polyps of the common jellyfish *Aurelia aurita* sl. *Plankton and Benthos Research*, 5, 98-105.
- HENSCHKE, N., STOCK, C. & SARMIENTO, J. 2018. Modeling population dynamics of scyphozoan jellyfish (*Aurelia* spp.) in the Gulf of Mexico. *Marine Ecology Progress Series*, 591, 167-183.
- IKEDA, T. 1985. Metabolic rates of epipelagic marine zooplankton as a function of body mass and temperature. *Marine Biology*, 85, 1-11.
- KALNAY, E., KANAMITSU, M., KISTLER, R., COLLINS, W., DEAVEN, D., GANDIN, L., IREDELL, M., SAHA, S., WHITE, G. & WOOLLEN, J. 1996. The NCEP/NCAR 40-year reanalysis project. *Bulletin of the American meteorological Society*, 77, 437-472.
- KEY, R. M., KOZYR, A., SABINE, C. L., LEE, K., WANNINKHOF, R., BULLISTER, J. L., FEELY, R. A., MILLERO, F. J., MORDY, C. & PENG, T. H. 2004. A global ocean carbon climatology: Results from Global Data Analysis Project (GLODAP). *Global biogeochemical cycles*, 18.
- LE QUÉRÉ, C., BUITENHUIS, E. T., MORIARTY, R., ALVAIN, S., AUMONT, O., BOPP, L., CHOLLET, S., ENRIGHT, C., FRANKLIN, D. J., GEIDER, R. J., HARRISON, S. P., HIRST, A., LARSEN, S., LEGENDRE, L., PLATT, T., PRENTICE, I. C., RIVKIN, R. B., SATHYENDRANATH, S., STEPHENS, N., VOGT, M., SAILLEY, S. & VALLINA, S. M. 2016. Role of zooplankton dynamics for Southern Ocean phytoplankton biomass and global biogeochemical cycles. *Biogeosciences*, 13, 4111-4133.

- LEBLANC, K., ARÍSTEGUI, J., ARMAND, L., ASSMY, P., BEKER, B., BODE, A., BRETON, E., CORNET, V., GIBSON, J., GOSSELIN, M. P., KOPCZYNSKA, E., MARSHALL, H., PELOQUIN, J., PIONTKOVSKI, S., POULTON, A. J., QUÉGUINER, B., SCHIEBEL, R., SHIPE, R., STEFELS, J., VAN LEEUWE, M. A., VARELA, M., WIDDICOMBE, C. & YALLOP, M. 2012. A global diatom database – abundance, biovolume and biomass in the world ocean. *Earth Syst. Sci. Data*, 4, 149-165.
- LEBRATO, M., MENDES, P. D. J., STEINBERG, D. K., CARTES, J. E., JONES, B. M., BIRSA, L. M., BENAVIDES, R. & OSCHLIES, A. 2013a. Jelly biomass sinking speed reveals a fast carbon export mechanism. *Limnology and Oceanography*, 58, 1113-1122.
- LEBRATO, M., MOLINERO, J.-C., CARTES, J. E., LLORIS, D., MÉLIN, F. & BENI-CASADELLA, L. 2013b. Sinking jelly-carbon unveils potential environmental variability along a continental margin. *PloS one*, 8, e82070.
- LEBRATO, M., PITT, K. A., SWEETMAN, A. K., JONES, D. O., CARTES, J. E., OSCHLIES, A., CONDON, R. H., MOLINERO, J. C., ADLER, L. & GAILLARD, C. 2012. Jelly-falls historic and recent observations: a review to drive future research directions. *Hydrobiologia*, 690, 227-245.
- LUCAS, C. H. & DAWSON, M. N. 2014. What Are Jellyfishes and Thaliaceans and Why Do They Bloom? *Jellyfish blooms*. Springer.
- LUCAS, C. H., GRAHAM, W. M. & WIDMER, C. 2012. JELLYFISH LIFE HISTORIES: ROLE OF POLYPS IN FORMING AND MAINTAINING SCYPHOMEDUSA POPULATIONS. *Advances in Marine Biology, Vol 63*, 63, 133-196.
- LUCAS, C. H., JONES, D. O. B., HOLLYHEAD, C. J., CONDON, R. H., DUARTE, C. M., GRAHAM, W. M., ROBINSON, K. L., PITT, K. A., SCHILDHAUER, M. & REGETZ, J. 2014. Gelatinous zooplankton biomass in the global oceans: geographic variation and environmental drivers. *Global Ecology and Biogeography*, 23, 701-714.
- LUO, Y. W., DONEY, S. C., ANDERSON, L. A., BENAVIDES, M., BERMAN-FRANK, I., BODE, A., BONNET, S., BOSTRÖM, K. H., BÖTTJER, D., CAPONE, D. G., CARPENTER, E. J., CHEN, Y. L., CHURCH, M. J., DORE, J. E., FALCÓN, L. I., FERNÁNDEZ, A., FOSTER, R. A., FURUYA, K., GÓMEZ, F., GUNDERSEN, K., HYNES, A. M., KARL, D. M., KITAJIMA,



- S., LANGLOIS, R. J., LAROCHE, J., LETELIER, R. M., MARAÑÓN, E., MCGILLICUDDY JR, D. J., MOISANDER, P. H., MOORE, C. M., MOURIÑO-CARBALLIDO, B., MULHOLLAND, M. R., NEEDOBA, J. A., ORCUTT, K. M., POULTON, A. J., RAHAV, E., RAIMBAULT, P., REES, A. P., RIEMANN, L., SHIOZAKI, T., SUBRAMANIAM, A., TYRRELL, T., TURK-KUBO, K. A., VARELA, M., VILLAREAL, T. A., WEBB, E. A., WHITE, A. E., WU, J. & ZEHR, J. P. 2012. Database of diazotrophs in global ocean: abundance, biomass and nitrogen fixation rates. *Earth Syst. Sci. Data*, 4, 47-73.
- MADEC, G. 2008. NEMO ocean engine Note du pole de mode' lisation. Institut Pierre-Simon Laplace, Paris.
- MALEJ, A. & MALEJ, M. 1992. Population dynamics of the jellyfish *Pelagia noctiluca* (Forsskål, 1775). In: COLOMBO, G., FERRARA, I. (ed.) *Marine Eutrophication and Populations Dynamics*. Denmark.
- MALEJ, A., TURK, V., LUČIĆ, D. & BENOVIĆ, A. 2007. Direct and indirect trophic interactions of *Aurelia* sp.(Scyphozoa) in a stratified marine environment (Mljet Lakes, Adriatic Sea). *Marine Biology*, 151, 827-841.
- MORIARTY, R. 2009. *The role of macro-zooplankton in the global carbon cycle*. Doctor of Philosophy, University of East Anglia.
- MORIARTY, R., BUITENHUIS, E. T., LE QUÉRÉ, C. & GOSSELIN, M. P. 2013. Distribution of known macrozooplankton abundance and biomass in the global ocean. *Earth Syst. Sci. Data*, 5, 241-257.
- MORIARTY, R. & O'BRIEN, T. D. 2013. Distribution of mesozooplankton biomass in the global ocean. *Earth Syst. Sci. Data*, 5, 45-55.
- O'BRIEN, C. J., PELOQUIN, J. A., VOGT, M., HEINLE, M., GRUBER, N., AJANI, P., ANDRULEIT, H., ARÍSTEGUI, J., BEAUFORT, L., ESTRADA, M., KARENTZ, D., KOPCZYŃSKA, E., LEE, R., POULTON, A. J., PRITCHARD, T. & WIDDICOMBE, C. 2013. Global marine plankton functional type biomass distributions: coccolithophores. *Earth Syst. Sci. Data*, 5, 259-276.
- PITT, K. A., KINGSFORD, M. J., RISSIK, D. & KOOP, K. 2007. Jellyfish modify the response of planktonic assemblages to nutrient pulses. *Marine Ecology Progress Series*, 351, 1-13.

- PITT, K. A., WELSH, D. T. & CONDON, R. H. 2009. Influence of jellyfish blooms on carbon, nitrogen and phosphorus cycling and plankton production. *Hydrobiologia*, 616, 133-149.
- PURCELL, J. 1992. EFFECTS OF PREDATION BY THE SCYPHOMEDUSAN CHRYSAORA-QUINQUECIRRHA ON ZOOPLANKTON POPULATIONS IN CHESAPEAKE BAY, USA. *Marine Ecology Progress Series*, 87, 65-76.
- PURCELL, J. 1997. Pelagic cnidarians and ctenophores as predators: Selective predation, feeding rates, and effects on prey populations. *Annales De L Institut Oceanographique*, 73, 125-137.
- PURCELL, J. 2003. Predation on zooplankton by large jellyfish, *Aurelia labiata*, *Cyanea capillata* and *Aequorea aequorea*, in Prince William Sound, Alaska. *Marine Ecology Progress Series*, 246, 137-152.
- PURCELL, J. E. 2009. Extension of methods for jellyfish and ctenophore trophic ecology to large-scale research. *Hydrobiologia*, 616, 23-50.
- PURCELL, J. E., FUENTES, V., ATIENZA, D., TILVES, U., ASTORGA, D., KAWAHARA, M. & HAYS, G. C. 2010. Use of respiration rates of scyphozoan jellyfish to estimate their effects on the food web. *Hydrobiologia*, 645, 135-152.
- RHEIN, M. S. R. R., S. AOKI, E. CAMPOS, D. CHAMBERS, R.A. FEELY, S. GULEV, G.C. JOHNSON, S.A. JOSEY, A. KOSTIANOY, C. MAURITZEN, D. ROEMMICH, L.D. TALLEY AND F. WANG, 2013. Observations: Ocean. In: STOCKER, T. F., D. QIN, G.-K. PLATTNER, M. TIGNOR, S.K. ALLEN, J. BOSCHUNG, A. NAUELS, Y. XIA, V. BEX AND P.M. MIDGLEY (ed.) *Climate Change 2013: The Physical Science Basis. Contribution of Working Group I to the Fifth Assessment Report of the Intergovernmental Panel on Climate Change*. Cambridge University Press, Cambridge, United Kingdom and New York, NY, USA.
- ROSA, S., PANSERA, M., GRANATA, A. & GUGLIELMO, L. 2013. Interannual variability, growth, reproduction and feeding of *Pelagia noctiluca* (Cnidaria: Scyphozoa) in the Straits of Messina (Central Mediterranean Sea): Linkages with temperature and diet. *Journal of Marine Systems*, 111, 97-107.
- SARMIENTO, J. L., DUNNE, J., GNANADESIKAN, A., KEY, R. M., MATSUMOTO, K. & SLATER, R. 2002. A new estimate of the CaCO<sub>3</sub> to organic carbon export ratio. *Global Biogeochemical Cycles*, 16, 1107.

- SCHNEDLER-MEYER, N. A., KIØRBOE, T. & MARIANI, P. 2018. Boom and Bust: Life History, Environmental Noise, and the (un)Predictability of Jellyfish Blooms. *Frontiers in Marine Science*, 5.
- SCHOEMANN, V., BECQUEVORT, S., STEFELS, J., ROUSSEAU, V. & LANCELOT, C. 2005. Phaeocystis blooms in the global ocean and their controlling mechanisms: a review. *Journal of Sea Research*, 53, 43-66.
- STOECKER, D., MICHAELS, A. & DAVIS, L. 1987. GRAZING BY THE JELLYFISH, AURELIA-AURITA, ON MICROZOOPLANKTON. *Journal of Plankton Research*, 9, 901-915.
- TIMMERMANN, R., GOOSSE, H., MADEC, G., FICHEFET, T., ETHE, C. & DULIERE, V. 2005. On the representation of high latitude processes in the ORCA-LIM global coupled sea ice–ocean model. *Ocean Modelling*, 8, 175-201.
- UYE, S. & SHIMAUCHI, H. 2005. Population biomass, feeding, respiration and growth rates, and carbon budget of the scyphomedusa Aurelia aurita in the Inland Sea of Japan. *Journal of Plankton Research*, 27, 237-248.
- VOGT, M., O'BRIEN, C., PELOQUIN, J., SCHOEMANN, V., BRETON, E., ESTRADA, M., GIBSON, J., KARENTZ, D., VAN LEEUWE, M. A., STEFELS, J., WIDDICOMBE, C. & PEPERZAK, L. 2012. Global marine plankton functional type biomass distributions: Phaeocystis spp. *Earth Syst. Sci. Data*, 4, 107-120.
- WEST, E. J., PITT, K. A., WELSH, D. T., KOOP, K. & RISSIK, D. 2009. Top-down and bottom-up influences of jellyfish on primary productivity and planktonic assemblages. *Limnology and Oceanography*, 54, 2058-2071.



CHAPTER 4. ROLE OF JELLYFISH  
FOR CARBON EXPORT



## Abstract

The biological carbon pump (BCP) plays an important role in transporting carbon out of the ocean surface, and the resulting balance of CO<sub>2</sub> between the atmosphere and the ocean. The structure of the marine plankton ecosystem is a key factor controlling the BCP. Jellyfish have unique characteristics of highly efficient grazers of zooplankton and bloom forming organisms. These two characteristics are thought to have a role in the BCP. Firstly, by acting as a control on the biomass of other zooplankton and therefore affecting the structure of the plankton ecosystem and secondly, by directly contributing to carbon export through bloom die-off and subsequent carcass sinking events known as jelly-falls. However, these roles are poorly quantified through observations and have not yet been examined with the use of global ocean biogeochemistry models. Here we use the PlankTOM11 global ocean biogeochemistry model (Chapter 3) to assess the influence of jellyfish on carbon export. The importance of each parameter that characterises the jellyfish plankton functional type (PFT) is also individually assessed with the use of five sensitivity simulations. Including jellyfish in PlankTOM11 produced a global annual carbon export of 7.11 PgC/y and a primary production of 41.5 PgC/y, with large spatial and seasonal variability in primary production, export and export efficiency. Changes to jellyfish affected the seasonal variation in primary production and export, through changes to the zooplankton community structure. The contribution of jellyfish mortality to carbon export is likely under-represented in the model because the large particulate organic carbon component from jellyfish mortality in the model is smaller and slower sinking than jelly-falls in reality. Results using PlankTOM11 suggest that the influence of jellyfish on export is most important through trophic cascades. There is also evidence that jellyfish mortality plays an important role in export, but this is not replicated in the model because of limited representation of mortality processes. A more detailed representation of particulate organic carbon is needed to improve the representation of jellyfish mortality in PlankTOM11, and its influence on the export.





## 4.1 Introduction

The oceans play a key role in the global carbon cycle (Le Quéré et al., 2018). The transfer of carbon from the atmosphere to the oceans is driven by the chemical dissolution of carbon dioxide (CO<sub>2</sub>) in the surface oceans, followed by the physical transport of carbon to depth. In addition to the physical transport is the biological carbon pump (BCP) which is estimated to export 5 - 12 PgC/y from the surface to the deep ocean through biological processes (McKinley et al., 2017), with physical transport returning this flux of carbon back to the surface when the BCP is in equilibrium. At equilibrium, the BCP does not influence the ocean CO<sub>2</sub> sink, but changes to the BCP can influence the sink. The downward section of the BCP is the collection of biological processes which influence the vertical gradient of dissolved inorganic carbon through production, export and remineralisation (Burd et al., 2016). In the BCP, phytoplankton fix carbon in the surface ocean via photosynthesis, transforming it from dissolved inorganic carbon to organic carbon. Phytoplankton are consumed by zooplankton, and the carbon is transferred and utilised in metabolic processes. Carbon leaves the surface waters through a number of biologically mediated routes including aggregation of particles, marine snow, messy-eating, defecation, shedding (i.e. crustacean exoskeletons and jellyfish mucus), carcasses sinking down the water column and diel vertical migration. Once carbon has sunk below the surface mixed-layer, it can become isolated from the atmosphere for decades and longer (McKinley et al., 2017). The carbon that sinks out of the mixed-layer depth is known as the carbon export and is usually defined in global studies as the sinking of organic carbon at 100m depth (Palevsky and Doney, 2018). Changes to the BCP contribute to changes in the air-sea CO<sub>2</sub> flux by changing the concentration of CO<sub>2</sub> in the surface ocean. Thus improving our understanding of the processes involved in the BCP, and how those processes are affected by climate, fisheries and other environmental changes, will improve our understanding of the evolution of the global carbon sink (Burd et al., 2016, McKinley et al., 2017).

The export efficiency ratio (*ef* ratio) is quantified as the ratio of the flux of organic matter exported across the base of the euphotic zone (here defined as 100m) to the integrated primary production within that layer (Laws et al., 2000, Laws et al., 2011, Cael et al., 2017). Temperature and primary production have been found to be the key

components in shaping the *ef* ratio, but simplistic relationships such as a linear, negative correlation between *ef* ratio and temperature (Laws et al., 2000) do not explain much of the global variance found in the *ef* ratio (Cael and Follows, 2016). The *ef* ratio varies proportionally to primary production, but both positive and negative correlation between *ef* ratio and primary production have been found in different ocean regions, indicating that significant control over the export of carbon is external to primary production (Maiti et al., 2013, Henson et al., 2015, Le Moigne et al., 2016, Cavan et al., 2017).

The carbon export is affected by several factors, including the primary production by phytoplankton, the types of phytoplankton present (in particular if they form shells or not), the presence of bloom conditions and the grazing by zooplankton (Cavan et al., 2015, Cael and Follows, 2016). Thus, the composition and activity of the marine ecosystem has a critical influence on the amount of carbon that is exported from surface waters. For a given primary production, the marine plankton ecosystem structure particularly influences the efficiency by which carbon is exported through depth (Henson et al., 2012, Henson et al., 2015, Cavan et al., 2017).

The composition of zooplankton is increasingly recognised as a factor in determining carbon export and the *ef* ratio (Boyd, 2015). However, the role of zooplankton diversity has been little explored (Boyd, 2015, Henson et al., 2015, Cavan et al., 2017). In particular, jellyfish are increasingly recognised as important in marine ecosystems and vertical fluxes but are not included in global biogeochemical models (Burd et al., 2016). Mass deposition events of jellyfish carcasses occur during and after jellyfish blooms and are known as jelly-falls. Jelly-falls have been shown to have a significant contribution to the fate of exported materials, including carbon (Yamamoto et al., 2008, Lebrato et al., 2012, Lebrato et al., 2013a, Li et al., 2015, Lamb et al., 2017, Stone and Steinberg, 2018). The standing stock of jellyfish carcasses along a continental margin (around 3000m depth) was found to vary from one-third of the annual organic carbon flux, up to an order of magnitude greater than the annual organic carbon flux (Billett et al., 2006). During their life, jellyfish also contribute to the flux of carbon through mucus production and faecal pellets (Pitt et al., 2009). Jellyfish are known to initiate top-down trophic cascades, as highly efficient grazers of zooplankton (Purcell, 1997, Purcell, 2003, West et al., 2009, Acuña et al., 2011). The

grazing by jellyfish will also influence the carbon flux through the control of other zooplankton types (Stone and Steinberg, 2018).

Here we use the PlankTOM11 global ocean biogeochemistry model (Chapter 3) to assess the influence of jellyfish on the BCP and carbon export to depth. Each parameter that represents the characteristics of the jellyfish plankton functional type (PFT) is also individually assessed through five additional simulations. These simulations are (1) parameterising the jellyfish PFT as the macrozooplankton PFT, then switching on in turn jellyfish (2) grazing preferences, (3) growth, (4) respiration and (5) mortality. The simulations are used to investigate the specific role of jellyfish characteristics (grazing, growth, respiration and mortality) beyond just the additional complexity from adding another zooplankton PFT (1).

## 4.2 Methods

PlankTOM11 was developed by introducing jellyfish as an additional trophic level at the top of the plankton food web. PlankTOM11 represents PFTs of six phytoplankton (Phyto), bacteria (BAC), protozooplankton (PRO), mesozooplankton (MES), macrozooplankton (MAC; representing crustacean zooplankton) and jellyfish (JEL). A full description of the model development is given in Chapter 3 including all equations and parameters. Some parameters are repeated here, where they directly relate to the differences between PlankTOM11 and the additional simulations used to assess the influence of jellyfish on carbon export.

### 4.2.1 Export in PlankTOM11

Carbon export within PlankTOM11 is controlled by the sinking of small particulate organic carbon (POC) and large particulate organic carbon (GOC). POC is generated by aggregation from dissolved organic carbon (DOC) and by protozooplankton

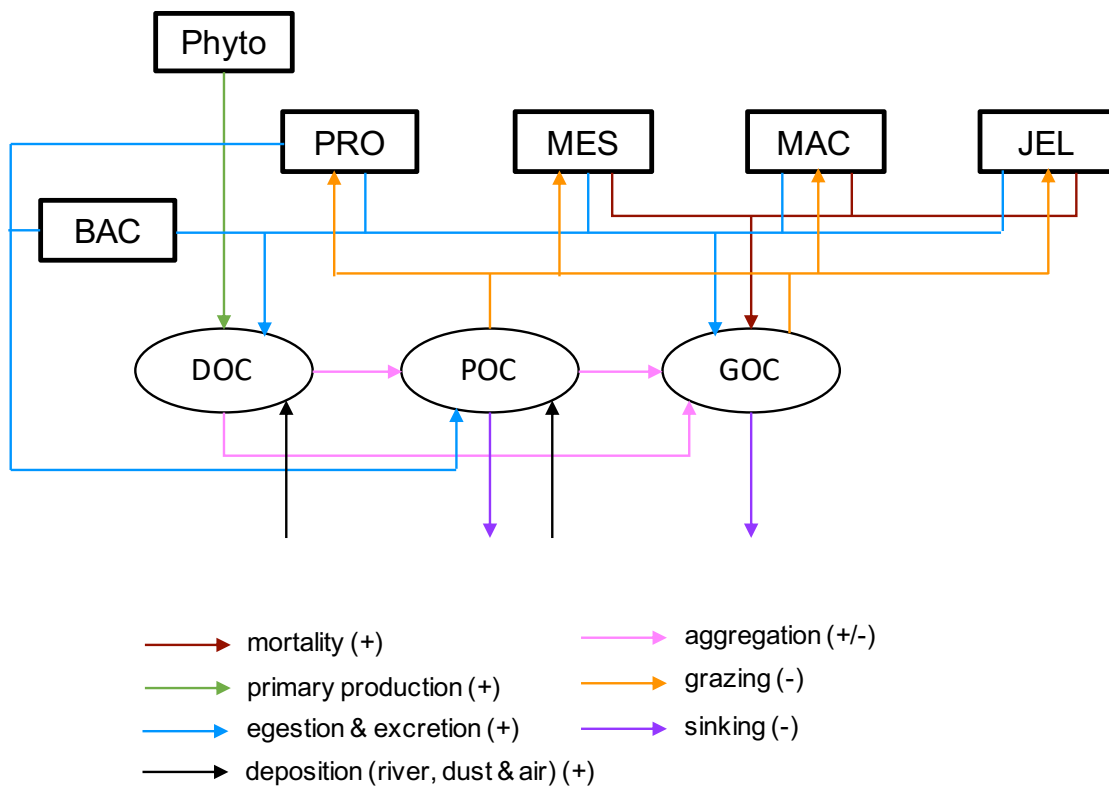


**Figure 4.1** The sources and sinks within PlankTOM11 for dissolved organic carbon (DOC) and small (POC) and large (GOC) particulate carbon. The sources (+) are additions to one or more of the organic carbon types and the sinks (-) are subtractions from one or more of the organic carbon types.

egestion and excretion and is consumed through grazing by all zooplankton. GOC is generated from aggregation from POC and DOC, egestion and excretion by all zooplankton, and mortality of mesozooplankton, macrozooplankton and jellyfish, and is consumed through grazing by all zooplankton (Fig. 4.1). The sinking speed of POC ( $V_{POC}$ ) is  $3 \text{ m/d}^{-1}$ , the sinking speed of GOC ( $V_{GOC}$ ) is dependent on particle density and sinking speed:

$$V_{GOC} = k_{GOC} \times \max(\rho_{GOC} - \rho_{seawater}, \rho_{min})^{S_{GOC}} \quad (4.1)$$

where  $k_{GOC}$  is  $0.0303 \text{ m}^2(\text{kg/d}^{-1})$  a sinking rate parameter for GOC,  $\rho_{GOC} - \rho_{seawater}$  is the density of GOC at a given density of seawater,  $\rho_{min}$  is the density at which GOC sinking speed is  $V_{POC}$ , and  $S_{GOC}$  is 0.6923, a unitless sinking rate parameter for GOC.

In order to help understand the effect of jellyfish on carbon export, the equations are provided here for the jellyfish processes that affect the sources and sinks of the three compartments of organic carbon (DOC, POC and GOC). The macrozooplankton PFT is parameterised using the same equations as for jellyfish but with different parameter rates (Fig. 4.1, Table 4.1). The influence of jellyfish on the evolution over time (t) of DOC is a source from egestion:

$$\frac{\partial DOC}{\partial t} = \sum [(1 - \sigma)(1 - \zeta - MGE) \sum_k g_{F_k}^{JEL} \times JEL \times F_k] \quad (4.2)$$

where  $1 - \sigma$  is the fraction of grazing by jellyfish that is converted to DOC (inorganic fraction of excretion),  $\zeta$  is the fraction of unassimilated grazing (particulate egestion) by jellyfish,  $MGE$  is the modelled growth efficiency of jellyfish, and  $g_{F_k}^{JEL}$  is the grazing of jellyfish on food source  $F_k$ . The influence of jellyfish on the evolution of POC is a sink from grazing:

$$\frac{\partial POC}{\partial t} = - \sum [g_{POC}^{JEL} \times JEL \times POC] \quad (4.3)$$

where  $g_{POC}^{JEL}$  is the grazing of jellyfish on POC. The influence of jellyfish on the evolution of GOC is sources from egestion, excretion and mortality, and a sink from grazing:

$$\frac{\partial GOC}{\partial t} = \sum \zeta \sum_k [g_{F_k}^{JEL} \times JEL \times F_k] + \sum [m_{0^\circ}^{JEL} \times T \times JEL] - \sum [g_{GOC}^{JEL} \times JEL \times GOC] \quad (4.4)$$

where  $m_{0^\circ}^{JEL}$  is the mortality of jellyfish,  $T$  is temperature and  $g_{GOC}^{JEL}$  is the grazing of jellyfish on GOC.

**Table 4.1** Temperature-dependent rates of macro- and jellyfish zooplankton. Respiration and mortality follow a simple exponential curve, where  $\mu_0$  is the rate at 0°C and  $Q_{10}$  is the temperature coefficient. Growth has a bell-shaped curve with a temperature optimum, where  $\mu_{max}$  is the maximum growth rate at  $T_{opt}$  (the optimal temperature) and  $dT$  is the temperature interval (see Chapter 3, section 3.2.2.1).

Parameters	Macrozooplankton			Jellyfish zooplankton		
	$\mu_0$ (d <sup>-1</sup> )	$Q_{10}$		$\mu_0$ (d <sup>-1</sup> )	$Q_{10}$	
Respiration	0.01	2.46		0.03	1.88	
Mortality	0.02	3.00		0.12	1.20	
	$\mu_{max}$ (d <sup>-1</sup> )	$T_{opt}$ (°C)	$dT$ (°C)	$\mu_{max}$ (d <sup>-1</sup> )	$T_{opt}$ (°C)	$dT$ (°C)
Growth	0.2	33.2	20.0	0.2	23.6	18.8

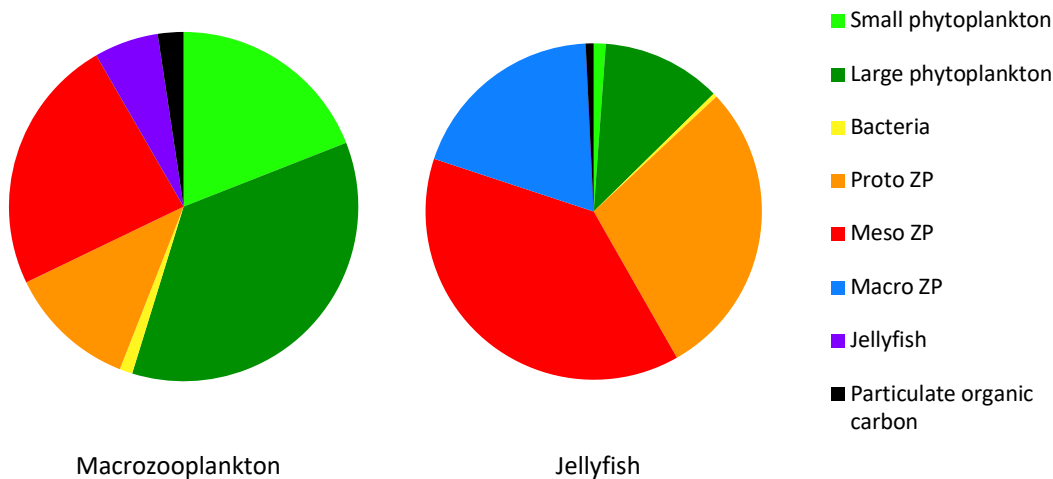


**Figure 4.2** Relative preference of (left) macrozooplankton and (right) jellyfish grazing for food used in PlankTOM11. Small phytoplankton is N<sub>2</sub>-fixers, pico-phytoplankton and coccolithophores, large phytoplankton is mixed phytoplankton, diatoms and Phaeocystis, and particulate organic carbon is POC and GOC. For values see Chapter 3, Table 3.3.

**Table 4.2** Sensitivity simulations to test the addition of a jellyfish PFT to PlankTOM. The parameterisation of the 11<sup>th</sup> PFT in PlankTOM as either jellyfish parameters (J) or macrozooplankton parameters (M) is indicated for each simulation. For grazing preferences, refer to Figure 4.2. For values used in growth, respiration and mortality parameters refer to Table 3.2 and Table 3.4.

Simulation Name	Parameters of the 11 <sup>th</sup> PFT			
	Grazing preference	Growth	Respiration	Mortality
PlankTOM11	J	J	J	J
PlankTOM10.5	M	M	M	M
PlankTOM10.5a	J	M	M	M
PlankTOM10.5b	M	J	M	M
PlankTOM10.5c	M	M	J	M
PlankTOM10.5d	M	M	M	J

#### 4.2.2 Model Simulations

In order to test the addition of a jellyfish PFT to PlankTOM, several sensitivity simulations were run. The central simulation is PlankTOM11, where jellyfish are parameterised as presented in Chapter 3. For a direct comparison, we also ran PlankTOM10.5, where jellyfish are parameterised as macrozooplankton, to test if the changes are due to the addition of jellyfish, or to the addition of an 11<sup>th</sup> PFT. The parameters for macrozooplankton and jellyfish are given in Table 4.1 and Figure 4.2. The four parameters that characterise jellyfish in PlankTOM11 (grazing preference, growth, respiration and mortality) were individually tested to identify which feature is the most influential (Table 4.2). Grazing preference determines the trophic level of the PFT. Jellyfish represents the highest trophic level in PlankTOM11, with the majority of grazing on other zooplankton PFTs (Fig. 4.2).

#### 4.2.3 Export Efficiency

The export efficiency, or *ef* ratio, is calculated;

$$ef = \frac{E_P}{P_P} \quad (4.5)$$

Where  $E_p$  is the export production at 100m, and  $P_p$  is the integrated primary production from 0 – 100m. An export efficiency of over one means that there is more carbon being exported at 100m than is being produced by the primary production in the water column above. This can occur where physical processes transport carbon from an area of high  $P_p$  to an area of low  $P_p$  where it is then exported (Laws et al., 2000, Laws et al., 2011). An *ef* ratio over one can also occur if there is a substantial time lag between  $P_p$  in the surface water and  $E_p$  due to biological processes slowing carbon transport. This may occur when  $P_p$  is declining just after a phytoplankton bloom,  $E_p$  may still be increasing due to the time taken for carbon to be transformed into GOC through the plankton food web and transported to depth (Henson et al., 2015). In reality the depth of the euphotic zone varies across the oceans and the seasons, and the choice of depth at which carbon export is calculated can impact results (Palevsky and Doney, 2018). A fixed depth of 100m is the standard depth horizon choice for global modelling studies. This fixed depth is used here as it has been shown to give *ef* ratio and carbon flux values around the centre of the spread of values when multiple depth horizons are used to calculate *ef* ratio and export across latitudes (Palevsky and Doney, 2018). For the results in this chapter, all plankton biomass is calculated for the top 100m, as this is where export and *ef* ratio are calculated.



## 4.3 Results

A description of PlankTOM11 ecosystem properties and spatial replication of chlorophyll and plankton types is given in Chapter 3.

### 4.3.1 Carbon Export in PlankTOM11

In PlankTOM11 primary production has large spatial and seasonal variability (Fig. 4.3). From June to August the highest primary production is 30 - 60°N, and from November to January, the highest primary production is 30 - 45°S. Primary production is high around the equator, with a slight variation between June to August and November to January. Primary production is consistently high in the Pacific equatorial upwelling region and is also elevated in the Atlantic equatorial upwelling (Fig. 4.3). Primary production is consistently low ( $<0.5 \text{ mol C/m}^2/\text{y}$ ) south of 50°S and in open ocean gyres (Fig. 4.3). Carbon export production has large spatial variability with the highest export ( $>5 \text{ mol C/m}^2/\text{y}$ ) in equatorial upwelling regions and around coastlines globally (Fig. 4.3). Export is elevated ( $1 - 3 \text{ mol C/m}^2$ ) in the open ocean for most of the Pacific and Indian Oceans, and in bands across the tropical and southern Atlantic Ocean, and in the northern Atlantic from June - August (Fig. 4.3). The strongest seasonal variability in export is in the southern Indian Ocean and around 30 - 40°S. Export is consistently low in the Southern Ocean south of 40°S (Fig. 4.3). The *ef* ratio has large spatial variation, the highest *ef* ratio for June to August is 0 - 30°S in the Indian, Pacific and Atlantic Ocean, at around 20°N in the western Atlantic and Pacific Ocean, and globally south of 60°S (Fig. 4.3). The highest *ef* ratio for November to January is 0 - 30°N in the western and central Pacific and Atlantic Ocean, extending to 20°S in the western Atlantic, and globally north of 60°N (Fig. 4.3). The *ef* ratio is lowest consistently at 30 - 60°S and 30 - 60°N with the exception of close to coasts (Fig. 4.3). The high *ef* ratio at latitudes higher than 60° in the respective hemispheres winter is driven by only slight changes in the low primary production and export in these regions.

The seasonal correlation between primary production and export production was divided into three regions; the North (30 - 90°N), Tropic (30°N - 30°S) and South (30 - 90°S; Fig 4.4). In the North and South regions, the correlation between primary

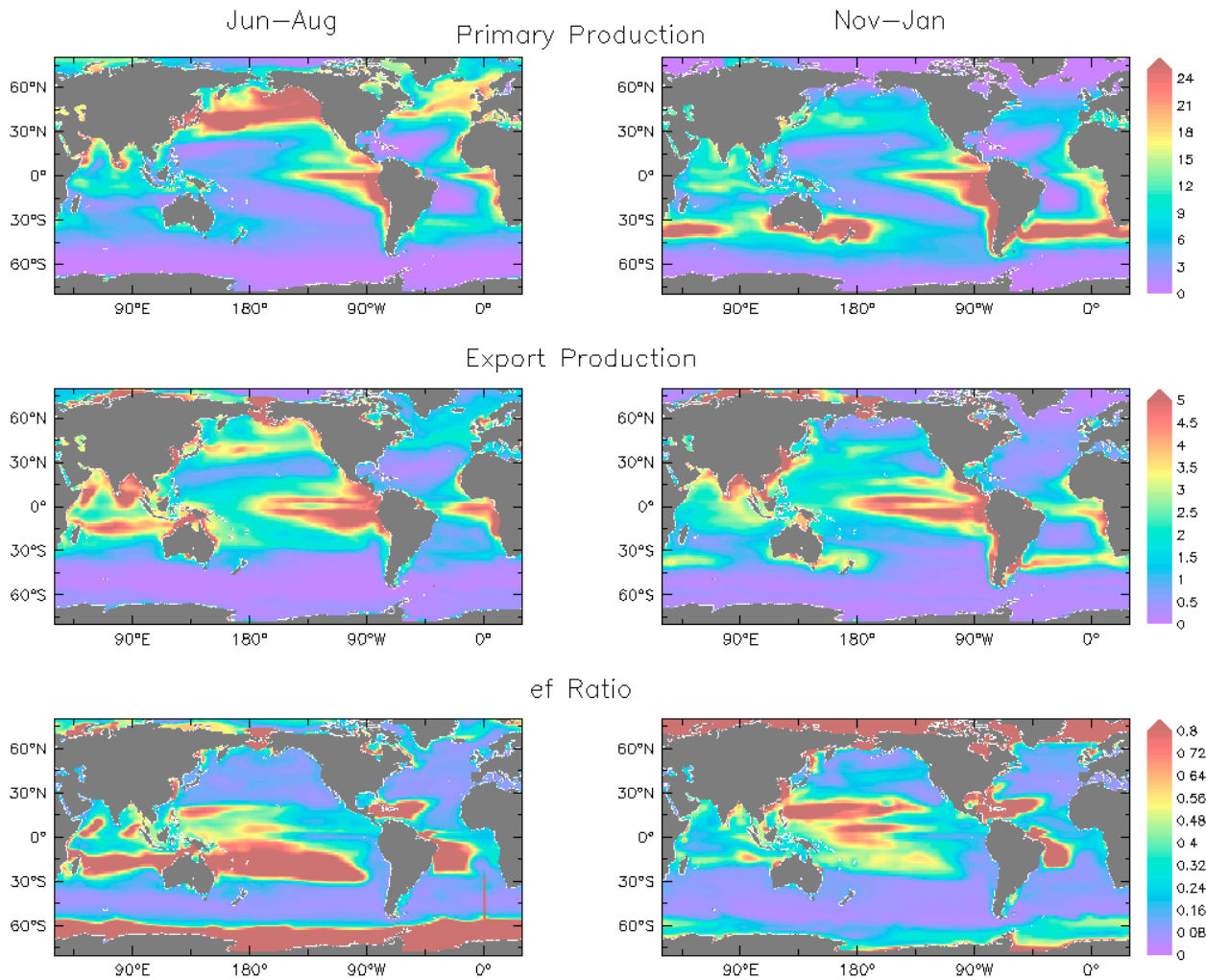


**Figure 4.3** PlankTOM11 results averaged for (left) June to August and (right) November to January. Data are for (top) primary production (mol C/m<sup>2</sup>/year) integrated over the top 100m, (middle) carbon export production at 100m (mol C/m<sup>2</sup>/year) and (bottom)  $ef$  ratio (export efficiency). All model results are averaged from 1985-2015.

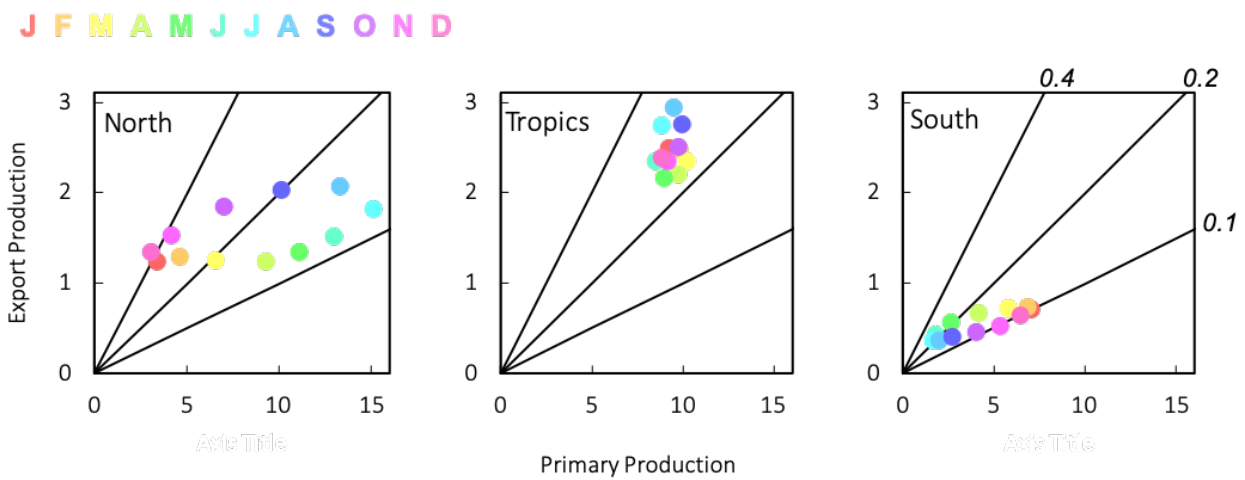


**Figure 4.4** PlankTOM11 seasonal variation of primary production and export production (mol/m<sup>2</sup>/year) at regions; (left) North 30°N–90°N, (middle) Tropics 30°N–30°S and (right) South 30°S–90°S. Points are coloured by months of the year, averaged from 1985-2015. Straight black lines indicate  $ef$  ratios of 0.1, 0.2 and 0.4.

production and export production is positive and follows a seasonal pattern, with higher production in the summer-autumn, lower production in winter-spring, and a higher *ef* ratio in the winter, for the respective hemisphere (Fig. 4.4). Both export and primary production are higher in the North region than in the South. In the North, from January to March the *ef* ratio drops from 0.4 to 0.2, is at its lowest from April to June (0.12), then increases from August to November back up to 0.4. In the South, from October to January the *ef* ratio is 0.1, it then increases to 0.2 from February to May, and stays at this value until September (Fig. 4.4). There is no correlation between primary production and export production in the Tropics, primary production stays around 10 mol/m<sup>2</sup>/y while export varies from 2 – 3 mol/m<sup>2</sup>/y (Fig. 4.4). The only seasonal variation in the Tropics occurs from July – September when export is elevated slightly above the rest of the year. The *ef* ratio in the Tropics is around 0.3 from July – September, and 0.25 for the rest of the year (Fig. 4.4).

The correlations over time between the *ef* ratio and primary production, sea surface temperature (SST), chlorophyll and zooplankton biomass were mapped globally (Fig. 4.5). Primary production and *ef* ratio show a negative correlation for the majority of the ocean. The negative correlation is largely due to the time lag between primary production and the conversion of DOC and POC into GOC by zooplankton, which is then exported. The strongest negative correlation (< -0.8) occurs in the Southern Ocean below 50°S. Little to no correlation occurs in the Indian Ocean, for 40 - 50°S and away from coastal regions for 40 - 60°N (Fig. 4.5). The SST and *ef* ratio show a mix of positive and negative correlation. Generally, at lower latitudes the correlation is negative and at higher latitudes the correlation is positive. At very high latitude in the Southern Ocean (>50°S) the correlation of SST and *ef* ratio is negative (Fig. 4.5). Chlorophyll and *ef* ratio show similar patterns of spatial correlation to primary production and *ef* ratio, with chlorophyll showing a weaker negative correlation (Fig. 4.5). Total zooplankton (tZP) biomass and *ef* ratio show a mix of negative and, mostly weak, positive correlation. In the Southern Ocean, below 30°S, tZP has a weak positive correlation to *ef* ratio, in the Pacific there are patches of negative or no correlation, and in the Atlantic there is positive correlation at the equator and in the east, with negative or no correlation elsewhere (Fig. 4.5). Jellyfish and *ef* ratio show similar patterns of correlation to total tZP and *ef* ratio, with stronger positive and weaker negative correlation to jellyfish than to total tZP (Fig. 4.5). Macrozooplankton and *ef* ratio show

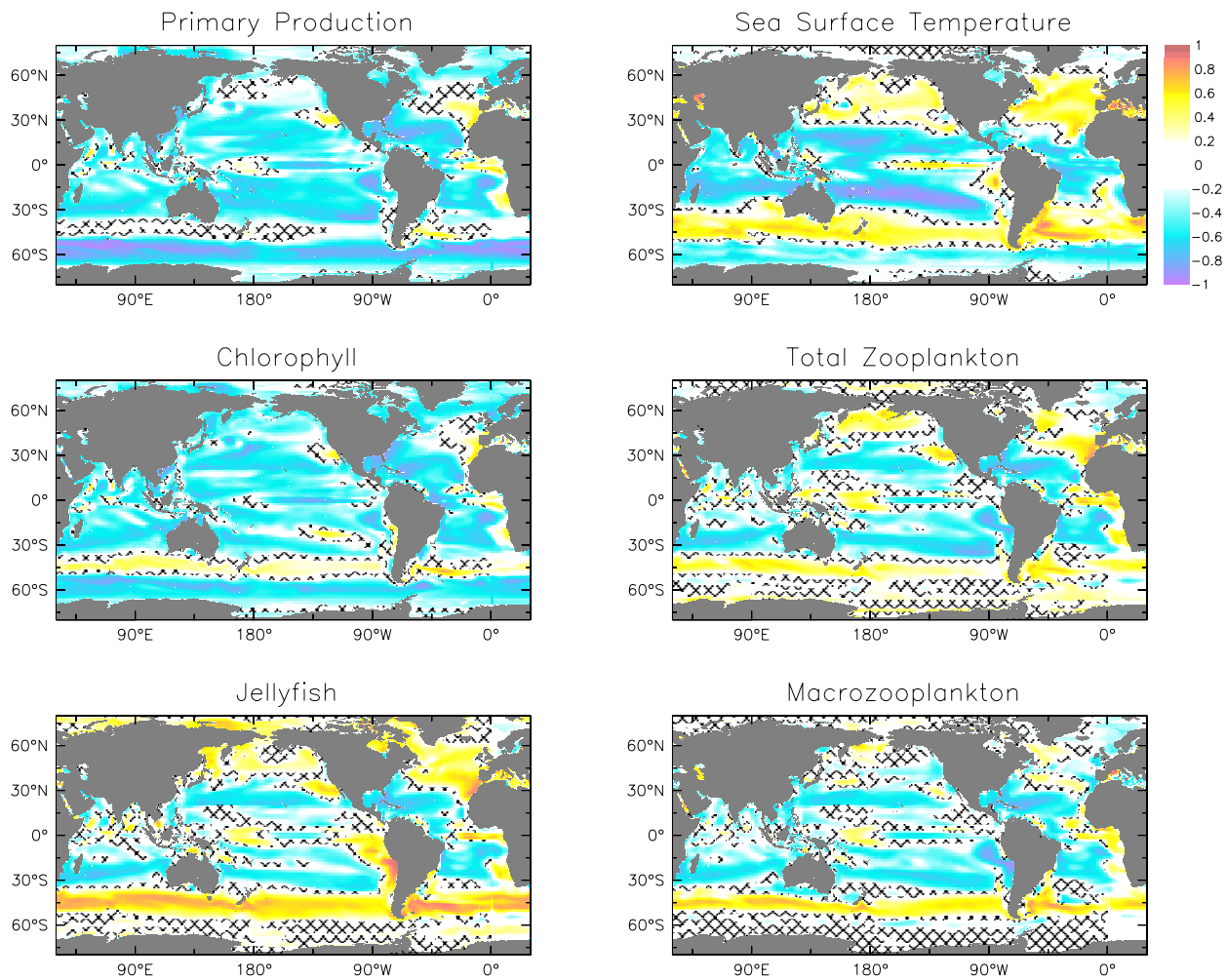


**Figure 4.5** PlankTOM11 correlations over time of the *ef* ratio with primary production (top left), sea surface temperature (top right), chlorophyll concentration (middle left), total zooplankton biomass (middle right), jellyfish biomass (bottom left) and macrozooplankton biomass (bottom right). Correlations are averaged over 0-100m except for sea surface temperature. Warm colours indicate a positive correlation, while cold colours indicate a negative correlation. Cross-hatched grid cells are where the correlation is not statistically significant ( $p$  values less than 0.05).

similar patterns of correlation to total tZP and *ef* ratio, with stronger positive correlation to macrozooplankton in the Southern Ocean, and weaker positive correlation elsewhere (Fig. 4.5). There is not a single variable that accounts for the seasonal fluctuations in *ef* ratio (Fig. 4.5). The patterns in SST and zooplankton are similar, and that may mean that SST could be a proxy for zooplankton. Within the zooplankton components, jellyfish have the largest correlations (in absolute values).

### 4.3.2 Role of Jellyfish Characteristics in Carbon Export

To assess the effect on carbon export of adding jellyfish to PlankTOM11, five sensitivity simulations were conducted; PlankTOM10.5 with the jellyfish PFT

parameterised as macrozooplankton (therefore leading to two identical macrozooplankton PFTs), and four intermediates between PlankTOM11 and 10.5, testing the individual characteristics of jellyfish by switching them on one at a time with all other parameters kept as in PlankTOM10.5 (Table 4.2). These characteristics are jellyfish grazing preferences (PlankTOM10.5a), jellyfish growth rate (PlankTOM10.5b), jellyfish respiration rate (PlankTOM10.5c) and jellyfish mortality rate (PlankTOM10.5d).

The global annual *ef* ratio, primary production and export production for all six simulations are given in Table 4.3, along with the tZP biomass. Out of the six runs investigating jellyfish characteristics, PlankTOM11 has the highest export of 7.11 PgC/y, but only the fourth-highest primary production (41.5 PgC/y) and the lowest tZP biomass (0.96 mol C/m<sup>3</sup>; Table 4.3). PlankTOM10.5a (grazing) has the highest primary production of 44.49 PgC/y, with the second highest export (6.91 PgC/y) and second lowest tZP biomass (1.14 mol C/m<sup>3</sup>; Table 4.3). PlankTOM10.5c (respiration) and PlankTOM10.5d (mortality) have the highest tZP biomass of 1.38 mol C/m<sup>3</sup>, with the second and third highest primary production (42.34 and 42.02 PgC/y respectively) and the third and fourth highest export (6.75 and 6.74 PgC/y respectively; Table 4.3). Fully parametrised jellyfish (PlankTOM11) gives the highest export and just using

**Table 4.3** Global annual *ef* ratio, primary production and export production rates (Pg carbon/year) and total zooplankton biomass (mol carbon/m<sup>3</sup>) averaged over 0-100m in PlankTOM11 and PlankTOM10.5 simulations.

Run	<i>ef</i> Ratio	Production (PgC/y)		Zooplankton Biomass (mol C/m <sup>3</sup> )
		Primary	Export	
<b>PlankTOM11</b> <i>jellyfish</i>	0.171	41.50	7.11	0.96
<b>PlankTOM10.5</b> <i>macro</i>	0.173	38.18	6.62	1.26
<b>PlankTOM10.5a</b> <i>grazing</i>	0.155	44.49	6.91	1.14
<b>PlankTOM10.5b</b> <i>growth</i>	0.159	37.23	5.91	1.32
<b>PlankTOM10.5c</b> <i>respiration</i>	0.159	42.34	6.75	1.38
<b>PlankTOM10.5d</b> <i>mortality</i>	0.160	42.02	6.74	1.38

jellyfish growth (PlankTOM10.5b) gives the lowest export. Total zooplankton biomass affects export, but not in a simple linear relationship. The highest total zooplankton biomass (PlankTOM10.5c/d) does not give the highest or lowest export, while the lowest total zooplankton biomass (PlankTOM11) does give the highest export. Export is not directly increased by more zooplankton biomass because zooplankton both consume and produce POC and GOC (Eq. 4.2 and 4.3). The composition of the zooplankton play a key role in controlling export; this is explored below.

The depth profiles of primary production, export production and tZP biomass in the six simulations are examined in Figure 6. The results are divided into three regions as for Figure 4.4; the North (30 - 90°N), Tropic (30°N - 30°S) and South (30 - 90°S). For the North (Fig. 4.6 top row) there is a substantial depth gradient from 0-200m, with the highest production and biomass at the surface, gradually decreasing as depth increases. The primary production is highest for PlankTOM10.5a (grazing preference) down to 50m; all other simulations have similar primary production throughout depth. The export production is highest and has the greatest depth gradient for PlankTOM11. The export is lowest and has the smallest depth gradient for PlankTOM10.5b (growth). The export for PlankTOM10.5a (grazing preferences) is the closest jellyfish characteristic simulation to PlankTOM11. The total zooplankton biomass is highest for PlankTOM10.5b (growth) down to 90m, below 90m PlankTOM10.5 (jellyfish = macrozooplankton) has the highest zooplankton biomass. The zooplankton biomass is lowest for PlankTOM11. Below 150m the zooplankton biomass is the same for all simulations (Fig. 4.6).

For the Tropics (Fig. 4.6 middle row) the highest production and biomass is from 0-75m, and then gradually decreases from 75-200m. The primary production peaks at the surface and then again at 75m for all simulations. There is no clear pattern of which simulation has the highest or lowest primary production through the depth profile. The export production is similar for all simulations, between 3 – 3.5 mol/m<sup>2</sup>/year at the surface dropping to 2.5 mol/m<sup>2</sup>/year at 100m, with no clear pattern of which simulation has the highest or lowest export through the depth profile. The total zooplankton biomass varies between simulations above 80m. The biomasses are similar below this depth horizon. At the surface the lowest zooplankton biomass is for

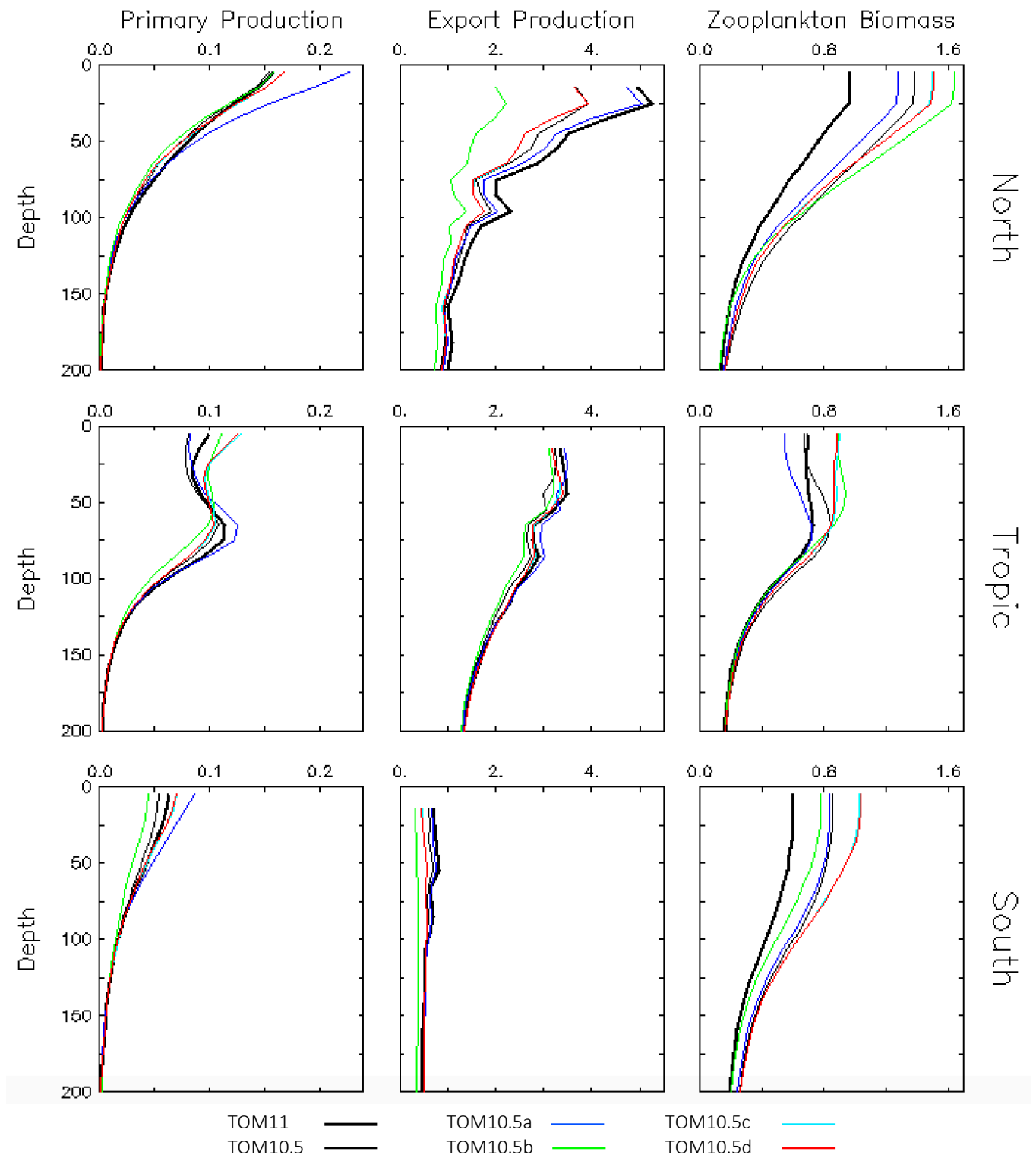


**Figure 4.6** Depth profiles of primary production, export production and total zooplankton biomass for PlankTOM11 (thick black line), PlankTOM10.5 (thin black line), PlankTOM10.5a (dark blue line; grazing preference), PlankTOM10.5b (green line; growth), PlankTOM10.5c (light blue line; respiration) and PlankTOM10.5d (red line; mortality). The top row of panels is results averaged for the Northern Hemisphere (30°N-90°N), the middle row is the Tropics (30°S-30°N) and the bottom row is the Southern Hemisphere (30°S-90°S). The left column of panels is for primary production ( $\text{mol}/\text{m}^2/\text{year}$ ), the middle column is export production ( $\text{mol}/\text{m}^2/\text{year}$ ) and the right column is total zooplankton biomass ( $\mu\text{m C L}^{-1}$ ). All results are averaged for 1985 – 2015.

PlankTOM10.5a (grazing preferences) at  $0.5 \mu\text{m C L}^{-1}$ . PlankTOM11 and PlankTOM10.5 have slightly higher zooplankton biomass of  $0.7 \mu\text{m C L}^{-1}$ , and the other three simulations have the highest biomass at the surface of  $0.9 \mu\text{m C L}^{-1}$  (Fig. 4.6).

For the South (Fig. 4.6 bottom row) production and biomass show a similar pattern over depth to the North, gradually decreasing as depth increases, but with a smaller gradient. The primary production is highest for PlankTOM10.5a (grazing preference) and lowest for PlankTOM10.5b (growth). The primary production for PlankTOM11 is about halfway between simulations a and b. The export production is low ( $<1 \text{ mol/m}^2/\text{year}$ ) for all the simulations. The export is lowest for PlankTOM10.5b (growth) with no depth gradient. The export is highest at the surface for PlankTOM11 and PlankTOM10.5a (grazing preferences), followed by PlankTOM10.5. At 100m export is the same for all simulations except for PlankTOM10.5b (growth) which is lower. The total zooplankton biomass has greater variation between simulations than export or primary production. The highest total zooplankton biomass is for PlankTOM10.5c (respiration) and PlankTOM10.5d (mortality) at  $1 \mu\text{m C L}^{-1}$  at the surface. The lowest zooplankton biomass is for PlankTOM11 at  $0.6 \mu\text{m C L}^{-1}$  at the surface (Fig. 4.6).

The differences in export and primary production, with jellyfish characteristic tests, exhibit variation between regions (Fig. 4.6). This spatial variation is further explored using global maps of PlankTOM11, and the difference between PlankTOM11 and each of the other simulations (Fig. 4.7). When the jellyfish PFT is parameterised as macrozooplankton (PlankTOM10.5) from PlankTOM11 overall export and primary production have the same pattern and direction of change. There is a decrease in both primary production and export in the equatorial Pacific and around  $40^\circ\text{N}$  and  $40^\circ\text{S}$ . There is a small increase in both primary production and export in the Indo-Pacific and Southern Ocean. Export and primary production differ in the eastern coastal equatorial Pacific where export increases while primary production decreases, and in the Bering Strait where export decreases while primary production increases (Fig. 4.7).

When jellyfish grazing preferences are switched on (PlankTOM10.5a), overall export and primary production have opposing directions of change where there is a substantial



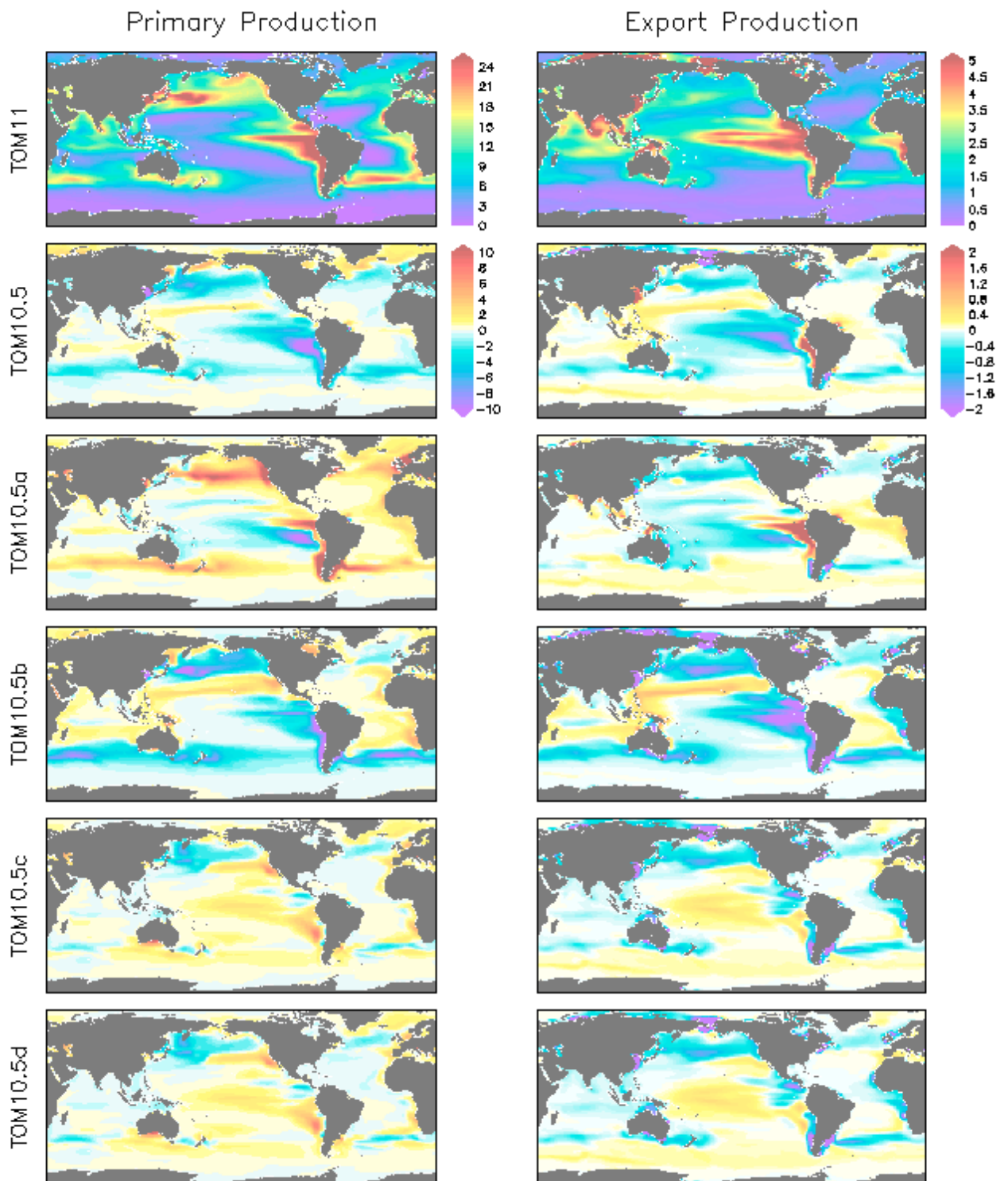


**Figure 4.7** Annual mean (left) primary production from 0-100m and (right) carbon export at 100m ( $\text{mol/m}^2/\text{year}$ ). Results shown for (top) PlankTOM11, then below the difference between PlankTOM11 and the other simulations, in descending order PlankTOM10.5, PlankTOM10.5a (grazing), PlankTOM10.5b (growth), PlankTOM10.5c (respiration) and PlankTOM10.5d (mortality). All model results are averaged for 1985-2015. For the difference between PlankTOM11 and other simulations, warm colours indicate that the values of the other simulation are higher than PlankTOM11, while cold colours indicate that the values of the other simulation are lower than PlankTOM11.

difference from PlankTOM11 (Fig. 4.7). North of 40°N globally and at 40°S in the Atlantic primary production increases while export decreases. In these areas' jellyfish grazing increases primary production, whilst increasing the retention of carbon within surface waters thus reducing export. Production follows the same direction of change in the eastern coastal equatorial Pacific where export and primary production increase, and in the central Pacific where they both decrease (Fig. 4.7).

When jellyfish growth is switched on (PlankTOM10.5b), overall export and primary production have the same pattern and direction of change (Fig. 4.7). Both export and primary production decrease compared to PlankTOM11 around 40°N and 40°S globally and in the eastern Pacific. Both export and primary production increase compared to PlankTOM11 in the Indo-Pacific and extending into the Pacific at 30°N. Export and primary production differ in the eastern coastal equatorial Atlantic and the Bering Strait where export decreases while primary production increases (Fig. 4.7).

When jellyfish mortality (PlankTOM10.5d) and respiration (PlankTOM10.5c) are switched on, they have the least impact of the characteristic runs and are very similar spatially in comparison to PlankTOM11 (Fig. 4.7). Export and primary production are slightly increased in most areas, except for at around 40°N globally and 40°S, excluding the Pacific, where they both decrease (Fig. 4.7).

Switching on jellyfish grazing (PlankTOM10.5a) has the biggest influence on the model processes that occur between primary production in the surface ocean and export production at 100m. Export and primary production mostly change in the same direction, such that as one increases so does the other, for all the other jellyfish characteristic simulations, compared to PlankTOM11 (Fig. 4.7). For the jellyfish grazing simulation, compared to PlankTOM11, there are large areas where export decreases as primary production increases (Fig. 4.7).

Figure 4.8 shows the seasonality of the *ef* ratio, primary production and export for each simulation for the North (30 - 90°N), while Figure 4.9 shows the seasonality of PFT biomass for the same region. From the exploration of PlankTOM11, the North is the region with the strongest seasonal variation (Fig. 4.4) and therefore the most useful to explore the mechanisms driving export. In Figure 4.8 export production is shown

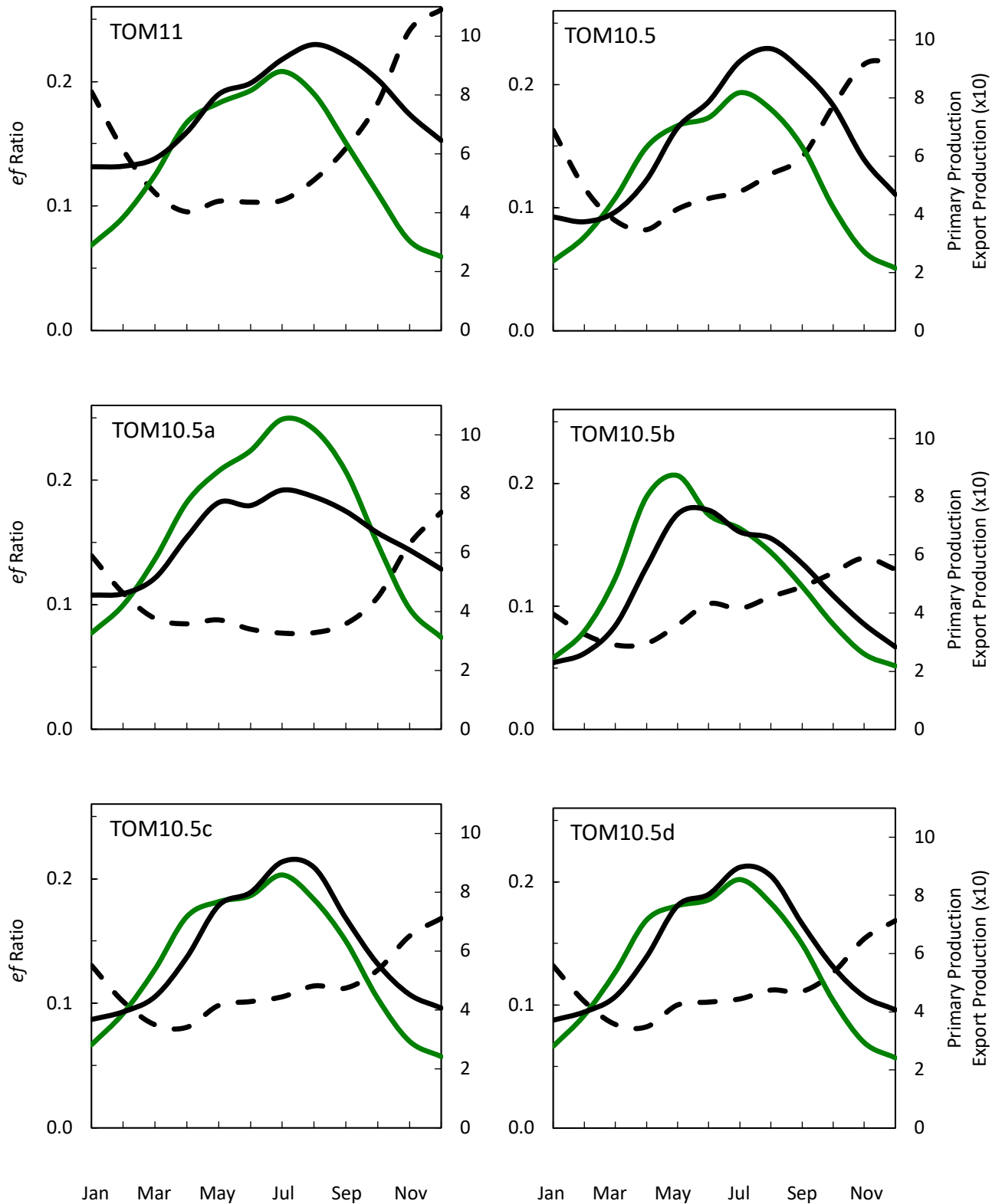


**Figure 4.8** Mean seasonal primary production, export production and the *ef* ratio for PlankTOM11 and the five PlankTOM10.5 simulations for the North (30-90°N). The *ef* ratio (dashed black line) is on the left vertical axis. Primary production (mol/m<sup>2</sup>; green line) and export production (mol/m<sup>2</sup>; black line) are on the right vertical axis. Export production is multiplied by a factor of 10 for visual clarity in comparison to primary production. Results are shown for (top left) PlankTOM11, (top right) PlankTOM10.5, (middle left) PlankTOM10.5a, (middle right) PlankTOM10.5b, (bottom left) PlankTOM10.5c, (bottom right) PlankTOM10.5d. All data are averaged for 1985-2015.

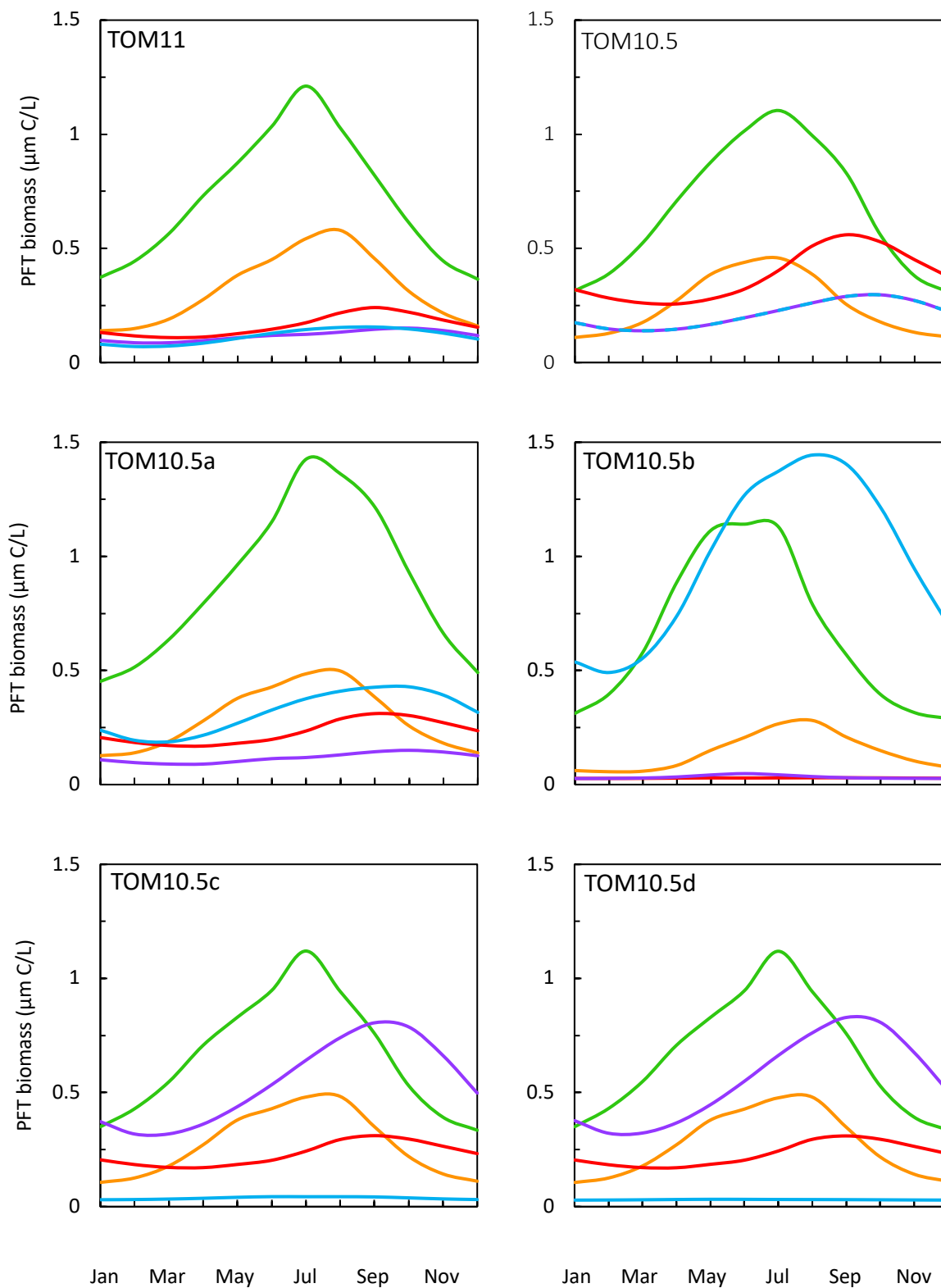


**Figure 4.9** Mean seasonal PFT biomass for PlankTOM11 and the five PlankTOM10.5 simulations for the North (30-90°N). The PFTs are total phytoplankton (green), protozooplankton (orange), mesozooplankton (red), macrozooplankton (purple) and jellyfish (blue). PFT biomass is averaged from 0 – 100m. Results are shown for (top left) PlankTOM11, (top right) PlankTOM10.5, (middle left) PlankTOM10.5a, (middle right) PlankTOM10.5b, (bottom left) PlankTOM10.5c, (bottom right) PlankTOM10.5d. All data are averaged for 1985-2015.

multiplied by a factor of 10 for visual clarity in comparison to primary production. In the text the values for export are not multiplied by a factor of 10.

In PlankTOM11 in the North, primary production increases through spring and summer to peak in July at 8.8 mol/m<sup>2</sup>, it then declines to the lowest production in December at 2.5 mol/m<sup>2</sup> (Fig. 4.8). Export production increases through spring and summer to peak in August at 0.97 mol/m<sup>2</sup>, a month after the peak in primary production. Export then declines to the lowest production in January to March at 0.56 mol/m<sup>2</sup> (Fig. 4.8). The *ef* ratio is highest in the winter, peaking in December at 0.26, and lowest in April to July at around 0.1 (Fig. 4.8). After the summer peak, primary production declines more rapidly and further than export, which results in the *ef* ratio peak in December. The seasonal variation of primary production is larger than the seasonal variation of export production. The mis-match in the amplitude of seasonal variation results in a larger seasonal variation in the *ef* ratio, than in the other simulations.

In PlankTOM10.5 in the North, primary production increases through spring and summer to peak in July at 8.2 mol/m<sup>2</sup>, it then declines to the lowest production in December at 2.2 mol/m<sup>2</sup> (Fig. 4.8). Primary production follows the same seasonal pattern as PlankTOM11, at slightly lower values. Export production increases through spring and summer to peak in August at 0.97 mol/m<sup>2</sup>, a month after the peak in primary production. Export then declines to the lowest production in February at 0.38 mol/m<sup>2</sup> (Fig. 4.8). Export follows a similar seasonal pattern as PlankTOM11, with the same peak value but a greater seasonal amplitude. The *ef* ratio is highest in the winter, peaking in November and December at 0.22, and lowest in April at around 0.08 (Fig. 4.8). The *ef* ratio is lower than in PlankTOM11, especially during the winter, due to the closer match in the amplitude of seasonal variation between primary production and export.

In PlankTOM10.5a in the North, primary production increases through spring and summer to peak in July at 10.5 mol/m<sup>2</sup>, it then declines to the lowest production in December at 3.1 mol/m<sup>2</sup> (Fig. 4.8). Primary production follows the same seasonal pattern as PlankTOM11 and 10.5, at higher values. Export production increases through spring and summer to peak in July at 0.81 mol/m<sup>2</sup>, the same month as the peak

in primary production. Export then declines to the lowest production in January and February at  $0.46 \text{ mol/m}^2$  (Fig. 4.8). Export is lower and has a slightly smaller amplitude than in PlankTOM11. The increased primary production in PlankTOM10.5a does not translate into export because primary production is only increased in the top 50m (Fig. 4.6). Switching on the grazing of jellyfish may have increased biological activity of the PFTs, cycling the carbon from primary production within surface waters, reducing the amount that is exported at 100m. The *ef* ratio is highest in the winter, peaking in December at 0.17, and lowest in June to August at around 0.08 (Fig. 4.8). The *ef* ratio is lower than in PlankTOM11, as the increased primary production does not translate to increased export.

In PlankTOM10.5b in the North, primary production increases through spring and summer to peak in May at  $8.7 \text{ mol/m}^2$ , it then declines to the lowest production in December at  $2.2 \text{ mol/m}^2$  (Fig. 4.8). Primary production peaks two months earlier in the year than in PlankTOM11 and 10.5, at a similar value to PlankTOM11. Switching on the growth of jellyfish in PlankTOM10.5b gives a high biomass of jellyfish which dominate the zooplankton (Fig. 4.9). The increased growth of the jellyfish PFT also results in an increased grazing rate, 55% of which is on phytoplankton (the jellyfish PFT grazing preference is that of macrozooplankton, Fig. 4.2). The primary production peaks earlier in the year; initially jellyfish keep the other zooplankton biomass low through grazing, and the jellyfish can only grow so fast in the lower winter temperatures, so in early spring phytoplankton can rapidly bloom as they have lower overall grazing pressure than in PlankTOM11 and 10.5. The increasing ocean temperature also allows jellyfish to bloom in spring, by increasing their growth and grazing rates, rapidly consuming the phytoplankton and reducing primary production (Fig. 4.9). Export production increases through spring and early summer to peak in June at  $0.75 \text{ mol/m}^2$ , a month after the peak in primary production. Export then declines to the lowest production in January at  $0.23 \text{ mol/m}^2$  (Fig. 4.8). Export is lower than PlankTOM11 and 10.5 but follows the same pattern of a month lag behind primary production. The *ef* ratio is highest in the winter, peaking in November at 0.14, and lowest in March and April at around 0.07 (Fig. 4.8). The *ef* ratio is lower than in PlankTOM11 and 10.5 and has a smaller seasonal variation.

In PlankTOM10.5c and 10.5d in the North, primary production, export and the *ef* ratio behave very similarly to each other (Fig. 4.8). Primary production increases through spring and summer to peak in July at  $8.6 \text{ mol/m}^2$ , it then declines to the lowest production in December at  $2.4 \text{ mol/m}^2$  (Fig. 4.8). Switching on the respiration and mortality of jellyfish in PlankTOM10.5c and 10.5d, respectively, reduces the biomass of jellyfish, allowing macrozooplankton biomass to increase. Macrozooplankton does not dominate the zooplankton in the same way as jellyfish in PlankTOM10.5b (Fig. 4.9). Macrozooplankton biomass peaks later in the year due to its lower growth and grazing rate, in comparison to jellyfish. The phytoplankton biomass, and thus primary production, is not over grazed in the spring due to this lower growth and grazing of the dominant zooplankton (Fig. 4.9). The biomass of jellyfish in PlankTOM10.5c and 10.5d is too low to have much impact on the ecosystem. Export production increases through spring and summer to peak in August at  $0.89 \text{ mol/m}^2$ , a month after the peak in primary production. Export then declines to the lowest production in January at  $0.37 \text{ mol/m}^2$  (Fig. 4.8). The *ef* ratio is highest in the winter, peaking in December at 0.17, and lowest in April at around 0.08 (Fig. 4.8). The *ef* ratio is lower than in PlankTOM11, especially during the winter, due to the closer match in the amplitude of seasonal variation between primary production and export.

## 4.4 Discussion

We have introduced jellyfish to the global ocean biogeochemical model PlankTOM11 and conducted simulations to investigate the influence of jellyfish characteristics on carbon export. PlankTOM11 gives a global carbon export production of 7.11 PgC/y, primary production of 41.5 PgC/y and an export efficiency (*ef* ratio) of 0.171 (Table 4.3), with large spatial and seasonal variability. Export and primary production are higher in the respective hemispheres summer, and generally lower in the Southern Ocean (Fig. 4.3). PlankTOM11 shows stronger seasonality in the *ef* ratio at higher latitudes, and weaker seasonality at lower latitudes. This latitudinal pattern matches observations from multiple studies (Fig. 4.3 and Fig. 4.4; Benitez-Nelson et al., 2001, Brix et al., 2006, Kawakami and Honda, 2007, Lutz et al., 2007, Baumann et al., 2013). The greater seasonality in the *ef* ratio at high latitudes is driven by greater seasonality in primary production and a greater lag to secondary production by zooplankton in the model, replicating the mechanisms shown in Henson et al. (2015). Importantly, these simulations highlight the influence of the top zooplankton, jellyfish, on export and export efficiency through the structuring of the plankton community, an area previously ignored in global biogeochemical models and global export studies.

Laws et al. (2000, 2011) derived simple equations from observations of primary production and SST to predict *ef* ratios. These equations assume *ef* ratios are positively correlated with primary production and negatively correlated with SST. Further studies have questioned these simple relationships. A negative correlation between *ef* ratios and primary production has been found in observations from the Southern Ocean (Maiti et al., 2013, Cavan et al., 2015, Le Moigne et al., 2016). Maiti et al. (2013) also showed that *ef* ratios are less sensitive to temperature in the Southern Ocean than global estimates suggest. A model including a simple plankton food web found that when zooplankton grazing was included there was a negative correlation between *ef* ratios and primary production, while when zooplankton grazing was not included the opposite (positive) correlation occurred (Cavan et al., 2017). Cavan et al. (2017) also found a negative correlation between *ef* ratios and primary production in observations from three geographical locations; the Southern Ocean, North Atlantic and equatorial North Pacific. Cavan et al. suggests three potential reasons for the negative correlation: (1) temporal decoupling between primary production and export, (2) seasonal



dynamics of the zooplankton community and (3) grazing by zooplankton. All three reasons are interlinked, in that temporal decoupling (1) is driven, at least in part, by zooplankton grazing (3), which is affected by the dynamics of the zooplankton community (2). The negative correlation of primary production and  $ef$  ratio in PlankTOM11 (Fig. 4.5) can be explained by seasonal variation in ecosystem dynamics (Fig. 4.8). The lag (temporal decoupling) between primary production and export production (as carbon is transformed through zooplankton grazing etc.) generates an  $ef$  ratio that peaks in winter, when primary production is lowest, and dips in summer, when primary production is highest (Fig. 4.8). Changing the parameters of jellyfish affected the zooplankton community dynamics and the zooplankton grazing, which affected primary production and export and thus the  $ef$  ratio (Fig. 4.8 and Fig. 4.9). The seasonal amplitude of the  $ef$  ratio was reduced and carbon export was decreased by the changes to jellyfish parameters, compared to PlankTOM11 (Fig. 4.8, Table 4.3). Changes to the zooplankton community structure have been shown to affect carbon export flux. Boyd (2015) altered mesozooplankton and microzooplankton trophic transfer efficiency in a 1-D coupled surface-subsurface carbon export flux model. They found that a shift in the zooplankton community structure (by increasing and decreasing the zooplankton transfer efficiencies) decreased carbon export, compared to the control simulation (Boyd, 2015). Changes to the zooplankton community structure in this study also decrease carbon export, compared to the control simulation, despite the different methods used to change the zooplankton community and the different types of model used by each study.

The  $ef$  ratio is strongly affected by the seasonal cycle of primary production and export production. These results have implications for the calculations of yearly  $ef$  ratio from observations, which are likely to be strongly dependent on the timing of data collection of export and primary production (Giering et al., 2017). For example, during the spring/summer primary production will be high but export low, as the BCP processes to repackage and move carbon down the water column are just beginning, so the  $ef$  ratio will be underestimated. For data collected during the autumn/winter, primary production will be lower and export higher as the carbon from the spring/summer production is now being exported, so the  $ef$  ratio will be overestimated. The effect of the seasonal cycle on the  $ef$  ratio increases as latitude increases. Clear and highlighted information on the timing of data collection for calculating  $ef$  ratios is vital to prevent

misrepresentation of data (Henson et al., 2015, Giering et al., 2017).

PlankTOM11 reproduces the complexity of processes influencing export production and export efficiency. The strength and direction of correlation with the *ef* ratio varied spatially for temperature, jellyfish and macrozooplankton. Primary production and chlorophyll showed largely negative correlation to the *ef* ratio, also with spatial variation in the strength of the correlation (Fig. 4.5). There is no clear one to one relationship between export efficiency and the total zooplankton biomass, or the biomass of any one of the zooplankton PFTs. Substantial spatial variation in the direction and strength of correlation between export efficiency and zooplankton (Fig. 4.5) increases the complexity of the analysis and highlights the spatial/regional variability in the key drivers of export. In PlankTOM11, the *ef* ratio is dependent on the seasonality of primary production and the processes mediating carbon into export production, both of which are influenced by the structure of the zooplankton community, which is in turn influenced by jellyfish. This may explain some of the variability outside of that predicted by primary production and SST. Jellyfish can play a key role in structuring the zooplankton community and thus, jellyfish influence export and export efficiency through trophic cascades.

Including jellyfish in PlankTOM11 increases the primary production, the export of carbon from surface waters and the export efficiency. This is not just an artefact of the additional zooplankton compartment in the model, but it is a reflection of the characteristics of jellyfish, primarily its trophic level. It is also reliant on the specific combination of growth and loss rates. The balance of high jellyfish growth and high jellyfish respiration and mortality, along with the high grazing preference for other zooplankton, combine to influence the ecosystem and increase export in PlankTOM11. The grazing preference, which determines the trophic level, is individually the most influential characteristic. Jellyfish in PlankTOM11 mostly affect export from top-down trophic cascades, rather than through their direct input to organic carbon (POC and GOC) from mortality, faecal matter production, messy eating, and other similar processes.

Phytoplankton are the key contributor to carbon export, by fixing inorganic carbon in the ocean surface into organic carbon, which eventually aggregates and sinks (Laws et

al., 2011). Jellyfish influence the biomass of other zooplankton through grazing and competition for food and therefore also influence carbon export. Zooplankton faecal pellets, especially those of macrozooplankton, are known to contribute to the carbon export, as they repackage organic carbon into larger particles. Larger particles generally sink more rapidly through the water column, allowing for less remineralisation and decomposition via grazing, thus leading to more sinking carbon out of the euphotic zone (Turner, 2002, Wilson et al., 2008, Wilson and Steinberg, 2010). Improving understanding of how jellyfish influence zooplankton biomass, and subsequently the volume and type of faecal pellets production and of packaging processes, will improve understanding of the processes governing the carbon sink. An observational study by Stone & Steinberg (2018) found no difference in total POC flux with or without jellyfish present, but did find a significant difference in copepod abundance which significantly decreased copepod faecal pellet production and thus carbon flux from copepods by 50%. The study only lasted for two days, and so jelly-falls and the influence of jellyfish mortality on flux was necessarily not included. This supports the findings of this study that during the life of jellyfish their greatest influence on carbon export is through trophic cascades.

The high mortality of jellyfish in the model does not contribute significantly to carbon export (Fig. 4.7). This is likely due to a number of reasons. High mortality without high growth (PlankTOM10.5d) results in low biomass of jellyfish and thus low production of organic carbon through mortality, faecal pellets and messy-eating and low carbon export. In reality, jellyfish carcasses are often many times larger than those of other zooplankton, with a much greater sinking speed (Lebrato et al., 2013a). However, jellyfish carcasses are not currently represented in the model. Additional partitioning of carbon, beyond the two current types of sinking organic matter (POC and GOC), would need to be introduced to the model to properly account for jellyfish mortality. Mass deposition events of jellyfish carcasses (jelly-falls), at depths where the carbon is unlikely to be recycled back into surface waters at short to medium time scales, are known to contain significant amounts of carbon and can contain in excess of a magnitude more carbon than the annual carbon flux (Billett et al., 2006, Yamamoto et al., 2008). PlankTOM11 likely gives a reasonable replication of the influence of jellyfish on export during their life, but substantially underestimates their contribution in death. Through rapidly sinking jelly-falls, jellyfish cause a large pulse

in export (Lebrato et al., 2012, Lebrato et al., 2013a), not yet accounted for in PlankTOM11. The global export in PlankTOM11 (7.11 PgC/y) is within global estimates of 5 - 12 PgC/y. The main reason for export being towards the lower end of observations is that the global primary production in PlankTOM11 is half the observed rate. Another potential explanation which may enhance the low export is that within the model jellyfish are high grazers and growers, thus taking in a high proportion of carbon, but they are not then acting as a direct rapid source of sinking carbon through their mortality. The similarity of the results from the respiration and mortality sensitivity simulations further highlights the under-representation of jellyfish mortality in the organic carbon flux. The similarity of the respiration and mortality simulations also suggests that once zooplankton are below a certain biomass, they have little to no effect on the ecosystem functioning (Fig. 4.8 and Fig. 4.9).

To include jelly-falls in global biogeochemical models you would need to increase the size partitioning of particulate organic carbon, so that they better represented jellyfish carcasses. This could be achieved in a relatively simple way by introducing an additional size class to the current POC and GOC, specifically parameterised to represent jellyfish carcasses. A more complex change to increase the size partitioning of particulate organic carbon could be achieved through introducing a size-resolving spectral model with a spectrum of particle size and size-dependent sinking velocity (Kriest and Oschlies, 2008). This second method has the advantage of improving the representation of particulate organic carbon production from all PFTs but is substantially more computer expensive and would be a substantial undertaking. The potential influence of introducing either of these methods on carbon export could be significant, with peaks in jellyfish biomass being followed by a pulse in carbon export because of the rapid sinking of large carcasses (Lebrato et al., 2012, Lebrato et al., 2013a).

## **4.5 Conclusion**

Ecosystem structures are known to be important for the export of carbon from surface waters. Increasing the complexity of food webs in biogeochemical models should thus improve understanding of the processes driving the BCP. This is especially true for modelling zooplankton, which lags behind compared to the advancements in

modelling greater complexity in the phytoplankton. More complex models should also better represent the global observed variation in export (Boyd and Trull, 2007, Cavan et al., 2017, Lutz et al., 2007). PlankTOM11 takes a step towards increasing the complexity of zooplankton food-webs in a biogeochemical model, by incorporating jellyfish, which are shown to influence export through trophic cascades. However, in order to fully account for the contribution of jellyfish to export, jellyfish mortality must be partitioned separately to other zooplankton in organic detritus, reflecting the large disparity in body size and composition (Lebrato et al., 2013a, Lebrato et al., 2013b, Lucas et al., 2011). The work presented here highlighted the importance of jellyfish in the export of carbon from the surface to the deep ocean. It also highlighted the need to further develop the dynamics of organic carbon export to better reflect the ecosystem dynamics active above the export horizon.

## References

- ACUÑA, J. L., LÓPEZ-URRUTIA, Á. & COLIN, S. 2011. Faking giants: the evolution of high prey clearance rates in jellyfishes. *Science*, 333, 1627-1629.
- BAUMANN, M. S., MORAN, S. B., LOMAS, M. W., KELLY, R. P. & BELL, D. W. 2013. Seasonal decoupling of particulate organic carbon export and net primary production in relation to sea-ice at the shelf break of the eastern Bering Sea: Implications for off-shelf carbon export. *Journal of Geophysical Research: Oceans*, 118, 5504-5522.
- BENITEZ-NELSON, C., BUESSELER, K. O., KARL, D. M. & ANDREWS, J. 2001. A time-series study of particulate matter export in the North Pacific Subtropical Gyre based on <sup>234</sup>Th: <sup>238</sup>U disequilibrium. *Deep Sea Research Part I: Oceanographic Research Papers*, 48, 2595-2611.
- BILLETT, D. S. M., BETT, B. J., JACOBS, C. L., ROUSE, I. P. & WIGHAM, B. D. 2006. Mass deposition of jellyfish in the deep Arabian Sea. *Limnology and Oceanography*, 51, 2077-2083.
- BOYD, P. & TRULL, T. 2007. Understanding the export of biogenic particles in oceanic waters: Is there consensus? *Progress in Oceanography*, 72, 276-312.
- BOYD, P. W. 2015. Toward quantifying the response of the oceans' biological pump to climate change. *Frontiers in Marine Science*, 2, 77.
- BRIX, H., GRUBER, N., KARL, D. M. & BATES, N. R. 2006. On the relationships between primary, net community, and export production in subtropical gyres. *Deep Sea Research Part II: Topical Studies in Oceanography*, 53, 698-717.
- BURD, A., BUCHAN, A., CHURCH, M. J., LANDRY, M. R., MCDONNELL, A. M., PASSOW, U., STEINBERG, D. K. & BENWAY, H. M. 2016. Towards a transformative understanding of the ocean's biological pump: Priorities for future research-Report on the NSF Biology of the Biological Pump Workshop. Ocean Carbon & Biogeochemistry (OCB) Program.
- CAEL, B., BISSON, K. & FOLLOWS, M. J. 2017. How have recent temperature changes affected the efficiency of ocean biological carbon export? *Limnology and Oceanography Letters*, 2, 113-118.
- CAEL, B. B. & FOLLOWS, M. J. 2016. On the temperature dependence of oceanic export efficiency. *Geophysical Research Letters*, 43, 5170-5175.

- CAVAN, E., LE MOIGNE, F. A., POULTON, A., TARLING, G., WARD, P., DANIELS, C., FRAGOSO, G. & SANDERS, R. 2015. Attenuation of particulate organic carbon flux in the Scotia Sea, Southern Ocean, is controlled by zooplankton fecal pellets. *Geophysical Research Letters*, 42, 821-830.
- CAVAN, E. L., HENSON, S. A., BELCHER, A. & SANDERS, R. 2017. Role of zooplankton in determining the efficiency of the biological carbon pump. *Biogeosciences*, 14, 177-186.
- GIERING, S. L., SANDERS, R., MARTIN, A. P., HENSON, S. A., RILEY, J. S., MARSAY, C. M. & JOHNS, D. G. 2017. Particle flux in the oceans: Challenging the steady state assumption. *Global Biogeochemical Cycles*, 31, 159-171.
- HENSON, S. A., SANDERS, R. & MADSEN, E. 2012. Global patterns in efficiency of particulate organic carbon export and transfer to the deep ocean. *Global Biogeochemical Cycles*, 26.
- HENSON, S. A., YOOL, A. & SANDERS, R. 2015. Variability in efficiency of particulate organic carbon export: A model study. *Global Biogeochemical Cycles*, 29, 33-45.
- KAWAKAMI, H. & HONDA, M. C. 2007. Time-series observation of POC fluxes estimated from <sup>234</sup>Th in the northwestern North Pacific. *Deep Sea Research Part I: Oceanographic Research Papers*, 54, 1070-1090.
- KRIEST, I. & OSCHLIES, A. 2008. On the treatment of particulate organic matter sinking in large-scale models of marine biogeochemical cycles. *Biogeosciences (BG)*, 5, 55-72.
- LAMB, P. D., HUNTER, E., PINNEGAR, J. K., CREER, S., DAVIES, R. G. & TAYLOR, M. I. 2017. Jellyfish on the menu: mtDNA assay reveals scyphozoan predation in the Irish Sea. *Royal Society Open Science*, 4.
- LAWS, E. A., D'SA, E. & NAIK, P. 2011. Simple equations to estimate ratios of new or export production to total production from satellite-derived estimates of sea surface temperature and primary production. *Limnology and Oceanography: Methods*, 9, 593-601.
- LAWS, E. A., FALKOWSKI, P. G., SMITH JR, W. O., DUCKLOW, H. & MCCARTHY, J. J. 2000. Temperature effects on export production in the open ocean. *Global Biogeochemical Cycles*, 14, 1231-1246.
- LE MOIGNE, F. A. C., HENSON, S. A., CAVAN, E., GEORGES, C., PABORTSAVA, K., ACHTERBERG, E. P., CEBALLOS-ROMERO, E., ZUBKOV, M. &

- SANDERS, R. J. 2016. What causes the inverse relationship between primary production and export efficiency in the Southern Ocean? *Geophysical Research Letters*, 43, 4457-4466.
- LE QUÉRÉ, C., ANDREW, R. M., FRIEDLINGSTEIN, P., SITCH, S., HAUCK, J., PONGRATZ, J., PICKERS, P., KORSBAKKEN, J. I., PETERS, G. P. & CANADELL, J. G. 2018. Global carbon budget 2018. *Earth System Science Data*, 10, 2141-2194.
- LEBRATO, M., MENDES, P. D. J., STEINBERG, D. K., CARTES, J. E., JONES, B. M., BIRSA, L. M., BENAVIDES, R. & OSCHLIES, A. 2013a. Jelly biomass sinking speed reveals a fast carbon export mechanism. *Limnology and Oceanography*, 58, 1113-1122.
- LEBRATO, M., MOLINERO, J.-C., CARTES, J. E., LLORIS, D., MÉLIN, F. & BENI-CASADELLA, L. 2013b. Sinking jelly-carbon unveils potential environmental variability along a continental margin. *PloS one*, 8, e82070.
- LEBRATO, M., PITT, K. A., SWEETMAN, A. K., JONES, D. O., CARTES, J. E., OSCHLIES, A., CONDON, R. H., MOLINERO, J. C., ADLER, L. & GAILLARD, C. 2012. Jelly-falls historic and recent observations: a review to drive future research directions. *Hydrobiologia*, 690, 227-245.
- LI, X., SONG, J., MA, Q., LI, N., YUAN, H., DUAN, L. & QU, B. 2015. Experiments and evidences: jellyfish (*Nemopilema nomurai*) decomposing and nutrients (nitrogen and phosphorus) released. *Acta Oceanologica Sinica*, 34, 1-12.
- LUCAS, C. H., PITT, K. A., PURCELL, J. E., LEBRATO, M. & CONDON, R. H. 2011. What's in a jellyfish? Proximate and elemental composition and biometric relationships for use in biogeochemical studies. *ESA Ecology*, 92, 1704.
- LUTZ, M. J., CALDEIRA, K., DUNBAR, R. B. & BEHRENFELD, M. J. 2007. Seasonal rhythms of net primary production and particulate organic carbon flux to depth describe the efficiency of biological pump in the global ocean. *Journal of Geophysical Research: Oceans*, 112.
- MAITI, K., CHARETTE, M. A., BUESSELER, K. O. & KAHRU, M. 2013. An inverse relationship between production and export efficiency in the Southern Ocean. *Geophysical Research Letters*, 40, 1557-1561.
- MCKINLEY, G. A., FAY, A. R., LOVENDUSKI, N. S. & PILCHER, D. J. 2017. Natural variability and anthropogenic trends in the ocean carbon sink. *Annual review of marine science*, 9, 125-150.



- PALEVSKY, H. I. & DONEY, S. C. 2018. How choice of depth horizon influences the estimated spatial patterns and global magnitude of ocean carbon export flux. *Geophysical Research Letters*, 45, 4171-4179.
- PITT, K. A., WELSH, D. T. & CONDON, R. H. 2009. Influence of jellyfish blooms on carbon, nitrogen and phosphorus cycling and plankton production. *Hydrobiologia*, 616, 133-149.
- PURCELL, J. 1997. Pelagic cnidarians and ctenophores as predators: Selective predation, feeding rates, and effects on prey populations. *Annales De L Institut Oceanographique*, 73, 125-137.
- PURCELL, J. 2003. Predation on zooplankton by large jellyfish, *Aurelia labiata*, *Cyanea capillata* and *Aequorea aequorea*, in Prince William Sound, Alaska. *Marine Ecology Progress Series*, 246, 137-152.
- STONE, J. P. & STEINBERG, D. K. 2018. Influence of top-down control in the plankton food web on vertical carbon flux: A case study in the Chesapeake Bay. *Journal of Experimental Marine Biology and Ecology*, 498, 16-24.
- TURNER, J. T. 2002. Zooplankton fecal pellets, marine snow and sinking phytoplankton blooms. *Aquatic microbial ecology*, 27, 57-102.
- WEST, E. J., PITT, K. A., WELSH, D. T., KOOP, K. & RISSIK, D. 2009. Top-down and bottom-up influences of jellyfish on primary productivity and planktonic assemblages. *Limnology and Oceanography*, 54, 2058-2071.
- WILSON, S. & STEINBERG, D. 2010. Autotrophic picoplankton in mesozooplankton guts: evidence of aggregate feeding in the mesopelagic zone and export of small phytoplankton. *Marine Ecology Progress Series*, 412, 11-27.
- WILSON, S. E., STEINBERG, D. K. & BUESSELER, K. O. 2008. Changes in fecal pellet characteristics with depth as indicators of zooplankton repackaging of particles in the mesopelagic zone of the subtropical and subarctic North Pacific Ocean. *Deep Sea Research Part II: Topical Studies in Oceanography*, 55, 1636-1647.
- YAMAMOTO, J., HIROSE, M., OHTANI, T., SUGIMOTO, K., HIRASE, K., SHIMAMOTO, N., SHIMURA, T., HONDA, N., FUJIMORI, Y. & MUKAI, T. 2008. Transportation of organic matter to the sea floor by carrion falls of the giant jellyfish *Nemopilema nomurai* in the Sea of Japan. *Marine Biology*, 153, 311-317.



CHAPTER 5. IMPACTS OF CLIMATE  
& FISHERIES ON JELLYFISH  
IN THE BENGUELA CURRENT  
SYSTEM

A case study using PlankTOM11



## Abstract

The Benguela Current System (BCS) is often cited as an example of historic overfishing causing an increase in jellyfish biomass. Within the BCS the Northern Benguela was heavily overfished during the 1960's leading to a collapse in fish stocks. It has been hypothesised that the collapse in fish stocks allowed zooplankton biomass to increase due to reduced predation by the fish, which in turn led to increased jellyfish biomass due to increased food availability. In contrast, the Southern Benguela was not subject to historic overfishing and is not reported to have experienced an increase in jellyfish biomass. Previous studies of jellyfish biomass in the BCS have used fisheries models with simplistic representations of climatic variability and jellyfish. Here I use PlankTOM11 to investigate the influence of historic fishing and climate variability on jellyfish biomass in the BCS. I introduce a representation of historic overfishing (1950-2012) through fish predation pressure on macrozooplankton. Fish predation pressure in the model does not affect jellyfish due to the existing evidence in the BCS. The influence of climatic variability and fishing are simulated individually and together. Without the inclusion of fishing, jellyfish show no long-term trend in biomass in the Northern or Southern Benguela. When fisheries are included, jellyfish biomass decreases in the Northern Benguela from 1980 to 2000 and is not substantially affected in the Southern Benguela. In the Northern Benguela macrozooplankton biomass is substantially increased (four-fold) by the inclusion of fisheries, but jellyfish respond to this by decreasing as they are outcompeted by the macrozooplankton. This is contrary to the patchy observations of jellyfish biomass and contrary to hypotheses on the key mechanism linking overfishing to increased jellyfish biomass. We suggest that the inclusion of fish predation on jellyfish as well as on macrozooplankton will affect these results, and that this predation of jellyfish by fish (not observed in the BCS but shown in other regions) is a key mechanism linking overfishing to increased jellyfish biomass. This mechanism should be tested in future experiments. In PlankTOM11 macrozooplankton have a coastal advantage to simulate enhanced growth and recruitment in this environment, while jellyfish do not. The results are dependent on the parameterisation of macrozooplankton and jellyfish grazing and growth rates. Further parameterisation of jellyfish within PlankTOM11, particularly the inclusion of a coastal advantage, need to be explored to solidify these findings. I

find that the full impact of overfishing on marine ecosystems cannot be understood without its interactions with climate variability.

## 5.1 Introduction

A global perceived increase in jellyfish biomass has been attributed to multiple causes, most prominently climate change, along with a range of other causes including fishing and coastal development (Chapter 1). Due to the nature of marine ecosystems, and the concurrent multiple stressors placed on them by human activities, it can be very difficult to attribute biomass changes to a single cause. The Northern Benguela (NB), part of the Benguela Current System (BCS), is often one of the cited examples of an increase in jellyfish having negative ecosystem and economic impacts, largely blamed on historic overfishing (Bakun and Weeks, 2006, Lynam et al., 2006, Richardson et al., 2009, Utne-Palm et al., 2010, Jensen et al., 2012, FAO, 2017). It has been widely reported that jellyfish biomass in the NB has increased significantly since the 1950's, but survey data is poor prior to the 1980's, with most reports being anecdotal, and since then data collection is "piece-meal... from once-off or incomplete data sets" (see Flynn et al., 2012). In the Southern Benguela (SB), where there has been an ecosystem approach to fisheries, jellyfish populations do not appear to have experienced any significant long-term trend (Cury and Shannon, 2004, Roux et al., 2013).

The implications of increasing jellyfish populations in the NB are wide ranging, including suppressing recovery of fish stocks, changes to the marine carbon cycle, marine ecosystem disruptions, and even affecting the diamond mining industry that in the NB mines sediment from the sea floor via suction pipes which can become clogged by jelly-falls (Venter, 1988, Heymans and Baird, 2000, Brierley et al., 2001, Lynam et al., 2006, Roux et al., 2013). The NB is often mentioned as a warning of the consequences of poor fisheries management, with relation to the SB and other ecosystems where planktivorous fish are a significant component of the system (Bakun and Weeks, 2006, Lynam et al., 2006, Richardson et al., 2009, Jensen et al., 2012). The NB can also be viewed as a warning for the combined effects of overfishing and climate change on jellyfish populations and marine ecosystems.

The BCS is one of the major eastern boundary upwelling ecosystems, characterised by high productivity from elevated primary production and planktivorous fish stocks. The upwelling is caused by a thermal pressure difference between the land and ocean, which causes wind stress northward along the coast. This results in Ekman transport of

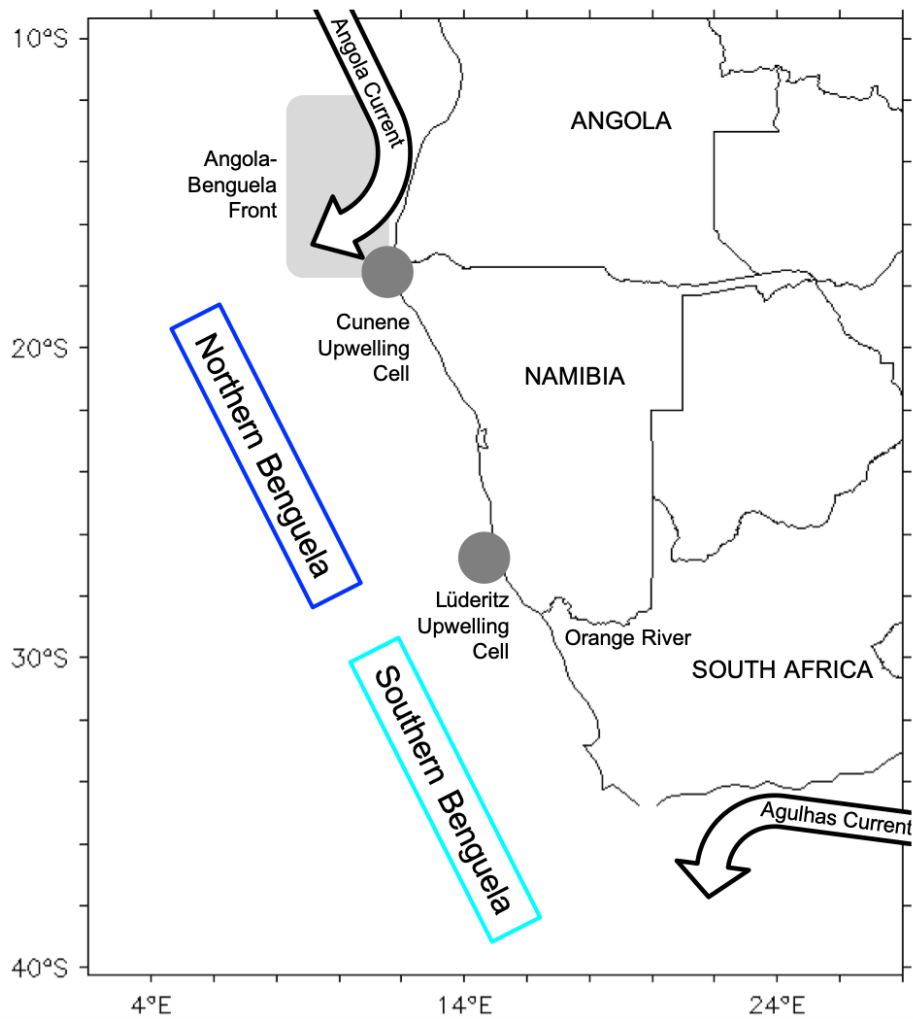


**Figure 5.1** The Benguela Current System with the key oceanographic features which form the Northern Benguela and Southern Benguela ecosystems. Upwelling cells (dark grey circles), the Angola-Benguela Front (light grey rectangle) and ocean currents (black arrows) are denoted in their approximate positions. See text for detail.

the surface waters offshore, driving upwelling of cold nutrient rich deep water along the coast, to replace the surface water (Hutchings et al., 2009, Bakun et al., 2010). This deep cool nutrient rich water is upwelled into the photic zone providing nutrients for phytoplankton, which in turn support zooplankton, and then planktivorous fish species, mostly sardines and anchovies. These provide a direct link to the top predators of the ecosystem, often including charismatic mega fauna; seabirds such as the African Penguin and Cape Gannet, and marine mammals such as the Cape Fur Seal, Southern Right Whales and Humpback Whales (Bakun et al., 2010, Roux et al., 2013). This relatively short food-chain, where a few species provide the crucial link between the plankton and top predators, is typical of eastern boundary upwelling ecosystems (Arntz et al., 2006).



The strength of the upwelling in the BCS varies intra- and inter-annually, with its peak in the spring and autumn (Hutchings et al., 2006). A longer-term variability in upwelling was discovered in the 1980's, and nick-named the 'Benguela Niño', after the El Niño/La Niña phenomenon in the Equatorial Pacific (Shannon et al., 1986). A Benguela Niño event is marked by a reduction in upwelling and the southward incursion of warm equatorial waters further into the BCS than usual. It leads to a decrease in plankton productivity, with consequences reverberating up the food-chain (Shannon et al., 1986). To date six Benguela Niño's have been confirmed; 1925-27, 1940-41, 1957-59, 1972-73, 1982-84 and 1997-98 (Arntz et al., 2006). The evidence on whether upwelling systems globally will strengthen or weaken with climate change is conflicting. There is a study reporting a long-term increase in upwelling-favourable winds for the BCS, however various data and collection method errors may drive this increasing trend (Shannon et al., 1992, Bakun et al., 2010).

The BCS is bordered at its northern edge by the southern reaches of the Angola Current, known as the Angola-Benguela Front region (12°S-18°S) and by the Cunene upwelling cell (18°S). The BCS is bordered at its southern and eastern edge by the Agulhas Current (around 36°S, 22°E; Fig. 5.1). These boundaries are variable depending on oceanographic and atmospheric conditions. The BCS can be considered as two regions; the Northern Benguela (NB) off the coast of Namibia and just into the coast of Southern Angola, and the Southern Benguela (SB) off the western coast of South Africa (Fig. 5.1). A strong permanent upwelling called the Lüderitz cell (26°S-27°S) acts as a biogeographical boundary between these two regions, with the official boundary at 29°S at the Namibian/South African border (Fig. 1; Brown et al., 1991, Hutchings et al., 2006, Hutchings et al., 2009). The positioning of this oceanographic feature near the country borders also means that marine management approaches of the two countries are separated here, making it a useful region for scientific study of a comparison between the NB and SB (Roux et al., 2013, Roux and Shannon, 2004). The NB is a typical coastal upwelling system, characterised by cool water, high productivity and low species diversity. The SB experiences a pulsed, seasonal upwelling and low-oxygen water close inshore, with lower productivity and higher species diversity than the NB (Hutchings et al., 2009).

### **5.1.1 Jellyfish in the Benguela Current System**

The dominant jellyfish species in the BCS are the Scyphozoa *Chrysaora (hysoscella) fulgida* and the Hydrozoa *Aequorea (aequorea) forskalea*, both pelagic Cnidaria species (Lynam et al., 2006). Since the 1970's fishermen in Namibia (NB) have complained of jellyfish clogging and damaging nets (Venter, 1988). Reports of Tunicates and Ctenophores in this region are limited, and have not been reported interacting with the fishing industry, either directly (clogging gear, contaminating catch) or indirectly (competing with planktivorous fish for resources) (Roux et al., 2013). Historically, scientific surveys of the BCS did not report jellyfish, likely because they were actively excluded, as was the case globally (Chapter 1). From the 1970's jellyfish abundance was measured using bongo-net surveys in the NB. The surveys found a combined mean biomass of 40.5 ( $\pm 5.3$ ) million tons for the period 1982-89, composed of *Aequorea* and *Chrysaora* (Fearon et al., 1992). While during a similar period (1981-1987) the fisheries by-catch of jellyfish totalled only 11.6 thousand tons (Venter, 1988). Fearon et al. (1992) also provide an estimate of the annual carbon biomass value for the jellyfish of 80-112 thousand tons. The survey period covered the 1984 Benguela Niño event (Shannon et al., 1986) and showed both a southward movement and significant reduction in biomass of jellyfish during the Niño months (warmer waters), compared to the rest of the survey period. This suggests a negative response of jellyfish to the Benguela Niño, following the reduced production of the NB ecosystem during this period (Shannon et al., 1986, Fearon et al., 1992). An 8-year study in the Northern California Current (2000 – 2007) found a strong negative correlation of jellyfish abundance to the Pacific Decadal Oscillation (PDO), with higher abundance in cooler years (negative PDO) (Suchman et al., 2012). In the Northern Californian Current region, negative PDO is associated with stronger upwelling, bringing cold, nutrient rich waters to surface and resulting in high marine productivity, and high jellyfish biomass. Suchman et al. (2012) note the importance of this negative correlation in an upwelling region, as it “run[s] counter to the prevailing trend for temperate species that warm temperatures lead to increased numbers” (Suchman et al., 2012). The studies by Fearon et al. 1992) and Shannon et al. (1986) suggest that this negative correlation between jellyfish and climate oscillations is also occurring in the BCS upwelling.

The inherent bias of bongo-net surveys of jellyfish (as used in Fearon et al., 1992), due

to the exclusion of larger specimens, have led to the development of acoustic survey techniques in the NB (Brierley et al., 2001). An acoustic survey in August 2003, including trawl nets for supplementary species information, along the entire Namibian shelf estimated a biomass of jellyfish (*Aequorea* and *Chrysaeroa*) of 12.2 million tons (Lynam et al., 2006). This is substantially lower than the biomass found by Fearon et al. (1992) of 40.5 million tons, which can be expected as it is a one off snapshot rather than a sustained survey. Of more relevance to the relationship between jellyfish and fishing Lynam et al., (2006) found that the jellyfish biomass was 3.4 times the total biomass of fish, and 15 times the biomass of sardines and anchovies (Lynam et al., 2006). Flynn et al. 2012) took a different approach to understanding the historic changes in jellyfish abundance by using frequency of capture (rather than biomass) from fisheries vessels and fisheries-dependent vessels (i.e. scientific surveys) from 1992 - 2006. This allowed for the inclusion of more data sets and provides a view of spatial patterns but is less useful for determining biomass, as is required for the validation of models. Jellyfish can be found in the NB throughout the year, with evidence of a winter-spring peak (Flynn et al., 2012, Venter, 1988). Jellyfish clearly represent a significant component of the NB ecosystem and are likely major zooplankton consumers. Data on jellyfish biomass in the SB is scarcer than in the NB. A winter-time survey of the St Helena Bay area in the SB from 1988-97, found 50 hydromedusae, one scyphozoan and two ctenophore species (including *Aequorea* and *Chrysaeroa*) reported as number of individuals per m<sup>3</sup>, but they are not observed at high abundances comparable to the NB (Buecher and Gibbons, 2000).

### **5.1.2 A Brief History of Fishing in the Benguela Current System**

As the BCS ecosystem spans multiple countries the different regions have experienced vastly different fisheries management practices. The Northern Benguela, mostly bordering Namibia has a turbulent fishing history (Roux and Shannon, 2004). During the 1950's and early 1960's catch of sardines rapidly increased, due to industrialisation of many vessels, as well as easing of quotas (Boyer and Hampton, 2001). The fishery peaked in 1968 followed by a rapid fall in catch (Fig. 5.2). Some of the fishery switched to anchovy, but this species catch never achieved the same volume as sardines, and in recent decades has collapsed to the point that no anchovies are caught (Fig. 5.2). The Namibian government only gained full authority of its marine

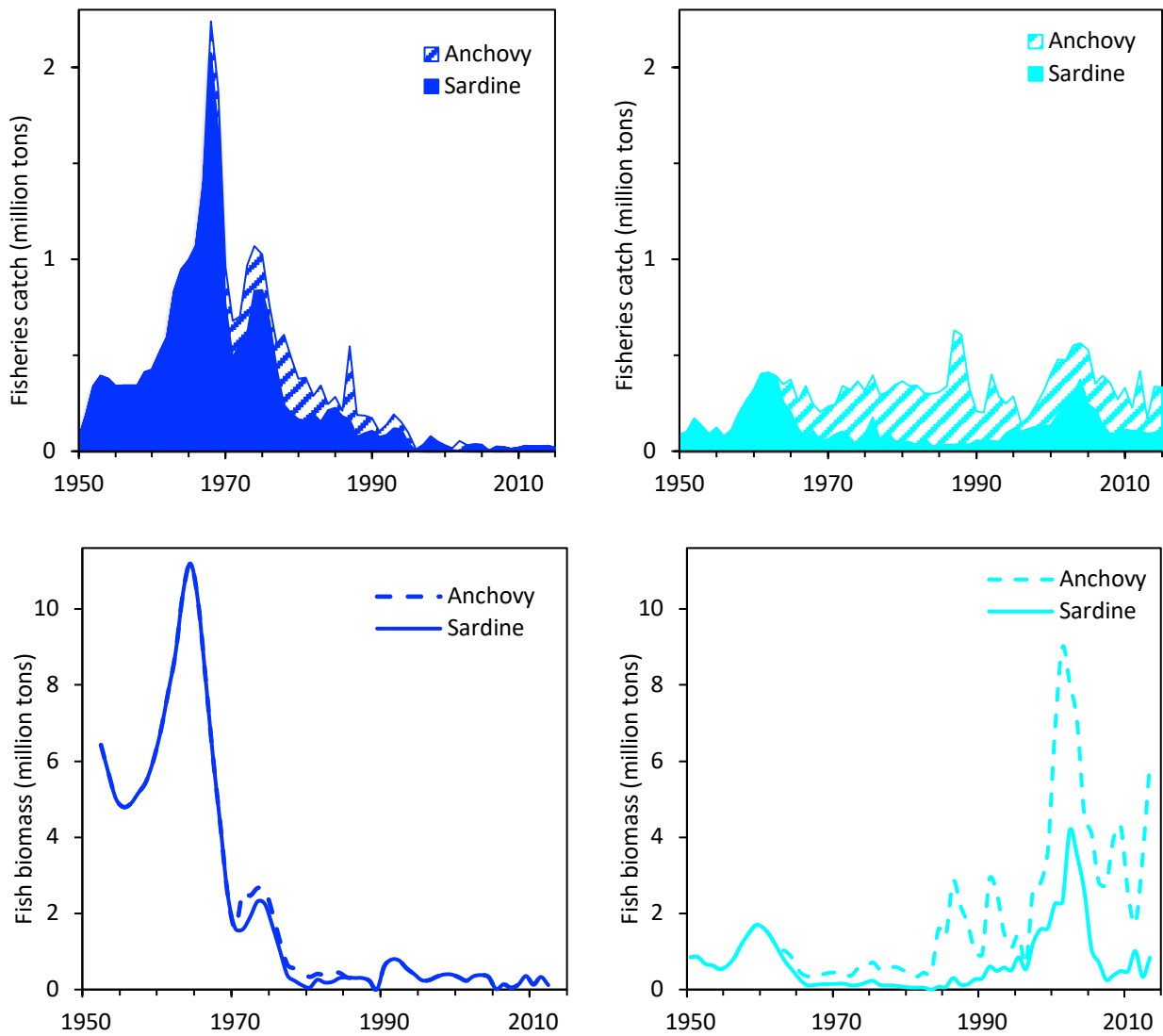


**Figure 5.2** Stacked (top) fisheries catch and (bottom) fish biomass in million tons in the (left) Northern Benguela and (right) Southern Benguela for sardines and anchovies. Fisheries catch data from (FAO, 2017) and fish biomass data collated from (FAO, 2017) and Crawford (2007) . Note that the catch and biomass panels have different scale bars.

environment in 1990 after achieving Independence, at which point fisheries management measures were rapidly implemented. However, catches continued to decline and are still at unsustainable levels (Roux and Shannon, 2004, Roux et al., 2013).

In contrast to Namibia (NB), South Africa's (SB) sardine and anchovy fishing industry has been relatively stable. Like Namibia, sardine were the targeted species in the 1950's and following a decline in the catch of sardines in the early 1960's, South Africa began targeting anchovy, the catch of which still regularly exceed the catch of sardine. By the 2000's sardine catches were recovering (Coetzee et al., 2008). The

catch levels have never reached the peak catch achieved in the NB (Fig. 5.2), as due to environmental forcing the SB ecosystem is naturally less productive (Shannon et al., 1986, Shannon et al., 2006). Catch of sardine and anchovies naturally fluctuates inter-annually due to their relatively short life cycle (Fig. 5.2). Presented here is a brief overview, based on several in depth papers reviewing the fishing history of the BCS (Boyer and Hampton, 2001, Coetzee et al., 2008, Roux et al., 2013).

### **5.1.3 Influence of Overfishing on Jellyfish Biomass**

Over fishing has been hypothesised as a cause of jellyfish biomass increase in numerous locations around the world, including in the Northern Benguela, supported by varying levels and quality of evidence. The causation between depleted planktivorous fish stocks and rising jellyfish biomass is linked to competition over prey, and mutual predation of juvenile stages. There is a strong dietary overlap between jellyfish and planktivorous fish, as both are voracious predators of zooplankton (Purcell and Arai, 2001, Purcell and Sturdevant, 2001, Sullivan and Kremer, 2011). Overfishing reduces the biomass of fish, which is hypothesised to release the pressure on their key prey, zooplankton, leading to an increase in the biomass of zooplankton. This provides a greater food source for jellyfish, which are rapid responders to environmental change, and so their biomass rapidly increases (Roux et al., 2013, Mills, 2001). It has been suggested that heavily fished ecosystems may reach a tipping point where jellyfish biomass is too large to allow for the recovery of fish stocks, even with strong fisheries management, such as reduced or removed fishing pressure (Roux et al., 2013, Roux and Shannon, 2004). The predation by jellyfish on ichthyoplankton (fish eggs and larvae) is thought to exacerbate this effect, as the elevated jellyfish numbers consume most of the reduced amounts of ichthyoplankton, making it very difficult for the fish to regain their previous population numbers (Purcell and Arai, 2001, Pauly et al., 2009, Sullivan and Kremer, 2011).

The predation of jellyfish by many fish species is now well known, including by clupeids, the fish order containing anchovies and sardines (Pauly et al., 2009). I have been unable to find direct evidence of sardine and anchovy predation on jellyfish in the BCS. The gelatinous soft-bodied nature of jellyfish means they have been overlooked

in traditional fish-stomach analysis, but new DNA techniques are rapidly adding fish species to the list of jellyfish predators (Arai, 2005, Sullivan and Kremer, 2011, Lamb et al., 2017). Ecosystem studies on the interactions between fish and jellyfish in the BCS do not include predation of fish on jellyfish (Roux and Shannon, 2004, Roux et al., 2013, Shannon et al., 2009). For other ecosystems such as the Black Sea, the relaxation of predation on jellyfish by over-fished species was given as an additional factor in the growth of the jellyfish population. However, for the Black Sea, there is direct stomach analysis evidence of the dominant fished species, mackerel, consuming the jellyfish species which became prevalent in the region (Daskalov et al., 2007, Purcell and Arai, 2001). For this study a system without predation by sardine and anchovy on jellyfish will be modelled due to the lack of evidence on this interaction.

The interactions between fish and jellyfish are varied and complex, as outlined above. A simplified interaction between the two groups will be modelled here. The limited quantitative data on the majority of these interactions and the complexity (Purcell and Arai, 2001) make them unrealistic to add to an already vastly complex and ‘computer expensive’ model. Fish will be represented in the model by changes to PFT predation mortality. This will be varied with the changes in sardine and anchovy fish stock over time.

Goby fish have been increasing along with jellyfish in the NB, and body-tissue isotope signatures reveal that they consume jellyfish (Utne-Palm et al., 2010). The same study shows evidence that gobies consume already dead or dying jellyfish near the seafloor. This predation would have no effect on the jellyfish population or mortality, but could increase the speed of transfer of resources back into the ecosystem (Utne-Palm et al., 2010). Cape Hake, although a key fished species in the BCS, both in terms of tonnage and stock collapse, is not considered in the model because its diet consists largely of fish (92% by mass) rather than the plankton groups within PlankTOM11 (Pillar and Wilkinson, 1995).

#### **5.1.4 Influence of Climate Variability on Jellyfish Biomass**

Another potential driver of jellyfish biomass changes in the BCS is climate variability such as changes in sea surface temperature and the strength of upwelling. Reduced

upwelling and the pole-ward intrusion of warm equatorial waters mark the Benguela Niño, leading to a decrease in biological productivity, with a much greater effect on the NB, than the SB. The Benguela Niño is known to have a strong negative influence on local fisheries and is likely to also influence jellyfish biomass through bottom-up control from changes to the plankton community (Arntz et al., 2006). Some studies have hypothesised that climate variability played a greater role in structuring the Benguela ecosystem than fishing (Roux et al., 2013, Shannon et al., 2009). The extremely patchy nature of jellyfish biomass data in the BCS, both spatially and temporally, makes it difficult to assess the role of the above drivers (fisheries and climate) in controlling local jellyfish biomass, if only observational data are used.

### **5.1.5 Models of Jellyfish in the Benguela Current System**

The NB ecosystem has undergone a regime shift since the 1950's. Regime shifts are generally defined as an abrupt change in the ecosystem status associated with sudden changes in climate variability (bottom-up drivers). Cury and Shannon (2004) argue that changes in fishing pressure (top-down driver) in addition to changes in climate variability are likely to have caused changes to the NB ecosystem state resulting in the regime shift. This hypothesis, of environment (bottom-up) plus fishing (top-down) triggering a regime shift, has been tested a few times in the BCS with ecosystem models where there is some representation of jellyfish. Roux and Shannon (2004) simulated potential fisheries management strategies in the NB, one of which was the removal of 50% of jellyfish, which resulted in an increase in the biomass of most fish groups modelled. A later study of the SB modelled the trophic impacts of fishing and climate change in the SB and in several other ecosystems (Shannon et al., 2009). The results agree with the circumstantial evidence that jellyfish may increase when planktivorous fish stocks decrease. Shannon et al. 2009) also found that climate variability explained up to 22% of the observed variability in the SB, more than is explained by fisheries in the model. The authors conclude that a conservative approach to fisheries management could avoid such an ecosystem shift elsewhere. Roux et al. (2013) used a fisheries model to explore the influence of fisheries on both the NB and SB ecosystems. They found that the existence of large populations of planktivorous fishes is fundamental in linking the plankton to the rest of the ecosystem and that their removal may promote an increase in jellyfish biomass, damaging this link from the

plankton. The Roux et al. (2013) model includes detail on top predators and multiple fish species, but much less detail on plankton groups at the base of the ecosystem, which are important in transferring bottom-up drivers through the ecosystem. All these models of the BCS including jellyfish so far are from the same lineage (ECOPATH with ECOSIM), focusing on top-down processes, rather than bottom-up, with limited representation of plankton types (Roux and Shannon, 2004, Roux et al., 2013, Shannon et al., 2009).

PlankTOM11 provides the opportunity for a study into the role of climate variability and fishing on the BCS and jellyfish biomass, with improved parameterisation of jellyfish biological functions and much more detailed representation of climate variability. The central question I will address in this chapter is; from 1950 did fishing have more of an impact on jellyfish biomass than climate variability? To address this central question, I will explore: how does the jellyfish biomass behave historically without fishing? What impact does the addition of fishing pressure have on jellyfish biomass? What are the impacts on the other PFTs? And does the climate variability or fishing have a greater impact?

The BCS is notoriously difficult to simulate with ocean models, generally over-estimating the temperature and under-estimating the salinity along the coast due to upwelling. Attempts to improve the accuracy of models by increasing the ocean grid resolution have only achieved limited improvements in surface conditions in the BCS (Small et al., 2015, Gent et al., 2010). PlankTOM is a relatively coarse resolution compared with regional models. However, investigation of the physical outputs (see section 2.3.2) shows reasonable upwelling properties, with biases that are no worse than other published models of the region. This analysis will focus on the differences between simulations to understand the processes driving changes in jellyfish biomass, rather than on exactly replicating the BCS. The model scenarios will include (1) climate variability and no fishing, (2) no climate variability and no fishing, (3) climate variability and fishing and (4) no climate variability and fishing. This chapter will use the differences between the model scenarios to address the questions outlined above.



## 5.2 Methods

### 5.2.1 Introducing Fishing Pressure to PlankTOM11

PlankTOM11, developed and described in Chapter 3, is used to explore the influence of fishing and climate variability on jellyfish in the BCS. Only model equations that were altered to introduce fishing pressure are given here. For the full model description see Chapter 3.

#### 5.2.1.1 Fish Predation Preference

Van der Lingen (1994) summarises the food web relationships between anchovies and sardines and the plankton in the BCS. Predicted fish clearance rates of zooplankton prey, expressed in particle size, show that clearance rates increase rapidly from near 0 across the size range of mesozooplankton (200 - 2000 $\mu\text{m}$ ), with rates increasing as the particle size increases. Clearance rates continue to rise and peak into the size range of macrozooplankton (>2000 $\mu\text{m}$ ). The preferred prey of sardines and anchovies is macrozooplankton, followed by mesozooplankton (Van der Lingen, 1994). There is no evidence of sardines or anchovies consuming jellyfish in the BCS. ‘Fish’ or ‘fishing pressure’ refers to the two planktivorous species, sardines and anchovies, unless otherwise specified.

#### 5.2.1.2 Mortality Through Predation

The temporal evolution of zooplankton biomass in PlankTOM11 is determined from growth and loss through grazing, respiration and mortality, as described in Chapter 3 section 3.2.2, Eq. 3.1. To include the effect of changes in fish biomass on grazing pressure in the model, without adding fish as another PFT, fish are considered as changes to the mortality of zooplankton. Fish are significant consumers of zooplankton in upwelling systems (Van der Lingen, 1994). The mortality of zooplankton in PlankTOM11 is calculated as:

$$\text{zooplankton mortality} = m_{0^{\circ}}^{Z_j} \times c_{Z_j}^T \times \frac{Z_j}{K^{Z_j+Z_j}} \times \sum_i P_i \quad (5.1)$$

where,  $Z_j$  is the zooplankton PFT,  $m_{0^\circ}^{Z_j}$  is the mortality rate at  $0^\circ$ ,  $c_{Z_j}^T$  is the temperature dependence of the mortality,  $K^{Z_j}$  is the half saturation constant for mortality.  $\sum_i P_i$  is the sum of all the PFTs, excluding bacteria, which is used as a proxy for the biomass of predators not explicitly included in the model. This proxy predator biomass is altered here to correspond to the fish biomass over the same period (see Section 5.2.2.3). Only the mortality of macrozooplankton is altered to the fish biomass. This is because the mortality of proto- and mesozooplankton in the model is entirely accounted for through pressure by zooplankton represented in the model (Buitenhuis et al., 2013, Le Quéré et al., 2016). Also, macrozooplankton is the dominant food source of the fish (Van der Lingen, 1994). As there is no evidence of sardines or anchovies consuming jellyfish in the BCS, the mortality of jellyfish is not altered through the changes in fish biomass.

### 5.2.1.3 Fish Biomass and Proxy Predator Biomass

The biomass of fish prior to 1990 in the NB, and 1984 in the SB is estimated using virtual population analysis from the catch data. The biomass of fish after 1990 in the NB, and 1984 in the SB is estimated using acoustic surveys (Crawford, 2007, FAO, 2017, Butterworth, 1983). Although combining results from these two methods is not ideal, they are the best historic biomass estimates available (Crawford, 2007, Pauly and Zeller, 2017). The total sardine and anchovy fish stock biomass ( $B_F$ ) is converted to carbon units ( $0.06\text{gC} = 1\text{gWW}$ ) to match the proxy predator biomass ( $P_i$ ) in PlankTOM11 (Walsh, 1981). For 1989 in the Northern Benguela where no stock estimate is available, an interpolation of 1988 and 1990 is used. Fish biomass is surveyed in November and December for both the NB and SB. The biomass is interpolated between these months for each year. There is no seasonal cycle in the biomass data due to the way they are sampled. Although sardine and anchovy are significant consumers of zooplankton, they are not the only predators of zooplankton not included in the model. To prevent a shock to the biomass of top predators represented in the model the fish biomass is normalised ( $P_F$ ) as follows:

$$P_F^{NB} = \frac{B_F^{NB}}{B_F^{BCS}} \quad (5.2)$$

$$P_F^{SB} = \frac{B_F^{SB}}{\overline{B_F^{BCS}}} \quad (5.3)$$

Where  $B_F$  is the fish biomass of either the NB or the SB, and  $\overline{B_F^{BCS}}$  is the average fish biomass of the BCS (both the NB and the SB) over the whole period. The normalised fish biomass for the NB and SB is masked to the respective region, with equal weight

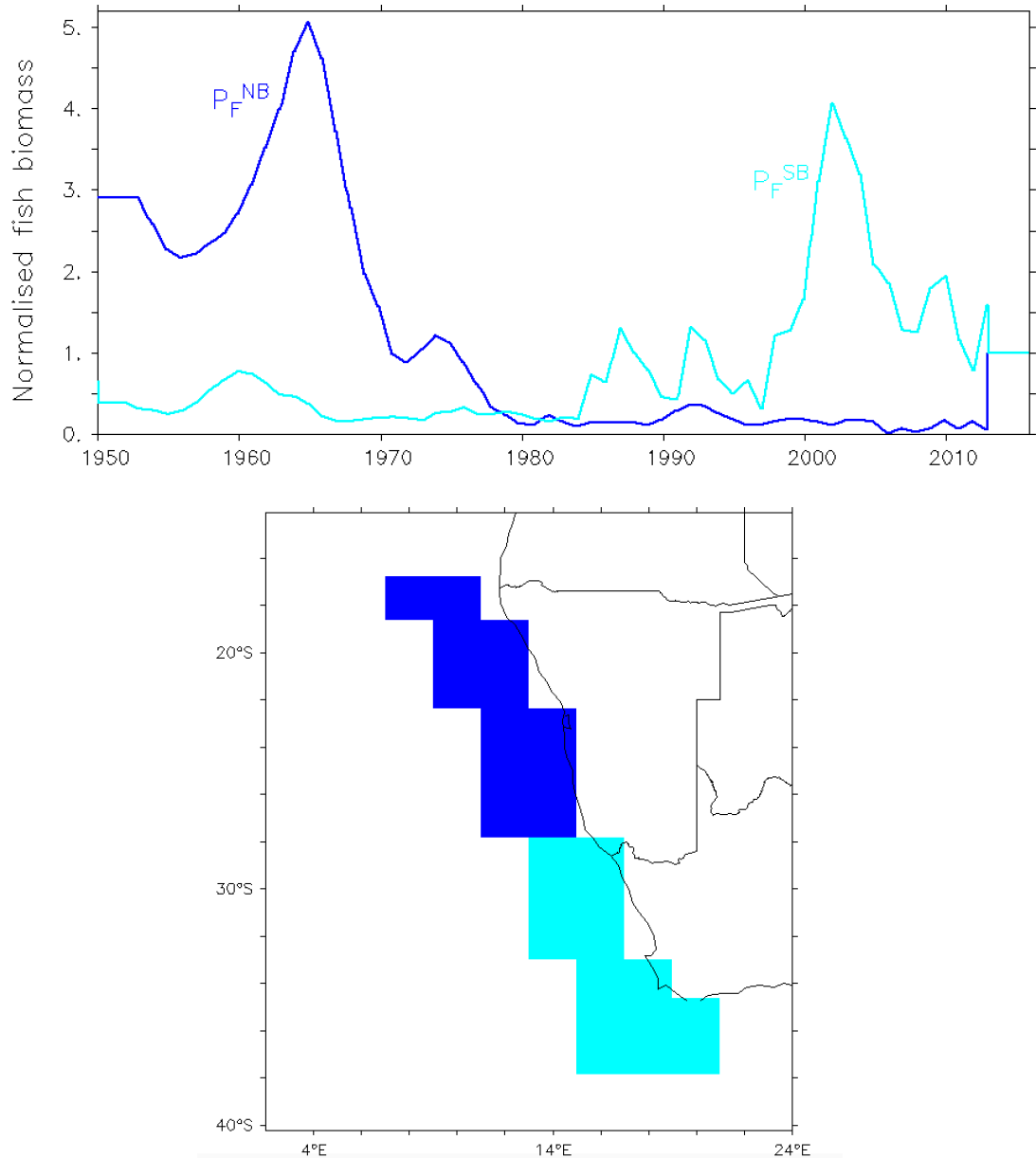


**Figure 5.3** The top panel shows the normalised fish biomass for the Northern Benguela (dark blue) and Southern Benguela (cyan) as used in PlankTOM11 to simulate fish PP. The normalised fish biomass is masked to the Northern and Southern Benguela, the area of these masks is shown in the bottom panel using the same colour key. The fish biomass data ends in 2012 so after this time the normalised fish biomass returns to 1.

for each grid box (see Figure 5.3). The proxy predator biomass is scaled to the normalised fish biomass to represent fish predation pressure (fish PP):

$$fish\ PP = P_F^{NB,SB} \times \sum_i P_i \quad (5.4)$$

## 5.2.2 Model Validation

### 5.2.2.1 Plankton Observations

Hutchings et al. (1991) assessed and compiled surveys on meso- and macrozooplankton in the BCS. These observations of meso- and macrozooplankton are used to validate the model, along with the observations of jellyfish (Fearon et al., 1992, Lynam et al., 2006) because the meso- and macrozooplankton observations have a higher validity, cover a longer period and cover both regions of the Benguela (see Section 5.1.1; Flynn et al., 2012). The global tuning of PlankTOM11 carried out in Chapter 3 gives meso- and macrozooplankton biomass within the observed range for the Northern and Southern Benguela (Table 5.1). The mesozooplankton average in the NB is a third of observations, and in the SB is half the observations, but still well within the range observed range (Table 5.1). The jellyfish average in the NB is double

**Table 5.1** The annual average (min – max) zooplankton biomass ( $\mu\text{mol C L}^{-1}$ ) in the Benguela for the top 200m. Observations are converted into  $\mu\text{mol C L}^{-1}$  from Hutchings et al. (1991) for mesozooplankton and macrozooplankton, and from Fearon et al. (1992) for jellyfish, with the Lynam et al. (2006) snapshot observations in parenthesis. Jellyfish observations are converted into carbon weight using the conversions in Lucas et al. (2011). PlankTOM11 results are for 1950-2015, 0-200m, using the regional masks shown in Figure 5.3.

	Mesozooplankton	Macrozooplankton	Jellyfish
<b>Northern Benguela</b>			
<b>Observations</b>	0.42 (0.04 - 0.42)	0.25 (0.04 - 0.42)	0.14 (0.0001)
<b>PlankTOM11</b>	0.13 (0.06 - 0.36)	0.23 (0.05 - 2.53)	0.26 (0.05 - 1.04)
<b>Southern Benguela</b>			
<b>Observations</b>	0.33 (0.08 - 0.83)	0.21 (0.04 - 0.42)	-
<b>PlankTOM11</b>	0.18 (0.06 - 1.76)	0.19 (0.05 - 1.17)	0.20 (0.05 - 0.68)

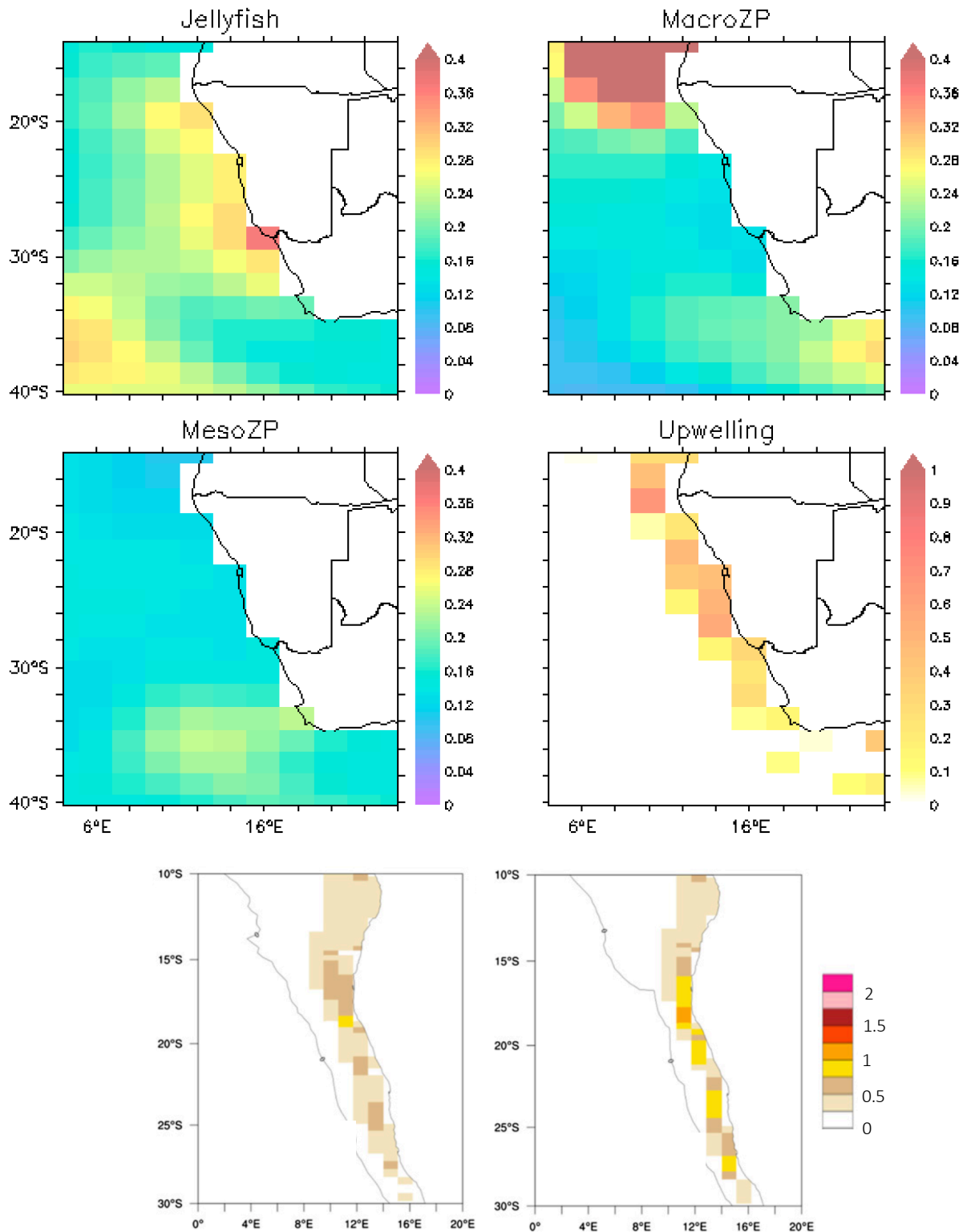


**Figure 5.4** Zooplankton biomass and upwelling for the BCS region. PlankTOM11 jellyfish (top left), macrozooplankton (top right) and mesozooplankton (middle left) biomass are in  $\mu\text{molC L}^{-1}$  averaged over 0-200m. Upwelling is the vertical velocity in  $\text{m day}^{-1}$ , positive values indicate upwelling. PlankTOM11 upwelling (middle right) is averaged over 40-50m and upwelling modelled by Small et al. (2015) is at 45m (bottom; panels are adapted from Figure 5 in Small et al., 2015). All PlankTOM11 results are averaged over 1950 – 2015.

the observations, with no observations in the SB. PlankTOM11 shows slightly higher jellyfish biomass in the NB than the SB (Table 5.1 and Fig. 5.4). The model may underestimate mesozooplankton biomass in the BCS because the global biomass is also slightly underestimated (see Chapter 3) and because jellyfish are overestimated (in the NB) which may reduce mesozooplankton through predation. No further tuning of PlankTOM11 was deemed necessary for this study. In PlankTOM11 jellyfish are ubiquitous across the NB and into the northern SB, with higher concentration along the coast and near the Lüderitz Cell (Fig. 5.4). Macrozooplankton biomass is concentrated in the north around the Angola-Benguela Front and the Cunene Cell (Fig. 5.4).

### **5.2.2.2 Physical Observations**

PlankTOM11 replicates the pattern of upwelling along the coast in the Benguela Current, with stronger upwelling at the Lüderitz Cell (26-28°S) and Cunene Cell (18°S; Fig. 5.4) although the strength of upwelling is underestimated (Small et al. 2015). The strength of upwelling in PlankTOM11 is similar to the model results in Small et al. (2015), with most of the upwelling in the NB between 0.25 – 1 m day<sup>-1</sup> (Fig. 5.4). Models of the Benguela Current systematically underestimate upwelling, the similarity of PlankTOM11 upwelling strength to Small et al. (2015) means that we accept this as a reasonable replication of the Benguela Current. The upwelling in PlankTOM11 extends further from the coast than would be ideal, but this is expected with the grid resolution in the model (Fig. 5.4).

### **5.2.3 Model Simulations**

Four simulations are used to assess the individual as well as combined influence of climate variability and fisheries (as fish PP) on the BCS ecosystem (Table 5.2). The simulations are TOM11-CN with climatic variability and without fish PP (PlankTOM11 as in Chapter 3), TOM11-NN without climatic variability and without fish PP, TOM11-CF with climatic variability and with fish PP and TOM11-NF without climate variability and with fish PP (Table 5.2).

All the simulations are run from 1920-2015. We apply a 28-year spin up during 1920 – 1947 by repeating meteorological forcing corresponding to year 1980 (see Chapter 3 for detail). For the simulation with climate variability, we apply meteorological forcing of the corresponding year during 1948 – 2015. For the simulation without climate variability, we maintain the meteorological forcing corresponding to year 1980 throughout the simulation.

Results from the simulations are presented for 1950-2012, as fish biomass data ends in 2012. Results are averaged using the Northern and Southern Benguela masks shown in Figure 5.3. Differences between the simulations are used to assess the influence of climatic variability and fishing. The simulation TOM11-NN is used as a baseline. Each of the other simulations is subtracted from TOM11-NN to calculate differences due to climate variability and fisheries individually (TOM11-CN and TOM11-NF respectively) and combined (TOM11-CF).

**Table 5.2** PlankTOM11 simulations to assess the influence of climate variability and fisheries (as fish predation pressure) on the BCS ecosystem.

<b>PlankTOM11 simulations</b>	<b>Climatic Variability</b>	<b>Fish Predation Pressure</b>
<b>TOM11-CN</b>	Yes	No
<b>TOM11-NN</b>	No	No
<b>TOM11-CF</b>	Yes	Yes
<b>TOM11-NF</b>	No	Yes

## 5.3 Results

### 5.3.1 The Northern Benguela

Figure 5.5 shows each of the four simulations subtracted from TOM11-NN. The normalised fish biomass, representing fish PP, in the Northern Benguela is also shown. Figure 5.6 shows jellyfish and macrozooplankton biomass for each of the four simulations. In the Northern Benguela fish PP is between 2 – 3 during the 1950's. Fish PP then increases to peak at 5 in 1964 after which it rapidly decreases to 1 by 1970 (Fig. 5.5). For the next few years fish PP stays close to 1; at 1 fish PP has minimal influence on macrozooplankton mortality. From the late 1970's onwards fish PP is low (less than 0.3; Fig. 5.5).

In the Northern Benguela with climate variability and without fish PP (TOM11-CN; black line) jellyfish biomass shows year-to-year oscillations. This oscillation due to climate variability is reduced from 1983 to 1994, followed by a period of increased jellyfish biomass until ~2000 (Fig. 5.5). Without climate variability and with fish PP (TOM11-NF; green line) jellyfish biomass is only affected after 1990 when it rapidly declines and remains lower until the end of the simulation (Fig. 5.5). With climate variability and fish PP (TOM11-CF; red line) the oscillations in jellyfish biomass are slightly larger than without fish PP (TOM11-CN) until 1972, where it matches TOM11-CN oscillations for a few years until 1978, after which jellyfish biomass rapidly declines. Jellyfish biomass stays at a reduced level with some small oscillations for 20 years. From 2001 jellyfish biomass rapidly increases again to match TOM11-CN oscillations for the remainder of the simulations (Fig. 5.5). The period from 1972 to 1978 where jellyfish biomass is the same in TOM11-CN and TOM11-CF is the period where fish PP is closest to 1 (where it has little effect on macrozooplankton predation mortality). The high fish PP before this period has a slight impact on increasing jellyfish biomass, after this period the reduced fish PP has a substantial impact on decreasing jellyfish biomass. However, after 2001 jellyfish biomass substantially increases while fish PP remains low (Fig. 5.5).

In the Northern Benguela with climate variability and without fish PP (TOM11-CN; black line) macrozooplankton experience an increase in biomass due to climate from



1995 to 1975 and from 1989 to 1994. Outside of these two periods, climate variability has a small influence on macrozooplankton biomass (Fig. 5.5). Without climate variability and with fish PP (TOM11-NF; green line) macrozooplankton biomass is only affected after 1990 when it rapidly increases and remains elevated until the end of the simulation (Fig. 5.5). With climate variability and fish PP (TOM11-CF; red line) macrozooplankton biomass is lower than without fish PP (TOM11-CN) from 1955 to

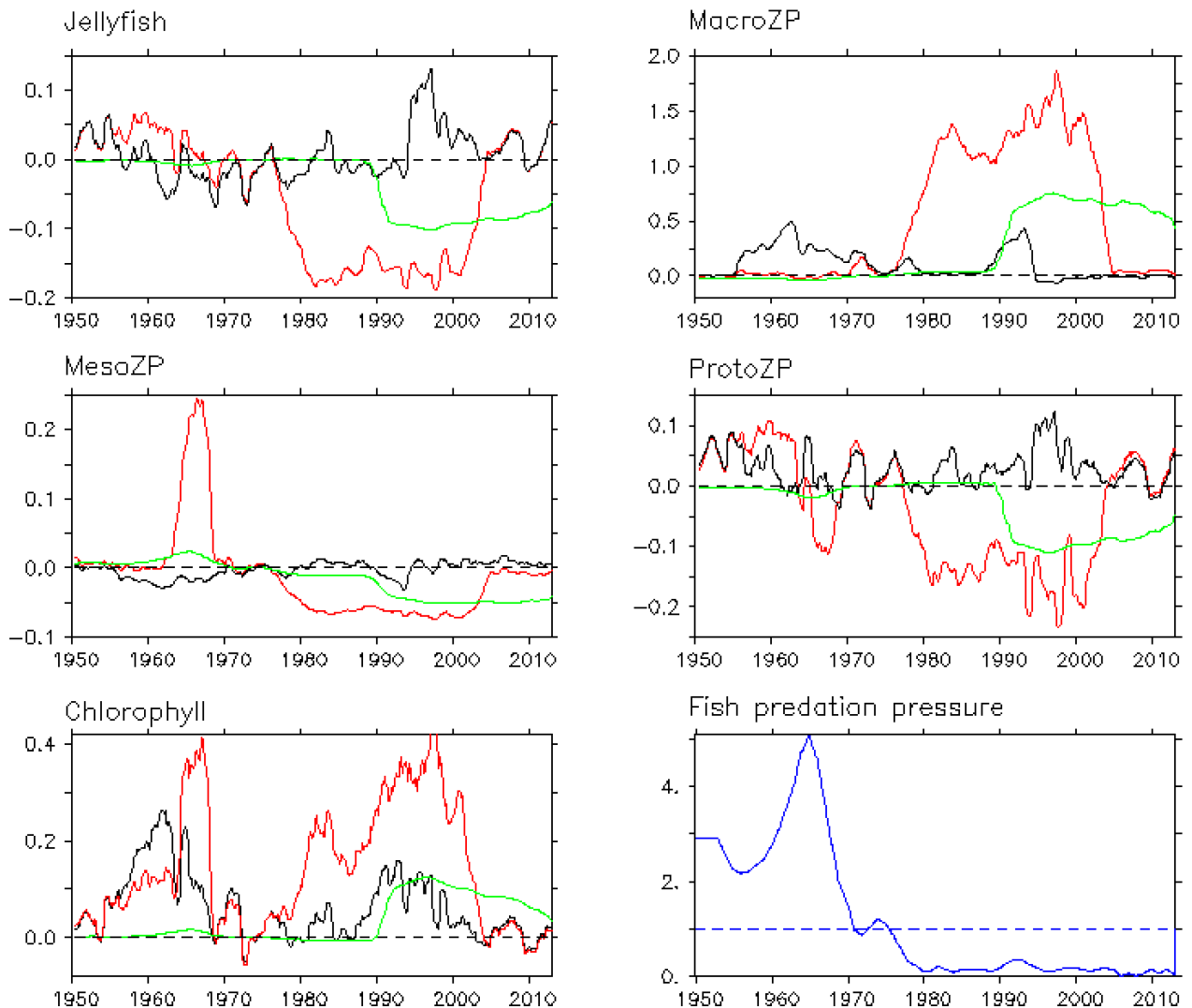


**Figure 5.5** The effect of climate and fishing on zooplankton biomass and chlorophyll concentration in the Northern Benguela. Each of the simulations TOM11-CF (red line), TOM11-CN (black line), TOM11-NF (green line) and TOM11-NN (dashed black line), is subtracted from TOM11-NN, so that the y-axis is the difference due to fish PP, climate or fish PP and climate. Results are shown for (top left) jellyfish, (top right) macrozooplankton, (middle left) mesozooplankton, (middle right) protozooplankton and (bottom left) surface chlorophyll. Note that the panels have different y-axis. Fish PP (bottom right) for the Northern Benguela as in Figure 5.3 with the dashed line at 1 where fish predation does not have an influence on proxy predator biomass (Eq. 5.2). All simulation results are seasonally smoothed to show year to year variability, zooplankton are averaged over 0-200 meters in  $\mu\text{mol C L}^{-1}$  and chlorophyll is averaged over 0-10 meters in  $\mu\text{mol chl L}^{-1}$ .

1970, but almost the same as the simulation with no climate variability or fish PP (TOM11-NN; dashed black line). As with jellyfish, from 1972 to 1978 macrozooplankton biomass in TOM11-CF matches TOM11-CN oscillations. After 1978 macrozooplankton biomass rapidly increases and stays elevated for 20 years. From 2001 biomass rapidly declines to be just above TOM11-CN for the remainder of the simulation (Fig. 5.5). The period from 1972 to 1978 where macrozooplankton biomass is the same in TOM11-CN and TOM11-CF is the period where fish PP is closest to 1 (where it has little effect on macrozooplankton predation mortality). The high fish PP before this period decreases macrozooplankton biomass, after this period the reduced fish PP has a substantial impact on increasing macrozooplankton biomass. However, after 2001 macrozooplankton biomass substantially decreases while fish PP remains low (Fig. 5.5).

In the Northern Benguela with climate variability and without fish PP (TOM11-CN; black line) mesozooplankton biomass is slightly reduced from 1955 to 1970 and then has small oscillations in biomass for the rest of the simulation period (Fig. 5.5).

Without climate variability and with fish PP (TOM11-NF; green line) mesozooplankton biomass increases slightly around 1965 and decreases from 1990 to the end of the simulation (Fig. 5.5). With climate variability and fish PP (TOM11-CF; red line) mesozooplankton biomass increases substantially more than TOM11-NF around 1965 and decreases earlier (1978) than TOM11-NF (1990). Mesozooplankton biomass in TOM11-CF increases after 2002 to slightly below TOM11-CN. In the Northern Benguela protozooplankton behaves in a similar pattern and to a similar degree of change to jellyfish for all the simulations (Fig. 5.5).

In the Northern Benguela with climate variability and without fish PP (TOM11-CN; black line) chlorophyll concentration shows multi-decadal cycles with year-to-year oscillations, with higher chlorophyll from 1955 to 1968 and from 1990 to 1998 and lower chlorophyll outside of these periods. Chlorophyll is higher in the 1960's than in the 1990's (Fig. 5.5). Without climate variability and with fish PP (TOM11-NF; green line) chlorophyll is only affected after 1990 when it rapidly increases for a year and then gradually declines to the end of the simulation (Fig. 5.5). With climate variability and fish PP (TOM11-CF; red line) chlorophyll has similar multi-decadal cycles to TOM11-CN but in the 1960's elevated concentration chlorophyll begins lower and

then increases to more than in TOM11-CN and for the later elevated concentration period chlorophyll concentration increases earlier (1980 compared to 1990) and increases more than in TOM11-CN. From 2003 chlorophyll in TOM11-CF is the same as in TOM11-CN (Fig. 5.5).

The addition of fish PP on macrozooplankton, simulating overfishing in the Northern Benguela, has not caused an increase in jellyfish biomass over time (Fig. 5.5). This

**Table 5.3** The effect of climate and fishing on zooplankton and chlorophyll in the Northern Benguela. Each of the simulations TOM11-CF, TOM11-CN and TOM11-NF is subtracted from TOM11-NN (no climate or fishing). CN + NF is the addition of the results from TOM11-CN and TOM11-NF. Results are given as a total of 1950 - 2012 for all zooplankton ( $\mu\text{mol C L}^{-1}$ ) and chlorophyll ( $\mu\text{mol chl L}^{-1}$ ) and broken down into the total of each decade for macrozooplankton, jellyfish and chlorophyll.

	<b>TOM11-CF</b>	<b>TOM11-CN</b>	<b>TOM11-NF</b>	<b>CN + NF</b>
<b>PFT</b>	<b>1950 – 2012 total</b>			
<b>ProtoZP</b>	110.6	33.8	45.2	79.0
<b>MesoZP</b>	56.6	11.4	29.0	40.4
<b>MacroZP</b>	744.8	161.9	358.8	520.6
<b>Jellyfish</b>	87.8	32.5	35.2	67.8
<b>Chlorophyll</b>	42.2	20.5	12.6	33.1
	<b>1950 - 1959</b>			
<b>MacroZP</b>	4.1	24.5	3.9	28.4
<b>Jellyfish</b>	5.3	3.7	0.3	4.0
	<b>1960 - 1969</b>			
<b>MacroZP</b>	4.1	65.0	6.5	71.5
<b>Jellyfish</b>	4.3	6.4	0.9	7.3
	<b>1970 - 1979</b>			
<b>MacroZP</b>	44.7	23.2	2.2	25.4
<b>Jellyfish</b>	8.3	6.3	0.1	6.3
	<b>1980 - 1989</b>			
<b>MacroZP</b>	256.0	7.8	10.0	17.8
<b>Jellyfish</b>	29.7	3.7	0.4	4.1
	<b>1990 - 1999</b>			
<b>MacroZP</b>	326.9	37.8	147.9	185.6
<b>Jellyfish</b>	28.8	8.7	15.3	24.0
	<b>2000 - 2009</b>			
<b>MacroZP</b>	106.4	3.2	151.2	154.4
<b>Jellyfish</b>	10.5	2.9	14.6	17.5

lack of increase in jellyfish biomass is contrary to observations and hypothesis for the region (see Section 5.1). The macrozooplankton instead become dominant in the environment, due to reduced predation pressure after the 1970's (Fig. 5.5). This advantage allows them to outcompete jellyfish, which in PlankTOM11 do not have this advantage of reduced fish PP.

In the NB macrozooplankton shows behaviour typical of tipping points, when their biomass rapidly increases following continuous forcing, affecting jellyfish and other zooplankton biomass. These tipping points are most prevalent in the TOM11-CF simulation, where combined climate variability and fish PP reduction allow macrozooplankton biomass to increase four-fold above the biomass in TOM11-CN, and double that of the biomass in TOM11-NF (Fig. 5.5). The changes to macrozooplankton biomass are substantially greater than the changes to the biomass of the other zooplankton.

The differences between the simulations are provided by decade and for the whole period in Table 5.3. In the Northern Benguela over the whole period (1950-2012) when acting individually, climate variability and fish PP had a similar level of influence on jellyfish biomass ( $32.5 \mu\text{mol C L}^{-1}$  for TOM11-CN versus  $35.2$  for TOM11-NF). The combination of climate variability and fish PP (TOM11-CF) had a greater influence on jellyfish biomass than the sum of the two factors alone ( $87.8 \mu\text{mol C L}^{-1}$  versus  $67.8$ ; Table 5.3). For macrozooplankton over the whole period, fish PP had a greater influence on biomass than climate variability ( $358.8 \mu\text{mol C L}^{-1}$  for TOM11-NF versus  $161.9$  for TOM11-CN; Table 5.3). Here also, the combination of climate variability and fish PP (TOM11-CF) had a greater influence on macrozooplankton biomass than the addition of the two factors alone ( $744.8 \mu\text{mol C L}^{-1}$  versus  $520.6$ ; Table 5.3). For chlorophyll over the whole period, climate variability (TOM11-CN;  $20.5 \mu\text{mol C L}^{-1}$ ) had a greater influence on chlorophyll concentration than fish PP (TOM11-NF;  $12.6$ ). The combination of climate variability and fish PP (TOM11-CF) had a greater influence on chlorophyll concentration than the sum of the two factors alone ( $42.2 \mu\text{mol C L}^{-1}$  versus  $33.1$ ; Table 5.3). For all zooplankton the combination of climate variability and fish PP (TOM11-CF) had a greater influence on biomass than the sum of the two factors alone (CN + NF; Table 5.3).

Before 1990 jellyfish biomass is more influenced by climate variability (TOM11-CN,  $3.7 - 6.4 \mu\text{mol C L}^{-1}$ ) than fish PP (TOM11-NF,  $0.1 - 0.9 \mu\text{mol C L}^{-1}$ ; Table 5.3). After 1990 jellyfish biomass is more influenced by fish PP ( $14.6 - 15.3 \mu\text{mol C L}^{-1}$ ) than climate variability ( $2.9 - 8.7 \mu\text{mol C L}^{-1}$ ; Table 5.3). Before 1970 when fish PP is over 1 (Fig. 5.5) macrozooplankton are more influenced by climate variability ( $24.5 + 65$ ) than fish PP ( $3.9 + 6.5 \mu\text{mol C L}^{-1}$ ; Table 5.3). During the 1970's when fish PP is close to 1 (Fig. 5.5) macrozooplankton are more influenced by climate variability ( $23.2 \mu\text{mol C L}^{-1}$ ) than fish PP ( $2.2 \mu\text{mol C L}^{-1}$ ; Table 5.3) as expected because fish PP is having a small influence over macrozooplankton predation mortality. From 1980 fish PP is low ( $<0.4$ ) but it takes until the 1990's for fish PP to have significantly more influence on macrozooplankton biomass than climate variability ( $146.9$  versus  $37.8 \mu\text{mol C L}^{-1}$ ; Table 5.3). Before 1970 the combined simulation of climate variability and fish PP (TOM11-CF) has less of an influence on macrozooplankton biomass than either factor does alone. After 1970 TOM11-CF has more of an influence on macrozooplankton biomass than either factor does alone, or summed (CN + NF; Table 5.3). The low influence of fish PP prior to 1970, is due to the low macrozooplankton biomass without climate during this period (Fig. 5.5). PlankTOM11 contains protection mechanisms to prevent plankton biomass decreasing below a critical level and becoming extinct. It is likely that the addition of high fish PP to an already low macrozooplankton biomass triggers this protection mechanism, preventing macrozooplankton biomass from reducing further and thus suppressing the influence of fish PP.

### 5.3.2 The Southern Benguela

Figure 5.6 is similar to Figure 5.5 but for the Southern Benguela. In the Southern Benguela fish PP is less than 1 from 1950 to the mid-1980's. From the mid-1980's to late 1990's fish PP oscillates between 0.5 and 1.2. Fish PP then rapidly increases to peak in 2001 at 4. Fish PP then rapidly declines into the mid-2000's after which it oscillates between 1 and 2.

In the Southern Benguela with climate variability and without fish PP (TOM11-CN; black line) jellyfish biomass shows multi-decadal cycles with year-to-year oscillations. Jellyfish biomass is higher from 1950 to 1970, lower from 1970 to 1992, then higher

for a shorter period from 1993 to 2001 and lower from 2001 to 2012 (Fig. 5.6). Without climate variability and with fish PP (TOM11-NF; green line) jellyfish biomass has slight variations from no climate variability and no fish predation (TOM11-NN) with a slightly lower biomass from 1965 to 1985 and slightly higher biomass from 2000 to 2011 (Fig. 5.6). With climate variability and fish PP (TOM11-CF; red line) jellyfish biomass is very similar to TOM11-CN, with some years of

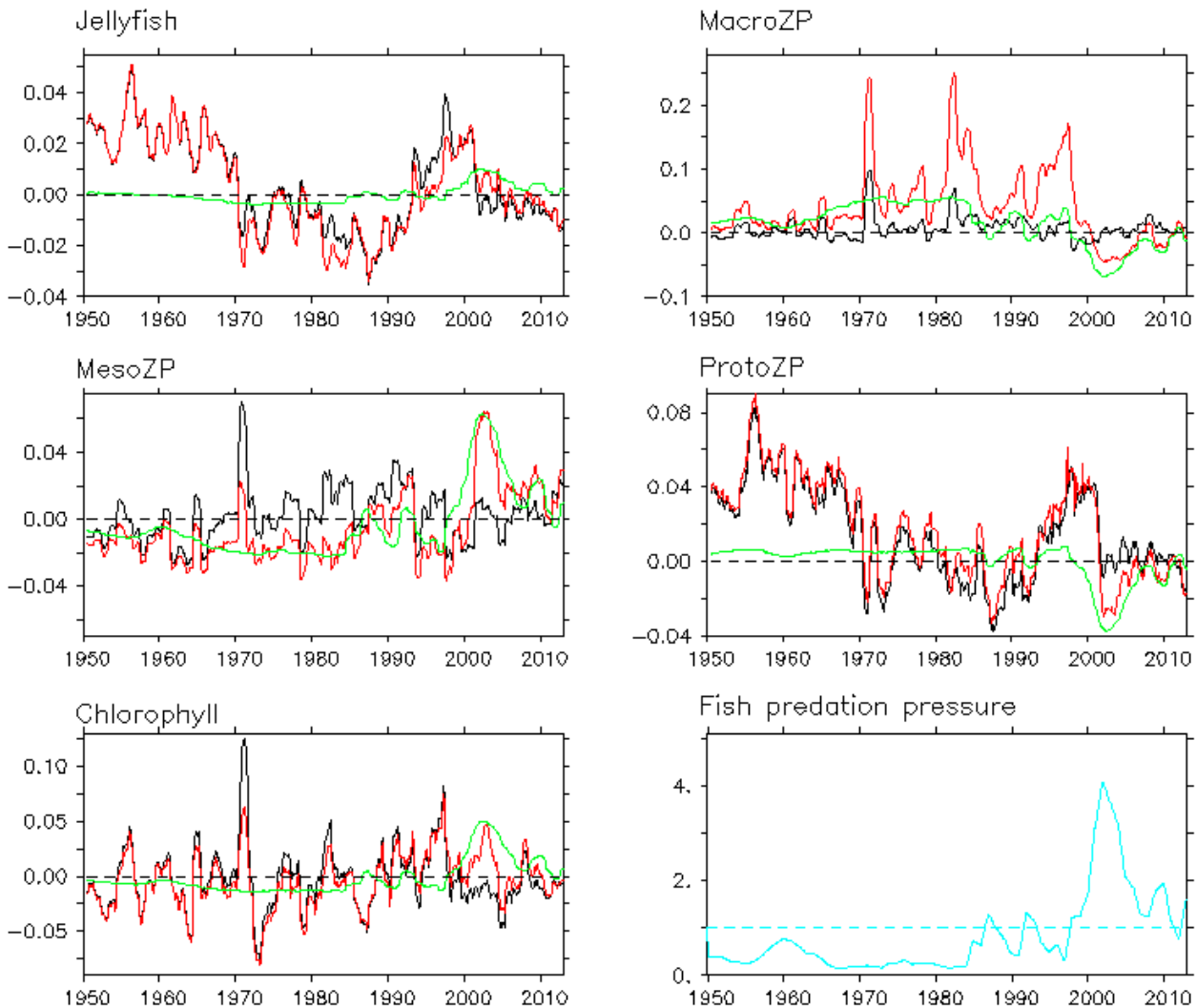


**Figure 5.6** The effect of climate and fishing on zooplankton and chlorophyll in the Southern Benguela. Each of the simulations TOM11-CF (red line), TOM11-CN (black line), TOM11-NF (green line) and TOM11-NN (dashed black line), is subtracted from TOM11-NN, so that the y-axis is the difference due to fishing, climate or fishing and climate. Results are shown for (top left) jellyfish, (top right) macrozooplankton, (middle left) mesozooplankton, (middle right) protozooplankton and (bottom left) surface chlorophyll. Fish PP (bottom right) for the Northern Benguela as in Figure 5.3 with the dashed line at 1 where fish predation does not have an influence on proxy predator biomass (Eq. 5.3). All simulation results are seasonally smoothed to show year to year variability, zooplankton are averaged over 0-200 meters in  $\mu\text{mol C L}^{-1}$  and chlorophyll is averaged over 0-10 meters  $\mu\text{mol chl L}^{-1}$ .

**Table 5.4** The effect of climate and fishing on zooplankton and chlorophyll in the Southern Benguela. Each of the simulations TOM11-CF, TOM11-CN and TOM11-NF is subtracted from TOM11-NN (no climate or fishing). CN + NF is the addition of the results from CN and NF. Results are given as a total of 1950 – 2012 for all zooplankton ( $\mu\text{mol C L}^{-1}$ ) and chlorophyll ( $\mu\text{mol chl L}^{-1}$ ) and broken down into the total of each decade for macrozooplankton, jellyfish and chlorophyll.

	CF	CN	NF	CN + NF
<b>PFT</b>	<b>1950 – 2012 total</b>			
<b>ProtoZP</b>	30.8	28.6	8.2	36.7
<b>MesoZP</b>	24.4	16.9	22.3	39.2
<b>MacroZP</b>	66.7	17.0	41.5	58.5
<b>Jellyfish</b>	21.1	20.2	3.9	24.1
<b>Chlorophyll</b>	12.3	10.9	9.0	19.9
	<b>1950 - 1959</b>			
<b>MacroZP</b>	3.3	1.3	3.7	5.1
<b>Jellyfish</b>	4.3	4.2	0.1	4.3
	<b>1960 - 1969</b>			
<b>MacroZP</b>	4.6	2.2	6.3	8.5
<b>Jellyfish</b>	4.0	4.0	0.4	4.4
	<b>1970 - 1979</b>			
<b>MacroZP</b>	15.6	3.8	11.3	15.1
<b>Jellyfish</b>	3.0	2.2	0.9	3.0
	<b>1980 - 1989</b>			
<b>MacroZP</b>	19.4	4.0	6.8	10.8
<b>Jellyfish</b>	4.9	4.1	0.5	4.6
	<b>1990 - 1999</b>			
<b>MacroZP</b>	17.8	3.3	4.3	7.5
<b>Jellyfish</b>	2.5	3.5	0.4	3.9
	<b>2000 - 2009</b>			
<b>MacroZP</b>	5.3	2.2	8.4	10.6
<b>Jellyfish</b>	1.6	1.5	1.5	3.0

slightly lower biomass from 1970 to 2000 and slightly higher biomass from 2000 (Fig. 5.6). The changes in jellyfish biomass are small for all the effects.

In the Southern Benguela with climate variability and without fish PP (TOM11-CN; black line) macrozooplankton biomass shows year to year oscillations with no long-term trend (Fig. 5.6). Without climate variability and with fish PP (TOM11-NF; green line) macrozooplankton biomass is increased from 1950 to 1985, then in 2000 declines before slowing increasing until the end of the simulation (Fig. 5.6). With climate

variability and fish PP (TOM11-CF; red line) macrozooplankton biomass shows the same pattern of year-to-year oscillations as TOM11-CN at higher biomass with stronger peaks from 1950 to 2000 and lower biomass from 2000 to the end of the simulation (Fig. 5.6). Before 1985 fish PP is less than 1 and so reduces macrozooplankton predation mortality, from 1985 to 2000 fish PP oscillates around 1, and after 2000 fish PP rapidly increases and peaks at 4 before declining to between 1 and 2 increasing macrozooplankton predation mortality (Fig. 5.6).

In the Southern Benguela with climate variability and without fish PP (TOM11-CN; black line) mesozooplankton biomass shows year to year oscillations with no long-term trend (Fig. 5.6). Without climate variability and with fish PP (TOM11-NF; green line) mesozooplankton is decreased from 1950 to 1985, where it oscillates before rapidly increasing from 2000 to 2002 and then decreases to 2012 (Fig. 5.6). With climate variability and fish PP (TOM11-CF; red line) mesozooplankton biomass shows the same pattern of year-to-year oscillations as TOM11-CN at lower biomass from 1950 to 1992 and higher biomass from 2000 to 2011 (Fig. 5.6). In the Southern Benguela protozooplankton biomass behaves in a similar pattern to jellyfish for all the simulations, except for the fish predation runs (TOM11-CF and TOM11-NF) from 2000 to 2005 where protozooplankton biomass declines unlike jellyfish biomass which increases over this period (Fig. 5.6).

In the Southern Benguela with climate variability and without fish PP (TOM11-CN; black line) chlorophyll concentration shows year-to-year oscillations with no long-term trend (Fig. 5.6). Without climate variability and with fish PP (TOM11-NF; green line) chlorophyll is slightly decreased from 1950 to 1985 and increased from 2000 (Fig. 5.6). With climate variability and fish PP (TOM11-CF; red line) chlorophyll concentration is similar to TOM11-CN except from 2000 to 2005 where it increases (Fig. 5.6).

In the Southern Benguela, jellyfish (both with and without fish PP) seem to show a decadal to multi-decadal cycle in biomass, similar to the cycle shown by protozooplankton. Biomass of jellyfish is higher from 1950-1970, lower from 1970-1992, higher again from 1992 – 2003, and lower from 2003 – 2012 (Fig. 5.6). In the Southern Benguela over the whole period (1950-2012) when acting individually



climate variability has a greater level of influence on jellyfish biomass than fish PP (20.2 for TOM11-CN versus 3.9  $\mu\text{mol C L}^{-1}$  for TOM11-NF). The combination of climate variability and fish PP (TOM11-CF) had a slightly lower influence on jellyfish biomass than the addition of the two factors alone (21.1 versus 24.1  $\mu\text{mol C L}^{-1}$ ; Table 5.4). For macrozooplankton over the whole period, fish PP has a greater level of influence on biomass than climate variability (41.5 versus 17.0  $\mu\text{mol C L}^{-1}$ ). The combination of climate variability and fish PP (TOM11-CF) had a greater influence on macrozooplankton biomass than the addition of the two factors alone (66.78 versus 58.7  $\mu\text{mol C L}^{-1}$ ; Table 5.4). For chlorophyll over the whole period, climate variability and fish PP individually have a similar influence on concentration (10.9 versus 9.0  $\mu\text{mol C L}^{-1}$ ). The combination of climate variability and fish PP (TOM11-CF) had a greater influence on macrozooplankton biomass than the sum of the two factors alone (66.7 versus 58.5  $\mu\text{mol C L}^{-1}$ ; Table 5.4). For protozooplankton over the whole period, climate variability had a greater influence on biomass than fish PP (28.6 versus 8.2  $\mu\text{mol C L}^{-1}$ ) and for mesozooplankton fish PP had a greater influence on biomass than climate variability (22.3 versus 16.9  $\mu\text{mol C L}^{-1}$ ; Table 5.4).

Before 2000 jellyfish biomass is more influenced by climate variability (TOM11-CN, 3.7 – 6.4  $\mu\text{mol C L}^{-1}$ ) than fish PP (TOM11-NF, 0.1 – 0.9  $\mu\text{mol C L}^{-1}$ ; Table 5.4), during this period fish PP is mostly below 1 (Fig. 5.7). After 2000 jellyfish biomass is equally influenced by climate variability and fish PP individually (1.5  $\mu\text{mol C L}^{-1}$ ) as well as by the combination of the two factors (TOM11-CF, 1.6  $\mu\text{mol C L}^{-1}$ ), during this period fish PP is above 1 (Fig. 5.7). For every decade macrozooplankton biomass is more influenced by fish PP (3.7 - 11.3  $\mu\text{mol C L}^{-1}$ ) than by climate variability (1.3 – 4.0  $\mu\text{mol C L}^{-1}$ ; Table 5.4). The influence of fish PP on macrozooplankton is greatest during the 1970's, when fish PP is at its lowest (Fig. 5.6).

In the Southern Benguela, the effect of fish PP on macrozooplankton has the largest knock-on effect on mesozooplankton, where macrozooplankton biomass is higher, mesozooplankton biomass is lower. This is likely due to increase predation by macrozooplankton on meso (Fig. 5.6). The effect of fish PP on macrozooplankton biomass is far lower in the Southern Benguela than in the Northern Benguela (Fig. 5.5 and 5.8).

## JELLYFISH

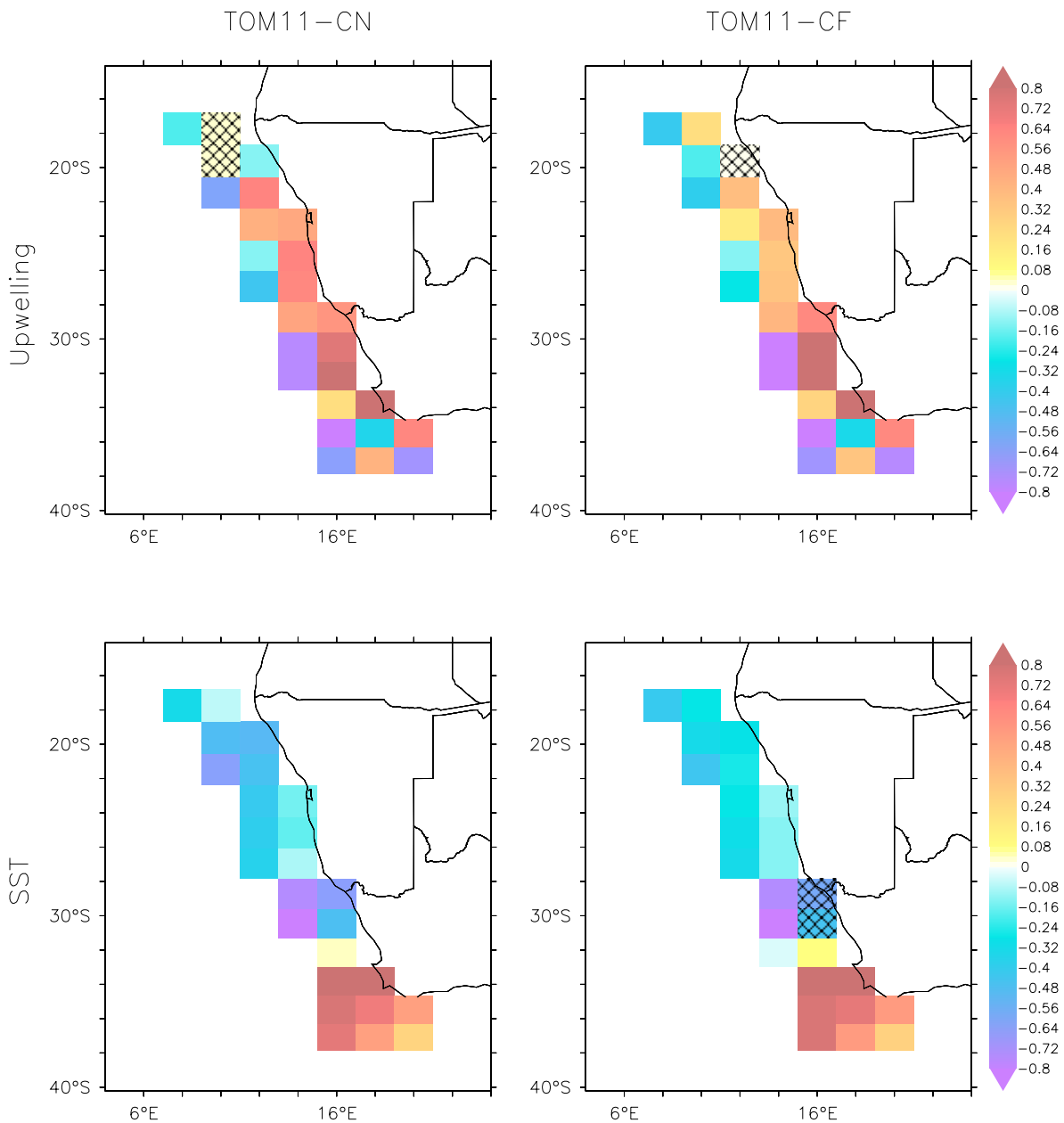


**Figure 5.7** The correlation over time of jellyfish with (top) upwelling and (bottom) SST for the simulations (left) TOM11-CN (Climate & No fish predation) and (right) TOM11-CF (Climate & Fish predation). Correlations are calculated for 1950-2012 for the Northern and Southern Benguela masks where fish predation is applied, as shown in Figure 5.3. Warm colours indicate positive correlation and cold colours indicate negative correlation. Cross-hatched grid cells are where the correlation is not statistically significant ( $p$  values less than 0.05).

### 5.3.3 Correlation to Physical Conditions

Climatic variability in the BCS is largely driven by upwelling and SST. Figure 5.7 and 5.8 show the correlation of jellyfish and macrozooplankton with upwelling and SST

## MACROZOOPLANKTON

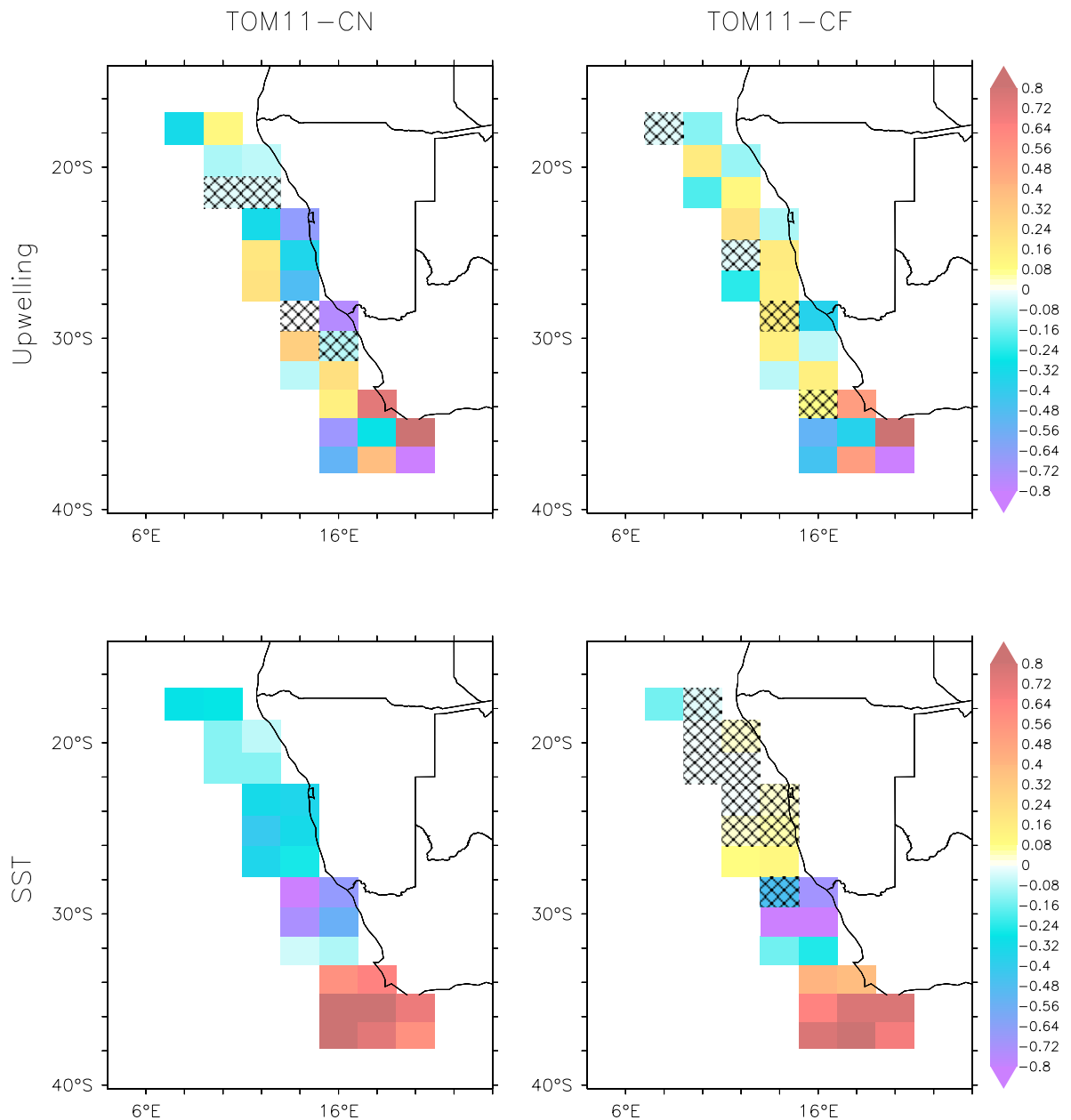


**Figure 5.8** The spatial correlation of macrozooplankton with (top) upwelling and (bottom) SST for the simulations (left) TOM11-CN (climate and no fish PP) and (right) TOM11-CF (climate and fish PP). Correlations are calculated for 1950-2012 for the Northern and Southern Benguela masks where fish predation is applied, as shown in Figure 3. Warm colours indicate positive correlation and cold colours indicate negative correlation. Cross-hatched grid cells are where the correlation is not statistically significant ( $p$  values less than 0.05).

over time averaged for 1950 to 2012. Grid cells are cross-hatched where the correlation between zooplankton and physical conditions is not statistically significant ( $p = 0.05$ ). Along the coast jellyfish are positively correlated to upwelling, the correlation decreases and becomes negative just away from the coast (Fig. 5.7). The positive correlation between jellyfish and upwelling is stronger in the northern

Benguela in TOM11-CN, without fish predation, than in TOM11-CF with fish predation. In the Northern Benguela and the northern half of the Southern Benguela jellyfish are negatively correlated to SST (Fig. 5.7). In the southern half of the Southern Benguela jellyfish are positively correlated to SST. The negative correlation in the Northern Benguela is slightly stronger in TOM11-CN than in TOM11-CF. In the Southern Benguela the strength of correlation is the same with and without fish PP, except in two grid cells where there is no significant correlation with fish PP (Fig. 5.7). In the Northern Benguela TOM11-CN has stronger correlation between jellyfish and physical conditions than TOM11-CF (Fig. 5.7). The simulation of fish PP adds another influence on jellyfish biomass and reduces the influence of physical conditions.

Negative correlation between jellyfish and SST is contrary to the general expectation of higher temperatures increasing growth and thus increasing biomass. Lower SST occurs where upwelling is stronger (above 34°S, see Fig. 5.4) as the upwelling brings colder deep water to the surface. The cold deep water brings nutrients to the surface enhancing biomass despite the colder temperature. The model simulates this enhanced biomass in colder upwelled coastal waters, despite the relatively coarse model resolution. In the southern half of the Southern Benguela where upwelling is reduced (below 34°S, see Fig. 5.4) jellyfish are positively correlated with temperature (Fig. 5.7). In the north of the Northern Benguela (above 21°S) jellyfish have a weaker, or no, correlation to upwelling (Fig. 5.7). The high biomass of macrozooplankton in this region (see Fig. 5.4) outcompetes jellyfish, so that macrozooplankton have a greater influence on jellyfish biomass than physical conditions.

Macrozooplankton biomass and upwelling do not have a clear spatial pattern of correlation, unlike jellyfish biomass with upwelling (Fig. 5.7 and 5.8). In the Northern Benguela without fish PP (TOM11-CN), macrozooplankton biomass has a mostly negative correlation to upwelling, when fish PP is introduced (TOM11-CF) the negative correlation decreases in strength and in some areas becomes a weak positive correlation (Fig. 5.8). In the Southern Benguela without fish PP (TOM11-CN), correlation along the coast between macrozooplankton biomass and upwelling changes from strongly negative in the north, through neutral correlation, to strongly positive correlation in the south. When fish PP is introduced (TOM11-CF), the strength of coastal correlation weakens but largely remains in the same direction (Fig. 5.8).

Macrozooplankton biomass and SST have a negative correlation north of 33°S and a positive correlation below 33°S. The strongest negative correlation between macrozooplankton biomass and SST is between 28 -31°S (Fig. 5.8). When fish PP is introduced (TOM11-CF) correlation in the Northern Benguela largely disappears. In the Southern Benguela the spatial correlations remain mostly the same. Fish PP has a stronger influence on macrozooplankton in the Northern Benguela than in the Southern Benguela (Fig. 5.8).

#### **5.3.4 External Influence**

Figure 5.9 shows jellyfish and macrozooplankton biomass in the BCS mapped annually from 1975 – 1984 for TOM11-CF. This covers a period of rapid increase in macrozooplankton biomass in the Northern Benguela and a concurrent decrease in jellyfish biomass (Fig. 5.5). Figures and Tables in this chapter are calculated for the masked BCS region shown in Figure 5.3, for the Northern and Southern Benguela, as this is the region where the fish PP is applied. PFT biomass Northern and Southern Benguela is influenced by PFT biomass and physical conditions outside of this region as well as by conditions within the region. This influence can be seen in Figure 5.9 for jellyfish, which have a persistent background offshore biomass that may supplement the coastal population. Macrozooplankton biomass is concentrated closer to the coast than jellyfish biomass, particularly in the north of the Northern Benguela (Fig. 5.9). Over the period shown, macrozooplankton biomass moves southwards beginning from north of the Northern Benguela region. Within the Northern Benguela the macrozooplankton biomass increases substantially (due to fish PP), and this elevated biomass moves southwards across the Northern Benguela (Fig. 5.9). When assessing the results from introducing fishing pressure to the Benguela, it is important to keep in mind the potential influence from conditions external to the masked Benguela region, as shown in Figure 5.9.

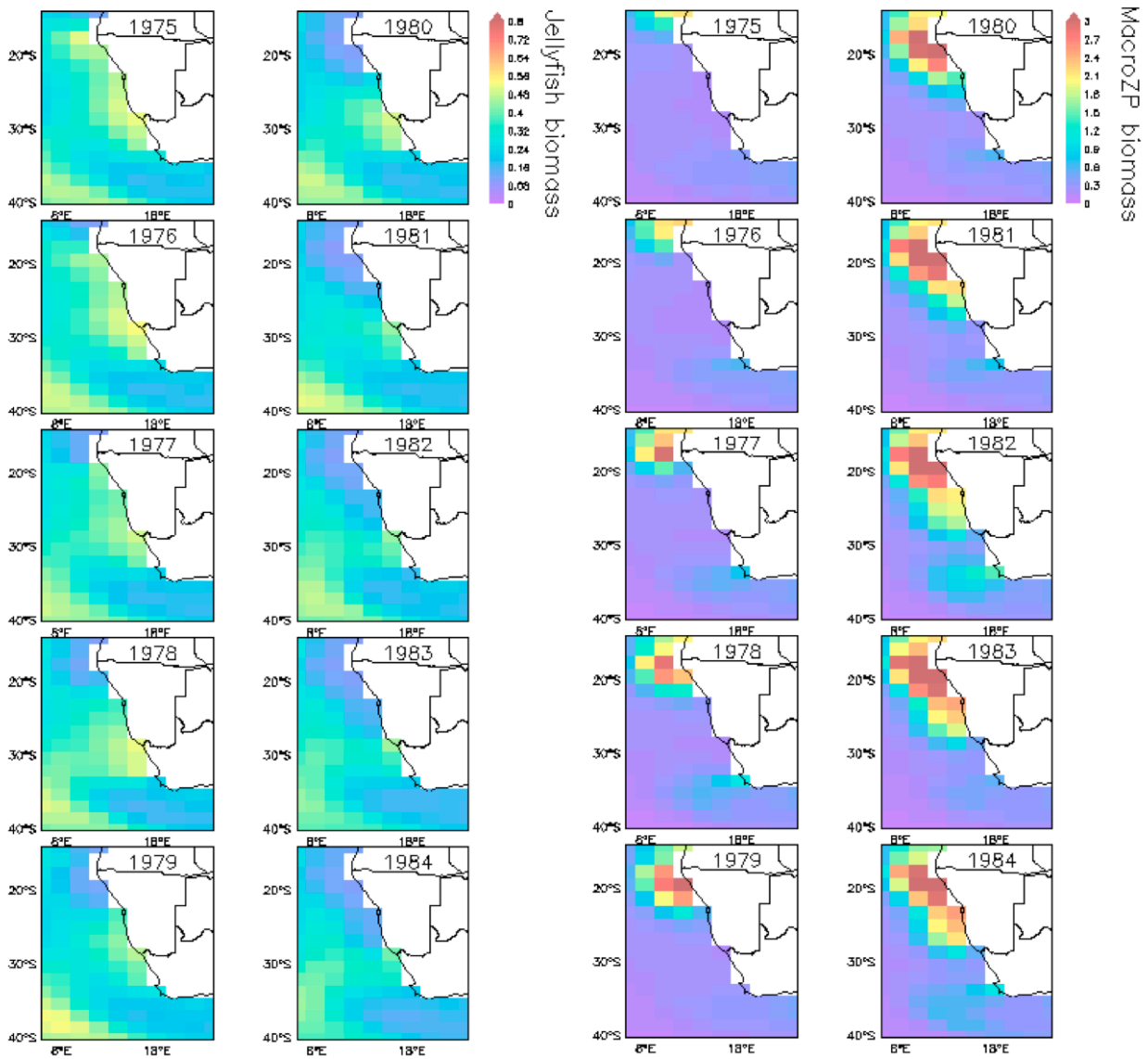


**Figure 5.9** Annual average maps of (left) jellyfish and (right) macrozooplankton biomass ( $\mu\text{mol C L}^{-1}$ ) for TOM11-CF from 1975 – 1984, covering a period of rapid increase in macrozooplankton biomass in the Northern Benguela. Note that the zooplankton are mapped to different scales.

## 5.4 Discussion

The addition of fish PP to simulate historical overfishing in the Northern Benguela does not cause an increase in jellyfish biomass in PlankTOM11, but instead it causes a decline in jellyfish from 1980 to 2000. Without simulating historical overfishing (TOM11-CN) in the Northern Benguela, the biomass of jellyfish shows a slight increase during the 1990's, but no long-term trend.

In PlankTOM11 in the Northern Benguela macrozooplankton outcompete jellyfish when fish PP is reduced, causing the decline in jellyfish biomass. The central hypothesis behind the apparent observed increase in jellyfish biomass in the Northern Benguela is that reduced fish biomass releases predation pressure on macrozooplankton allowing them to bloom, which in turn causes jellyfish to bloom due to an increased availability of food (Roux et al., 2013). There are several possible reasons for the opposing results presented here to the ECOPATH with ECOSIM modelling results (discussed in Section 5.1.5) which support the hypothesis (Roux and Shannon, 2004, Roux et al., 2013, Shannon et al., 2009). Firstly, in PlankTOM11, macrozooplankton have a built-in coastal advantage which enhances recruitment in coastal areas. Jellyfish in PlankTOM11 do not have this coastal advantage. The consequences of this may be that when macrozooplankton gain an advantage over jellyfish in a coastal environment (here reduced predation in the BCS) they can rapidly proliferate and overtake the ecosystem. Future work could introduce a coastal advantage to jellyfish in PlankTOM11, to simulate enhanced recruitment of jellyfish in coastal areas due to their meroplanktonic life cycle (see Chapter 1). Secondly, jellyfish experience no explicit predation pressure from fish in PlankTOM11. There is currently no evidence of sardines and/or anchovies preying on jellyfish in the BCS. However, research into this area is expanding, and recent studies have shown fish predation on jellyfish where it was previously assumed to not occur (Lamb et al., 2017). Fish predation on the adult stage of the jellyfish life cycle is highly unlikely due to the substantial size difference between the fish and jellyfish and the feeding strategies of sardines and anchovies. However, predation could occur on the planula larvae and ephyrae stages of the jellyfish life cycle. If this were the case in the BCS then it would have implications on the jellyfish biomass (see Chapter 3). Overfishing resulting in a release of predation pressure on jellyfish has been shown to be a contributing factor in

increasing jellyfish biomass in other regions (i.e. the Black Sea; Daskalov et al., 2007, Purcell and Arai, 2001); this may be a missing part of the story in the BCS. Future work could test the inclusion of varying levels of fish PP on jellyfish within PlankTOM11. Thirdly, mesozooplankton and protozooplankton experience no explicit predation pressure from fish in PlankTOM11. This lack of simulated predation by fish is because within PlankTOM11 all of the biomass of meso and protozooplankton is consumed by explicitly simulated PFTs. A release on the mortality of protozooplankton and mesozooplankton would also be ideal, but this requires additional work on the model, as there is currently no calculation of mortality due to proxy predator biomass for these two PFTs.

In PlankTOM11 in the Southern Benguela fish PP has a substantially smaller effect on macrozooplankton and jellyfish biomass than in the Northern Benguela, with no long-term trend in biomass. Fish PP has a greater influence on macrozooplankton than climate variability, but this influence does not propagate far into the ecosystem; mesozooplankton are also more influenced by fish PP but jellyfish, protozooplankton and chlorophyll are more influenced by climate variability. Climate variability has a greater influence on jellyfish than fish PP, except in the 2000's where fish PP peaks. The low fish PP in the Southern Benguela during the 1970's is a similar level to the low fish PP in the Northern Benguela after 1980 (Fig. 5.3). In both regions this increases macrozooplankton biomass and decreases jellyfish biomass. However, the influence of similar fish PP is substantially greater in the Northern Benguela than in the Southern Benguela. This result is consistent with observations of the Southern Benguela where changes to jellyfish biomass has not been reported (Roux et al., 2013).

In PlankTOM11 in the Northern Benguela jellyfish are negatively correlated to SST, and positively correlated to upwelling. This supports the findings in Fearon et al. (1992) and Shannon et al. (1986) which suggest that negative correlation between jellyfish and climate oscillations is occurring in the BCS upwelling. Negative correlation between jellyfish and climate oscillations has been demonstrated for the PDO in the Northern Californian Current (Suchman et al., 2012). Negative correlation between temperate marine species and SST is counter to general growth and population trends, which are usually positively correlated to SST. The negative correlation likely occurs in upwelling regions like the Northern Benguela as the cold



upwelled waters bring nutrients to the surface stimulating enhanced phytoplankton growth which cascades up through the ecosystem (Suchman et al., 2012).

A key result is the impact of simulating climate variability and fish PP together, rather than individually. In the Northern Benguela, the influence on the ecosystem of TOM11-CF was greater than the influence of TOM11-CN and TOM11-NF together (Table 5.3). In the Southern Benguela the influence on the ecosystem of TOM11-CF was less (except for macrozooplankton) than the influence of TOM11-CN and TOM11-NF together (Table 5.4). PlankTOM11 shows regional differences despite the relatively low resolution. The full impact of overfishing on marine ecosystems cannot be understood without its interactions with climate variability. In the Northern Benguela climate and fisheries act synergistically to influence the ecosystem. This influence is greater than would be expected from the sum of the individual simulations of climate and fisheries. In the Southern Benguela climate and fisheries act in opposition to influence the ecosystem, reducing the overall effect. The Northern Benguela experiences stronger upwelling and is more affected by the Benguela Niño than the Southern Benguela (Shannon et al., 1986, Arntz et al., 2006). This difference affects the way each region interacts with the climate, and also likely with fisheries perturbations. Marine ecosystems face pressure from multiple factors at the same time including climate change, fisheries, pollution and oxygen depletion (Richardson et al., 2009, Purcell, 2012). Improving understanding of how these various factors interact and potentially increase or decrease the influence of one another is vital in understanding how the marine environment will behave in the future with the pressure from many of these factors increasing.

## **5.5 Conclusion**

Increased food availability is often named as the key mechanism driving an increase in jellyfish biomass following overfishing of planktivorous fish species (Bakun and Weeks, 2006, Lynam et al., 2006, Pauly et al., 2009, Robinson et al., 2014). Only including this mechanism in PlankTOM11 has resulted in a decrease in jellyfish biomass following overfishing of planktivorous fish species. These results have implications for the hypothesised mechanisms linking over fishing to increases in jellyfish biomass. Without some release in predation pressure on jellyfish, other large

zooplankton (which do experience a release in predation pressure) have an advantage and may outcompete jellyfish. Indeed, the behaviour of macrozooplankton in the Northern Benguela looks similar to that expected for jellyfish. Further work on the jellyfish PFT is required to investigate these results, particularly introducing a coastal advantage and testing the inclusion of fish predation on jellyfish.

## References

- ARAI, M. N. 2005. Predation on pelagic coelenterates: a review. *Journal of the Marine Biological Association of the United Kingdom*, 85, 523-536.
- ARNTZ, W. E., GALLARDO, V. A., GUTIÉRREZ, D., ISLA, E., LEVIN, L. A., MENDO, J., NEIRA, C., ROWE, G. T., TARAZONA, J. & WOLFF, M. 2006. El Niño and similar perturbation effects on the benthos of the Humboldt, California, and Benguela Current upwelling ecosystems. *Advances in geosciences*, 6, 243-265.
- BAKUN, A., FIELD, D. B., REDONDO-RODRIGUEZ, A. & WEEKS, S. J. 2010. Greenhouse gas, upwelling-favorable winds, and the future of coastal ocean upwelling ecosystems. *Global Change Biology*, 16, 1213-1228.
- BAKUN, A. & WEEKS, S. J. 2006. Adverse feedback sequences in exploited marine systems: are deliberate interruptive actions warranted? *Fish and Fisheries*, 7, 316-333.
- BOYER, D. & HAMPTON, I. 2001. An overview of the living marine resources of Namibia. *South African Journal of Marine Science*, 23, 5-35.
- BRIERLEY, A. S., AXELSEN, B. E., BUECHER, E., SPARKS, C. A., BOYER, H. & GIBBONS, M. J. 2001. Acoustic observations of jellyfish in the Namibian Benguela. *Marine Ecology Progress Series*, 210, 55-66.
- BROWN, P., PAINTING, S. & COCHRANE, K. 1991. Estimates of phytoplankton and bacterial biomass and production in the northern and southern Benguela ecosystems. *South African Journal of Marine Science*, 11, 537-564.
- BUECHER, E. & GIBBONS, M. J. 2000. Interannual variation in the composition of the assemblages of medusae and ctenophores in St. Helena Bay, Southern Benguela Ecosystem. *Scientia Marina*, 64, 123-134.
- BUITENHUIS, E. T., HASHIOKA, T. & LE QUERE, C. 2013. Combined constraints on global ocean primary production using observations and models. *Global Biogeochemical Cycles*, 27, 847-858.
- BUTTERWORTH, D. 1983. Assessment and management of pelagic stocks in the southern Benguela region [South Africa, Namibia]. *FAO Fisheries Report (FAO). no. 291*.
- COETZEE, J. C., VAN DER LINGEN, C. D., HUTCHINGS, L. & FAIRWEATHER, T. P. 2008. Has the fishery contributed to a major shift in the distribution of

- South African sardine? *ICES Journal of Marine Science: Journal du Conseil*, 65, 1676-1688.
- CRAWFORD, R. J. 2007. Food, fishing and seabirds in the Benguela upwelling system. *Journal of Ornithology*, 148, 253-260.
- CURY, P. & SHANNON, L. 2004. Regime shifts in upwelling ecosystems: observed changes and possible mechanisms in the northern and southern Benguela. *Progress in Oceanography*, 60, 223-243.
- DASKALOV, G. M., GRISHIN, A. N., RODIONOV, S. & MIHNEVA, V. 2007. Trophic cascades triggered by overfishing reveal possible mechanisms of ecosystem regime shifts. *Proceedings of the National Academy of Sciences*, 104, 10518-10523.
- FAO 2017. Fishery and Aquaculture Statistics. Global capture production 1950-2015 (FishstatJ). Rome: FAO Fisheries and Aquaculture Department [online].
- FEARON, J., BOYD, A. & SCHÜLEIN, F. 1992. Views on the biomass and distribution of *Chrysaora hysoscella* (Linné, 1766) and *Aequorea aequorea* (Forskål, 1775) off Namibia, 1982-1989. *Sci. mar*, 56, 75-85.
- FLYNN, B. A., RICHARDSON, A. J., BRIERLEY, A. S., BOYER, D. C., AXELSEN, B. E., SCOTT, L., MOROFF, N. E., KAINGE, P. I., TJIZOO, B. M. & GIBBONS, M. J. 2012. Temporal and spatial patterns in the abundance of jellyfish in the northern Benguela upwelling ecosystem and their link to thwarted pelagic fishery recovery. *African Journal of Marine Science*, 34, 131-146.
- GENT, P. R., YEAGER, S. G., NEALE, R. B., LEVIS, S. & BAILEY, D. A. 2010. Improvements in a half degree atmosphere/land version of the CCSM. *Climate Dynamics*, 34, 819-833.
- HEYMANS, J. J. & BAIRD, D. 2000. A carbon flow model and network analysis of the northern Benguela upwelling system, Namibia. *Ecological Modelling*, 126, 9-32.
- HUTCHINGS, L., PILLAR, S. & VERHEYE, H. 1991. Estimates of standing stock, production and consumption of meso- and macrozooplankton in the Benguela ecosystem. *South African Journal of Marine Science*, 11, 499-512.
- HUTCHINGS, L., VAN DER LINGEN, C., SHANNON, L., CRAWFORD, R., VERHEYE, H., BARTHOLOMAE, C., VAN DER PLAS, A., LOUW, D., KREINER, A. &

- OSTROWSKI, M. 2009. The Benguela Current: An ecosystem of four components. *Progress in Oceanography*, 83, 15-32.
- HUTCHINGS, L., VERHEYE, H. M., HUGGETT, J. A., DEMARCO, H., CLOETE, R., BARLOW, R. G., LOUW, D. & DA SILVA, A. 2006. Variability of plankton with reference to fish variability in the Benguela current large marine ecosystem—An overview. *Large Marine Ecosystems*, 14, 91-124.
- JENSEN, O. P., BRANCH, T. A. & HILBORN, R. 2012. Marine fisheries as ecological experiments. *Theoretical Ecology*, 5, 3-22.
- LAMB, P. D., HUNTER, E., PINNEGAR, J. K., CREER, S., DAVIES, R. G. & TAYLOR, M. I. 2017. Jellyfish on the menu: mtDNA assay reveals scyphozoan predation in the Irish Sea. *Royal Society Open Science*, 4.
- LE QUÉRÉ, C., BUITENHUIS, E. T., MORIARTY, R., ALVAIN, S., AUMONT, O., BOPP, L., CHOLLET, S., ENRIGHT, C., FRANKLIN, D. J., GEIDER, R. J., HARRISON, S. P., HIRST, A., LARSEN, S., LEGENDRE, L., PLATT, T., PRENTICE, I. C., RIVKIN, R. B., SATHYENDRANATH, S., STEPHENS, N., VOGT, M., SAILLEY, S. & VALLINA, S. M. 2016. Role of zooplankton dynamics for Southern Ocean phytoplankton biomass and global biogeochemical cycles. *Biogeosciences Discuss.*, 12, 11935-11985.
- LYNAM, C. P., GIBBONS, M. J., AXELSEN, B. E., SPARKS, C. A., COETZEE, J., HEYWOOD, B. G. & BRIERLEY, A. S. 2006. Jellyfish overtake fish in a heavily fished ecosystem. *Current biology*, 16, R492-R493.
- MILLS, C. E. 2001. Jellyfish blooms: are populations increasing globally in response to changing ocean conditions? *Hydrobiologia*, 451, 55-68.
- PAULY, D., GRAHAM, W., LIBRALATO, S., MORISSETTE, L. & PALOMARES, M. L. D. 2009. Jellyfish in ecosystems, online databases, and ecosystem models. *Hydrobiologia*, 616, 67-85.
- PAULY, D. & ZELLER, D. The best catch data that can possibly be? Rejoinder to Ye et al. "FAO's statistic data and sustainability of fisheries and aquaculture". *Marine Policy*.
- PILLAR, S. & WILKINSON, I. 1995. The diet of Cape hake *Merluccius capensis* on the south coast of South Africa. *South African Journal of Marine Science*, 15, 225-239.

- PURCELL, J. E. 2012. Jellyfish and ctenophore blooms coincide with human proliferations and environmental perturbations. *Annual Review of Marine Science*, 4, 209-235.
- PURCELL, J. E. & ARAI, M. N. 2001. Interactions of pelagic cnidarians and ctenophores with fish: a review. *Hydrobiologia*, 451, 27-44.
- PURCELL, J. E. & STURDEVANT, M. V. 2001. Prey selection and dietary overlap among zooplanktivorous jellyfish and juvenile fishes in Prince William Sound, Alaska. *Marine Ecology Progress Series*, 210, 67-83.
- RICHARDSON, A. J., BAKUN, A., HAYS, G. C. & GIBBONS, M. J. 2009. The jellyfish joyride: causes, consequences and management responses to a more gelatinous future. *Trends in Ecology & Evolution*, 24, 312-322.
- ROBINSON, K. L., RUZICKA, J. J., DECKER, M. B., BRODEUR, R. D., HERNANDEZ, F. J., QUIÑONES, J., ACHA, E. M., UYE, S.-I., MIANZAN, H. & GRAHAM, W. M. 2014. Jellyfish, forage fish, and the world's major fisheries. *Oceanography*, 27, 104-115.
- ROUX, J. & SHANNON, L. 2004. Ecosystem approach to fisheries management in the northern Benguela: the Namibian experience. *African Journal of Marine Science*, 26, 79-93.
- ROUX, J.-P., VAN DER LINGEN, C. D., GIBBONS, M. J., MOROFF, N. E., SHANNON, L. J., SMITH, A. D. & CURY, P. M. 2013. Jellyfication of marine ecosystems as a likely consequence of overfishing small pelagic fishes: lessons from the Benguela. *Bulletin of Marine Science*, 89, 249-284.
- SHANNON, L., BOYD, A., BRUNDRIT, G. & TAUNTON-CLARK, J. 1986. On the existence of an El Niño-type phenomenon in the Benguela system. *Journal of marine Research*, 44, 495-520.
- SHANNON, L., CRAWFORD, R., POLLOCK, D., HUTCHINGS, L., BOYD, A., TAUNTON-CLARK, J., BADENHORST, A., MELVILLE-SMITH, R., AUGUSTYN, C. & COCHRANE, K. 1992. The 1980s—a decade of change in the Benguela ecosystem. *South African Journal of Marine Science*, 12, 271-296.
- SHANNON, L. J., COLL, M., NEIRA, S., CURY, P. & ROUX, J.-P. 2009. Impacts of fishing and climate change explored using trophic models.
- SHANNON, V., HEMPEL, G., MOLONEY, C., WOODS, J. D. & MALANOTTE-RIZZOLI, P. 2006. *Benguela: predicting a large marine ecosystem*, Elsevier.

- SMALL, R. J., CURCHITSER, E., HEDSTROM, K., KAUFFMAN, B. & LARGE, W. G. 2015. The Benguela upwelling system: Quantifying the sensitivity to resolution and coastal wind representation in a global climate model. *Journal of Climate*, 28, 9409-9432.
- SUCHMAN, C. L., BRODEUR, R. D., DALY, E. A. & EMMETT, R. L. 2012. Large medusae in surface waters of the Northern California Current: variability in relation to environmental conditions. *Hydrobiologia*, 690, 113-125.
- SULLIVAN, L. J. & KREMER, P. 2011. Gelatinous Zooplankton and Their Trophic Roles. *Treatise on Estuarine and Coastal Science*. Waltham: Academic Press.
- UTNE-PALM, A. C., SALVANES, A. G. V., CURRIE, B., KAARTVEDT, S., NILSSON, G. E., BRAITHWAITE, V. A., STECYK, J. A. W., HUNDT, M., VAN DER BANK, M., FLYNN, B., SANDVIK, G. K., KLEVJER, T. A., SWEETMAN, A. K., BRÜCHERT, V., PITTMAN, K., PEARD, K. R., LUNDE, I. G., STRANDABØ, R. A. U. & GIBBONS, M. J. 2010. Trophic Structure and Community Stability in an Overfished Ecosystem. *Science*, 329, 333-336.
- VAN DER LINGEN, C. D. 1994. Effect of Particle-Size and Concentration on the Feeding-Behavior of Adult Pilchard *Sardinops-Sagax*. *Marine Ecology Progress Series*, 109, 1-13.
- VENTER, G. 1988. Occurrence of jellyfish on the west coast off south west Africa/Namibia. *Long-term data series relating to southern Africa's renewable natural resources, IAW Macdonald, and RJM Crawford, eds. S. African Nat. Sci. Progs*, 157, 56-61.
- WALSH, J. J. 1981. A carbon budget for overfishing off Peru. *Nature*, 290, 300-304.





# CHAPTER 6. CONCLUSION



## 6.1 Introduction

Gelatinous zooplankton (GZ) play a key role in marine ecosystems and may be increasing due to climate change and other anthropogenic pressures. The need for GZ inclusion in global biogeochemical models has been noted several times in the literature (Burd et al., 2016, Fuentes et al., 2018, Lebrato et al., 2013). The focus of this PhD thesis was to investigate the role of GZ in the marine ecosystem through its inclusion in a global biogeochemical model, in particular the influence of GZ on other zooplankton and how this may influence the carbon cycle. Another goal was to assess the relative and cumulative influence of overfishing and climate change on GZ populations. It was necessary, due to data limitations, to focus the development of a GZ PFT to one of the three phylum types: Cnidaria medusa, also termed jellyfish. The largest portion of work for this thesis was undoubtedly the development of PlankTOM11 (Chapter 3) which included the incorporation of the jellyfish PFT by characterising their physiological and ecological process rates and determining their trophic level. The model development also included changing the growth rate calculation for all the PFTs, subsequent tuning and learning to navigate such a complex ocean model. Within this thesis, five key questions have been addressed;

- 1) Can GZ be represented in a global biogeochemical model?
- 2) What is the global biomass of GZ and how does it compare to other zooplankton types?
- 3) How do jellyfish affect the plankton ecosystem structure?
- 4) What is the role of jellyfish in global carbon export?
- 5) What is the relative effect on jellyfish biomass of overfishing and climate variability?

## 6.2 Key Questions and Findings

The five key questions addressed throughout this thesis are summarised below.

- 1) Can GZ be represented in a global biogeochemical model?

Yes, Cnidaria (jellyfish) have sufficient physiological data and are cohesive enough within the group to be defined as a PFT and are successfully incorporated into PlankTOM11 in Chapter 3. This is the first inclusion of jellyfish (or any GZ) in a global ocean biogeochemical model. Mortality is found to be a key tuning factor for

the jellyfish PFT and is also the characteristic with the least data available and therefore the largest uncertainty (Chapter 3). Representing GZ as one type in a global biogeochemical model is not ideal. Tunicata fill a different ecological niche and trophic level to Ctenophora and Cnidaria, so do not fulfil the requirements for a PFT as outlined in Le Quéré et al. (2005). Ctenophora and Cnidaria fill a similar ecological niche, but the dominance of physiological data on Cnidaria would mean that if the two were combined, the PFT would greatly represent Cnidaria over Ctenophora. Cnidaria also represent >90% of the global GZ biomass and so are arguably the most important of the three groups to understand (Lucas et al., 2014). This is addressed in Chapter's 1, 2 and 3.

2) What is the global biomass of GZ and how does it compare to other zooplankton types?

The global biomass of GZ from observations (MAREDAT) is range of 0.14 to 1.33 PgC, and for jellyfish (Cnidaria) is 0.46 to 3.11 PgC (Chapter 2; following the methods from Buitenhuis et al., 2013). GZ biomass is similar to and possibly lower than the biomass range for macrozooplankton and jellyfish biomass is almost as high as the microzooplankton and higher than meso- and macrozooplankton. Key caveats to these values include that (almost) all of the biomass data for GZ is from the Northern Hemisphere, there is a potential under reporting of zero biomass values and for jellyfish there is a greater variance between the results from the different averaging methods, than between the MAREDAT and JeDI databases. The global biomass of jellyfish in PlankTOM11 is 0.13 PgC (Chapter 3) towards the lower end of observational analysis. PlankTOM11 overall underestimates the biomass and rates of most components, likely contributing to a possible underestimation of jellyfish biomass. However, within the context of lower biomass and rates, PlankTOM11 results are consistent overall with observations. The zooplankton community in PlankTOM11 was highly sensitive to the jellyfish mortality rate, with low jellyfish mortality allowing jellyfish biomass to increase and dominate the zooplankton. This sensitivity of the zooplankton community to the mortality of jellyfish could help explain why jellyfish may be increasing globally, as pressures on their mortality in early-life stages decrease (reduced predation due to overfishing and increased habitat for planula settling), allowing them to outcompete other zooplankton.

### 3) How do jellyfish affect the plankton ecosystem structure?

Jellyfish exert substantial control on the plankton community structure (Chapter 3). This control is both direct, through grazing on (mostly) other zooplankton, and indirect, through trophic cascades. Jellyfish biomass and macrozooplankton (crustaceans) biomass have a negative correlation, i.e. when one is high, the other is low. If one gains an advantage (environmental or prey driven) then it rapidly outcompetes the other, despite occupying different trophic levels. This negative correlation can be seen firstly in the jellyfish mortality experiments in Chapter 3, where macrozooplankton respond the most strongly of the PFTs to changes to jellyfish mortality, secondly throughout the jellyfish characteristic tests in Chapter 4, and thirdly in the fishing experiments in Chapter 5 where macrozooplankton have the advantage of reduced predation pressure and they rapidly dominate the region reducing jellyfish biomass. Jellyfish influence global chlorophyll concentration and spatial patterns, through trophic cascades, improving the north/south chlorophyll ratio in PlankTOM11.

### 4) What is the role of jellyfish in global carbon export?

Chapter 4 specifically addresses the role of jellyfish in carbon export. In PlankTOM11 jellyfish influence carbon export mostly during their life through trophic cascades (see Question 3). Carbon export is higher with jellyfish included in the model than with 'just another' top zooplankton, suggesting that the characteristics of jellyfish act to increase carbon export. The influence of jellyfish mortality on carbon export is most likely underrepresented in PlankTOM11, as the mortality simulation gives almost identical results to the respiration simulation. Observations of jelly-falls suggest that jellyfish mortality has a substantial influence on carbon export in areas of jellyfish blooms, as the high biomass of blooms coupled with the large body size and rapid sinking transport a substantial amount of carbon to the seafloor (Lebrato et al., 2012, Lebrato et al., 2013). The size and sinking speed of large OC in PlankTOM11 is far less than the size and sinking speed of jellyfish carcasses in reality, thus the model is likely not reflecting the influence of jellyfish mortality on carbon export.

### 5) What is the relative effect on jellyfish biomass of overfishing and climate variability?

Chapter 5 specifically addresses how overfishing and climate variability affect jellyfish biomass using a case study of the Benguela Current System. Overfishing impacts

jellyfish biomass in the Northern Benguela but in the opposite way to that expected from hypotheses and circumstantial observations. In PlankTOM11 overfishing reduces jellyfish biomass due to macrozooplankton biomass increasing and outcompeting the jellyfish. In PlankTOM11 jellyfish are not predated by fish. This gives macrozooplankton an advantage over jellyfish and allows them to dominate the regional ecosystem. Introducing jellyfish predation by fish, cited as a hypothesis alongside competition for prey in other regions, will change these results and give insight into the relative importance of each in the relationship between jellyfish biomass and overfishing. In PlankTOM11 climate variability and overfishing act synergistically in the Northern Benguela, to such an extent that the effect of the two simulated together is greater than the effect of them individually simulated and added together. This is not the case in the Southern Benguela, which appears less sensitive to both changes in fishing and climate. Climate and fisheries ecosystem impacts, both individually and cumulatively, are regionally dependent.

### **6.3 Future Work**

This is the first representation of jellyfish in a global ocean biogeochemical model, as a result there are further refinements to the jellyfish PFT which could be made in the future. A key refinement could be adding a coastal advantage to the jellyfish PFT to represent enhanced recruitment in coastal regions. This will likely have interesting implications for the current relationship between macrozooplankton and jellyfish in PlankTOM11. A coastal advantage will also introduce an element of jellyfish life cycle strategy (enhanced recruitment and settlement of planulae larvae onto hard substrate) into the model, without the need to wait for more observational data on life cycles. PlankTOM11 currently demonstrates some increase of jellyfish biomass in coastal regions (Chapter 3) but is likely under estimating their biomass in these regions.

The representation of large OC in PlankTOM11 could be expanded to include multiple sizes so that carbon export associated with jellyfish processes (as well as other plankton) are better represented, especially in death. There is growing evidence that jelly-falls can contribute significant volumes of carbon to the sea floor (Lebrato et al., 2012, Lebrato et al., 2013). Jelly-falls are currently underrepresented in PlankTOM11 and may have substantial implications for the role of jellyfish in carbon export. Further

observations of the fate of carbon underneath active jellyfish blooms, during bloom formation and subsequent jelly-falls, would be very useful in furthering our understanding of the mechanisms linking jellyfish to carbon export. Observations of carbon export (through analysis of marine snow) during bloom formation could provide further information on potential changes to the sources of the carbon being exported, i.e. changing from mesozooplankton faecal matter to jellyfish mucus. Such observations would help to both validate and further development PlankTOM11.

A key refinement for understanding the influence of overfishing on jellyfish biomass would be to test the predation pressure of historical fishing directly on jellyfish. The relative importance of the two mechanisms (jellyfish and fish competition for prey, and fish predation on jellyfish) in driving jellyfish biomass could then be investigated, and the hypothesis from Chapter 5 could be readdressed. The inclusion of fish predation on the other zooplankton, especially mesozooplankton, would also be ideal in order to further investigate the importance on ecosystem responses of food webs.

The introduction of a higher grid resolution in PlankTOM11 will allow the representation of small-scale physical mixing such as eddies and frontal regions, which have been shown to influence bloom formation. For example many jellyfish blooms occur around fronts, upwelling regions, tidal and estuarine regions and shelf-breaks where currents can aggregate and retain organisms (Graham et al., 2001). Higher grid resolution will likely improve the representation of spatial and temporal patchiness of jellyfish biomass, along with improved representation of patchiness for the other PFTs.

Data on the physiological rates of jellyfish required for PFT biogeochemical modelling are currently sparse. More data are needed to improve the parameterisation of jellyfish physiological rates. This is especially apparent for jellyfish mortality rates across all life stages. Further experiments on growth rates at a wider range of temperatures and for a wider range of jellyfish species would also help to better constrain the model growth parameter. Observational data on the biomass and abundance of jellyfish are sparse for the majority of the ocean. Increased observations would be beneficial to the further improvement of jellyfish in PlankTOM11, especially of open ocean regions and the Southern Hemisphere where data coverage is particularly poor. The inclusion of jellyfish in general ecosystem surveys and fisheries surveys is increasing and will

hopefully continue to increase. In the future this will provide valuable quantitative data that can be used for model validation, among many other uses.

With some of these further refinements to the jellyfish PFT, long-term simulations of PlankTOM11 can be undertaken to investigate the role of climate change and climate indices on jellyfish both historically and into the future under various climate change projections. PlankTOM11 can now be used to investigate many questions beyond those we had time to address in this thesis project.

#### **6.4 Closing Statement**

The development and use of the PlankTOM11 model is a successful first step in understanding the role of jellyfish in global ocean biogeochemical cycles. Models can always be improved and can never perfectly and fully replicate the huge complexities of the ocean. The quote by the statistician George E. P. Box that “all models are wrong, but some are useful” is valuable in reminding us of the worth of models such as PlankTOM11 in understanding jellyfish.

Jellyfish blooms are responsible for economic losses to a wide variety of coastal industries and have a substantial role within ecosystems, but we lack the observations to understand the role of climate change and overfishing on jellyfish populations. Now is a good time to look closely at the effects of climate change and overfishing on jellyfish, as global biogeochemical models have developed to a point where the inclusion of jellyfish is possible, as demonstrated in this thesis.

No living organism is without a role in the natural world. Jellyfish (and GZ in general) are a prime example of a group of organisms largely overlooked by the scientific community and wider society because they were deemed ‘dead-end’ and ‘nuisance’ organisms, without an obvious monetary gain. Growing evidence is dismantling the idea of jellyfish (and all GZ) as trophic dead-ends (Lamb et al., 2017). Jellyfish make up a substantial proportion of the global marine ecosystem, likely play an important role in the biological carbon pump, are fascinating ancient organisms and much about them remains to be discovered.



Climate change, along with other human pressures, represent a huge challenge to marine ecosystems. To understand the impacts of humankind and perhaps limit or even reverse these impacts, we must understand the ecosystems we are trying to protect. Scientific evidence is needed to support good and proportionate action. Only through improving scientific evidence and understanding can we help to resolve the climate crisis. There is still much work to be done, particularly with improving public and political understanding of the oceans and how they will be impacted by climate change and how this in turn will affect all of us.

*“For most of history, man has had to fight nature to survive; in this century he is beginning to realise that, in order to survive, he must protect it.”*

*Jaques Cousteau*

## References

- BUITENHUIS, E. T., VOGT, M., MORIARTY, R., BEDNARSEK, N., DONEY, S. C., LEBLANC, K., LE QUERE, C., LUO, Y. W., O'BRIEN, C., O'BRIEN, T., PELOQUIN, J., SCHIEBEL, R. & SWAN, C. 2013. MAREDAT: towards a world atlas of MARine Ecosystem DATa. *Earth System Science Data*, 5, 227-239.
- BURD, A., BUCHAN, A., CHURCH, M. J., LANDRY, M. R., MCDONNELL, A. M., PASSOW, U., STEINBERG, D. K. & BENWAY, H. M. 2016. Towards a transformative understanding of the ocean's biological pump: Priorities for future research-Report on the NSF Biology of the Biological Pump Workshop. Ocean Carbon & Biogeochemistry (OCB) Program.
- FUENTES, V. L., PURCELL, J. E., CONDON, R. H., LOMBARD, F. & LUCAS, C. H. 2018. Jellyfish blooms: advances and challenges. *Marine Ecology Progress Series*, 591, 3-5.
- GRAHAM, W., PAGÈS, F. & HAMNER, W. 2001. A physical context for gelatinous zooplankton aggregations: a review. *Hydrobiologia*, 451, 199-212.
- LAMB, P. D., HUNTER, E., PINNEGAR, J. K., CREER, S., DAVIES, R. G. & TAYLOR, M. I. 2017. Jellyfish on the menu: mtDNA assay reveals scyphozoan predation in the Irish Sea. *Royal Society Open Science*, 4.
- LE QUÉRÉ, C., HARRISON, S. P., COLIN PRENTICE, I., BUITENHUIS, E. T., AUMONT, O., BOPP, L., CLAUSTRE, H., COTRIM DA CUNHA, L., GEIDER, R., GIRAUD, X., KLAAS, C., KOHFELD, K. E., LEGENDRE, L., MANIZZA, M., PLATT, T., RIVKIN, R. B., SATHYENDRANATH, S., UITZ, J., WATSON, A. J. & WOLF-GLADROW, D. 2005. Ecosystem dynamics based on plankton functional types for global ocean biogeochemistry models. *Global Change Biology*, 11, 2016-2040.
- LEBRATO, M., MENDES, P. D. J., STEINBERG, D. K., CARTES, J. E., JONES, B. M., BIRSA, L. M., BENAVIDES, R. & OSCHLIES, A. 2013. Jelly biomass sinking speed reveals a fast carbon export mechanism. *Limnology and Oceanography*, 58, 1113-1122.
- LEBRATO, M., PITT, K. A., SWEETMAN, A. K., JONES, D. O., CARTES, J. E., OSCHLIES, A., CONDON, R. H., MOLINERO, J. C., ADLER, L. &

- GAILLARD, C. 2012. Jelly-falls historic and recent observations: a review to drive future research directions. *Hydrobiologia*, 690, 227-245.
- LUCAS, C. H., JONES, D. O. B., HOLLYHEAD, C. J., CONDON, R. H., DUARTE, C. M., GRAHAM, W. M., ROBINSON, K. L., PITT, K. A., SCHILDHAUER, M. & REGETZ, J. 2014. Gelatinous zooplankton biomass in the global oceans: geographic variation and environmental drivers. *Global Ecology and Biogeography*, 23, 701-714.



---

# APPENDICES



**Table A1.** Taxonomic information for gelatinous zooplankton from MAREDAT. The last filled column for each row is the taxonomic level given in MAREDAT. Provided in parenthesis are alternative or historic names for the same organism.

Phylum	Subphylum	Class	Subclass	Order	Suborder	Family	Genus	Species
Chordata	Tunicata	Appendicularia		Copelata		Fritillaridae	Fritillaria	<i>Fritillaria borealis</i>
Chordata	Tunicata	Appendicularia		Copelata		Fritillaridae	Fritillaria	<i>Fritillaria formica</i>
Chordata	Tunicata	Appendicularia		Copelata		Fritillaridae	Fritillaria	<i>Fritillaria haplostoma</i>
Chordata	Tunicata	Appendicularia		Copelata		Fritillaridae	Fritillaria	<i>Fritillaria megachile</i>
Chordata	Tunicata	Appendicularia		Copelata		Fritillaridae	Fritillaria	<i>Fritillaria pellucida</i>
Chordata	Tunicata	Appendicularia		Copelata		Fritillaridae	Fritillaria	
Chordata	Tunicata	Appendicularia		Copelata		Fritillaridae		
Chordata	Tunicata	Appendicularia		Copelata		Okiopleuridae	Okiopleura	<i>Okiopleura dioica</i>
Chordata	Tunicata	Appendicularia		Copelata		Okiopleuridae	Okiopleura	<i>Okiopleura labradoriensis</i>
Chordata	Tunicata	Appendicularia		Copelata		Okiopleuridae	Okiopleura	<i>Okiopleura longicauda</i>
Chordata	Tunicata	Appendicularia		Copelata		Okiopleuridae	Okiopleura	<i>Okiopleura parva</i>
Chordata	Tunicata	Appendicularia		Copelata		Okiopleuridae	Okiopleura	<i>Okiopleura vanhoeffeni</i>
Chordata	Tunicata	Appendicularia		Copelata		Okiopleuridae	Okiopleura	
Chordata	Tunicata	Appendicularia		Copelata				
Chordata	Tunicata	Ascidiacea						
Chordata	Tunicata	Thaliacea		Doliolida	Doliolidina	Doliolidae	Doliolides	<i>Dolioloides rarum</i>
Chordata	Tunicata	Thaliacea		Doliolida	Doliolidina	Doliolidae	Doliolum	

**Table A1.** Taxonomic information for gelatinous zooplankton from MAREDAT. The last filled column for each row is the taxonomic level given in MAREDAT. Provided in parenthesis are alternative or historic names for the same organism.

Phylum	Subphylum	Class	Subclass	Order	Suborder	Family	Genus	Species
Chordata	Tunicata	Thaliacea		Doliolida	Doliolidina	Doliolidae		
Chordata	Tunicata	Thaliacea		Doliolida (Cyclomyaria)				
Chordata	Tunicata	Thaliacea		Pyrosomatida		Pyrosomatidae (Pyrosomidae, Pyrosomida)	Pyrosoma	
Chordata	Tunicata	Thaliacea		Pyrosomatida		Pyrosomatidae (Pyrosomidae, Pyrosomida)		
Chordata	Tunicata	Thaliacea		Salpida		Salpidae	Ihlea	<i>Ihlea punctata</i>
Chordata	Tunicata	Thaliacea		Salpida		Salpidae	Ihlea	
Chordata	Tunicata	Thaliacea		Salpida		Salpidae	Salpa	<i>Salpa fusiformis</i>
Chordata	Tunicata	Thaliacea		Salpida		Salpidae	Salpa	<i>Salpa maxima</i>
Chordata	Tunicata	Thaliacea		Salpida		Salpidae	Salpa	
Chordata	Tunicata	Thaliacea		Salpida		Salpidae	Thalia	<i>Thalia democratica</i>
Chordata	Tunicata	Thaliacea		Salpida		Salpidae	Thalia	
Chordata	Tunicata	Thaliacea		Salpida		Salpidae		
Chordata	Tunicata	Thaliacea		Salpida				
Chordata	Tunicata	Thaliacea			Hemimyaria			
Chordata	Tunicata	Thaliacea						
Chordata	Tunicata							



**Table A1.** Taxonomic information for gelatinous zooplankton from MAREDAT. The last filled column for each row is the taxonomic level given in MAREDAT. Provided in parenthesis are alternative or historic names for the same organism.

Phylum	Subphylum	Class	Subclass	Order	Suborder	Family	Genus	Species
Cnidaria		Anothzoa						
Cnidaria		Hydrozoa	Hydroida (Hydroidae, Hydroidolina)	Anthoathecata (Anthomedusae)	Capitata	Capitata incertae sedis	Plotocnide	<i>Plotocnide borealis</i>
Cnidaria		Hydrozoa	Hydroida (Hydroidae, Hydroidolina)	Anthoathecata (Anthomedusae)	Capitata	Capitata incertae sedis	Plotocnide	
Cnidaria		Hydrozoa	Hydroida (Hydroidae, Hydroidolina)	Anthoathecata (Anthomedusae)	Capitata	Corynidae	Polyorchis	<i>Polyorchis penicillatus</i>
Cnidaria		Hydrozoa	Hydroida (Hydroidae, Hydroidolina)	Anthoathecata (Anthomedusae)	Capitata	Corynidae	Polyorchis	
Cnidaria		Hydrozoa	Hydroida (Hydroidae, Hydroidolina)	Anthoathecata (Anthomedusae)	Capitata	Corynidae	Sarsia	<i>Sarsia princeps</i>
Cnidaria		Hydrozoa	Hydroida (Hydroidae, Hydroidolina)	Anthoathecata (Anthomedusae)	Capitata	Corynidae	Sarsia	<i>Sarsia tubulosa</i>
Cnidaria		Hydrozoa	Hydroida (Hydroidae, Hydroidolina)	Anthoathecata (Anthomedusae)	Capitata	Corynidae	Sarsia	
Cnidaria		Hydrozoa	Hydroida (Hydroidae, Hydroidolina)	Anthoathecata (Anthomedusae)	Capitata	Porpitidae	Porpita	
Cnidaria		Hydrozoa	Hydroida (Hydroidae, Hydroidolina)	Anthoathecata (Anthomedusae)	Capitata	Porpitidae	Veleva	
Cnidaria		Hydrozoa	Hydroida (Hydroidae, Hydroidolina)	Anthoathecata (Anthomedusae)	Filifera	Bougainvilliidae	Bougainvillia (Perigonimus)	<i>Bougainvillia multitentaculata</i>
Cnidaria		Hydrozoa	Hydroida (Hydroidae, Hydroidolina)	Anthoathecata (Anthomedusae)	Filifera	Bougainvilliidae	Bougainvillia (Perigonimus)	<i>Bougainvillia superciliaris</i>
Cnidaria		Hydrozoa	Hydroida (Hydroidae, Hydroidolina)	Anthoathecata (Anthomedusae)	Filifera	Bougainvilliidae	Bougainvillia (Perigonimus)	<i>Perigonimus multicirratu</i>
Cnidaria		Hydrozoa	Hydroida (Hydroidae, Hydroidolina)	Anthoathecata (Anthomedusae)	Filifera	Bougainvilliidae	Bougainvillia (Perigonimus)	

**Table A1.** Taxonomic information for gelatinous zooplankton from MAREDAT. The last filled column for each row is the taxonomic level given in MAREDAT. Provided in parenthesis are alternative or historic names for the same organism.

Phylum	Subphylum	Class	Subclass	Order	Suborder	Family	Genus	Species
Cnidaria		Hydrozoa	Hydroida (Hydroidae, Hydroidolina)	Anthoathecata (Anthomedusae)	Filifera	Bougainvilliidae		
Cnidaria		Hydrozoa	Hydroida (Hydroidae, Hydroidolina)	Anthoathecata (Anthomedusae)	Filifera	Pandeidae	Halitholus	<i>Halitholus yoldiaearcticae</i>
Cnidaria		Hydrozoa	Hydroida (Hydroidae, Hydroidolina)	Anthoathecata (Anthomedusae)	Filifera	Pandeidae	Leuckartiara	<i>Leuckartiara annexa</i>
Cnidaria		Hydrozoa	Hydroida (Hydroidae, Hydroidolina)	Anthoathecata (Anthomedusae)	Filifera	Pandeidae	Leuckartiara	<i>Leuckartiara nobilis</i>
Cnidaria		Hydrozoa	Hydroida (Hydroidae, Hydroidolina)	Anthoathecata (Anthomedusae)	Filifera	Pandeidae	Leuckartiara	<i>Leuckartiara octona</i>
Cnidaria		Hydrozoa	Hydroida (Hydroidae, Hydroidolina)	Anthoathecata (Anthomedusae)	Filifera	Pandeidae	Leuckartiara	
Cnidaria		Hydrozoa	Hydroida (Hydroidae, Hydroidolina)	Anthoathecata (Anthomedusae)	Filifera	Pandeidae	Neoturris	<i>Neoturris breviconis</i> ( <i>Perigonimus breviconis</i> )
Cnidaria		Hydrozoa	Hydroida (Hydroidae, Hydroidolina)	Anthoathecata (Anthomedusae)	Filifera	Pandeidae	Pandea	
Cnidaria		Hydrozoa	Hydroida (Hydroidae, Hydroidolina)	Anthoathecata (Anthomedusae)	Filifera	Pandeidae	Stomotoca	<i>Stomotoca atra</i>
Cnidaria		Hydrozoa	Hydroida (Hydroidae, Hydroidolina)	Anthoathecata (Anthomedusae)	Filifera	Pandeidae	Stomotoca	
Cnidaria		Hydrozoa	Hydroida (Hydroidae, Hydroidolina)	Anthoathecata (Anthomedusae)	Filifera	Proboscidactylidae	Proboscidactyla	<i>Proboscidactyla flavicirrata</i>
Cnidaria		Hydrozoa	Hydroida (Hydroidae, Hydroidolina)	Anthoathecata (Anthomedusae)	Filifera	Proboscidactylidae	Proboscidactyla	<i>Proboscidactyla ornata</i>
Cnidaria		Hydrozoa	Hydroida (Hydroidae, Hydroidolina)	Anthoathecata (Anthomedusae)	Filifera	Rathkeidae	Rathkea	<i>Rathkea jaschnowi</i>
Cnidaria		Hydrozoa	Hydroida (Hydroidae, Hydroidolina)	Anthoathecata (Anthomedusae)	Filifera	Rathkeidae	Rathkea	<i>Rathkea octopunctata</i>

**Table A1.** Taxonomic information for gelatinous zooplankton from MAREDAT. The last filled column for each row is the taxonomic level given in MAREDAT. Provided in parenthesis are alternative or historic names for the same organism.

Phylum	Subphylum	Class	Subclass	Order	Suborder	Family	Genus	Species
Cnidaria		Hydrozoa	Hydroida (Hydroidae, Hydroidolina)	Anthoathecata (Anthomedusae)	Filifera	Rathkeidae	Rathkea	
Cnidaria		Hydrozoa	Hydroida (Hydroidae, Hydroidolina)	Leptothecata		Campanulariidae	Clytia (Phialidium)	<i>Clytia gregaria</i> ( <i>Phialidium gregaria</i> )
Cnidaria		Hydrozoa	Hydroida (Hydroidae, Hydroidolina)	Leptothecata		Campanulariidae	Clytia (Phialidium)	<i>Clytia hemisphericum</i> ( <i>Phialidium hemisphericum</i> )
Cnidaria		Hydrozoa	Hydroida (Hydroidae, Hydroidolina)	Leptothecata		Campanulariidae	Clytia (Phialidium)	
Cnidaria		Hydrozoa	Hydroida (Hydroidae, Hydroidolina)	Leptothecata		Campanulariidae	Obelia	<i>Obelia geniculata</i>
Cnidaria		Hydrozoa	Hydroida (Hydroidae, Hydroidolina)	Leptothecata		Campanulariidae	Obelia	<i>Obelia longissima</i> ( <i>Obelia flabellate</i> )
Cnidaria		Hydrozoa	Hydroida (Hydroidae, Hydroidolina)	Leptothecata		Campanulariidae	Obelia	
Cnidaria		Hydrozoa	Hydroida (Hydroidae, Hydroidolina)	Leptothecata		Eirenidae	Eutonina	<i>Eutonina indicans</i>
Cnidaria		Hydrozoa	Hydroida (Hydroidae, Hydroidolina)	Leptothecata		Laodiceidae	Ptychogena	<i>Ptychogena lactea</i>
Cnidaria		Hydrozoa	Hydroida (Hydroidae, Hydroidolina)	Leptothecata		Laodiceidae	Staurophora	<i>Staurophora mertensii</i>
Cnidaria		Hydrozoa	Hydroida (Hydroidae, Hydroidolina)	Leptothecata		Laodiceidae	Staurophora	
Cnidaria		Hydrozoa	Hydroida (Hydroidae, Hydroidolina)	Leptothecata		Merlicertidae	Melicertum	<i>Melicertum octocostatum</i>
Cnidaria		Hydrozoa	Hydroida (Hydroidae, Hydroidolina)	Leptothecata		Mitrocomidae		

**Table A1.** Taxonomic information for gelatinous zooplankton from MAREDAT. The last filled column for each row is the taxonomic level given in MAREDAT. Provided in parenthesis are alternative or historic names for the same organism.

Phylum	Subphylum	Class	Subclass	Order	Suborder	Family	Genus	Species
Cnidaria		Hydrozoa	Hydroida (Hydroidae, Hydroidolina)	Leptothecata		Tiaropsidae	Tiaropsidium	
Cnidaria		Hydrozoa	Hydroida (Hydroidae, Hydroidolina)	Leptothecata		Tiaropsidae	Tiaropsis	<i>Tiaropsis multicirrata</i>
Cnidaria		Hydrozoa	Hydroida (Hydroidae, Hydroidolina)	Leptothecata		Tiaropsidae	Tiaropsis	
Cnidaria		Hydrozoa	Hydroida (Hydroidae, Hydroidolina)	Leptothecata				
Cnidaria		Hydrozoa	Hydroida (Hydroidae, Hydroidolina)	Siphonophorae	Calyconectae (Calycophorae)	Abylidae	Abylopsis	<i>Abylopsis tetragona</i>
Cnidaria		Hydrozoa	Hydroida (Hydroidae, Hydroidolina)	Siphonophorae	Calyconectae (Calycophorae)	Abylidae	Abylopsis	
Cnidaria		Hydrozoa	Hydroida (Hydroidae, Hydroidolina)	Siphonophorae	Calyconectae (Calycophorae)	Diphyidae	Lensia	<i>Lensia beryi</i>
Cnidaria		Hydrozoa	Hydroida (Hydroidae, Hydroidolina)	Siphonophorae	Calyconectae (Calycophorae)	Diphyidae	Lensia	<i>Lensia campanella</i>
Cnidaria		Hydrozoa	Hydroida (Hydroidae, Hydroidolina)	Siphonophorae	Calyconectae (Calycophorae)	Diphyidae	Lensia	<i>Lensia conoidea</i>
Cnidaria		Hydrozoa	Hydroida (Hydroidae, Hydroidolina)	Siphonophorae	Calyconectae (Calycophorae)	Diphyidae	Lensia	<i>Lensia fowleri</i>
Cnidaria		Hydrozoa	Hydroida (Hydroidae, Hydroidolina)	Siphonophorae	Calyconectae (Calycophorae)	Diphyidae	Lensia	<i>Lensia subtilis</i>
Cnidaria		Hydrozoa	Hydroida (Hydroidae, Hydroidolina)	Siphonophorae	Calyconectae (Calycophorae)	Diphyidae	Lensia	<i>Lensia subtiloides</i>
Cnidaria		Hydrozoa	Hydroida (Hydroidae, Hydroidolina)	Siphonophorae	Calyconectae (Calycophorae)	Diphyidae	Lensia	
Cnidaria		Hydrozoa	Hydroida (Hydroidae, Hydroidolina)	Siphonophorae	Calyconectae (Calycophorae)	Diphyidae	Muggiaea	<i>Muggiaea atlantica</i>

**Table A1.** Taxonomic information for gelatinous zooplankton from MAREDAT. The last filled column for each row is the taxonomic level given in MAREDAT. Provided in parenthesis are alternative or historic names for the same organism.

Phylum	Subphylum	Class	Subclass	Order	Suborder	Family	Genus	Species
Cnidaria		Hydrozoa	Hydroida (Hydroidae, Hydroidolina)	Siphonophorae	Calyconectae (Calycophorae)	Diphyidae	Muggiaea	<i>Muggiaea kochi</i>
Cnidaria		Hydrozoa	Hydroida (Hydroidae, Hydroidolina)	Siphonophorae	Calyconectae (Calycophorae)	Diphyidae	Muggiaea	
Cnidaria		Hydrozoa	Hydroida (Hydroidae, Hydroidolina)	Siphonophorae	Calyconectae (Calycophorae)	Diphyidae	Sulculeolaria	<i>Sulculeolaria quadrivalvis</i>
Cnidaria		Hydrozoa	Hydroida (Hydroidae, Hydroidolina)	Siphonophorae	Calyconectae (Calycophorae)	Diphyidae	Sulculeolaria	
Cnidaria		Hydrozoa	Hydroida (Hydroidae, Hydroidolina)	Siphonophorae	Cystonectae	Physaliidae	Physalia	
Cnidaria		Hydrozoa	Hydroida (Hydroidae, Hydroidolina)	Siphonophorae	Physonectae	Agalmatidae	Nanomia	
Cnidaria		Hydrozoa	Hydroida (Hydroidae, Hydroidolina)					
Cnidaria		Hydrozoa	Hydromedusae					
Cnidaria		Hydrozoa	Trachylinae	Narcomedusae		Aeginidae	Aegina	<i>Aegina rosea</i>
Cnidaria		Hydrozoa	Trachylinae	Narcomedusae		Aeginidae	Aegina	
Cnidaria		Hydrozoa	Trachylinae	Narcomedusae		Aeginidae	Aeginopsis	<i>Aeginopsis laurentii</i>
Cnidaria		Hydrozoa	Trachylinae	Narcomedusae		Aeginidae	Aeginopsis	
Cnidaria		Hydrozoa	Trachylinae	Narcomedusae		Aeginidae	Solmundella	<i>Solmundella bitentaculata</i>
Cnidaria		Hydrozoa	Trachylinae	Narcomedusae		Aeginidae		
Cnidaria		Hydrozoa	Trachylinae	Narcomedusae		Tetraplatidae	Tetraplatia	
Cnidaria		Hydrozoa	Trachylinae	Trachymedusae		Geryoniidae	Liriope	<i>Liriope tetraphylla</i>

**Table A1.** Taxonomic information for gelatinous zooplankton from MAREDAT. The last filled column for each row is the taxonomic level given in MAREDAT. Provided in parenthesis are alternative or historic names for the same organism.

Phylum	Subphylum	Class	Subclass	Order	Suborder	Family	Genus	Species
Cnidaria		Hydrozoa	Trachylinae	Trachymedusae		Halicreatidae	Homoeonema	<i>Homoeonema platygonon</i>
Cnidaria		Hydrozoa	Trachylinae	Trachymedusae		Ptychogastridae		
Cnidaria		Hydrozoa	Trachylinae	Trachymedusae		Rhopalonematidae	Aglantha	<i>Aglantha digitale</i>
Cnidaria		Hydrozoa	Trachylinae	Trachymedusae		Rhopalonematidae	Aglantha	
Cnidaria		Hydrozoa	Trachylinae	Trachymedusae		Rhopalonematidae	Aglaura	<i>Aglaura hemistoma</i>
Cnidaria		Hydrozoa	Trachylinae	Trachymedusae		Rhopalonematidae	Aglaura	
Cnidaria		Hydrozoa	Trachylinae	Trachymedusae		Rhopalonematidae	Sminthea	<i>Sminthea arctica</i>
Cnidaria		Hydrozoa	Trachylinae	Trachymedusae		Rhopalonematidae		
Cnidaria		Hydrozoa		Anthoathecata (Anthomedusae)	Aplanulata	Corymorphidae	Euphysa (Corymorpha)	<i>Euphysa flammea</i> ( <i>Corymorpha flammea</i> )
Cnidaria		Hydrozoa		Anthoathecata (Anthomedusae)	Aplanulata	Corymorphidae	Euphysa (Corymorpha)	<i>Euphysa tentaculata</i>
Cnidaria		Hydrozoa		Anthoathecata (Anthomedusae)	Aplanulata	Corymorphidae	Euphysa (Corymorpha)	
Cnidaria		Hydrozoa		Anthoathecata (Anthomedusae)	Aplanulata	Tubulariidae	Hybocodon	<i>Hybocodon prolifer</i> ( <i>Tubularia prolifer</i> )
Cnidaria		Hydrozoa		Anthoathecata (Anthomedusae)	Aplanulata	Tubulariidae	Hybocodon	
Cnidaria		Hydrozoa		Anthoathecata (Anthomedusae)	Capitata	Corynidae	Coryne	<i>Coryne principes</i>
Cnidaria		Hydrozoa		Anthoathecata (Anthomedusae)	Capitata	Corynidae	Coryne	<i>Coryne pusilla</i>
Cnidaria		Hydrozoa		Anthoathecata (Anthomedusae)	Capitata	Corynidae	Coryne	<i>Coryne tubulosa</i>

**Table A1.** Taxonomic information for gelatinous zooplankton from MAREDAT. The last filled column for each row is the taxonomic level given in MAREDAT. Provided in parenthesis are alternative or historic names for the same organism.

Phylum	Subphylum	Class	Subclass	Order	Suborder	Family	Genus	Species
Cnidaria		Hydrozoa		Anthoathecata (Anthomedusae)	Capitata	Corynidae	Coryne	
Cnidaria		Hydrozoa		Anthoathecata (Anthomedusae)	Capitata	Corynidae	Dipurena	<i>Dipurena halterata</i>
Cnidaria		Hydrozoa		Anthoathecata (Anthomedusae)	Capitata	Corynidae		
Cnidaria		Hydrozoa		Anthoathecata (Anthomedusae)	Capitata	Halimedusidae	Halimedusa	<i>Halimedusa typus</i>
Cnidaria		Hydrozoa		Anthoathecata (Anthomedusae)	Filifera	Bythotiaridae	Calycopsis	<i>Calycopsis birulai</i>
Cnidaria		Hydrozoa		Anthoathecata (Anthomedusae)	Filifera	Bythotiaridae	Calycopsis	<i>Calycopsis nematophora</i>
Cnidaria		Hydrozoa		Anthoathecata (Anthomedusae)	Filifera	Cyaeidae	Cyaeis	
Cnidaria		Hydrozoa		Anthoathecata (Anthomedusae)	Filifera	Pandeidae	Catablema	<i>Catablema vesicarium</i> ( <i>Perigonimus vesicarius</i> )
Cnidaria		Hydrozoa		Anthoathecata (Anthomedusae)	Filifera	Pandeidae	Halitholus	<i>Halitholus cirratus</i>
Cnidaria		Hydrozoa		Anthoathecata (Anthomedusae)				
Cnidaria		Hydrozoa		Leptothecata		Aequoreidae	Aequorea	<i>Aequorea aequorea</i>
Cnidaria		Hydrozoa		Leptothecata		Aequoreidae	Aequorea	<i>Aequorea forskalea</i>
Cnidaria		Hydrozoa		Leptothecata		Aequoreidae	Aequorea	
Cnidaria		Hydrozoa		Leptothecata		Campanulinidae	Cuspidella	<i>Cuspidella mertensi</i>
Cnidaria		Hydrozoa		Leptothecata		Campanulinidae	Cuspidella	

**Table A1.** Taxonomic information for gelatinous zooplankton from MAREDAT. The last filled column for each row is the taxonomic level given in MAREDAT. Provided in parenthesis are alternative or historic names for the same organism.

Phylum	Subphylum	Class	Subclass	Order	Suborder	Family	Genus	Species
Cnidaria		Hydrozoa		Leptothecata		Campanulinidae		
Cnidaria		Hydrozoa		Leptothecata		Mitrocomidae	Halistaura	
Cnidaria		Hydrozoa		Limnomedusae		Olindiidae	Gonionemus	<i>Gonionemus vertens</i>
Cnidaria		Hydrozoa		Limnomedusae		Olindiidae	Gonionemus	
Cnidaria		Hydrozoa		Siphonophorae	Calyconectae (Calycophorae)	Diphyidae	Chelophyes	<i>Chelophyes appendiculata</i>
Cnidaria		Hydrozoa		Siphonophorae	Calyconectae (Calycophorae)	Diphyidae	Chelophyes	
Cnidaria		Hydrozoa		Siphonophorae	Calyconectae (Calycophorae)	Diphyidae	Dimophyes	<i>Dimophyes (Diphyes arctica)</i>
Cnidaria		Hydrozoa		Siphonophorae	Calyconectae (Calycophorae)	Diphyidae	Diphyes	<i>Diphyes dispar</i>
Cnidaria		Hydrozoa		Siphonophorae	Calyconectae (Calycophorae)	Diphyidae	Diphyes	
Cnidaria		Hydrozoa		Siphonophorae	Calyconectae (Calycophorae)	Diphyidae	Eudoxoides	<i>Eudoxoides spiralis</i>
Cnidaria		Hydrozoa		Siphonophorae	Calyconectae (Calycophorae)	Diphyidae	Eudoxoides	
Cnidaria		Hydrozoa		Siphonophorae	Calyconectae (Calycophorae)	Diphyidae		
Cnidaria		Hydrozoa		Siphonophorae	Physonectae	Agalmatidae	Agalma	<i>Agalma elegans</i>
Cnidaria		Hydrozoa		Siphonophorae	Physonectae	Agalmatidae	Agalma	



**Table A1.** Taxonomic information for gelatinous zooplankton from MAREDAT. The last filled column for each row is the taxonomic level given in MAREDAT. Provided in parenthesis are alternative or historic names for the same organism.

Phylum	Subphylum	Class	Subclass	Order	Suborder	Family	Genus	Species
Cnidaria		Hydrozoa		Siphonophorae	Physonectae	Agalmatidae	Cordagalma	<i>Cordagalma cordiforme</i>
Cnidaria		Hydrozoa		Siphonophorae	Physonectae	Agalmatidae	Halistemma	<i>Halistemma rubrum</i>
Cnidaria		Hydrozoa		Siphonophorae	Physonectae	Agalmatidae		
Cnidaria		Hydrozoa		Siphonophorae		Abylidae	Bassia	<i>Bassia bassensis</i>
Cnidaria		Hydrozoa		Siphonophorae		Abylidae	Bassia	
Cnidaria		Hydrozoa		Siphonophorae		Aglamidae		
Cnidaria		Hydrozoa		Trachymedusae		Halicreatidae	Botrynema	<i>Botrynema brucei</i>
Cnidaria		Hydrozoa						
Cnidaria		Scyphozoa	Coronamedusae	Coronatae		Periphyllidae	Periphylla	<i>Periphylla periphylla</i>
Cnidaria		Scyphozoa		Semaeostomeae		Cyaneidae	Cyanea	<i>Cyanea capillata</i>
Cnidaria		Scyphozoa		Semaeostomeae		Pelagiidae	Chrysaora	<i>Chrysaora helova</i>
Cnidaria		Scyphozoa		Semaeostomeae		Pelagiidae	Chrysaora	<i>Chrysaora melanaster</i>
Cnidaria		Scyphozoa		Semaeostomeae		Pelagiidae	Chrysaora	
Cnidaria		Scyphozoa		Semaeostomeae		Ulmaridae	Aurelia	<i>Aurelia aurita</i>
Cnidaria		Scyphozoa		Semaeostomeae		Ulmaridae	Aurelia	<i>Aurelia limbata</i>
Cnidaria		Scyphozoa						
Cnidaria		Siphonophorae						
Cnidaria								

**Table A1.** Taxonomic information for gelatinous zooplankton from MAREDAT. The last filled column for each row is the taxonomic level given in MAREDAT. Provided in parenthesis are alternative or historic names for the same organism.

Phylum	Subphylum	Class	Subclass	Order	Suborder	Family	Genus	Species
Ctenophore		Nuda		Beroidea		Beroidea	Beroe	
Ctenophore		Tentaculata		Cydippida		Mertensiidae	Mertensia	<i>Mertensia ovum</i>
Ctenophore		Tentaculata		Cydippida		Mertensiidae	Mertensia	
Ctenophore		Tentaculata		Cydippida		Pleurobrachiidae	Hormiphora	<i>Hormiphora cucumis</i>
Ctenophore		Tentaculata		Cydippida		Pleurobrachiidae	Pleurobranchia	<i>Pleurobranchia pileus</i>
Ctenophore		Tentaculata		Cydippida		Pleurobrachiidae	Pleurobranchia	
Ctenophore		Tentaculata		Lobata		Bolinopsidae	Bolinopsis	<i>Bolinopsis infundibulum</i>
Ctenophore		Tentaculata		Lobata		Bolinopsidae	Bolinopsis	
Ctenophore								
Jellyfish								

